

THE RELATIONSHIP BETWEEN NECK STRENGTH AND HEAD ACCELERATIONS IN A RUGBY TACKLE

Alasdair R Dempsey¹, Timothy J Fairchild¹, and Brendyn B Appleby²

School of Psychology and Exercise Science, Murdoch University, Perth, Australia¹

Australian Institute of Sport, Perth, Australia²

The purpose of this study was to investigate the relationship between neck strength and head accelerations during a rugby tackle. Ten elite rugby players had their neck strength assessed and head accelerations tracked using a three dimensional motion analysis system during a rugby tackle. Higher levels of strength were related to lower head accelerations. Significant relationships were found between coronal plane accelerations and flexion and extension strength. The findings support those in the literature suggesting that increasing neck strength is a potential target to reduce sport concussions.

KEY WORDS: concussion, injury, neck strength.

INTRODUCTION: Over recent years there has been an increase in interest in understanding and moving towards prevention of concussion in sports. This interest arises from both the management of the initial incident and return to play, but also with regards to the long term effects of concussion, in particular repeated concussions (McCroly et al., 2013; Pearce et al., 2014). A recent systematic review has estimated the incidence of concussion in rugby union to be 4.73 per 1000 player match hours (Gardner, Iverson, Williams, Baker, & Stanwell, 2014).

Much of the work undertaken to identify the aetiology of the injury has focused on the assessment of head accelerations in game during American Football using in helmet accelerometers (Broglio, Martini, Kasper, Eckner, & Kutcher, 2013; Young, Rowson, & Duma, 2014). We are only aware of one study that has investigated head accelerations in a controlled contact situation (Hasegawa et al., 2014). Recently it has been identified that increased neck strength may reduce concussion risk in high school sports (Collins et al., 2014). The aim of this study was to investigate the relationship between neck strength parameters and head accelerations during a rugby tackle.

METHODS: Ten elite Rugby Union players (height 1.89 (SD 0.07) meters, weight 98 (SD 10.5) kilograms) were recruited to undertake this study. Four players were current professional players with a Super 15 team with the remainder being drawn from the wider training squad and academy. All procedures were approved by the Murdoch University Human Research Ethics Committee.

All testing was performed in the Performance Laboratory at Murdoch University. Peak isometric neck strength was assessed using a load cell (HBM 2007 S40 100kg) connected to the player using a head harness made of seatbelt webbing and velcro. All measurements were done while the participant was lying and strapped to a bench to minimise movement.

The tackle situation was designed to mimic a "one off the ruck" hit up. The attacking player was located four meters in front of two opposing defenders holding a regulation rugby ball. On the command to start, the attacking player moved forward to be met by one of the two defenders. The attacker was instructed to run to the centre of the two defenders and attempt to drive past the defenders. The defender used their inside shoulder to attempt to drive the attacker back and to the side where large mats were located. For instance the defender on the attacker's right would drive the attacker to the left. Prior to the start of the trial the

attacker was not aware of which defender would make the tackle, and initially both defenders were instructed to move forward, however only one would make contact. This was done to increase the similarity of the tackle scenario to the game. See Appendix 1.

The following markers were placed on the attacking players head, torso and pelvis: left and right forehead, left and right behind head, C7, sternal notch, left and right acromioclavicular joints, left and right anterior and posterior superior iliac spines. An additional two markers were located inferiorly to the left and right of C7, with a further marker located superior to and mid-way between the left and right posterior superior iliac spines. These markers were used to enable tracking of the torso and pelvis segments during the dynamic trials, as markers on the anterior body were occluded at contact. All motion was captured using a 12 camera (Oqus 3+, Qualysis, Gothenburg, Sweden) with 11 cameras capturing marker data 200Hz and with one capturing high speed video at 100Hz to identify contact. Data was recorded in Qualysis Track Manager (Qualysis, Gothenburg, Sweden).

Data was transferred to Visual3D where head, torso and pelvis segments were created based on a static posture. Head angular acceleration relative to both the lab and torso were calculated as well as the linear acceleration of both the torso and head along the anterior-posterior and medial lateral axes of the relevant segment. The peak values for linear accelerations following contact identified on video was used for further analysis. For flexion/extension and lateral flexion angular accelerations, two peaks were identified, one positive and one negative. Both peaks were identified and the range between two peaks also calculated.

Subject means for all data were calculated. Following this Pearson correlations were identified between neck strength data with head linear and angular accelerations using SPSS Version 21. P was set at 0.05.

RESULTS: Subject means for all data is presented in Table 1. In general, an increase in neck strength variables were correlated with a reduction in head accelerations (Table 2). Increased neck flexion strength was significantly correlated to a reduction in the range of lateral flexion angular acceleration ($r = -0.671$) and peak medial/lateral acceleration ($r = -0.911$). A decrease in peak medial/lateral accelerations were also significantly related to an increase in neck extensor strength ($r = -0.843$) and right lateral flexion strength ($r = -0.754$). Finally an increase in right lateral flexion strength was significantly correlated to a decrease in peak lateral flexion angular velocity away from the direction of travel (0.722). A number of other correlations approached significance.

DISCUSSION: All correlations indicated relationships in the expected direction, specifically an increase in neck muscular strength is related to a decrease in head accelerations. Only a few variables indicated significant relationships, despite a number showing moderate relationships around $r = 0.6$. It would appear that currently the study is underpowered and we are currently seeking to increase our participant numbers. The findings of the current study support previous work indicating that increased strength can reduce concussion risk (Collins et al., 2014). It also supports controlled laboratory based studies that have found that there is a relationship between neck strength and head accelerations in all three planes during controlled head perturbations (Eckner, Oh, Joshi, Richardson, & Ashton-Miller, 2014).

What is interesting in this study is the fact that the strongest correlations were found between neck flexion and extension strength and medial/lateral angular and linear accelerations. This may be indicative of the fact that muscles utilised in lateral flexion unilaterally are utilised bilaterally during flexion and extension. Therefore if participants were to preactivate their flexors and extensors in preparation for contact they may be protecting from movement more than a reactive lateral activation. Increase pre-activation has been shown to reduce head accelerations in a controlled experimental situation (Eckner et al., 2014). Instructions to clench

Table 1 Mean and standard deviation of all measured variables

Variable	Mean (Standard Deviation)
Flexion Strength (N)	293.8 (65.1)
Extension Strength (N)	222.0 (49.3)
Left Lateral Flexion Strength (N)	221.9 (38.8)
Right Lateral Flexion Strength (N)	216.6 (43.2)
Peak Positive Flexion/Extension ω (rad/s ²)	89.8 (48.2)
Peak Negative Flexion/Extension ω (rad/s ²)	-73.7 (39.1)
Peak Lateral Flexion ω in direction of travel (rad/s ²)	55.0 (18.9)
Peak Lateral Flexion ω away from the direction of travel (rad/s ²)	-51.5 (18.9)
Flexion/Extension ω range (rad/s ²)	172.7 (87.3)
Lateral Flexion ω range (rad/s ²)	114.1 (45.8)
Peak Anterior/Posterior acceleration (g)	-2.6 (0.6)
Peak Medial/Lateral acceleration (g)	2.1 (0.5)
Peak Superior/Inferior acceleration (g)	1.7 (0.6)

Table 2 Correlation of strength and neck anthropometrics with head accelerations. * indicates significance a $p < 0.05$.

	Flexion Strength	Extension Strength	Left Lateral Flexion Strength	Right Lateral Flexion Strength
Peak Positive Flexion/Extension ω	-0.294	-0.430	-0.209	-0.348
Peak Negative Flexion/Extension ω	0.346	-0.554	0.401	0.476
Peak Lateral Flexion ω in direction of travel	-0.628	-0.668	-0.405	-0.476
Peak Lateral Flexion ω away from the direction of travel	0.470	0.309	0.416	0.772*
Flexion/Extension ω range	-0.416	-0.521	-0.364	-0.474
Lateral Flexion ω range	-0.671*	-0.531	-0.508	-0.431
Peak Anterior/Posterior acceleration	0.551	0.259	0.509	0.277
Peak Medial/Lateral acceleration	-0.911*	-0.843*	-0.629	-0.754*
Peak Superior/Inferior acceleration	0.365	-0.605	-0.418	-0.522

the jaw prior to contact, and therefore inducing pre-activation have also been shown to reduce head accelerations in a contact situation (Hasegawa et al., 2014). While we have collected muscle activation for this study it has yet to be analysed. Coronal plane accelerations may also be subsequent to sagittal plane accelerations following contact, allowing for increases in muscle activation post contact to mitigate the magnitude of the coronal accelerations in stronger participants.

Finally further investigation is required to identify what other factors influence head accelerations during the tackle situation. While this and previous studies have identified muscle strength and muscle activation, factors such as applied tackle force and direction have yet to be assessed. In part this is due to these variables being technically difficult to assess, however moving forward, this should be considered either through direct measurement or derived values such as assessing full body center of mass velocity changes and calculating applied force via the impulse-momentum relationship.

CONCLUSION: Increases in neck strength are related to reductions in head accelerations during a rugby tackle. The greatest relationship was to coronal plane accelerations, however further work is required to understand the difference between relationships of neck strength to sagittal and coronal plane accelerations. This study supports the proposition that increasing neck strength may reduce concussion risk in contact sports.

REFERENCES:

- Broglio, S. P., Martini, D., Kasper, L., Eckner, J. T., & Kutcher, J. S. (2013). Estimation of head impact exposure in high school football: implications for regulating contact practices. *The American Journal of Sports Medicine*, 41(12), 2877-2884.
- Collins, C. L., Fletcher, E. N., Fields, S. K., Kluchurosky, L., Rohrkemper, M. K., Comstock, R. D., & Cantu, R. C. (2014). Neck strength: a protective factor reducing risk for concussion in high school sports. *The Journal of Primary Prevention*, 35(5), 309-319.
- Eckner, J. T., Oh, Y. K., Joshi, M. S., Richardson, J. K., & Ashton-Miller, J. A. (2014). Effect of neck muscle strength and anticipatory cervical muscle activation on the kinematic response of the head to impulsive loads. *The American Journal of Sports Medicine*, 42(3), 566-576.
- Gardner, A. J., Iverson, G. L., Williams, W. H., Baker, S., & Stanwell, P. (2014). A systematic review and meta-analysis of concussion in rugby union. *Sports Medicine*, 44(12), 1717-1731.
- Hasegawa, K., Takeda, T., Nakajima, K., Ozawa, T., Ishigami, K., Narimatsu, K., & Noh, K. (2014). Does clenching reduce indirect head acceleration during rugby contact? *Dental Traumatology*, 30(4), 259-264.
- McCorry, P., Meeuwisse, W. H., Aubry, M., Cantu, B., Dvořák, J., Echemendia, R. J., . . . Turner, M. (2013). Consensus statement on concussion in sport: the 4th International Conference on Concussion in Sport held in Zurich, November 2012. *British Journal of Sports Medicine*, 47(5), 250-258.
- Pearce, A. J., Hoy, K., Rogers, M. A., Corp, D. T., Maller, J. J., Drury, H. G., & Fitzgerald, P. B. (2014). The long-term effects of sports concussion on retired Australian football players: a study using transcranial magnetic stimulation. *Journal of Neurotrauma*, 31(13), 1139-1145.
- Young, T., Rowson, S., & Duma, S. M. (2014). High magnitude head impacts experienced during youth football practices. *Biomedical Sciences Instrumentation*, 50, 100-105.

Acknowledgement

We would like to thank RugbyWA and the Western Force for their assistance in player recruitment.

VALIDITY, SENSITIVITY AND REPRODUCIBILITY OF STAGES AND GARMIN VECTOR POWER METERS WHEN COMPARED WITH SRM DEVICE

Anthony Bouillod^{1,4}, Julien Pinot^{1,2}, Georges Soto-Romero^{3,4} and Frederic Grappe^{1,2}

EA4660, C3S Health - Sport Department, Sports University, Besancon, France¹
Professional Cycling Team FDJ²
ISIFC, Université de Franche-Comté³
LAAS-CNRS, Toulouse, France⁴

The measurement of power output (PO) during cycling has led some manufacturers to develop mobile power meters. However, such devices have to provide a valid, sensitive and reproducible PO. This study aimed to determine the validity, sensitivity and reproducibility of the Stages and Garmin Vector during both laboratory and field cycling tests. The results demonstrate that the Stages and the Garmin Vector systems appear to be reproducible. However, the validity and the sensitivity of the two systems must be treated with some caution.

KEYWORDS: mobile power meter, power output, comparison, laboratory, field, cycling.

INTRODUCTION: The measurement of power output (PO) during cycling allows the assessment of the cyclist's training and racing intensity zones according to their skills and thus, to their race performance profile (Pinot & Grappe, 2011). In this way, several manufacturers developed mobile power meters. To be used, such devices have to provide a valid, sensitive and reproducible PO (Bertucci, Duc, Villerius, Pernin, & Grappe, 2005). The SRM power meter (SRM, Schoberer, Rad, Messtechnik, Julich, Germany) is the most commonly used system in cycling (Sparks, Dove, Bridge, Midgley, & McNaughton, 2015). It is considered as a gold standard due to the high validity, sensitivity and reproducibility of the measurement. The high cost of the SRM led manufacturers to develop less expensive systems. Some of them have been studied for their validity, sensitivity and reproducibility (Max one, Polar S710, Ergomo, Look Keo Power, Powertap), whereas others newer power meter have not been yet studied (Stages, Garmin Vector).

The aim of this study was to assess the validity, sensitivity and reproducibility of the Stages and Garmin Vector systems during both laboratory and field cycling tests.

METHODS: After a familiarisation session, a national level male competitive cyclist (age: 23 years old, height: 1.88 m, body mass: 80 kg) performed all testing sessions with the same road racing bicycle fitted with a SRM crank set (SRM 9000 comprising 8 strain gauges), a Stages left-arm crank (STG, Boulder, USA) and Garmin Vector pedals (VCT, Olathe, USA). The validity, the sensitivity and the reproducibility of Stages and Garmin Vector were investigated in the laboratory at submaximal and maximal intensities from three experimental protocols which included 1) a sub-maximal incremental test, 2) a sub-maximal 30-min continuous test, and 3) a sprint test. The incremental and continuous sub-maximal tests were performed on a motorized treadmill, whereas the sprint test was performed on a Cateye ergometer (CS-1000, Cateye, Osaka, Japan). The subject performed the three protocols on the same day and repeated each protocol three times on three different days. One extra test was performed in the field to study the validity of the three systems during real cycling locomotion.

A sub-maximal incremental test was performed on a motorized treadmill with 19.5, 21, 22.5, 24 and 25.5 km.h⁻¹ velocities (150 to 350 W). The mass of the system (subject + bicycle) contributes to the PO required to ride on a treadmill at a given speed, that's why we controlled this parameter adding or removing water from two bottles in the bottle cages of the bicycle. On each velocity, both the pedalling cadence (60, 80 and 100 rpm) and the position (seated and standing) effects on PO were tested. The combinations of the different speeds, pedalling cadences and positions resulted in 30 different data sets.

A 30-min continuous exercise test was performed in seated position at 21 km.h⁻¹ on a 3 % slope with a pedalling cadence of 80 rpm.

The sprint test consisted of three 8-sec sprints in a seated position to determine the maximal 1-sec PO (PO_{max}) and 5-sec PO (PO_{5sec}). The magnetic resistance of the Cateye ergometer was set at a simulated grade of 7 %. Three different gear ratios were used (53/15, 53/17 and 53/19) to determine three different maximal pedalling cadences. Sprints were separated by 5-min of active recovery periods at low intensity (<150 W).

The field test consisted of a 2-h road cycling session on a hilly terrain including the different laboratorial experimental conditions.

Bland-Altman plots and 95 % limits of agreement were applied to assess agreement between PO_{STG}, PO_{VCT} and PO_{SRM} during sub-maximal incremental test. The data of the four protocols were not normally distributed. Thus, the analysis of differences between the mean PO_{STG}, the mean PO_{VCT} and the mean PO_{SRM} of each protocol were assessed with a non-parametric Kruskal-Wallis test. Pedalling cadence and cycling position effects on PO_{STG}, PO_{VCT} and PO_{SRM} during sub-maximal incremental test were evaluated with a non-parametric two-way repeated measures test (Friedman). To assess the reproducibility, the mean coefficient of variation (CV) and the intraclass correlation coefficient (ICC) were calculated. In all statistical tests significance was set at p < 0.05.

RESULTS: During the sub-maximal incremental test there were strong correlations between PO_{SRM} and PO_{STG} (r = 0.985, p < 0.001) and PO_{VCT} (r = 0.996, p < 0.001). The mean PO from 19.5 to 25.5 km.h⁻¹ (150 to 350 W) was not significantly different between the three systems. Bland-Altman analysis (fig. 1) shows that the mean bias between PO_{SRM} and PO_{STG} was -13.7 ± 12.4 W (95 % CI: -37.9 and 10.6 W) and 0.6 ± 6.2 W (95 % CI: -11.6 and 12.7 W) between PO_{SRM} and PO_{VCT}.

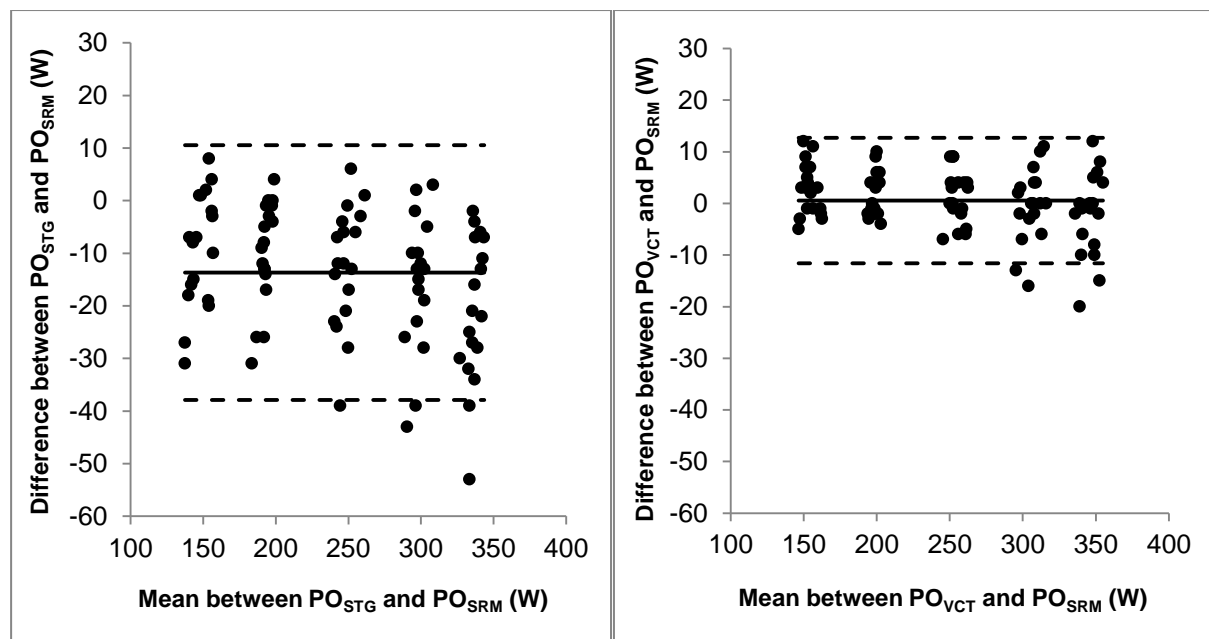


Figure 1: Bland-Altman plots of the differences between PO_{SRM} and PO_{STG} and PO_{VCT} during sub-maximal incremental test. The dashed lines represent the high and low 95 % confidence interval (CI), whereas the solid line represents the bias.

No significant difference was measured between the mean POs during the 30-min continuous tests and the mean CV was 3.6 %, 2.0 % and 2.8 % for PO_{STG}, PO_{VCT} and PO_{SRM}. However, the figure 2 shows that the 5-sec PO_{VCT} was significantly lower (-36.9 %, p < 0.05) compared to PO_{SRM} with the lowest gear.

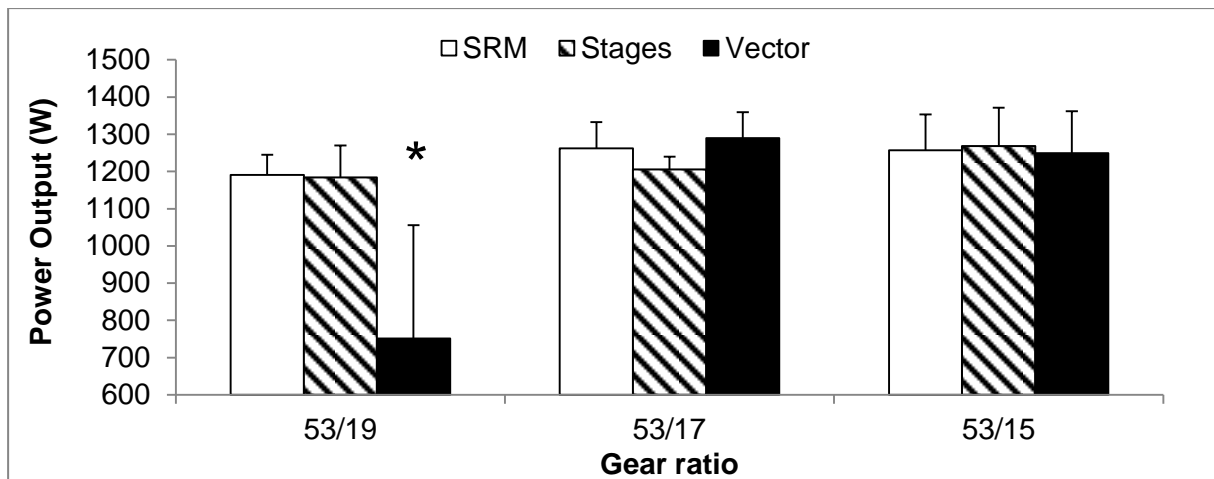


Figure 2: SRM, Stages and Garmin Vector 5-sec PO obtained during the sprint tests.

* Significant difference ($p < 0.05$)

The mean PO was not significantly different with SRM (178.5 ± 200.4 W) and Stages devices (168.3 ± 166.7 W) during the field test. However the Garmin Vector under estimates ($p < 0.001$) the PO of 16.5 % (149.1 ± 187.7 W) compared to the SRM.

The pedalling cadence had no effect on PO among the different power meters. However, the cycling position had a significant effect on PO_{STG} and PO_{SRM} (fig. 3). Indeed, with the SRM device PO was significantly higher in standing position (+ 2.1 %, $p < 0.001$). In contrast, PO_{STG} was significantly lower in standing position (-4.4 %, $p < 0.001$).

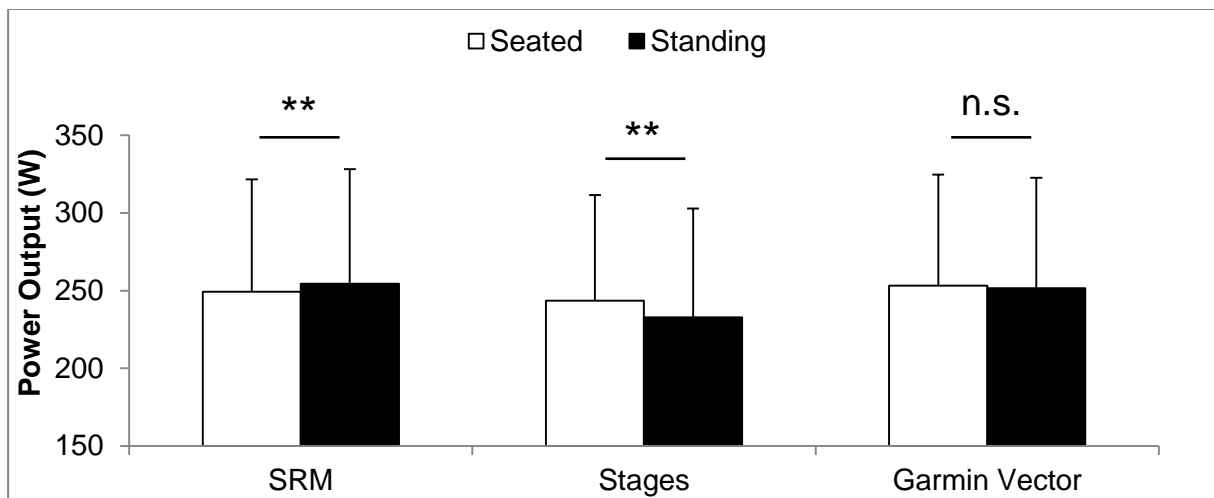


Figure 3. Effect of cycling position on PO during sub-maximal incremental test.

** Significant difference ($p < 0.001$)

n.s. Non-significant difference ($p > 0.05$)

For all the incremental tests, the mean CVs for all the cycling conditions (5 velocities, 3 pedalling cadences, 2 pedalling postures) were 3.0 ± 1.9 % for PO_{STG} , 2.5 ± 1.3 % for PO_{VCT} and 1.9 ± 1.3 % for PO_{SRM} . Additionally, ICC was 0.87, 0.87 and 0.92 respectively whereas no difference was detected with the Kruskal-Wallis analysis.

DISCUSSION: This is the first study that analyse the validity, sensitivity and reproducibility of the Stages and Garmin Vector power meters in comparison with the SRM. The results demonstrate that the Garmin Vector provide a valid PO during sub-maximal exercise in laboratory. However, this power meter under estimates the PO during both the sprints with the low gear ratio (-36.9 %) and the field test (-16.5 %). Concerning the Stages power meter,

the large CI cannot consider this system as valid during the sub-maximal incremental test. PO_{STG} was significantly lower in standing position compared with seated position, probably due to the only left-crank measurement. Because asymmetry depends on the subject, further studies must be realised on several cyclists controlling this parameter especially with the Stages device.

The Garmin Vector system didn't measure the PO change between seated and standing positions. Both Stages and Garmin Vector power meters are not considered as sensitive given that the PO_{SRM} was significantly higher in standing position compared with seated position (Bouillod *et al.*, 2014).

The importance of reproducible power meters to detect small changes in performance has been emphasised in a review (Hopkins, Schabert, & Hawley, 2001). The detectable change in performance represents a magnitude less than 2 % in elite athletes. The mean CVs obtained with the Stages and Garmin Vector devices are slightly higher than 2 % but the statistical analysis indicates that the three power meters provide reproducible PO during sub-maximal tests in laboratory.

CONCLUSION: Our study demonstrates that the Stages and Garmin Vector systems are reproducible mobile power meters. However, the validity and the sensitivity of the two systems must be treated with some caution.

REFERENCES:

- Bertucci, W., Duc, S., Villerius, V., Pernin, J.N., & Grappe, F. (2005). Validity and reliability of the Powertap mobile cycling powermeter when compared with the SRM device. *International Journal of Sports Medicine*, 26, 868–873.
- Bouillod, A., Pinot, J., Valade, A., Cassirame, J., Soto Romero, G., & Grappe, F. (2014). Gross efficiency is improved in standing position with an increase of the power output. *Journal of Science and Cycling*, 3, 6.
- Hopkins, W.G., Schabert, E.J., & Hawley, J.A. (2001). Reliability of power in physical performance tests. *Sports Medicine*, 31, 211-234.
- Pinot, P., & Grappe, F. (2011). The record power profile to assess performance in elite cyclists. *International Journal of Sports Medicine*, 32, 839-844.
- Sparks, S.A., Dove, B., Bridge C.A., Midgley, A.W., & McNaughton, L.R. (2015). Validity and reliability of the look keo power pedal system for measuring power output during incremental and repeated sprint cycling. *International Journal of Sports Physiology and Performance*, 10, 39-45.

SWIM START STANDPOINTS ON THE OSB11 STARTING BLOCK

Armin Kibele, Kristina Biel and Sebastian Fischer

Institute for Sports and Sport Science, University of Kassel, Germany

Systematic variations of the preferred stance positions of 17 elite swimmers on the OSB11 were analyzed in regard to block time, swim start times to 5 m, horizontal take-off velocities, and horizontal vs. vertical peak force values. The variations encompassed changes of the front leg (left vs. right), the centre of mass (CM) height (low vs. high), the stance width (narrow vs. wide), and a rear vs. a front weighted stance. For half of the subjects, at least one stance alternative provided a better swim start time than the preferred stance with an average gain of 0,06s and extreme improvements of up to 0,14s. The majority of the improvements were associated with a change to the front weighted stance, a narrow foot displacement, and an elevated CM position.

KEY WORDS: swim start, OSB11, stance position.

INTRODUCTION: Although clear advantages have been reported for the new OSB11 as compared to the old OSB9 starting block model (e.g. Honda et al., 2010; Biel et al., 2010) there is a dearth of research about the optimal stance position on the OSB11 with respect to the swimmers' leg preference, the stance width, and the CM position. While, for the old OSB9, the rear-weighted track start has been shown to offer advantages over the front-weighted track start (Welcher et al. (2008) it remains unclear whether this virtue is maintained with the use of the OSB11 and its new foot plate and a slightly longer and more inclined start block surface. While swim start positions on the new block have been examined regarding leg preference and stance width already (e.g., Slawson et al., 2011; Takeda et al., 2012; Barlow et al. 2014), only limited knowledge is available about the optimal position of the centre of mass (CM) as this measure has been shown earlier to influence block time as a major prerequisite of swim start performance (Hay & Guimaraes, 1983; Fischer, 2013). A comparative study was conducted to analyze systematic variations of the preferred stance position in the track start of 5 female and 12 male elite swimmers on the OSB11. Variations of the individually preferred stance were examined regarding the front leg (left vs. right), the CM height (low vs. high), the stance width (narrow vs. wide), and a weighted stance (rear vs. front) estimated by the horizontal distance of the hip joint to the front edge of the block. The size of the variations was expressed relative to the individual leg length. Kinematic and kinetic measures were analyzed to evaluate the swim start performance. In addition, a cluster analysis on joint angles (shoulder, elbow, hip, knee, and foot) was conducted to identify the most typical strategies in the preferred stance condition.

METHODS:

Subjects: 17 elite swimmers (5 females: 24,8 ±2,7y age; 1,74 ±0,02m height, 63,8 ±5,09kg body mass; 12 males: 23 ±1,5y age; 1,88 ±0,07m height, 83,6 ±11,7kg body mass) participated in the study. All subjects reported crawl to be their preferred swimming style except for one male and one female with a preference on butterfly swimming.

Instrumentation: For the kinematic data analysis, 2 video cameras (Sony DCR-TRV900E Pal operated at 50Hz) were placed vertically at a height of 1,35 m above the water level and horizontally in parallel to the front edge of the block, and at 5m after the block. While the first camera was used to analyze the take-off behaviour on the block, the second camera was utilized to capture the time between the starting signal and the head passage at 5m. A 2D-strain gauge equipped starting block (Kibele, 2004) with an OSB11 surface measured the horizontal and vertical ground reaction forces.

Procedures: Systematic variations of the preferred stance position accounting for the CM heights and distances relative to the front edge of the block, as well as the stance width, were related to the standard deviations (SD) found in a preceding pilot study (Experiment 1 in Kibele, Biel, & Fischer, 2013) with six male and seven female elite swimmers (females: $22,1 \pm 4,0$ y age; $1,78 \pm 0,06$ m height, $65,2 \pm 5,4$ kg body mass; males: $23,8 \pm 2,3$ y age; $1,90 \pm 0,03$ m height, $85,8 \pm 5,4$ kg body mass). Here, the means and SDs in the above measures were expressed relative to the individual leg lengths of the male and female swimmers separately. For the present study, these SDs were reconverted to metres for male and females separately according to the leg length of each subject. These measures were then added or subtracted to the preferred stance configurations (Fig. 1 left side). Thus, in addition to the preferred stance, 8 configurations were possible for each leg: CM height (low vs. high) x CM distance (rear vs. front weighted stance), and stance width (narrow vs. wide). However, because of motor coordination demands, for each leg, only four of the eight possible configurations could be eventually maintained on the block. The configurations consisted of: a narrow stance with CM position high-front (No.1), a wide stance with CM position high-back (No.2), a wide stance with CM position low-front (No.3), and a wide stance with CM position low-back (No.4). Hence, aside from the preferred stance, a total of eight swim start variations were analyzed. Three trials were used for each configuration. Prior to the various trials, the subjects performed starts in their preferred stance conditions. Subsequently, the variations of the stance configuration were analyzed in random order and across three non-consecutive days. For simplicity reasons, the hip-joint landmark was used as an estimate of the CM location. For the stance width of a male subject, for example, the SD 0,66 from the pilot study was multiplied with the given leg length of a subject and the result was added to the preferred stance width (wide) or subtracted (narrow). Then, the closest footplate position was used for the swim start trial. A video display was used to control the required stance configurations. Here, an overlay reference grid (Fig. 1 right side) was used to indicate the various hip joint positions.

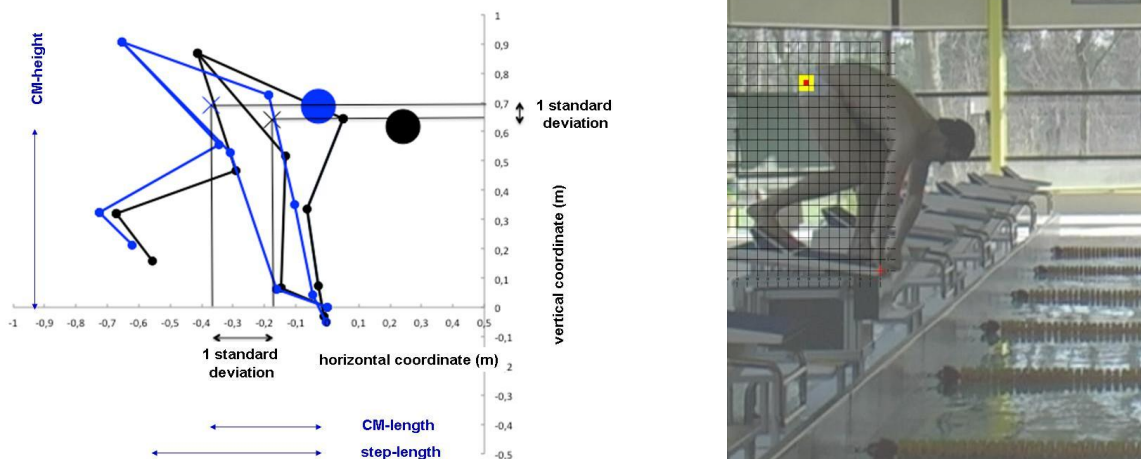


Fig. 1 left side: stance parameters: CM-length (rear weighted vs. front weighted start), CM-height (high vs. low), and step length (narrow vs. wide), right side: video display to control for the required CM location.

Parameters: For each subject, the mean values across valid trials were evaluated for the following kinematic take-off parameters: block time, horizontal take-off velocity (mean velocity across the first three images in the flight phase), take-off angle (inclination of CM trajectory during the first 3 images in the flight phase), flight distance (between front end of

the block and the point of hip entry) relative to the body height, entry angle (inclination of the CM-hand interconnection), and hip angle at entry (angle between shoulder, hip, and knee joint at hand entry). For the take-off dynamics, the vertical and horizontal peak forces were evaluated across the valid trials. Swim start performance was evaluated by the time between the starting signal and the head passage at 5m

Statistics: For the statistical data evaluation, an analysis on variance for repeated measures was conducted with the stance configurations and preferred vs. non-preferred leg as factors. For the cluster analysis, the Ward-Method was adopted.

RESULTS: For the evaluation of typical strategies in the preferred stance, 3 clusters were identified: a) elevated CM height, large step size, rear-weighted CM position (N=3), b) intermediate CM height, large step size, front-weighted CM position (N=8), and c) low CM height, small step size, intermediate CM position (N=6). Across all stance variations, the deviations for the hip joint landmark from the target position were $-0,049 \pm 0,039\text{m}$ in the vertical direction and $-0,040\text{m} \pm 0,053\text{m}$ in the horizontal direction. To prevent overlapping in CM locations in the different stance configurations, trials were excluded from the statistical data analysis if their CM deviation from the target was larger than the smallest difference between the various target CM locations. Subsequently, 12% of all the trials were excluded. For the valid trials, 9 of the 17 subjects showed swim start improvements for the stance alternatives better than the preferred stance position. However, for 6 swimmers, alterations of their preferred stance configuration caused a deteriorated swim start time. Across all subject, the mean improvements were found as large as 0,06s. The largest increase in the swim start time was 0,14s.

In the analysis of variance for repeated measures, a significant main effect for the front leg factor could not be found in any of the kinematic and dynamic variables, or in the swim start time. For the stance factor, swim start parameters with significant main effects are listed in Tab. 1. For the remaining variables the level of significance was missed.

Tab. 1 Significant main effects for the stance variations (1 = CM high-front narrow stance, 2 = CM high-back wide stance, 3 = CM low-front wide stance, 4 = CM low-back wide stance) with F-values and effect sizes (expressed as partial eta²-values) for the multivariate tests in the analysis of variance for repeated measures and post-hoc differences (* p < 0,05; ** p < 0,01).

<i>repeated measures variables</i>	<i>stance factor</i>	<i>stance differences</i>
block time	32,2** : 0,92	1-2**, 1-4**, 2-3**, 3-4**
swim start time at 5m	7,9* : 0,80	1-4**, 2-3*, 2-4*, 3-4**
horizontal take-off velocity	6,1* : 0,70	2-3*, 3-4**
horizontal peak force	11,6** : 0,81	1-2**, 1-4**, 2-3*, 2-4*, 3-4**
take-off angle	6,5* : 0,71	2-3**, 3-4**

Shortest block times were found for the front-weighted CM positions (No. 1 and 3). No differences were observed between the preferred and non-preferred leg except for the high-front narrow stance (No. 1) with superior values for the non-preferred leg. Accordingly, an interaction effect was found between the front leg factor and the stance factor ($F=5,2^*$; $\eta^2 = 0,66$). Best swim start times to 5m were found in for the front-weighted CM positions as well. No differences between the preferred and non-preferred leg were identified except for the high CM positions (No. 1 and 2). Here, best values were observed for the non-preferred leg. In contrast, the largest horizontal take-off velocities were found independent of the leg in the back CM positions. For the front-high CM position with narrow stance width a slightly smaller take-off velocity was found in the non-preferred leg. The largest horizontal peak forces were present for front CM positions. A significant difference between the preferred and the non-preferred leg was not observed.

DISCUSSION: The presented results indicate that for the majority of the elite swimmers the best swim start performance is in other stance configurations than their preferred one. There was a clear tendency showing that a forward shift to high CM position with a narrow stance would provide best biomechanical conditions for a fast swim start to 5m. Here, subjects were able to produce large horizontal peak forces while block times remained small. These benefits were not counterbalanced by the smaller horizontal take-off velocities observed for the frontal stance positions. These advantages in the take-off velocity are based on the longer block times and acceleration pathways with lower forces amplitudes. A main objection towards the presented results regards swimmers (33 percent) who have found their best stance positioning from the beginning. Variations in their stance configuration led to a deterioration of the swim start performance. In addition, it is unclear whether swim start performance is unambiguously evaluated by the time to the 5m mark.

CONCLUSION: The presented results show that swimmers looking for their best stance positioning a shift to the front with a high CM position and a narrow stance might offer the best chances to improve their swim start performance.

REFERENCES:

- Barlow, H., Halaki, M., Stuelcken, M., Greene, A. & Sinclair, P.J. (2014). The effect of different kick start positions on OMEGA OSB11 blocks on free swimming time to 15 m in developmental level swimmers. *Human Mov Science*, 34, 178–186.
- Biel, K., Fischer, S. & Kibele, A. (2010) Kinematic analysis of take-off performance in elite swimmers: new OSB11 versus traditional starting block. *Biom Med Swimming XI. Proc XI Int Symposium Biom Med Swimming* (p. 75). Oslo: Norwegian School of Sport Sciences.
- Honda, K.E., Sinclair, P.J., Mason, B.R. & Pease, D.L. (2010). A biomechanical comparison of elite swimmers start performance using the traditional track start and the new kick start. *Biom Med Swimming XI. Proc XI Int Symposium Biom Med Swimming* (p. 94-96). Oslo: Norwegian School of Sport Sciences.
- Fischer, S. (2013). Kinematische und dynamische Analyse des Schwimmstarts vom Block unter besonderer Berücksichtigung der Eintauch- und Übergangsphase. PhD Thesis University of Kassel Germany (<http://nbn-resolving.de/urn:nbn:de:hebis:34-2013012242433>)
- Hay, J.G. & Guimaraes, A.C.S. (1983). A quantitative look at swimming biomechanics. *Swimming Technique* 29, 2, 11-17.
- Kibele A (2004). Mobiler Mess-Startblock. Abschlussbericht zu einem Betreuungsprojekt des Bundesinstituts für Sportwissenschaft (VF 0407150102). Universität Kassel.
- Kibele, A., Biel, K. & Fischer, S. (2013) Zur Optimierung des Trackstarts im Schwimmen auf dem neuen Startblock OSB11. Abschlussbericht zu einem Betreuungsprojekt des Bundesinstituts für Sportwissenschaft (VF IIA1-070621/12). Universität Kassel.
- Slawson, S., Conway, P., Cossor, J., Chakravorti, N., Le-Sage, T. & West, A. (2011). The effect of start block configuration and swimmer kinematics on starting performance in elite swimmers using the Omega OSB11 block. *Proc Engineering* 13, 141–147.
- Takeda, T., Takagi, H. & Tsubakimoto, S. (2012). Effect of inclination and position of new swimming starting block's back plate on track-start performance. *Sport Biom* 11, 3, 370-381.
- Welcher, R.L., Hinrichs, R.N. & George, T.R. (2008). Front- or rear-weighted track start or grab start: which is the best for female swimmers? *Sports Biom* 7, 1, 100-113.

Acknowledgement

The study was supported by the Federal Institute of Sport Science Germany IIA1-070621_12

PERFORMANCE RELATED TECHNIQUE FACTORS IN OLYMPIC SPRINT KAYAKING

Barney Wainwright, Carlton Cooke, and Chris Low

The Institute for Sport, Physical Activity and Leisure, Leeds Beckett University, Leeds, UK.

A sprint kayaking specific deterministic model was used to identify key performance related technique factors using data from 12 international-level kayakers. There was large variability in the strength of the between-factor relationships across the group. The pull phase was split into 3 components with the 1st phase contributing the most to increases in boat velocity and the 3rd phase causing a decrease in velocity. The propulsive impulse had the largest influence on velocity, but the magnitude of the impact was moderated by blade slip. Large propulsive impulses in the 3rd phase of the pull were associated with larger decreases in velocity. The results show that the model can be used to identify key technique factors on an individual level, although the use of the model should be confirmed on additional kayakers before being used in an applied setting by practitioners.

KEYWORDS: Deterministic model, biomechanics, performance.

INTRODUCTION: There is little research on technique and style of Olympic sprint kayaking that identifies biomechanical factors that underpin performance. Previous research has described the kinematics of kayakers of different standard (e.g. Kendal & Sanders, 1992), or gender (Baker, Rath, Sanders, & Kelly, 1999), while some have started to explore the influence of equipment on performance (Jackson, 1995) and changes in kayaking proficiency (Pendergast et al., 2005). However, from a coaching and performance perspective, the underlying mechanical relationships between previously identified factors and the requirements of technique are unclear. Recently, an 8-level deterministic model was proposed that identified technique factors that determined performance in Olympic sprint kayaking (Wainwright, Cooke, & Low, 2014) (Figure 1). The purpose of this study was to populate the Wainwright et al. (2014) deterministic model with on-water performance data from a group of international-level kayakers to 1) establish whether the model could explain individual levels of performance, and 2) identify factors in the model that play a key role in determining performance.

METHODS: Data from 12 international-level kayakers completing 250m at race pace were used to create 24 individual deterministic models. Paddle forces and forwards kayak acceleration were measured using a kayaking specific measurement system (Sperlich & Sperlich, Germany) that recorded data at 100 Hz, and was calibrated prior to each trial and checked for drift post-trial. Kinematic variables were measured from video that was recorded from a moving vehicle (motor boat or car) keeping pace with the kayak using Dartfish software (Fribourg, Switzerland), with the length of the kayak (5.20 m) used as a moving calibration frame. The synchronised data were used to calculate a number of variables that were subsequently employed to calculate model factors. The pull phase was divided into three phases for more detailed analysis: Phase 1 – from paddle contact to paddle vertical; Phase 2 – from paddle vertical to maximum velocity; Phase 3 – from maximum velocity to paddle extraction (when the paddle starts to be removed from the water). The transition phase was from the position of paddle extraction to the paddle contact on the opposite side stroke. The model factors determined from the recorded data can be seen in Table 1. The values used in the deterministic models were generated from between 34 and 55 strokes (mean 42). Quadratic and linear regression models were used to establish relationships between factors on adjacent levels in the model to develop a greater understanding of how the factors in the model interact to create average stroke velocity. An important aspect of the methodology was to enable the observation of individual differences in the manipulation of

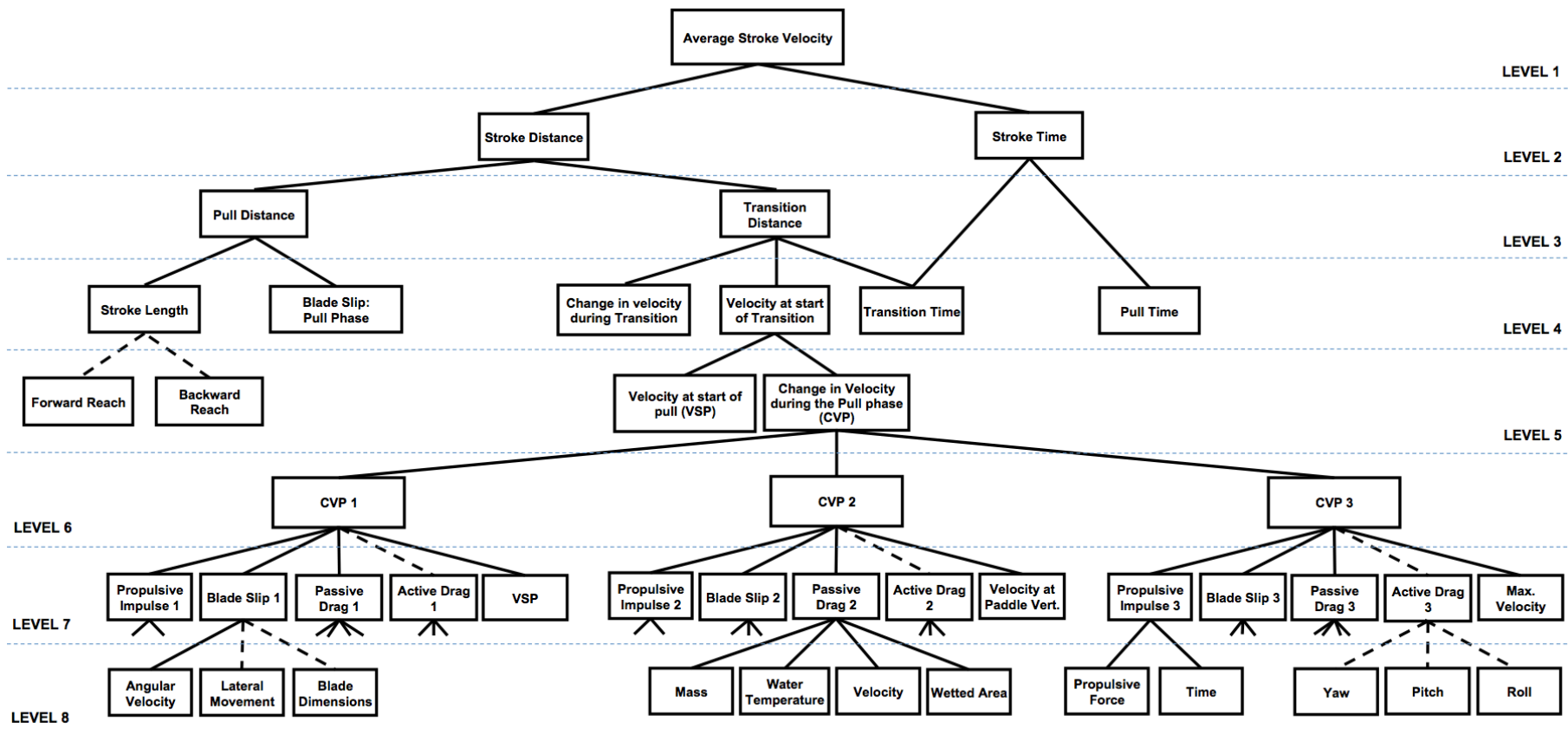


Figure 1. The Wainwright et al. (2014) sprint kayaking deterministic model.

the model factors that were used to achieve velocity. By observing differences between left and right strokes within an individual, and differences between individuals a greater understanding of the key factors that determine performance was developed.

RESULTS: The results of the regression equations between each of the model factors are shown in Table 1. Most kayakers exhibited asymmetry in their models for left and right sides, and therefore had differences in the magnitude and strength of relationships between the model factors that were used to create an average stroke velocity. When examining the change in velocity during the pull (CVP), phase 1 showed the largest change (mean increase 0.233, $s = 0.077$ m/s), with phase 2 increasing velocity to a smaller degree (mean increase 0.098, $s = 0.063$ m/s), and phase 3 experiencing a decrease in velocity (mean increase - 0.138, $s = 0.074$ m/s). The sum of the CVP in phases 1, 2 and 3 was most strongly determined by changes in CVP 3, rather than CVP 1 or 2 as shown by the coefficients of determination. The propulsive impulse (PI) was the largest in phase 3 (average phase 1 = 17.6 n·s, phase 2 = 20.0 n·s, phase 3 = 21.3 n·s). On an individual basis increases in PI increased velocity in phases 1 and 2, but were associated with decreases in velocity in phase 3. Blade slip (BS) (average phase 1 = 0.03 m, phase 2 = -0.11 m, phase 3 = 0.10 m) was the second strongest determinant of CVP, where larger positive blade slip were associated with smaller increases in velocity. In general BS had its strongest influence on CVP in the second phase, where in 22 out of the 24 models blade slip was negative meaning that the blade had a net forwards movement, rather than in phases 1 and 3 where on average the blade moved backwards.

Table 1
The strength and range of the regressions between factors in the model. Only coefficients of determination of significant relationship ($p < 0.05$) are included.

	Dependent Variable	Independent Variable	n	Av. r^2	Min. r^2	Max. r^2
Level 1	Average Stroke Velocity	Stroke Time	14	0.35	0.17	0.68
		Stroke Distance	18	0.47	0.20	0.85
Level 2	Stroke Distance	Transition Distance	23	0.54	0.17	0.85
		Pull Distance	20	0.42	0.12	0.86
	Stroke Time	Transition Time	23	0.55	0.17	0.85
		Pull Time	17	0.33	0.09	0.81
Level 3	Pull Distance	Stroke Length	23	0.37	0.07	0.80
		Blade Slip (whole pull)	13	0.39	0.12	0.75
	Transition Distance	Velocity at Start of Transition	17	0.31	0.13	0.61
		Change in Velocity during Transition	18	0.35	0.12	0.79
Level 4	Velocity at Start of Glide	Transition Time	24	0.95	0.82	0.99
		Velocity at Start of Pull	24	0.75	0.14	0.96
		Change in Velocity during Pull (whole pull)	9	0.22	0.10	0.33
Level 5	Change in Velocity during Pull (whole pull)	CVP 1	10	0.27	0.12	0.52
		CVP 2	20	0.38	0.11	0.76
		CVP 3	23	0.44	0.23	0.78
Level 6	CVP 1	Propulsive Impulse 1	20	0.49	0.17	0.89
		Blade Slip 1	9	0.24	0.13	0.36
		Passive Drag 1	3	0.21	0.33	0.09
		Velocity at Start of Pull	8	0.17	0.11	0.32
	CVP 2	Propulsive Impulse 2	23	0.57	0.26	0.80
		Blade Slip 2	18	0.28	0.10	0.61
		Passive Drag 2	6	0.24	0.12	0.38
		Velocity at Paddle Vertical	14	0.29	0.10	0.57
	CVP 3	Propulsive Impulse 3	16	0.30	0.09	0.66
		Blade Slip 3	8	0.21	0.15	0.36
		Passive Drag 3	8	0.18	0.08	0.27
		Maximum Velocity	6	0.20	0.14	0.27
Level 7	Blade Slip 1	Angular Velocity 1	14	0.34	0.11	0.72
	Blade Slip 2	Angular Velocity 2	6	0.28	0.10	0.64
	Blade Slip 3	Angular Velocity 3	6	0.17	0.08	0.25

DISCUSSION: Although many of the temporo-spatial factors are interesting and have been reported elsewhere (Baker, Rath, Sanders, & Kelly, 1999; Kendal & Sanders, 1992), the factors of most interest are those that directly influence distance the kayak moves during the stroke: the transition distance (TD) and CVP 1, 2 and 3. The most important factors that can be manipulated to maximise TD are the change in velocity during the transition (CVT), and the velocity at the start of the transition (VST). Although the strength of the relationships are variable, the regression models describe a scenario where the TD is determined by the magnitude of decrease in velocity during transition, presumably due to unwanted active drag (Pendergast et al., 2005), and by the VST that has been created during the pull phase. The CVP in each phase was most strongly determined by the magnitude of PI and BS, with the strength and nature of the relationships varying between phases. A strong relationship between the PI and CVP in each phase of the pull was expected, but it was unexpected that BS was found to play a key role in moderating the effect of the PI. While increases in CVP 1 and 2 were very important in increasing velocity during the pull, CVP 3 had the strongest influence upon the increase in velocity during the pull due to its' effect of decelerating the kayak. In general increases in PI lead to increases CVP in phases 1 and 2, but decreases in velocity in phase 3. The examination of the individual results applied to the deterministic model suggest that in general athletes should attempt to maximise the PI in phases 1 and 2, while aiming to minimise it in phase 3 once maximum velocity has been reached. The BS should be minimised where possible, and ideally be negative during phase 2. Athletes should also adopt strategies to minimise the decrease in velocity that occurs during the transition phase.

CONCLUSION: The findings demonstrate that the Wainwright, Cooke, and Low (2014) deterministic model can be used to explain individual levels of performance by examining and comparing both the relationships between factors and the magnitudes of the factors across the group. A number of novel factors have been identified that have a strong influence on other factors within the model, and determine kayak velocity. In particular was the changing role of PI in the pull phase that both increased and decreased velocity. Of additional significance was the variability and importance of BS in moderating the effectiveness of the PI on CVP. The between-athlete variation showed that each athlete used an individual style to create velocity, which suggests that standardised technique interventions used by coaches may not be equally effective in improving performance in different individuals. The approach and methods used in this study were based on a need to provide coaches and practitioners with an analysis process that would identify technique-related factors that presented opportunities to improve performance. Given the effectiveness of the model to do this, it would seem sensible to evaluate it on other high performance kayakers before recommending this approach as a valid tool for practitioners to adopt, but the findings of the present study are encouraging.

REFERENCES:

- Baker, J., Rath, D., Sanders, R., & Kelly, B. (1999). A 3-D analysis of male and female elite sprint kayak paddlers. In R.H. Sanders & B.J. Gibson (Eds), *Scientific proceedings of the XVII International Symposium on Biomechanics in Sports*, Perth, Australia. (pp. 53-56).
- Jackson P.S. (1995). Performance prediction for Olympic kayaks. *Journal of Sports Sciences*. 13, 239-245.
- Kendal, S.H., & Sanders, R.H. (1992). The technique of elite flatwater kayak paddlers using the wing paddle. *Journal of Applied Biomechanics*, 8, 233-250.
- Pendergast, D., Mollendorf, J., Zamparo, P., Termin, A., Bushnell, D., & Paschke, D. (2005). The influence of drag on human locomotion in water. *Undersea and Hyperbaric Medicine*, 32, 45-57.
- Wainwright, B., Cooke, C.B., & Low, C. (2014). A deterministic model for Olympic Sprint kayaking. *Journal of Sports Sciences*, 32(Suppl. 1), s107.

USING INERTIAL SENSORS FOR RECONSTRUCTING 3D FULL-BODY MOVEMENT IN SPORTS – POSSIBILITIES AND LIMITATIONS ON THE EXAMPLE OF ALPINE SKI RACING

Benedikt Fasel¹, Jörg Spörri², Josef Kröll², Erich Müller², and Kamiar Aminian¹

Laboratory of Movement Analysis and Measurement, Ecole Polytechnique Fédérale de Lausanne, Lausanne, Switzerland¹

Department of Sport Science and Kinesiology, University of Salzburg, Hallein-Rif, Austria²

The present study investigates if inertial sensors could be used for reconstructing 3D full body movements in sports. On the example of alpine ski racing, it was demonstrated that inertial sensors allow computing meaningful parameters related to a skier's overall posture. While some parameters were obtained with sufficient accuracy and precision, others were not obtained reliably using inertial sensor-based systems. Main error sources were discussed and it was found that an accurate and precise functional calibration is most important for short duration measurements. In cases where it is not possible fixing inertial sensors to all relevant body segments (e.g. skis and arms) their orientations could be estimated. In this case parameter validity needs to be carefully verified, as even strongly related parameters may show different validities, as demonstrated in this study.

KEY WORDS: inertial sensors, validation, centre of mass, alpine skiing, fore-aft position, vertical distance, posture.

INTRODUCTION: In sports, motion capture is a key tool for a dynamic posture analysis and may provide essential information for efficient coaching. In alpine ski racing, for example, the skier's dynamic posture during a turn is commonly analysed using specific aspects of vertical and anterior/posterior movement (Kipp et al., 2008; Reid, 2010): (1) $d_{CoM-ankle}$, the distance between the skier's centre of mass (CoM) and the ankle joint of the outside leg; (2) $p_{fore-aft}$, the projection of the outside leg's ankle-CoM vector onto the outside ski's longitudinal axis (Fig. 1). Furthermore, these variables have been suggested to be related to performance (Kipp et al., 2008; Läubli et al., 2014; Reid, 2010) and are specifically trained on different athlete levels (Läubli et al., 2014).

Traditionally, motion capture is performed using video-based 3D kinematics, as this method is known to provide the highest possible accuracy under field conditions (Reid, 2010). Alternatively, in recent days inertial measurement units (IMU) composed of accelerometers, gyroscopes and magnetometers have been used (Chardonens et al., 2012; Fasel et al., 2013). IMUs allow measuring an unlimited capture volume and data processing can be fully automatized. However, unlike the method of video-based 3D kinematics, IMUs do not allow a direct measurement of the skier's posture. Finding a posture based on IMUs involves the following three processing steps: 1) obtain sensor orientation through integration of inertial signals, 2) relate sensor orientations to segment orientations using functional calibration movements, and 3) estimate posture from the individual segment orientations using biomechanical models. Each of these three steps may induce errors in the final posture estimation. The five most important error sources are the following: i) drift in the sensor orientations from the integration of the inertial signals, ii) bias in the alignment sensor frame – segment anatomical frame because of inaccuracies from the functional calibration movements, iii) soft tissue artefact from muscle contractions and wobbling changing temporarily the sensor frame – segment anatomical frame alignment, iv) errors in the interpolation of segment orientations that were not directly measured, and v) inaccuracies in the underlying biomechanical model for posture estimation. Since all of these errors might be amplified when applying higher sophisticated or model-based algorithms, it is important to know the impact of each error source on specific parameter outcomes.

In order to illustrate this methodological challenge and to emphasise the importance of a careful, sport-/ and parameter-specific in-field validation prior using IMUs, the aims of the current study were the following: first, it was to compute $d_{CoM-ankle}$ and $p_{fore-aft}$ based on inertial measurements and to validate these ski racing specific parameters using a video-based reference system. Second, it was to discuss the impact of the above cited error sources on the parameter validity.

METHODS: Six European Cup level alpine ski racers were selected for the study. Two runs per athlete on a 12 gate giant slalom course were recorded. Gates were set with a constant gate distance of 27.2m and offset of 8m where the left turn of gate 7 was analysed. The study was approved by the University Ethics Committee of the Department of Sport Science and Kinesiology at the University of Salzburg.

Seven IMUs (Physilog[®] III, GaitUp, Switzerland; 3D accelerometers, 3D gyroscopes, sampling rate 500Hz) were fixed to the skier's helmet, sacrum, sternum, left and right thigh, and left and right shank using a custom underwear suit. Squat movements and upright standing posture were used for the functional calibration (Chardonens et al., 2012; Fasel et al., 2013). Strapdown integration with gravity drift and joint drift correction adapted from (Dejnabadi et al., 2006; Favre et al., 2006) was used to estimate each segment's orientation. A seven segment (head, upper trunk, lower trunk, left and right thigh, and left and right shank) and eight ball joint (neck, trunk centre, left and right hip, left and right knee, and left and right ankle) body model was used for pose estimation. The segment lengths were obtained from the video-based reference system described below. Segment inertia parameters and body CoM were obtained according to Dumas et al. (2007). Left and right arm centre of mass was hypothesized to lay 5cm anterior and 10cm inferior of the trunk centre. The ski's longitudinal axis was fixed perpendicular to the shank's medio-lateral anatomical axis and 17 degrees rotated with respect to the shank's anterior-posterior anatomical axis. Feet and skis were ignored for the computation of the body centre of mass. ${}^{imu}d_{ankle-CoM}$ was defined as the norm of ${}^{imu}v_{ankle_CoM}$, the vector relying the outside leg's ankle joint centre with the body CoM. ${}^{imu}p_{fore-aft}$ was defined as the length of ${}^{imu}v_{ankle_CoM}$ projected onto the ski's longitudinal axis (Fig. 1).

Six panned, tilted and zoomed HDV cameras recording at 50Hz were used as a reference system to record joint centres' positions over one turn cycle (left turn) as described in (Gilgien et al., 2015). An electronic trigger was used to synchronize the cameras with the inertial sensors. The ski's longitudinal axis was defined as the vector relying the ski's tail and tip. ${}^{ref}d_{ankle-CoM}$, and ${}^{ref}p_{fore-aft}$ were defined the same way as for the wearable system. The curves for ${}^{imu}d_{ankle-CoM}$ and ${}^{imu}p_{fore-aft}$ were low-pass filtered and resampled to 50Hz to match the sampling rate of the reference system. All data were time normalized prior to computing mean curves and errors. Accuracy (precision) was defined as the mean (standard deviation) of the difference between the curves of the wearable and reference systems.

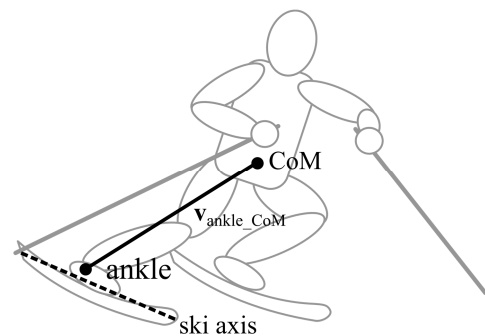


Figure 1: Illustration of the athlete's center of mass (CoM), ankle joint, ski axis and v_{ankle_CoM} , the vector connecting the ankle with CoM.

RESULTS: Accuracy and precision of ${}^{imu}d_{ankle-CoM}$ were -0.65cm and 2.67cm, respectively. For ${}^{imu}p_{fore-aft}$ accuracy and precision were -5.02cm and 4.03cm, respectively. Fig. 2 and 3 show the mean curves and standard deviations for all the twelve turns. From a purely descriptive perspective, it can be seen that ${}^{imu}d_{ankle-CoM}$ and ${}^{ref}d_{ankle-CoM}$ had a similar shape. ${}^{imu}p_{fore-aft}$ and ${}^{ref}p_{fore-aft}$ did not only have a curve offset but a different shape: the range for ${}^{imu}p_{fore-aft}$ was smaller than for ${}^{ref}p_{fore-aft}$. The peak at around 25% of turn cycle was less pronounced in the wearable system than the reference. The peak at around 85% of turn cycle was not present in the wearable system.

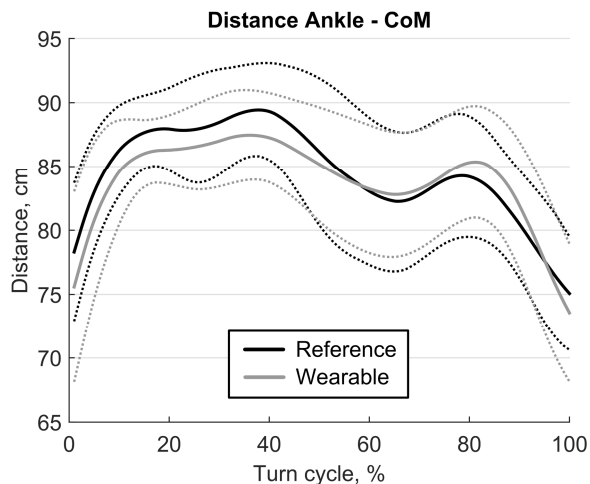


Figure 2: Mean curves (solid lines) \pm standard deviation (dotted lines) for the distance ankle-CoM. The reference system is shown in black; the wearable system is shown in grey.

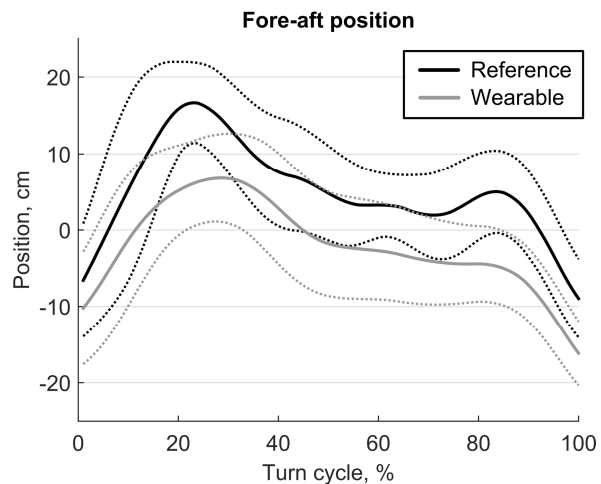


Figure 3: Mean curves (solid lines) \pm standard deviation (dotted lines) for the fore-aft position. The reference system is shown in black; the wearable system is shown in grey.

DISCUSSION: For twelve turns in giant slalom skiing, ankle-CoM distance, $d_{ankle-CoM}$, and fore-aft position, $p_{fore-aft}$, were computed using a wearable IMU system and compared to a video-based reference. Mean differences of $d_{ankle-CoM}$ of 2cm and range of motion differences of 8cm have been reported for two different course settings in slalom skiing (Reid, 2010). Additionally, the same study reported different mean curve shapes between the two course settings. ${}^{imu}d_{ankle-CoM}$ would allow measuring the same differences: mean curve differences could be measured as long as they are larger than the system's precision (2.67cm). Curve shape differences (e.g. range of motion) could also be found, as ${}^{imu}d_{ankle-CoM}$ was well correlated to ${}^{ref}d_{ankle-CoM}$ (Pearson's correlation coefficient of 0.89). Therefore, it can be concluded that $d_{ankle-CoM}$ can be computed with sufficient accuracy and precision using IMU-based systems.

In contrast to ${}^{imu}d_{ankle-CoM}$, ${}^{imu}p_{fore-aft}$ may not be accurate and precise enough. A case study by Spörri et al. (2015) reported differences in the order of 5-10cm for the fore-aft position for the second half of the turn. Larger horizontal gate offsets led to a less pronounced forward position. As ${}^{imu}p_{fore-aft}$ was underestimated and missed the peak at 85% turn cycle in the current study, the validity for analysing the absolute fore-aft position values might not be considered sufficient when using the IMU-based approach. However, ${}^{imu}p_{fore-aft}$ may still give valuable partial information about the fore-aft position of the athlete when comparing different dependent interventions: as all twelve turns were the same, the curves of individual turns must be similar. Indeed, the coefficient of multiple correlation (adapted from Kadaba et al., 1989) was higher for the wearable IMU system (0.66) than for the video-based reference system (0.35), indicating that the wearable IMU system was able to measure the parameter with a good repeatability.

Relating the results of ${}^{imu}d_{ankle-CoM}$ and ${}^{imu}p_{fore-aft}$ to the error sources cited in the introduction, the following can be concluded: i) the drift in orientation from integration of inertial signals did not impact the results substantially because of the short measurement period (<30sec). For longer measurements results should be critically inspected for drift. In the presence of drift, the curves' shapes would show a higher variability between trials; ii) the functional calibration plays an important role for the correct computation of the segment's orientation. For both ${}^{imu}d_{ankle-CoM}$ and ${}^{imu}p_{fore-aft}$ some outlier curves were observed and could be related to inaccurate functional calibration; iii) the present setup did not allow quantifying the effect of soft tissue artefacts on the computed parameters: its impact remains unclear; iv) the interpolation of unknown segment orientations (e.g. arms and skis) did most likely affect ${}^{imu}p_{fore-aft}$. Already small arm movements might have a considerable influence on the CoM with regards to its

fore-aft position, while their influence on the vertical position of CoM remains small. The relative orientation of the skis with respect to the shanks may not be fixed as ski boots may allow minor ankle flexion. Hence, these two effects could serve as an explanation for the attenuated peak in ${}^{imu}p_{fore-aft}$ at 25% and 85% of the turn cycle; v) inaccuracies in the underlying biomechanical model could be assumed to play only a minor role as other error sources were much larger. Joint rotation was not restricted to natural range of motion (e.g. for removing soft tissue artefact) which could be an error source. However, restrictions of joint rotations may be problematic, especially if the joint model does not fit the reality well.

CONCLUSION: The current study has illustrated the possibilities and limitations of using IMUs for reconstructing 3D full-body movement on the example of alpine ski racing. Two variables, which are commonly used to analyse vertical movement ($d_{ankle-CoM}$) and anterior/posterior movement ($p_{fore-aft}$) in research and coaching practice, have been computed. The validity of ${}^{imu}d_{ankle-CoM}$ has been demonstrated. However, ${}^{imu}p_{fore-aft}$ seemed not to provide enough precision for a full quantification of the fore-aft position. As this example demonstrates, knowing the impact of each error source is essential before applying more sophisticated or model-based algorithms as they might amplify certain errors. In this context, the use of simple algorithms has been demonstrated to be helpful for understanding and separating different error sources. Moreover, the current study has emphasised the importance of sport and parameter specific in-field validated algorithms: while one parameter might be valid (e.g. $d_{ankle-CoM}$), a closely related parameter (e.g. $p_{fore-aft}$) may not be valid. Nevertheless, once these methodological aspects have been carefully assessed, IMUs might open a broad spectrum of new possibilities for reconstructing 3D full-body movement in sports, particularly for in-field conditions.

REFERENCES:

- Chardonens, J., Favre, J., Le Callennec, B., Cuendet, F., Gremion, G., & Aminian, K. (2012). Automatic measurement of key ski jumping phases and temporal events with a wearable system. *Journal of Sports Sciences*, 30(1), 53–61.
- Dejnabadi, H., Jolles, B. M., Casanova, E., Fua, P., & Aminian, K. (2006). Estimation and visualization of sagittal kinematics of lower limbs orientation using body-fixed sensors. *IEEE Transactions on Bio-Medical Engineering*, 53(7), 1385–93.
- Dumas, R., Chèze, L., & Verriest, J.P. (2007). Adjustments to McConville et al. and Young et al. body segment inertial parameters. *Journal of Biomechanics*, 40(3), 543–53.
- Fasel, B., Spörri, J., Chardonens, J., Gilgien, M., Kröll, J., Müller, E., & Aminian, K. (2013). 3D measurement of lower limb kinematics in alpine ski racing using inertial sensors. *Abstract book international congress on science and skiing 2013*.
- Favre, J., Jolles, B.M., Siegrist, O., & Aminian, K. (2006). Quaternion-based fusion of gyroscopes and accelerometers to improve 3D angle measurement. *Electronics Letters*, 42(11), 612.
- Gilgien, M., Spörri, J., Chardonens, J., Kröll, J., Limpach, P., & Müller, E. (2015). Determination of the centre of mass kinematics in alpine skiing using differential global navigation satellite systems. *Journal of Sports Sciences*.
- Kadaba, M.P., Ramakrishnan, H.K., Wootten, M.E., Gaine, J., Gorton, G., & Cochran, G. V. (1989). Repeatability of kinematic, kinetic, and electromyographic data in normal adult gait. *Journal of Orthopaedic Research*, 7(6), 849–60.
- Kipp, R.W., Reid, R.C., Gilgien, M., Moger, T., Tjorhom, H., Haugen, P., & Smith, G. (2008). Slalom Performance in Elite Alpine Ski Racing can be Predicted by Fore / Aft Movement Dynamics. *Medicine and Science in Sports and Exercise*, 40(5), S165.
- Läuppi, P. & Spörri, J. (2014). *Ski Alpin Racing Concept*. Muri bei Bern: Swiss-Ski.
- Reid, R.C. (2010). A kinematic and kinetic study of alpine skiing technique in slalom. *Dissertation from the Norwegian School of Sport Sciences*.
- Spörri, J., Kröll, J., Schwameder, H., Schiefermüller, C., & Müller, E. (2012). Course setting and selected biomechanical variables related to injury risk in alpine ski racing: an explorative case study. *British Journal of Sports Medicine*, 46(15), 1072–7.

CHARACTERISTICS OF ELITE SWIM TURN PERFORMANCES

Bruce R. Mason^{1,2}, Gina Sacilotto¹, Pendar Hazrati¹ and Colin Mackintosh²
Australian Institute of Sport, Canberra, Australia¹
The Appsen Company, Brogo, Australia²

It is generally undisputed that the turn is of paramount importance in distance and middle distance competitive swimming. Accordingly, there is a need to identify the value of those parameters in the turn that are typical of international elite performance. This will be of vital importance in coaching, to assist swimmers to improve their performance in this aspect of competition. Using the Wetplate analysis system, many elite international swimmers were analysed performing a turn. Selected parameters for elite freestyle, butterfly, backstroke and breaststroke swimming in both genders, that represented the superior turners in each group, were analysed to identify a value for these parameters. A Pearson product moment correlation statistic was also performed on the data to identify those parameters that were of most significant interest in performance enhancement.

KEY WORDS: swimming, competition, turn, analysis, elite, Wetplate

INTRODUCTION: The Australian Institute of Sport developed a unique analysis system called Wetplate in 2006, to analyse the start and turn performances of elite competitive swimmers in a training environment (Mason et al 2012). The system provided immediate computerised quantitative analysis of each swimmer's turn performance along with an above/below water video recording of the swimmer from the 5m mark going into the wall to the 10m mark going out from the wall. The quantitative information supplied for each trial included: overall time on the wall in s, the period the feet were in contact with the wall in s, the depth of the foot plant on the wall and under the water in m, the change in the horizontal velocity of the swimmer's CoG during the time on the wall in ms^{-1} , the peak power generated by the swimmer on the wall in watts/kg of body mass, the force generated against the wall in body weight (Bwt) at peak power output, the projected vertical thrust angle of the swimmer from the wall at peak power output in deg (-ve in a downward direction), the distance from the wall that maximum depth was reached in m, the actual depth of the swimmer at maximum depth in m, the distance from the wall at breakout in m as well as the following times. Time from the 5m mark until wall contact in s, time from wall contact until the 5m, 7.5m and 10m marks were reached in s. The body segment to determine body location in all measurements was the centre of the head. The criterion measure of turn performance was the time taken from the 5m mark travelling into the wall until the 10m mark was reached travelling out from the wall in s. The quantitative information provided by the Wetplate system is used by Australian national team coaching staff to objectively evaluate a swimmer's turns and provide feedback to enhance turn performance. In order for the coach to effectively assess a swimmer's turn technique, the coach must be provided with some suggested ideal parameter values associated with elite turn performance. This paper provides such information so that coaches, technicians and biomechanists are familiar with the biomechanical characteristics of elite swim turns.

METHOD: Since 2006 many of the Australian national swim team members as well as a large number of elite international swimmers have had their turn performances analysed using the Wetplate system. The swimmer's data used in this project was that of the quickest turn for the fastest turners in each stroke, as defined by the time taken from the centre of the head passing the 5m mark on the way into the wall until the centre of the head passed the 10m mark travelling out from the turn. Most of the swimmers whose data was used in this

research were at the level of finalists at world championships and Olympic swim meets. Several of the swimmers were actually world champions and gold medalists in Olympic competition. The data from nine to fourteen swimmers were utilised in each gender category and each of the four stroke categories to be included in the analysis. Most of the parameters were obtained from force measurements on the instrumented turning wall or from digitising the video images of the performance. Both the vertical and horizontal components of force were used to compute the projected angle of the swimmer's thrust when leaving the wall. These two components of force were used to determine the direction of the swimmer's thrust on the wall. Power is the product of force and velocity and both these were derived from the force transducers in the instrumented turn wall. Most of the other parameters were obtained from digitisation of points on the video image. The maximum depth reached and the distance of breakout from the wall in m was obtained from digitisation of the video image. Time at the start of the turn (5m out) (0.0s) and time to reach the 10m mark (in s) was obtained from stationary video cameras (50 fields/s) synchronised with the wall touch signal and located high on the pool wall and facing perpendicularly across the pool at the 5m and 10m mark out from the wall.

RESULTS The four summary tables below, list the turn parameter values obtained from the four swimming strokes. Tables 1 and 2 contain the data for males and table 3 and 4 for females. The tables include the mean value and the standard deviation value obtained for each parameter over all turns in the specific gender group. Group sizes were generally 10 in number but there were two with 9 and one with 14. The Pearson product moment correlation coefficient for each parameter is listed to indicate the relationship between that variable and the criterion variable which was Overall Turn Time. The correlation coefficient provides a good indication of the importance of that particular parameter variable to overall turn performance. As the criterion variable in this instance was the time to complete the turn, quicker turns were categorised by smaller numbers in the criterion variable. Correlation coefficient values may range from 1 to -1. The higher the absolute value of the correlation coefficient, the stronger the relationship between that of the parameter in question and the criterion variable.

Table 1
Turn parameter values obtained from the four swimming strokes for males (mean and SD)

Table 1 MALE		Touch to Off. Wall time (s)	Foot Contact Duration (s)	Foot Depth in Water (m)	Change in Velocity (m/s)	Peak Power (W/Kg)	Horz Force at Peak Power (Bwt)	Projection Angle Off Wall (Deg)
Freestyle	Mean	0.26	0.26	0.26	3.92	59.80	1.83	-10
	SD	0.03	0.03	0.06	0.48	12.30	0.25	6
n=11	r	0.01	0.01	-0.18	-0.01	0.08	0.27	0.09
Butterfly	Mean	1.21	0.30	0.31	4.13	64.60	1.93	-4
	SD	0.17	0.04	0.07	0.38	8.60	0.20	4
n=13	r	0.29	0.15	0.04	0.02	0.05	-0.08	-0.11
Backstroke	Mean	0.25	0.25	0.18	3.99	62.50	1.82	-14
	SD	0.04	0.04	0.08	0.20	6.50	0.20	5
n=9	r	0.69	0.69	-0.01	-0.05	-0.81	-0.91	-0.20
Breaststroke	Mean	1.18	0.29	0.32	3.98	58.20	1.73	-2
	SD	0.08	0.04	0.04	0.33	8.10	0.30	4
n=10	r	-0.36	-0.24	-0.89	-0.24	-0.35	-0.24	-0.27

Table 2

Turn parameter values obtained from the four swimming strokes for males (mean and SD)

Table 2 MALE		Dist to Max Depth (m)	Max Depth (m)	Breakout Distance (m)	Time. 5m to Touch (s)	Time. Touch to 5m (s)	Time. Touch to 10m (s)	Overall Turn Time 15m (s)
Freestyle	Mean	3.4	0.50	7.3	2.69	1.68	4.33	7.03
	SD	0.9	0.10	1.8	0.09	0.09	0.15	0.17
n=11	r	-0.02	0.26	-0.19	0.46	0.55	0.86	1.00
Butterfly	Mean	5.9	0.81	11.9	2.58	2.62	5.40	7.98
	SD	1.7	0.22	1.3	0.10	0.09	0.13	0.21
n=13	r	-0.27	0.24	-0.25	0.85	0.67	0.91	1.00
Backstroke	Mean	5.6	0.97	12.2	3.03	1.76	4.65	7.57
	SD	0.9	0.17	2.0	0.13	0.10	0.57	0.37
n=9	r	-0.11	-0.57	-0.76	0.72	0.54	0.79	1.00
Breaststroke	Mean	5.4	0.93	9.3	3.22	2.82	6.50	9.72
	SD	0.7	0.14	1.0	0.14	0.09	0.21	0.29
n=10	r	-0.24	-0.10	-0.05	0.72	0.62	0.89	1.0

Table 3

Turn parameter values obtained from the four swimming strokes for females (mean and SD)

Table 3 FEMALE		Touch to Off. Wall time (s)	Foot Contact Duration (s)	Foot Depth in Water (m)	Change in Velocity (m/s)	Peak Power (W/Kg)	Horz Force at Peak Power (Bwt)	Projection Angle Off Wall (Deg)
Freestyle	Mean	0.27	0.27	0.24	3.66	52.30	1.69	-12
	SD	0.02	0.02	0.06	0.29	6.20	0.16	4
n=10	r	0.10	0.10	-0.09	-0.36	-0.44	-0.22	-0.02
Butterfly	Mean	1.15	0.31	0.28	3.82	50.00	1.53	-5
	SD	0.09	0.02	0.05	0.30	6.30	0.13	5
n=10	r	0.44	-0.42	0.37	-0.65	-0.61	-0.28	0.51
Backstroke	Mean	0.28	0.28	0.19	3.66	49.40	1.56	-14
	SD	0.05	0.05	0.07	0.44	6.80	0.16	3
n=9	r	0.33	0.33	-0.71	0.26	0.11	-0.29	-0.28
Breaststroke	Mean	1.26	0.30	0.31	3.57	45.60	1.52	-2
	SD	0.11	0.05	0.08	0.61	9.70	0.13	5
n=10	r	0.20	-0.60	0.17	-0.31	-0.27	0.02	0.09

Table 4

Turn parameter values obtained from the four swimming strokes for females (mean and SD)

Table 4 FEMALE		Dist to Max Depth (m)	Max Depth (m)	Breakout Distance (m)	Time. 5m to Touch (s)	Time. Touch to 5m (s)	Time. Touch to 10m (s)	Overall Turn Time 15m (s)
Freestyle	Mean	3.3	0.61	7.5	3.03	1.97	4.98	8.00
	SD	0.7	0.15	1.3	0.11	0.09	0.14	0.21
n=10	r	-0.51	-0.44	-0.43	0.80	0.48	0.88	1.00
Butterfly	Mean	3.8	0.60	8.8	2.87	2.88	6.03	8.90
	SD	0.8	0.15	2.3	0.11	0.18	0.32	0.39
n=10	r	0.10	-0.51	-0.54	0.75	0.90	0.98	1.00
Backstroke	Mean	4.7	0.87	10.8	3.41	2.08	5.27	8.68
	SD	0.7	0.15	0.9	0.12	0.12	0.22	0.24
n=9	r	0.08	0.28	-0.20	0.39	0.87	0.92	1.00
Breaststroke	Mean	4.7	0.76	8.5	3.35	3.08	7.01	10.36
	SD	0.6	0.11	0.6	0.20	0.13	0.37	0.45
n=10	r	0.58	0.23	-0.33	0.59	0.62	0.90	1.00

The table cells marked in yellow denote at least a 0.2 significance level: two tailed/non/directional. Those cells that denote the swimmer's times before and after the wall touch are obviously likely to be related to overall turn time. However the other related parameter values, that occurred particularly in the form strokes, provide some insight as to the importance of specific parameters to turn performance. Overall there are not many significant correlations in these tables and this is probably due to the fact that each group of swimmers was very much at a homogeneous elite level resulting in most of the parameters having little variability within the subject cohort.

CONCLUSION: The descriptive statistics derived from this study are able to be used by coaches, swimmers and technicians to identify strengths and weaknesses of particular swimmer turn performances. Without such information it is difficult to ascertain where a swimmer should concentrate their efforts to improve performance when working with the Wetplate and other swim start analysis systems such as the new Kistler Pas-S Analysis system. Coaches often require such information when working with swimmers without the use of an analysis system, just to visualise how the swim turn should be performed. The Pearson product moment correlation coefficients in the data tables provide information concerning an indication of the general importance that the particular parameter has to the overall performance of a turn. A similar paper based on the parameters that influence start performance was presented at ISBS2014 (Mason et al 2014). This data in this paper should also dispel many coaching myths about turn performance.

REFERENCES:

Mason, B.R., Mackintosh, C., & Pease, D. (2012) The Development of an Analysis System to Assist in the Correction of Inefficiencies in Starts and Turns for Elite Competitive swimmers. Paper presented at the *30th International Society of Biomechanics in Sports Conference*, Melbourne, Australia

Mason, B.R., Franco, R., Sacilotto, G and Hazrati, P. (2014) Characteristics of Elite Swim Start Performances. Paper presented at the *32nd International Society of Biomechanics in Sports Conference*, Johnson City, USA

INFLUENCE OF TRADITIONAL AND NON-TRADITIONAL ENTRIES ON FIGURE SKATING JUMPS

Bryanna L. Nevius and Pamela J. Russell

**Movement Arts, Health Promotion, and Leisure Studies Department at
Bridgewater State University, Bridgewater MA, United States of America**

The choice of performing jumps from traditional entries or nontraditional entries are left to the discretion of the skater. The purpose of this study was to examine the influence of non-traditional entries on the kinematics of two figure skating jumps using a simple quantitative tool available to coaches. It was hypothesized that non-traditional entries would alter jump kinematics. Ten skilled figure skaters were videotaped while performing toe loops or salchows with both traditional and non-traditional entries. Kinematic variables were determined with Dartfish. Results indicated that non-traditional entries had significantly more jump height and ankle plantar flexion at landing in the toe loop, and significantly more horizontal displacement in the salchow. Coaches may wish to examine these subtleties to determine a skater's readiness to practice non-traditional entries.

KEY WORDS: angular position, Dartfish, jump height, linear displacement

INTRODUCTION: Jumping is a basic movement that children master fairly quickly as they grow (Haywood, 1993). Jumping is also a valuable skill in many sports such as gymnastics, track and field, and figure skating. The United States Figure Skating Association dictates that three of the required elements in the ladies short program be jump elements, and a maximum of seven of the required elements in the ladies long program also be jumps (USFSA, 2013). These requirements essentially make up more than half of the elements in both the ladies short and long programs. Since jumping is such an important factor in a figure skating program, a great deal of emphasis is placed on the skater's performance of their jump elements. Over the years, judges have also started to reward skaters for making a traditional jump more difficult. Skaters receive more points for a jump with a difficult entry than they would receive for the same jump with a traditional entry (USFSA, 2013). With the creative freedom that skaters have in determining their jump entry and the incentive of extra points, more often than not a skater will perform a more difficult version of a traditional jump by selecting a non-traditional entry to earn more points (USFSA, 2013). However, this trend may become a cause for concern if skaters are not proficient at their non-traditional jump entries, yet they include them in the program in hopes that they will earn extra points anyways. Thus the purpose of this study was to examine the influence of non-traditional entries on the kinematics of two figure skating jumps using a simple quantitative tool available to amateur coaches. It was hypothesized that non-traditional entries would alter jump kinematics. Findings might help coaches examine readiness for non-traditional entry attempts.

METHODS: Ten female figure skaters volunteered for the study. All skaters were able to perform both double salchows and double toe loops proficiently from a traditional take off and a non-traditional take off. Skaters, or their parent, signed a University approved consent form. Data collection took place at several skating rinks. Upon arrival at the rink, skaters completed a short demographic survey then placed joint markers on the lateral aspects of both legs at the hip, knee and ankle joints under the direction of the researcher. While skaters took 20 minutes to warm up, cameras were placed at mid ice in the hockey box to capture the toe loop trials (Cannon ZR960) and at the end of the ice rink to capture the salchow trials (Sony Cybershot DSC-S750). One skater performed a double salchow and a double toe loop in front of the cameras to verify that the field of view captured the entire jump. The spot on the ice where she initiated her jump was marked with permanent marker to show the other skaters where they should also initiate their jumps. Five trials of each skater's self-selected jump, double salchow or double toe loop with a traditional entry, were

filmed first, followed by five trials of the same jump with a non-traditional entry. In total one hundred trials were filmed. Trials that contained falls or step outs were excluded, leaving 43 trials for analysis (21 toe loops; 22 salchows). Data from both cameras were analyzed at 60 Hz using DartFish ProSuite (version 6.0). In each trial with both traditional and non-traditional entries, ankle, knee, and hip joint angles were determined at take-off and landing. Take-off position for the toe loop was defined as the last backward movement where both feet were still in contact with the ice and the take-off position for the salchow was defined as the last backward movement when the full blade was in contact with the ice. After calibration using each skater's height, maximum jump height, airtime, and horizontal displacement were also determined. Jump height was determined by subtracting the skater's height from her greatest vertical displacement from the surface of the ice. Horizontal displacement was calculated as the distance from the moment the skater's blade left the ice at take off to the moment the toe-pick first made contact with the ice at landing. Airtime was defined as the time between take-off and landing, when the skater's blade left the ice to when it first landed on the ice again. Paired samples t-tests compared the ankle, knee and hip angles at take-off and at landing, maximum jump height, airtime, and horizontal displacement between traditional and non-traditional entries for all jumps, just toe loops, and just salchows. Significance was set at .05 and a Bonferonni correction was used as needed.

RESULTS: The skaters that completed the study had a mean age of 15.2 (3.7) years, were 1.5 (.09) m tall, weighed 447 (90.2) N and had 10.2 (3.6) years of skating experience. Comparison of the take-off angles for the hip, knee and ankle joints showed no significant differences between traditional and non-traditional entries (Table 1). Across all jumps, ankle ($p=.023$) and hip joint ($p=.028$) angles approached significance. At take-off the ankle was more plantarflexed and the hip was slightly more extended for non-traditional entry trials compared to traditional entry trials (Table 1)

Table 1
Take-off Angles for Traditional (T) and Non-Traditional (NT) Entries

Jump	Ankle T	Ankle NT	Knee T	Knee NT	Hip T	Hip NT
Toe Loop	83.6±10.6	86.6±8.9	126.6±18.1	128.8±19.2	127.8±21.1	135.5±28.6
Salchow	79.8±12.0	82.5±6.1	125.9±5.8	122.7±7.83	126.9±8.1	129.2±13.5
All Jumps	81.8±11.3	84.5±7.8	126.3±13.6	125.7±14.7	127.4±16.1	132.3±22.1

Note: measures in degrees; Traditional=T; Non-Traditional=NT; Bonferroni Correction $p<.005$

Across both jumps ($p=.001$) and for the toe loop ($p=.0005$) there was a difference in maximum jump height. Non-traditional entries showed significantly more height (Table 2). In the salchow, the non-traditional entry provided for significantly more ($p=.001$) horizontal displacement than the traditional entry (Table 2)

Table 2
Flight Characteristics for Traditional (T) and Non-Traditional (NT) Entries

Jump Type	Max Jump Height T (m)	Max Jump Height NT (m)	Airtime T (s)	Airtime NT (s)	Horizontal displacement T (m)	Horizontal displacement NT (m)
Toe Loop	0.33±.13*	.46±.171*	.62±.07	.63±.11	1.31±.53	1.04±.17
Salchow	.38±.14	.43±.117	.78±.12	.77±.09	1.56±.64*	1.83±.72*
All Jumps	.36±.14*	.44±.145*	.69±.12	.70±.12	1.43±.59	1.45±.66

*Significant difference $p= <.005$

At landing there were significant differences in the ankle angle across both jumps ($p=.001$) and for the toe loop ($p=.001$) (Table 3). Non-traditional trials showed greater plantar flexion at landing.

Table 3
Landing Angles for Traditional (T) and Non-Traditional (NT) Entries

Jump	Ankle T	Ankle NT	Knee T	Knee NT	Hip T	Hip NT
Toe Loop	83.9±12.5*	88.7±9.1*	135.1±6.3	135.8±7.9	129.5±14.4	136.1±14.7
Salchow	87.5±13.2	92.2±7.9	134.6±8.7	129.3±9.5	128.2±19.6	133.4±15.2
All Jumps	85.6±12.9*	90.5±8.6*	134.8±7.4	132.5±9.2	128.9±16.9	134.7±14.8

Note: All measures in degrees; Traditional=T Non-Traditional=NT; *= Significant difference at $p < .005$.

DISCUSSION: The purpose of this study was to examine the influence of non-traditional entries on the kinematics of two figure jumps using a simple quantitative tool available to amateur coaches. As hypothesized non-traditional entries altered jump kinematics.

There were no statistically significant differences between traditional and non-traditional entries in the ankle, knee and hip joint angles at take-off, but across both jumps non-traditional jump entries tended to produce slightly more plantar flexion and hip extension. These tendencies could indicate that with non-traditional entries skaters are slightly further along in the jumping motion at takeoff, executing the extension phase of the jump already, or perhaps skaters took less time to perform the preparatory flexion motions associated with jumping. Traditional entries may constrain the take-off position, thus the skater's preparation for and execution of the jump. The knee and other joints contribute to successful completion of the jump and the success of the landing (Johnson & King 2001), thus these tendencies should be further investigated to determine how they might influence other aspects of the jump and the skater's readiness for non-traditional entries.

Comparison of flight parameters indicated that, especially for the toe loop, maximum jump height was greater with a non-traditional as opposed to a traditional entry. For the salchow, the non-traditional entry provided for greater horizontal displacement than the traditional entry. The non-traditional entry may have allowed skaters to emphasize technique differences in these jumps. To perform a toe loop from either a traditional and a non-traditional entry, the skater applies most of their weight on their favored leg and places the toe-pick of their free leg into the ice, which helps to propel them into the air. Use of the toe pick slows the horizontal aspect of the jump and permits increased vertical motion (King, 2000). The salchow is an edge jump, thus the toe-pick is not utilized at all during take-off, which allows for more horizontal movement (King, 2000). In each jump the increases could be due to lack of technical limitations associated with the traditional take-off position (USFSA, 2013). Non-traditional entries may be more effective at providing for greater height in the toe loop and greater horizontal distance for edge jumps. If coaches can detect these subtle differences with a simple quantitative tool, they could make more informed decisions about skaters' readiness for non-traditional entries.

During the landing phase the ankle showed greater plantar flexion during nontraditional entries when compared to traditional entries, especially for the toe loop jumps. Increased plantarflexion could be related to the increased jump height associated with toe loops done with non-traditional entries. Also skaters may not be as far into the lower extremity flexion sequence associated with landing if they jumped higher. Non-traditional entries seem to allow a less structured technique throughout the jump because skaters do not have to start in a specific take-off position. Landing a jump is very important to the skater, thus the mechanics of the landing should be carefully considered as non-traditional entries are attempted.

CONCLUSION: The purpose of this study was to examine the influence of non-traditional entries on the kinematics of two figure skating jumps using a simple quantitative tool available to coaches. Results indicated that non-traditional entries had significantly more jump height and ankle plantar flexion at landing in the toe loop, and significantly more horizontal displacement in the salchow. Detecting these increases in jump height and horizontal displacement may be important for coaches as they could influence a skater's

readiness to focus their practice on non-traditional entries. These differences could make the entire jump, take-off through landing, more difficult to control, or they could give a skater an opportunity to add complexity to their jump. Coaches may wish to examine these subtle jump characteristic differences with a simple video analysis tool to determine a skater's readiness to practice non-traditional entries. The findings of this research could be further supported through a larger sample size as well as through acquiring the score given to the jump from an accredited figure skating judge. This would allow further insight into which jump take-off is more effective at earning more points from the perspective of the skater and the coach.

REFERENCES:

Haywood, Kathleen M. (1993). *Life span motor development*. (2nd ed.). Champaign, IL: Human Kinetics. p. 135.

Johnson, M., & King, D. L. (2001). *A kinematic analysis between triple and quadruple revolutions figure skating jump*. University of California San Diego, CA: American Society of Biomechanics. Retrieved from <http://www.asbweb.org/conferences/2001/pdf/063.pdf>

King, D. L. (2000). Jumping in Figure Skating. *Biomechanics in Sport*, 9, 312-325.

United States Figures Skating Association. (2013, May 10). *Technical Info: Singles/Pairs*. Colorado Springs, CO: United Skates Figure Skating Association. Retrieved from http://www.usfsa.org/New_Judging.asp?id=355

Acknowledgement

I would like to acknowledge everyone who was a part of this research, especially the subjects, thesis committee members, and my mentor Dr Pamela Russell.

SPINAL MUSCLE ACTIVITY DURING DIFFERENT RUGBY SCRUM ENGAGEMENT PROCEDURES

Dario Cazzola¹, Benjamin Stone¹, Tim P. Holsgrove¹, Grant Trewartha¹ and Ezio Preatoni¹

Department for Health, University of Bath, UK¹

Biomechanical studies of rugby union scrummaging have focussed on kinetic and kinematic analyses, whilst muscle activation strategies employed by front row players during scrummaging are still unknown. The aim of this study was to investigate the activity of the sternocleidomastoid, upper trapezius and erector spinae muscles during machine and live scrums. Nine male front-row forwards scrummaged individually against a scrum machine under 'crouch-touch-set' and 'crouch-bind-set' conditions, and against a two-player opposition in a simulated live condition. Results suggest that the pre-bind technique, may effectively prepare the cervical spine by stiffening joints before the impact phase. Additionally, machine scrummaging does not replicate the muscular demands of live scrummaging for the erector spinae.

KEY WORDS: biomechanics, scrummaging technique, sport injury, cervical spine, EMG.

INTRODUCTION: Rugby scrummaging places intense biomechanical demands on players, particularly those playing in the front row. Due to its physical nature, the scrum is associated with approximately 6 to 8% of all rugby injuries (Trewartha et al., 2014), 40% of catastrophic injuries (Brown et al., 2013), and may lead to chronic degenerative spinal injuries. Machine and live scrummaging biomechanics have been described in terms of the forces generated and motions observed (Cazzola et al., 2014; Preatoni et al., 2014). From these investigations, the scrum has undergone a number of rule changes, most recently from a 'crouch-touch-set' (CTS, in 2012/2013) to a 'crouch-bind-set' (CBS, in 2013/2014) procedure, in an attempt to improve safety by de-emphasising the initial impact of the scrum engagement (Cazzola et al., 2014; Preatoni et al., 2014). Currently, no study has investigated the effects of rule and technique changes on spinal muscle activity. The analysis of neuromuscular activation patterns under different engagement conditions is fundamental to elucidate the strategies employed by front row players as they prepare their bodies for the engagement and pushing actions. The aim of this study was to determine the activity of the bilateral upper trapezius, sternocleidomastoid and erector spinae muscles under three scrummaging conditions; two machine scrummaging conditions, the 'crouch-bind-set' and 'crouch-touch-set' and a single live scrummaging condition were investigated

METHODS: In a repeated measures design, a group of rugby union front row forwards performed multiple trials in three different simulated scrummage conditions (within-group factor) and throughout the phases of scrummaging (within-group factor) to assess and compare spinal muscle activity (dependent variable). Nine male rugby union players (age 20.3 ± 1.3 year, height 1.80 ± 0.10 m, weight 102.36 ± 15 kg), of at least University 1st XV standard with a minimum of 3 years playing experience in the front row and no history of spinal injuries in the 12 months prior to testing, participated in the study.

Data collection: For electromyography (EMG) collection, six wireless electrodes (DelsysTrigno, DelsysInc), sampling at 2000 Hz, were attached to: the sternocleidomastoid, and upper trapezius accordingly to Sharp et al. (2014).

Two isometric maximal voluntary contractions (MVC) trials were performed for each muscle of interest. The three different engagement techniques: crouch-touch-set (CTS), crouch-bind-set (CBS) and live 1-versus-2 scrummaging (Live) were presented in a blocked random order. The machine scrummaging conditions involved a single participant engaging with an instrumented scrum machine using the CTS and CBS variants followed by a sustained push

(Preatoni et al., 2012). The live condition involved a single participant passively engaging, for safety reasons, with two other participants prior to the sustained push. A bespoke control and acquisition system was programmed to synchronously trigger the acquisition hardware, collect and store the forces measured through the instrumented scrum machine, and playback pre-recorded cues given by the referee (Preatoni et al., 2013). Muscle activity was measured for 10 s from 1 s prior to the “crouch” call.

Data Processing: Raw electromyograms were filtered by applying a bi-directional second-order Butterworth low pass and high pass filter between 20-200 Hz. The data were then rectified and smoothed using a moving average over 50 ms windows. EMG signals were normalised to the MVCs. Average muscle activity (average rectified EMG amplitude) during scrum trials was calculated over three phases of each scrum: the pre-engagement, the engagement and the sustained push phases.

Statistics: Separate one-way repeated measure analysis of variance (ANOVA) (with scrummage conditions as the within-group factor) and Bonferroni post-hoc analysis were applied (SPSS software, IBM Corp, USA) to determine if there were any differences ($p < 0.05$) in muscles' activation across scrummage conditions during the sustained push phase (CBS vs CTS vs Live). A paired t-test was performed to determine the differences in muscle activation in the pre-engagement phase (CBS vs CTS), and the engagement phase (CBS vs CTS), as Live engagement included only the sustained push phase. Further one-way repeated measure ANOVAs (with scrum phases as the within-group factor) were used to test possible changes in muscles activation across the different phases of the scrum for the CTS and CBS machine trials, followed by Bonferroni post-hoc comparisons ($p < 0.05$). Pairwise effect sizes calculated using Cohen's d_z statistic ($|d_z| > 1$ large effects; $|d_z| > 0.8$ moderate effects; $|d_z| > 0.5$ small effects) were also calculated.

RESULTS: Comparing Conditions: In the pre-engagement phase, all the measured muscles in both machine conditions were activated in excess of 25% MVC (Figure 1). The activity of the sternocleidomastoid and upper trapezius was significantly higher ($p < 0.01$) in the CBS condition than the CTS condition. The activity of the erector spinae tended to be more activated (large effect size, $d > 0.8$), although not significantly ($p > 0.05$), in the CTS condition during pre-engagement than the CBS condition. During the engagement phase all the measured muscles were more active in the CBS than CTS condition. The activity of the upper trapezius and sternocleidomastoid were significantly higher ($p < 0.05$ – paired t-test), showing an average increase of $20\% \pm 12\%$ and $22\% \pm 20\%$ respectively (Figure 1).

During the sustained push phase the activity of the muscles across all three conditions (CBS, CTS and Live) could be compared. The activity of the erector spinae during the sustained push phase was significantly higher in live scrummaging than in either of the CBS ($56\% \pm 26\%$ greater) or CTS ($62\% \pm 18\%$ greater) conditions ($p < 0.01$), with the erector spinae activity approximately $56\% \pm 26\%$ lower (CBS vs Live) and $62\% \pm 18\%$ lower (CTS vs Live). The activity of the upper trapezius tended to be lower in the CTS than in the CBS and Live conditions, whereas the activity of the sternocleidomastoid was similar across conditions.

Comparing across phases: The activity of the sternocleidomastoid and erector spinae showed a decreasing trend ($p < 0.05$) moving from pre-engagement through engagement to the sustained push in both the CBS and CTS conditions (Figure 1). The activity of the sternocleidomastoid was significantly higher during the pre-engagement and engagement phase than sustained push in CBS ($p < 0.05$), and in CTS pre-engagement tended to be higher than sustained push ($p = 0.059$). The activity of the erector spinae during both CBS and CTS conditions was significantly higher during both the pre-engagement phase ($p < 0.05$) and engagement phase ($p < 0.05$) when compared with the sustained push (Figure 1). There was a significant pattern of decreasing activation from i) pre-engagement to engagement and from ii) engagement to sustained push.

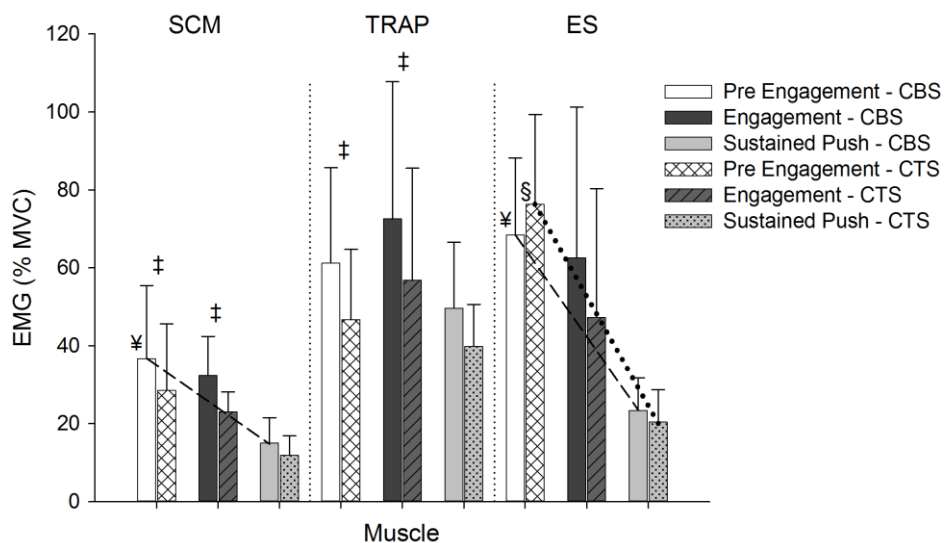


Figure 1: Normalised values (% MVC) of muscles activation (mean and SD) of sternocleidomastoid (SCM), upper trapezius (TRAP) and erector spinae (ES) during CBS and CTS engagements. Muscles activation during CBS and CTS engagements are shown throughout the three scrum phases: pre-engagement, engagement and sustained push. Live engagement is not included because in that condition EMG measures were carried out only during sustained push phase. The dashed and dotted lines show the muscles activation trend in respectively CTS and CBS, and are representative of the differences (ANOVA) between i) pre-engagement and sustained push and ii) engagement and sustained push. ‡ = significant difference between CBS and CTS ($p < 0.05$ – paired t-test); ¥ = significant difference between both i) pre-engagement and sustained push, and ii) engagement and sustained push in CBS ($p < 0.05$ - ANOVA); § = significant difference between both i) pre-engagement and sustained push, and ii) engagement and sustained push in CTS ($p < 0.05$ - ANOVA).

DISCUSSION: The aim of this study was to gain more insight into the activity of sternocleidomastoid, upper trapezius and erector spinae muscles during machine (CBS and CTS) and live scrummaging. Compared with the machine conditions, the live condition resulted in significantly higher activation of erector spinae during the sustained push phase. Also, the activity of sternocleidomastoid, upper trapezius and erector spinae tended to be greater during the CBS condition than the CTS condition throughout the three phases of the scrum. Spinal muscle activity in both machine scrummaging conditions was characterised by a considerable pre-activation of all 6 muscles ($>25\%$ MVC) prior to engagement. This pre-activation can functionally lead to an increase in cervical and lumbar spine stiffness, which may better prepare the player's spinal structures for the high biomechanical loads placed upon the spine during engagement. A high level of muscle pre-activation may potentially mitigate the effect of loads on spinal posture and help maintain optimal neutral spine position (Brooks & Kemp, 2011). However, the stabilisation of the spine due to high-level of muscles activation may not be enough to limit cervical spine hyperflexion or buckling mechanisms (Dennison et al., 2012) during catastrophic injury, and further analyses are needed to elucidate the actual contribution that muscle activations can make in certain high-risk loading conditions. The activity of the spinal muscles was comparable between the conditions and the activity of sternocleidomastoid and upper trapezius was found, in the engagement phase, to be significantly greater in the CBS condition. This pre-bind posture may effect spinal muscle activation, where greater upper trapezius and sternocleidomastoid activation increase cervical spine stiffness and may better maintain cervical spine posture during the engagement. This indicates that a pre-bind procedure makes the upper spine more prepared for the scrum engagement.

The activation of the erector spinae was significantly higher throughout the sustained push phase of the live scrummaging condition than either of the machine scrummaging conditions.

Live scrummaging is an unstable dynamic condition when compared with machine scrummaging, therefore the forces applied to the opposition players are not equally matched in direction or magnitude, as they are during a scrum against the machine. These findings demonstrate that although machine and live scrummaging show comparable kinematic and kinetic characteristics, machine scrummaging does not accurately replicate live scrummaging in terms of muscle activation strategies required to maintain the sustained phase. Thus, it can be suggested that front row players should be required to train in live situations and not only against scrum machines. Therefore, a relative increase in live scrummaging practise may be beneficial for all front row players from the perspective of training appropriate and specific neuromuscular activation patterns. This may be particularly important under current rugby practice since the duration of the sustained phase has markedly increased under the CBS engagement procedure.

CONCLUSION:In conclusion, the activation of selected spinal muscles is greater in the CBS condition than the CTS condition, particularly in the pre-engagement phase. This indicates that the muscles of the cervical spine, in the CBS condition, are better prepared for the forces experienced during the scrum engagement than in the CTS condition as cervical spine stiffness is greater. Furthermore, this research provides evidence that the erector spinae is significantly more active during live scrummaging than machine scrummaging. This reinforces the requirement for individuals to practise and learn scrum techniques in a live situation, rather than purely against a machine, as machine scrummaging does not replicate the demands of a live contest. Future research should build on the foundations of the current study, with the objectives of improving its ecological validity through trials on natural turf and in a more complete scrummaging scenario (a full front row or a complete pack) either against a scrum machine or in live conditions.

REFERENCES:

- Brooks JHM, Kemp SPT. Injury-prevention priorities according to playing position in professional rugby union players. *British Journal of Sports Medicine*. 2011; 45: 765-775.
- Brown JC, Lambert MI, Verhagen E, Readhead C, van Mechelen W, Viljoen W. The incidence of rugby-related catastrophic injuries (including cardiac events) in South Africa from 2008 to 2011: a cohort study. *BMJ open*. 2013; 3.
- Cazzola D, Preatoni E, Stokes KA, England ME, Trewartha G. A modified prebind engagement process reduces biomechanical loading on front row players during scrummaging: a cross-sectional study of 11 elite teams. *British Journal of Sports Medicine*. 2014;49:541-546.
- Dennison CR, Macri EM, Crompton PA. Mechanisms of cervical spine injury in rugby union: is it premature to abandon hyperflexion as the main mechanism underpinning injury? *British Journal of Sports Medicine*. 2012; 46: 545-549.
- Preatoni E, Stokes KA, England ME, Trewartha G. Engagement techniques and playing level impact the biomechanical demands on rugby forwards during machine-based scrummaging. *British Journal of Sports Medicine*. 2014; 49: 520-528.
- Trewartha G, Preatoni E, England ME, Stokes KA. Injury and biomechanical perspectives on the rugby scrum: a review of the literature. *British Journal of Sports Medicine*. 2014.

Acknowledgement

The project was funded by RFU Injured Players Foundation.

OPTIMUM TECHNIQUE FOR MAXIMISING FORWARD SOMERSAULT ROTATION IN TRAMPOLINING

Dave Burke, Fred Yeadon, and Mike Hiley

School of Sport, Exercise, and Health Sciences, Loughborough University,
Loughborough, UK

The purpose of this study was to investigate the optimal technique to produce somersault rotation in forwards rotating somersaulting skills. A 7-segment planar, torque-driven simulation model of a trampolinist was developed. The trampoline was represented by horizontal and vertical force-displacement relationships. The model was evaluated using recorded performances of three forward somersaulting skills. Optimised takeoff technique produced an increase of 9% in rotation potential using a more open shoulder angle and a greater initial horizontal velocity.

KEY WORDS: trampolining, takeoff, simulation, model, optimisation, torque-driven.

INTRODUCTION: During each contact phase in trampolining, the trampolinist must create the required linear and angular momenta to enable themselves to have sufficient flight time and angular velocity to complete the desired skill in the subsequent flight phase. In order to achieve maximum rotation a trampolinist must have both a large vertical velocity and possess a large amount of angular momentum at takeoff (King & Yeadon, 2004). The generation of both linear and angular momenta are dependent on the vertical reaction force acting on a trampolinist (Vaughan, 1980), and it has been shown that the production of vertical linear momentum and angular momentum require opposing movement strategies; the production of vertical linear momentum requires a straight body position (Cheng & Hubbard, 2004) whereas the creation of forwards rotation requires a piked position at takeoff (Lephart, 1972). The inter-related nature of the two primary factors in the production of somersault rotation makes the identification of an optimal technique a complex problem. This study aims to investigate the optimal technique to produce maximum forward somersault rotation through the simulation of the trampoline contact phase.

METHODS: A planar seven-segment computer simulation model of a trampolinist with eight torque generators (four extensor, four flexor) was developed to investigate the mechanics of the contact phase in trampolining. Segments represented the head and trunk, upper arm, lower arm, thigh, shank, and a two-segment foot. The foot-trampoline interface was modelled as linear horizontal and non-linear vertical force-displacement relationships acting at the heel, metatarsal-phalangeal (MTP) joint and toe. The total reaction force was distributed between three points on the foot based on the relative depressions of each point.

The movements of the ankle, knee, hip, and shoulder joint were driven by pairs of torque generators representing the extensors and flexors. The movements of the elbow were driven by joint angle time histories calculated from 3D automatic motion capture of trampoline performances. The MTP joint was driven by two angle-displacement relationships that governed the MTP joint angle in the depression and recoil phases of the contact.

The torque generators represented the properties of muscle and tendon as a rotational muscle-tendon complex comprising a contractile element and a series elastic element. The torque exerted about a joint was calculated as the product of an activation level and the maximum voluntary torque as defined by a nine parameter, torque-angle-angular velocity function (King *et al.*, 2006; Yeadon *et al.*, 2006).

Input to the simulation model comprised the initial orientation and joint angles and angular velocities, the initial position and velocity of the centre of mass, and the parameters governing the activation profile of each torque generator. The output of the model consisted

of the orientation and joint angle time histories, and the linear and angular momenta of the trampolinist throughout the movement and at takeoff.

The simulation model was customised to an elite trampolinist by determining subject-specific segmental inertia parameters (Yeadon, 1990) and scaling the parameters governing isometric strength of each pair of torque generators to appropriate effective strength levels (King *et al.*, 2009) from torque parameters measured from a gymnast and a triple jumper.

The simulation model was evaluated against three recorded performances of forward somersaults with varying amounts of rotation; a single straight somersault (F_1), a piked $1\frac{3}{4}$ somersault (F_2), and a piked triffus (F_3). Simulated annealing was used to minimise a cost function whilst varying sixty parameters comprising 56 parameters governing the joint activation profiles and four allowing adjustments to the initial orientation angle, horizontal and vertical velocity of the centre of mass, and shoulder angular velocity. The cost function was an RMS score given to each simulation quantifying the differences between the recorded performances and simulation in four areas: orientation and joint angles throughout the contact phase, orientation and joint angles at takeoff, duration of the contact phase, and the movement outcomes of horizontal and vertical linear momentum and angular momentum at takeoff. The components of the cost function were weighted so that one degree difference was equivalent to 1% difference in the measures of duration and momentum (Yeadon & King, 2002).

The simulation model was used to investigate optimal technique to maximise rotation potential in forward rotating somersaults. Rotational potential is a normalised product of angular momentum and flight time and is expressed as the number of somersaults the trampolinist would be capable of completing in a straight position. The optimisation procedure varied 57 parameters: 56 joint activation parameters and one parameter allowing adjustment to the initial horizontal velocity. Rotation potential was maximised whilst permitting travel (in the preceding and subsequent flight phases) up to a total of half the length of the jumping zone (1.075 m) and the full length of the jumping zone (2.15 m). Penalties were imposed on the simulations if they utilised joint movements beyond the limits of ranges of motion observed in the recorded performances or exceeded the permitted allowance of horizontal travel.

RESULTS & DISCUSSION: The simulation model was capable of providing a close match to the recorded performances of the trampolinist. On average the simulation model was able to match the performance to within 4.4%, with the individual trials matched to 3.2%, 4.8% and 5.3% for F_1 , F_2 , and F_3 respectively. The individual component scores are presented in Table 1.

Table 1
Cost function component scores resulting evaluation procedure

	Component Score						RMS (%)
	S_{RMS}	S_{ABS}	S_1	S_2	S_3	S_4	
F_1	2.7	1.5	0.2	1.3	0.2	0.0	3.2
F_2	4.1	1.2	1.4	2.8	0.1	3.0	4.8
F_3	4.9	1.2	1.7	2.2	1.2	0.6	5.3
Mean	3.9	1.3	1.1	2.1	0.5	1.2	4.4

S_1 – average RMS difference in orientation and configuration angles during contact ($^\circ$), S_2 - average difference in orientation and configuration angles at takeoff ($^\circ$), S_3 - percentage difference in horizontal linear momentum (%), S_4 - percentage difference vertical linear momentum (%), S_5 - percentage difference angular momentum (%), S_6 - percentage difference contact duration (%)

The level of agreement shown between the simulated and recorded performances was sufficient to allow investigation of optimum takeoff technique.

The piked triffus skill (F_3) performed by the trampolinist had a rotation potential of 1.74 straight somersaults, whilst travelling a total distance of 1.88 m. The optimum simulations produced an increase of 9% in rotation potential when permitted to travel 2.15 m (1L) and a

reduction of 2% when limited to a total travel of 1.075 m ($0.5L$). The simulation model was capable of producing 1.71 and 1.89 straight somersaults when permitted to travel half and the full length of the jumping zone respectively. The $0.5L$ solution achieved this in a longer flight time of 1.47 s compared to 1.42 s for $1L$. Figure 1 shows the optimal takeoff techniques alongside the technique used to perform F_3 in the evaluation of the simulation model.

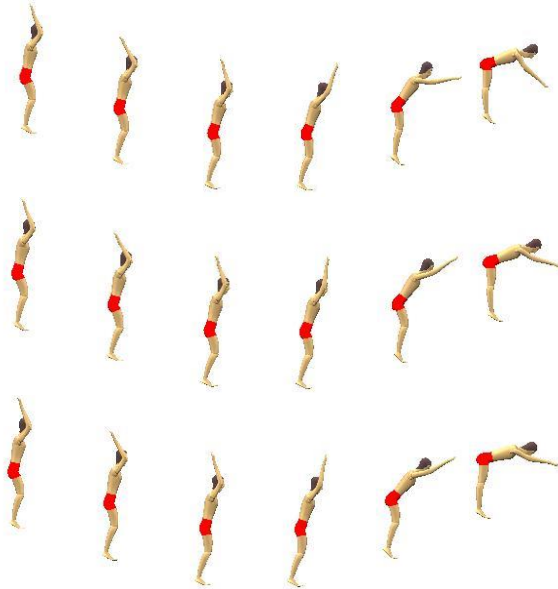


Figure 1: Comparison of torque-driven simulation of F_3 (top) and optimal technique to produce rotation potential for $0.5L$ (middle) and $1L$ (bottom).

The optimal techniques show greater flexion of the shoulders at takeoff, helping to produce angular momentum by moving the mass centre forward and increasing the moment arm of the vertical reaction force. During the recoil phase, the knee and hip both display greater flexion with $1L$ showing greater forward rotation with the hip in front of the ankle throughout.

The optimal techniques for $0.5L$ and $1L$ produced 1.00 m and 2.06 m of horizontal travel respectively, compared with 1.89 m for the recorded movement. The 47% decrease in horizontal travel for $0.5L$ was the result of a 4% increase in the travel in the preceding flight phase and an 87% decrease in the horizontal travel during the subsequent flight phase. $1L$ had a greater initial horizontal velocity, travelling 1.21 m before contact and 0.84 m afterwards. The initial horizontal velocity caused the model to rotate over the feet throughout the contact phase, promoting the production of angular momentum.

The differences in the optimal techniques were caused by differences in the activation profiles of the hip extensors and flexors, the knee extensors, and the ankle dorsi flexors, as well as a different horizontal velocity of the centre of mass at the beginning of the contact phase. The remaining joint torque activation profiles showed no significant differences between the two optimal techniques. The optimal solution for $0.5L$ decreased the initial horizontal velocity by 0.06 ms^{-1} whilst the solution for $1L$ increased the velocity by 0.10 ms^{-1} . Figure 2 shows the differences in the activation profiles. In $1L$, both the knee and hip extensors show a greater level of initial activation and a lesser maximum activation level in $1L$ than $0.5L$. The knee uses very similar activation timings but the hip extensor activation both increases to the maximum and decreases earlier than in $0.5L$. Both the hip flexor and dorsi flexor activation follow similar shapes but the activation of both is greater throughout in $1L$ and the difference constantly increases during the recoil phase.

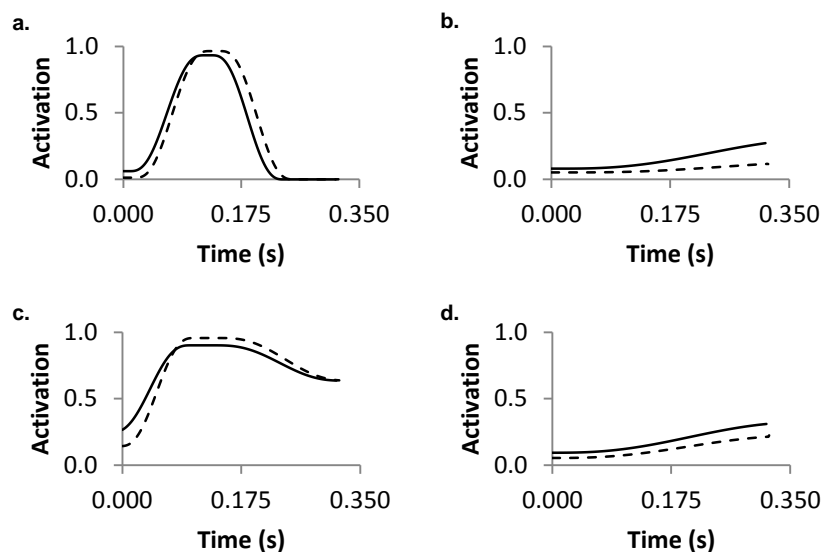


Figure 2: Activation profiles of (a) hip extensor (b) hip flexor (c) knee extensor (d) dorsi flexor

CONCLUSION: Optimal takeoff technique for maximal forward somersault rotation in trampolining was determined using a simulation model. The model utilised greater horizontal velocity of the centre of mass and greater flexion of the hips and shoulder to increase the moment arm of the vertical reaction force during the recoil phase. The larger moment arm enabled the increased production of angular momentum. A trade-off between flight time and angular momentum was seen but maintaining shoulder flexion helped to increase both of these. This knowledge can inform coaching practice through a better understanding of the use of the arms in forward somersaults.

REFERENCES:

Cheng, K.B. & Hubbard, M. (2004). Optimal jumping strategies from compliant surfaces: A simple model of springboard standing jumps. *Human Movement Science*, 23, 35-48.

King, M.A., Kong, P.W. & Yeadon, M.R. (2009). Determining effective subject-specific strength levels for forward dives using computer simulations of recorded performances. *Journal of Biomechanics*, 42, 2672-2677.

King, M.A. & Yeadon, M.R. (2004). Maximising somersault rotation. *Journal of Biomechanics*, 37, 471-477.

King, M.A., Wilson, C., Yeadon, M.R. (2006). Evaluation of a torque-driven model of jumping for height. *Journal of Applied Biomechanics*, 22, 264-274.

Lephart, S.A. (1972). A Mechanical analysis of forward somersaulting skills in rebound tumbling. *Unpublished Doctoral Thesis*. Ohio State University.

Vaughan, C.L. (1980). A kinetic analysis of basic trampoline stunts. *Journal of Human Movement Studies*, 6, 236-251.

Yeadon, M.R. (1990). The simulation of aerial movement--II. A mathematical inertia model of the human body. *Journal of Biomechanics*, 23(1), 67-74.

Yeadon, M.R., King, M.A. (2002). Evaluation of a torque driven simulation model of tumbling. *Journal of Applied Biomechanics*, 18, 195-206.

Yeadon, M.R., King, M.A. & Wilson, C. (2006). Modelling the maximum voluntary joint torque/angular velocity relationship in human movement. *Journal of Biomechanics*, 39, 476-482.

DIFFERENTIATING TOP-RANKED MALE TENNIS PLAYERS FROM LOWER-RANKED PLAYERS USING HAWK-EYE DATA: AN INVESTIGATION OF THE 2012–2014 AUSTRALIAN OPEN TOURNAMENTS

David Whiteside^{1,2}, Michael Bane^{1,2,3} and Machar Reid¹

Tennis Australia, Melbourne, Australia¹
Victoria University, Melbourne, Australia²
Australian Institute of Sport, Canberra, Australia³

The purpose of this study was to differentiate top- and lower-ranked professional tennis players, using Hawk-Eye derived performance metrics. Eighty players competing at the 2012–2014 Australian Open tournaments were assigned to either a top-ranked (n=40) or lower ranked (n=40) group, based on their ATP ranking. Hawk-Eye data from one of each player's matches were obtained for analysis and compared between groups. Top-ranked players achieved more success on serve (with respect to aces, accuracy and points won) and possessed a faster first serve return, compared with lower-ranked players. Top-ranked players also played more groundstrokes from behind the baseline, delivered the ball deeper into their opponent's court, and covered a greater distance during matches. Coaches may be able to use these findings to develop playing style and match tactics.

KEY WORDS: analytics, tactics, biomechanics, conditioning.

INTRODUCTION: During the 2015 ATP season, prize money on the men's tennis tour will exceed US\$100 million for the first time. Ostensibly, this bodes well for the 2184 players who obtained professional ranking points during the 2014 ATP season. However, a recent review of professional men's tennis revealed that 60% of the total prize money available is won by the top 1% (i.e., top 50) of players (ITF, 2015). Moreover, it was estimated that only players ranked higher than 336 earned enough to cover their basic playing expenses, suggesting that profits for those outside the top 1% are rather modest. For lower-ranked players, these findings highlight the importance of closing the performance gap between themselves and the world's top players.

Tennis is a multifaceted sport, with elite players required to possess expert stroke production abilities and physical capacities. Although research has been valuable for improving stroke biomechanics (Elliott, 2006) and conditioning programs (Reid & Schneiker, 2008), those factors that differentiate top-ranked tennis players remain somewhat unclear. Further, most objective data pertaining to elite tennis matchplay have emanated from controlled laboratory experiments involving restricted cohorts, thus limiting their application to professional tennis. However, the introduction of computer-assisted adjudication has redefined the possibilities for performance analysis in tennis. In equipped venues, Hawk-Eye tracks three-dimensional ball trajectories and player locations using cameras mounted in the stadium. Consequently, performance measurement is no longer restricted to a laboratory, and obtaining large datasets of top-level players has become a reality. Plausibly, these data could be used to supplement extant performance research in tennis and provide a direct insight into the professional game that coaches could use to improve player development.

Identifying the performance metrics that are unique to top-level tennis players may help coaches to develop players' ability and/or match strategies. The purpose of this study was to utilize Hawk-Eye data obtained during the 2012–2014 Australian Open tournaments to compare the performance of top-ranked players to that of lower-ranked players. It was hypothesised that top-ranked players would display superior serving, return of serve, groundstroke and movement abilities to their lower-ranked counterparts.

METHODS: During the 2012, 2013 and 2014 Australian Open tournaments, a total of 118 male players completed at least one match on a Hawk-Eye equipped court at Melbourne Park and were initially identified for inclusion in this study. During each of the analysed

matches, the Hawk-Eye system recorded ball and player movement data. At the conclusion of each match, a summary report was generated based on the recorded data. The report contained a total of twenty-eight performance metrics pertaining to serving, returning serve, groundstrokes and on-court movement that were analysed in this study.

One match, per player, was selected for analysis in this study. Where a player had completed more than one match on a Hawk-Eye court, only one was randomly selected for analysis. Each player's ATP ranking, at the time of their match was obtained manually from the ATP website. The players were then sorted according to their ranking and, using the 1/3 split technique (Murphy, Duffield, Kellett & Reid, In Press), the 38 players around the median removed, leaving two heterogeneous groups. The top 40 players were assigned to the "top-ranked" group, while the bottom 40 players were assigned to the "lower-ranked" group.

Given that the data were not normally distributed, nonparametric procedures were employed to compare performance metrics between the two groups. Significant differences between the groups were ascertained using Mann-Whitney U tests. With multiple comparisons being undertaken, significance was adjusted to the more conservative level of $P < 0.005$ and Cohen's d effect sizes were computed to aid interpretation. Conservatively, only effect sizes > 0.4 were considered meaningful, and were classified as either moderate ($0.4 < d < 0.5$), moderate-to-large ($0.5 > d > 0.8$) or large ($d > 0.8$).

RESULTS: The ATP ranking of the top-ranked group (≤ 53) was significantly better than those in the lower-ranked (≥ 73) (Table 1).

In the serve, top-ranked players hit significantly more aces, and won significantly more points on their first serve than lower-ranked players. A moderate-to-large effect size was associated with top-ranked players winning a greater percentage of points on their first serve, while moderate effect sizes were associated with top-ranked players winning a greater percentage of points on their second serve and also possessing greater maximum first serve speed.

Both groups returned first serves from similar locations; the same was true for second serves. The percentage of first serves returned and second serves returned also exhibited no significant difference between groups. Average first serve return speed was significantly greater in top-ranked players, but second serve return speed comparable in both groups.

Top-ranked players played a greater percentage of groundstrokes from behind the baseline and delivered a greater percentage of these shots to locations beyond the service line (both moderate effects). However, when considering groundstrokes, rally length, ball contact height, net clearance and average shot speed did not differ between the groups.

With respect to on-court movement, top-ranked players covered significantly greater distances during matches than lower ranked players. Similarly, top-ranked players covered greater distances during receiving points than lower-ranked players. Average speed and maximum speed did not differ between groups.

DISCUSSION: Several between-group differences suggested that the serve was superior in top-ranked players. Additionally, top-ranked players returned first serves with greater speed and were able to deliver groundstrokes deeper into their opponent's court from locations further behind the baseline. Top-ranked players also covered a greater distance during matches than their lower-ranked counterparts. Coaches may be able to use these findings to refine players' training programs and/or on-court strategies.

The data imply that players aiming to infiltrate the top 50 in professional tennis should possess a proficient serve. Top-ranked players achieved more aces ($d = 0.60$), which may relate to their capability of achieving faster maximal serve speeds ($d = 0.43$). Accuracy was also foremost in top-ranked players, who possessed a greater first serve percentage ($d = 0.51$). These factors might explain why top-ranked players won a greater percentage of points on their first ($d = 0.62$) and second serve ($d = 0.41$) and underlines the importance of being able to win points on serve in professional tennis. Interestingly, however, average serve speed did not differ between the groups and implies that velocity generation was similar in this cohort of professionals. This generally conforms to traditional serve speed "records", which are

Table 1
Statistical Comparison of Hawk-Eye Derived Performance Metrics Between the Two Groups.

Variable	Top-Ranked Mean ± SD	Lower-Ranked Mean ± SD	<i>P</i>	<i>d</i>
Ranking	20.2 ± 11.9	157.0 ± 90.2	<0.001*	1.46
<i>Serve</i>				
Aces	12.3 ± 8.0	7.8 ± 6.4	0.004*	0.60 [†]
1 st Serve (%)	64.6 ± 6.8	61.2 ± 6.0	0.031	0.51 [†]
Points Won on 1 st Serve (%)	65.7 ± 7.9	60.3 ± 8.8	0.003*	0.62 [†]
Serves Unreturned (%)	34.3 ± 10.6	30.3 ± 10.5	0.093	0.38
Fastest Serve Speed (km/h)	201.2 ± 9.3	196.5 ± 11.6	0.065	0.43 [‡]
Avg. 1 st Serve Speed (km/h)	175.0 ± 9.9	171.9 ± 8.7	0.095	0.34
Double Faults	3.9 ± 3.7	4.6 ± 3.0	0.112	0.21
Points Won on 2 nd Serve (%)	53.7 ± 11.3	49.7 ± 7.7	0.025	0.41 [‡]
Serves Unreturned (%)	17.1 ± 7.9	15.9 ± 9.3	0.438	0.14
Avg. 2 nd Serve Speed (km/h)	145.7 ± 9.3	144.4 ± 10.3	0.623	0.13
<i>Serve Return</i>				
Avg. 1 st Serve Return Location [#] (m)	-0.95 ± 0.8	-0.92 ± 0.7	0.751	0.05
Avg. 2 nd Serve Return Location [#] (m)	0.01 ± 1.09	0.16 ± 1.03	0.603	0.15
1 st Serve Returns Made (%)	65.7 ± 10.6	69.3 ± 10.4	0.143	0.34
2 nd Serve Returns Made (%)	82.9 ± 7.9	84.3 ± 9.0	0.355	0.17
Avg. 1 st Serve Return Speed (km/h)	76.2 ± 13.3	67.5 ± 9.9	0.003*	0.70 [†]
Avg. 2 nd Serve Return Speed (km/h)	104.7 ± 8.9	101.4 ± 9.5	0.073	0.35
<i>Groundstrokes</i>				
Shots Inside Baseline (%)	30.7 ± 7.9	34.0 ± 7.7	0.039	0.42 [‡]
Avg. Rally Length on 1 st Serve	3.7 ± 1.0	4.0 ± 1.2	0.240	0.28
Avg. Rally Length on 2 nd Serve	5.5 ± 1.2	5.2 ± 1.1	0.165	0.24
Avg. Ball Contact Height (m)	1.05 ± 0.09	1.07 ± 0.10	0.087	0.28
Avg. Net Clearance (m)	0.36 ± 0.02	0.37 ± 0.02	0.545	0.14
Avg. Shot Speed (km/h)	95.6 ± 6.6	94.3 ± 6.3	0.209	0.20
Shots Deep of Service Line (%)	64.7 ± 16.7	59.6 ± 5.6	0.019	0.40 [‡]
<i>Movement</i>				
Match Distance (m)	3082 ± 1075	2498 ± 898	0.002*	0.57 [†]
Avg. Speed (m/s)	1.3 ± 0.2	1.2 ± 0.2	0.491	0.12
Maximum Speed (m/s)	6.1 ± 2.5	6.5 ± 3.7	0.777	0.15
Avg. Distance Serving Points (m)	9.8 ± 2.8	9.5 ± 2.6	0.375	0.11
Avg. Distance Receiving Points (m)	8.7 ± 2.1	7.5 ± 2.1	0.003*	0.58 [†]

[#]Relative to baseline (-ve = behind baseline); *P* = Significance; *d* = Cohen's *d* effect size; *Significant at *P*<0.005 level. [†]Moderate-to-Large effect size; [‡]Moderate effect size.

typically not limited to top-ranked players. For this reason—and based on the first serve percentage data in this study—developing serve accuracy and/or direction should be at the forefront of coaches' intentions. It follows that future research in this area should appraise the dispersion of serve locations to identify patterns unique to top-ranked players.

All players returned first serves while standing 0.9–1.0 m behind the baseline, returned second serves fractionally inside the baseline, and were equally good at returning these balls into play. The primary difference in the return of serve—and largest effect size noted in this study (*d* = 0.70)—was the average speed of first serve return strokes (which was 8.7 km/h faster in the top-ranked group). Plausibly, a faster serve return may counteract the abovementioned advantage that is presented by a proficient first serve and better equip these players to break their opponents' serve. Although these data imply that serve return

speed is unrelated to the player's location on court, future research should explore other factors that might influence speed of the first serve return such as gaze, anticipation, movement time, and stroke mechanics. Such explorations would help coaches to develop what appears to be a critical component of elite tennis players' on-court strategies.

Although players stood in similar locations when returning serve, the same cannot be said for the ensuing groundstrokes. Top-ranked players executed a greater number of shots from behind the baseline ($d = 0.42$), which is consistent with a counter-punching strategy where the player aims to return as many balls into play as possible (standing deeper permits greater court coverage). Top-ranked players also delivered 5% more of these groundstrokes to a deeper location in their opponent's court ($d = 0.40$). This speaks to their offensive ability, as deeper balls are generally considered more difficult to play since they arrive faster, and may afford top-ranked players an advantage during rallies. Logically, these findings imply that practice drills should afford players ample opportunities to develop their stroke play from behind the baseline. However, it should be noted that average groundstroke speed, shot flatness (i.e., net clearance) and contact height did not significantly differentiate groups. Thus, for groundstrokes—as appeared to be the case with the serve—accuracy may be more a pivotal in differentiator of top- and lower-ranked players than speed.

Interestingly, top-ranked players covered greater distances during: (1) entire matches ($d = 0.57$), and; (2) points where they were receiving ($d = 0.58$). This is seemingly consistent with the counter-punching strategy noted previously, but could also indicate that top-ranked players: (1) recovered to centre court after each shot, and/or; (2) took extra steps to execute strokes from more favourable positions. Obviously further research is necessary, but these data underline the importance of movement and endurance capacities in professional men's tennis. In contrast, average and maximum movement speed data did not differentiate top- and lower-ranked players and—when considered alongside the stroke speed findings—presents the possibility that explosiveness is not a critical discriminator of ATP ranking.

This study was limited by the fact that only one match of data were analysed, per player. With Hawk-Eye in its infancy as an analytic tool, this was unavoidable and it follows that this study should be repeated and expanded as more data become available for analysis. These data also only pertain to professional male players at the Australian Open in recent years, thus restricting the generalizability of the findings.

CONCLUSION: This exploratory study identified a selection of match play parameters that differentiated top- and lower-ranked professional male tennis players. Top-ranked players appeared more successful on serve (with respect to aces, accuracy and points won) and possessed a faster first serve return, compared with lower-ranked players. Top-ranked players also played more groundstrokes from behind the baseline and delivered them deeper into their opponent's court, while covering a greater distance during matches. Consequently, it appears prudent for coaches to focus on developing these characteristics during practice. With average serve, groundstroke and movement speeds similar among all players, breaking into the top 50 may be more reliant on refining non-explosive capacities (e.g., accuracy, endurance and strategy) rather than velocity generation and explosiveness. Future research should utilize the growing volume of Hawk-eye data to further probe this question and advance the applications of tennis analytics.

REFERENCES:

- Elliott, B. (2006). Biomechanics and tennis. *British Journal of Sports Medicine*, 40(5), 392–396.
- International Tennis Federation. (2014). *Pro Circuit Review*. Retrieved from <http://www.itftennis.com/procircuit/about-pro-circuit/pro-circuit-review.aspx>
- Murphy, A. P., Duffield, R., Kellett, A., & Reid, M. (In Press). The relationship of training load to physical capacity changes during international tours in high performance junior tennis players. *International Journal of Sports Physiology and Performance*.
- Reid, M., & Schneiker, K. (2008). Strength and conditioning in tennis: current research and practice. *Journal of Science and Medicine in Sport*, 11(3), 248–256.

DO SWIMMERS ALWAYS PERFORM BETTER USING THEIR PREFERRED TECHNIQUE?

Elaine Tor^{1,2,3}, David Pease¹, Kevin Ball²

¹Movement Science, Australian Institute of Sport, ACT, Australia

²College of Exercise and Sport Science, ISEAL, Victoria University, Melbourne, Australia

³Victorian Institute of Sport, Melbourne, Australia

This study compared four underwater trajectories in order to determine if swimmers will always perform fastest using their preferred technique. Fourteen elite swimmers were asked to dive at three depths as well as their preferred dive. These conditions were labelled as Dive 1, Dive 2, Dive 3 and Preferred. The Wetplate Analysis System was used to collect all data before descriptive statistics were determined. Inter-trial variability on a group basis revealed little difference in variance between each dive type. Further individual analyses found that seven of the fourteen swimmers performed faster using a non-preferred technique. In contrast to other studies which have found that swimmers will favour their preferred start technique there is evidence in this study to suggest that elite swimmers are able to readily change their underwater trajectory.

KEYWORDS: dive, trajectory, swim start, elite

INTRODUCTION: In sport there have been multiple studies that have compared different techniques in order to determine if there is an “ideal movement pattern” which athletes must adopt in order to achieve superior performance. Specifically investigating the swimming start, there have also been a number of studies that have manipulated the swimmers’ technique with the aim of improving performance (Honda, Sinclair, Mason, & Pease, 2012; Kirner, Bock, & Welch, 1989; Slawson et al., 2011). Hay (1986) stated that most studies comparing different start techniques are flawed as swimmers will always perform better using their preferred start technique. Indeed, there are a number of studies that have shown swimmers will perform better with their preferred dive as this technique is more stable and reproducible (Hay, 1986; Jorgic et al., 2010; Vantorre, Seifert, Fernandes, Vilas-Boas, & Chollet, 2010).

There is also evidence in these studies that elite swimmers are able to readily change their technique, which suggests that these types of comparative studies are not flawed when using elite swimmers. Vantorre et al. (2010) compared elite swimmers preferential start technique with an un-preferential technique. They found that even through there were differences in kinematics prior to entry into the water, there were no differences in overall performance; stating that high-level swimmers are able to compensate lower block efficiency with effective underwater phases. Similarly, White et al. (2011) used experienced and less experienced swimmers to compare shallow and deep underwater trajectories and found that the more experienced swimmers were able to readily alter their technique.

The current study utilised a comparative design with elite swimmers only, aiming to determine if swimmers performed better using their preferred underwater trajectory. It was hypothesised that swimmers are likely to perform better using their preferred technique. Nevertheless, this study’s protocol will encourage swimmers to try a new technique, which may prove to be faster.

METHODS: Fourteen swimmers (11 male, 3 female, 19 ± 1 y) were recruited from the Australian Institute of Sport (AIS) Swimming Program and other state institute programs around Australia. All swimmers qualified for the National Championships in the 100 m freestyle (53.10 s for male, 59.00 s for female) and had at least 5 years of competitive swimming experience at the national level with an average FINA point score of 787 ± 19 . Swimmers were asked to perform a series of dives at three depths. The depths were categorised as Dive 1, Dive 2, Dive 3 and the swimmers’ preferred dive. Dive 1 is

typically characterised by swimmers resurfacing as fast as possible with minimal underwater kick. This is the dive used mostly by swimmers who are weak at underwater kick as they spent the shortest amount of time underwater. During Dive 1 the swimmers were asked to resurface and commence free swimming almost immediately after entry. Dive 2 can be described as a gradual descent followed by a gradual ascent. For Dive 2 the swimmers were asked to dive deeper and aim to resurface around the 10 m mark. Finally, Dive 3 is most commonly used by swimmers who are highly proficient in underwater kick, as the swimmer stays underwater for the longest amount of time during this dive. In Dive 3 the swimmers were asked to dive down deep and resurface to commence free swimming at the 15 m mark.

To assist the participants in achieving the prescribed trajectories, brightly coloured markers were placed at 5 m, 7.5 m and 9 m on the bottom of the pool, to indicate the point at which the participants needed to begin rising to the surface in order to achieve the Dive 1, Dive 2 and Dive 3 conditions respectively. The distances that the markers were placed at was determined from a previous study by Tor et al. (2014) which stated that the mean horizontal distance of maximum depth for elite swimmers is 6.06 m with a standard deviation (SD) of 0.97 m. Therefore, the markers were placed at -1 SD (5 m), +1.5 SD (7.5 m) and +3 SD (9 m) according to the results of that previous study. The swimmers performed 16 dives at maximum effort to 15 m (4 dives at each set condition and 4 dives at their preferred depth) with two minutes rest in between each dive. The 16 dives were completed over two testing sessions (one day rest in between each session); eight dives per session. Each swimmer performed two of each dive type during the session in a randomized order. Testing was divided into two testing sessions to ensure that each trial was performed maximally by the swimmer. Each dive trial was tested using the Wetplate Analysis System. The Wetplate Analysis System is a propriety system developed by the AIS Aquatic Testing, Training and Research Unit (ATTRU) and consists of an instrumented starting block with the same dimensions as the Omega OSB11 starting block (that used at all major international competitions) and a series of high-speed cameras (Mason, Mackintosh, & Pease, 2012; Tor, Pease, & Ball, 2015). The Swimtrak time system was used simultaneously to measure split times.

Individual analysis was first conducted on the data using standard deviation as a measure of inter-trial variability. Each swimmer's fastest dive condition was identified and tabulated. Means and standard deviations were then calculated for each parameter using SPSS Statistical Package (version 19.0, SPSS, Chicago, IL).

RESULTS: Performance time (time to 15 m) and descriptive statistics of selected parameters for each dive condition are shown in Table 1. The mean and standard deviation of each dive type for performance time was Dive 1 (mean \pm standard deviation, 6.62 \pm 0.40 s), Dive 2 (6.54 \pm 0.37 s), Dive 3 (6.56 \pm 0.42s) and Preferred (6.48 \pm 0.39s). Each swimmer's fastest dive condition was also identified on an individual basis. On seven occasions out of 14 the swimmer's preferred dive was not the fastest dive condition and on two occasions the fastest condition equalled the swimmer's preferred condition. Two swimmers each found that Dive 1 and Dive 3 were the fastest condition, while three swimmers found that Dive 2 was the fastest.

Table 1 Mean and standard deviation of selected parameters for each dive condition

Parameter	Preferred	Dive 1	Dive 2	Dive 3
Maximum Depth (m)	-0.98 ± 0.17	-0.74 ± 0.14	-0.92 ± 0.16	-1.03 ± 0.18
Distance at Max Depth (m)	5.86 ± 0.79	5.03 ± 0.58	5.75 ± 0.69	6.32 ± 1.21
Time at Max Depth (s)	1.78 ± 0.23	1.53 ± 0.18	1.75 ± 0.22	1.98 ± 0.46
Breakout Distance (m)	11.91 ± 1.52	8.11 ± 1.20	10.50 ± 1.41	12.43 ± 1.14
Breakout Time (s)	4.85 ± 0.69	2.94 ± 0.55	4.13 ± 0.68	5.22 ± 0.58
Depth of first kick (m)	-0.98 ± 0.20	-0.50 ± 0.24	-0.89 ± 0.18	-1.04 ± 0.17
Distance of first kick (m)	6.54 ± 0.68	6.16 ± 0.57	6.62 ± 0.68	6.65 ± 0.69
Time of First Kick (s)	2.04 ± 0.23	1.96 ± 0.19	2.08 ± 0.24	2.09 ± 0.24
Time to 15 m (s)	6.48 ± 0.39	6.62 ± 0.40	6.54 ± 0.37	6.56 ± 0.42

DISCUSSION: Most dive start studies have reported that swimmers' performed their best starts using a technique which they had the most practice with (Pearson, McElroy, Blitvich, Subic, & Blanksby, 1998). When examining different starting techniques, Hay (1986) stated that most studies are flawed because swimmers all have their own preferred start that is practiced almost exclusively. Therefore, studies which suggest one type of starting technique is superior to another may usually be associated with the swimmer's preference rather than real biomechanical advantages (Lyttle & Benjanuvatra, 2005). Further, an athlete's perception of their ability (sport confidence) and comfort in performing a skill (preference) may also affect their physical performance (Mills & Gehlsen, 1996). This study aimed to determine if swimmers always perform better with their preferred technique.

In this study, multiple individual analyses were used to determine if swimmers performed fastest using their preferred technique. Using standard deviation as a measure of inter-trial variability, there is very little difference in performance between each dive type and the swimmer's preferred condition. Even though previous research stated that the swimmers' preferred start technique is also the most stable and reproducible (Vantorre et al., 2010), there is evidence to suggest that this type of study is not flawed and that skilled swimmers are able to adjust from their preferred starting technique with similar amounts of inter-trial variability present for all dive conditions.

There is also evidence in this study that the swimmers' preferred technique is not the fastest. Each individuals fastest dive type was determined and showed that half of the participants performed faster using a non-preferred technique. Hence, even though the participants were considered highly competitive, a number of swimmers still had not optimised their performance and could further improve their start technique by altering their underwater trajectory. This was different to previous studies that have suggested swimmers will always perform better using their preferred or most practiced technique.

In addition, this study found that all swimmers were able to modify the maximum depth of their starts. White et al. (2011) tested 12 competitive and 13 less experienced swimmers at two different depths (preferred and shallow) and have shown swimmers with more competitive experience have been able to change the depth of their starts in comparison with less experiences swimmers. Conversely, in a study comparing two different start techniques Vantorre et al. (2010) found that there were no significant differences between the two techniques, stating that skilled swimmers were able to compensate lower block efficiency with effective underwater phases and there were no significant differences. Given that there was difference in maximum depth between each dive condition and some swimmers performed better using a non-preferred technique, the results from the present study and White et al. (2010) suggest that elite swimmers are able to adapt to a non-preferred technique with little training.

CONCLUSIONS: This study compared four underwater trajectories using an instrumented starting block and kick-start technique. Using this study design in the future coaches will be able to determine if their swimmers have optimised their underwater trajectory to improve start performance. Contrary to other studies this study found that elite swimmer's preferred movement pattern may not be their optimal technique. Elite swimmers, like the ones used in this study are able to change their technique with little training. Consequently, the findings of this study suggest that this type of design, when used with elite participants is not flawed and can be applied in the future.

REFERENCES:

- Hay, J. C. (1986). Swimming Biomechanics: A brief review. *Swimming Technique*, 23(3), 15-21.
- Honda, K., Sinclair, P., Mason, B., & Pease, D. (2012). *The effect of starting position on elite swim start performance using an angled kick plate*. Paper presented at the 30th Annual Conference of Biomechanics in Sports, Melbourne, ACU.166-168
- Jorgic, B., Puletic, M., Stankovic, R., Okicic, T., Bubanj, S., & Bubanj, R. (2010). The kinematic analysis of the grab and track start in swimming. *Physical Education and Sport*, 8(1), 31-36.
- Kirner, K., Bock, M., & Welch, J. (1989). A comparison of four different start combinations. *Journal of Swimming Research*, 5(2), 5-11.
- Lyttle, A., & Benjanuvatra, N. (2005). Start right? A biomechanical review of dive start performance Retrieved 13th Jan, 2010, from http://coachesinfo.com/index.php?option=com_content&view=article&id=89:swimming-start-style&catid=49:swimming-coaching&Itemid=86
- Mason, B., Mackintosh, C., & Pease, D. (2012). *The development of an analysis system to assist in the correction of inefficiencies in starts and turns for elite competitive swimming*. Paper presented at the 30th Conference for the International Society of Biomechanics in Sport, Melbourne.156-158
- Mills, B., & Gehlsen, G. (1996). A multidisciplinary investigation o the relation of start sport confidence with preference and velocity of swimming starts. *Perceptual and Motor Skills*, 83, 207-210.
- Pearson, C. T., McElroy, G. K., Blitvich, J. D., Subic, A., & Blanksby, B. (1998). A comparison of the swimming start using traditional and modified starting blocks. *Journal of Human Movement Studies*, 34, 49-66.
- Slawson, S. E., Conway, P. P., Cosser, J., Chakravort, N., Le-Sage, T., & West, A. A. (2011). The effect of start block configuration and swimming kinematics on starting performance in elite swimmers using the Omega OSB11 block. *Procedia Engineering*, 13, 141-147.
- Tor, E., Pease, D., & Ball, K. (2014). *Characteristics of an elite swimming start*. Paper presented at the Biomechanics and Medicine in Swimming Conference 2014, Canberra.257-263
- Tor, E., Pease, D., & Ball, K. (2015). The reliability of an instrumented start block analysis system. *Journal of Applied Biomechanics*, 31, 62-67.
- Vantorre, J., Seifert, L., Fernandes, R. J., Vilas-Boas, J. P., & Chollet, D. (2010). Biomechanical influence of start technique preference for elite track starters in front crawl. *The Open Sports Sciences Journal*, 3, 137-139.
- White, J. C., Cornett, A. C., Wright, B. V., Willmott, A. P., & Stager, J. M. (2011). Competitive swimmers modify racing start depth upon request. *International Journal of Aquatic Research & Education*, 5, 187-198.

EFFECT OF POST-ACTIVATION POTENTIATION ON KINEMATICS AND KICKING PERFORMANCE IN A ROUNDHOUSE KICK WITH TRAINED MARTIAL ARTS PRACTITIONERS

Håkon Strand Aandahl, Roland Van den Tillaar, Erna Von Heimburg
Department of Teacher Education and Sports, University College of Nord
Trøndelag, Levanger, Norway

The purpose of this study was to examine if kicking with elastic resistance (ER) during warming up could initiate Post-Activation Potentiation (PAP), and increase kinematics and performance on subsequent explosive kicking. Five woman and eleven men (n=16) with a background in kickboxing and/or TaeKwonDo performed two warming up strategies with subsequent testing. Kicking performance, defined as kicking velocity with the foot was measured 3D. In addition, muscle activity of the prime movers was measured. Kicking velocity of the foot increased by 3.3% after performing a warming-up strategy including kicking with ER ($p=0.009$). Increases were also recorded in muscle activity in m. vastus medialis (35.2%, $p=0.05$), rectus femoris (43.9%, $p=0.04$). The study show a positive effect on kicking performance after performing a warmup strategy including kicking with ER.

KEY WORDS: Warmup, explosive, PAP, elastic, resistance, ballistic.

INTRODUCTION: Warming up before a performance is used to prepare and enhance the upcoming performance. A mechanism that is associated with warming up and has positive effect upon performance in explosive movements is Post-Activation Potentiation (PAP) (Mitchell & Sale, 2011; Bergmann, et al., 2013; Miarka, et al., 2011). The muscles' ability to develop force is dependent on what has happened earlier within the muscle and improvements in performance that follow a submaximal or a maximal contraction has been referred to as PAP (Baudry & Duchateau, 2007). These improvements could come from changes in pennation angle (Tillin & Bishop, 2009), physiological improvements (Paasuke, et al., 1996; Rassier & Macintosh, 2000; Sale, 2002; Hodgson, et al., 2005) or neurological improvements (Chiu, et al., 2003; Güllich & Schmidtbleicher, 1996; Aagard, 2003; Aagard, et al., 2002). Previous studies presented inconsistent findings of PAP and improvements in performance. Some studies have shown improvements in performance (Chiu, et al., 2003; Mitchell & Sale, 2011; Batista, et al., 2007; Rixon, et al., 2007), while other studies have not been able to measure an effect of PAP (Behm, et al., 2004). Some studies have used maximal voluntary contractions (MVC) (Behm, et al., 2004; Batista, et al., 2007), while other studies have used heavy resistance weightlifting exercises (Chiu, et al., 2003; Mangus, et al., 2006; Rixon, et al., 2007; Mitchell & Sale, 2011) with the intention to initiate PAP. Even so, for many sports there is a lack of specificity in using such exercises to initiate a short-term positive effect on performance.

Only a few studies have applied more specific exercises to initiate PAP to enhance performance. Smith et al. (2014) applied sprinting with resistance in form of a sleigh with the intention of initiating PAP, which is more biomechanically similar and specific to the following sprinting exercise. Kicking with elastic resistance (ER) has previously shown to chronically increase kicking performance in terms of velocity (Jakubiak & Saunders, 2008). However, using elastic resistance as an exercise to initiate a short-term positive effect (PAP) on performance is not studied yet.

Therefore, the purpose of this study was to examine if kicking with ER could initiate PAP, increase kinematics and thereby performance on subsequent explosive kicking. It was hypothesized that kicking with elastic resistance at the end of a warming up protocol will improve short-term kicking kinematics and performance of the trained martial arts practitioners.

Furthermore, that this was caused by the increase muscle activity in the kicking legs' knee extensors due to PAP.

METHODS: A randomised crossover study was conducted to examine differences in the trained martial arts practitioners (n=16) kicking performance subsequent to two warming up protocols. One warming up protocol included a standardized pre-competition warming up routine and ballistic hip movements. The second warmup protocol included the same standardized pre-competition warmup routine with an additional 10 kicks with ER (X-ERFIT FITNESS TUBE, high resistance, black colour) in three sets with 90 seconds pause, which was sufficient for maintaining maximal performance and complies with the theory of recovery of power (Rahimi, et al.,2009). Between the two protocols participants had a minimum 30 minutes break before starting the next warming up protocol to ensure that any effects of PAP had diminished. Three roundhouse kicks with maximal effort were conducted on a hanging heavy-bag 5-8 min after warming up. The three test kicks were measured by using six 3D cameras at 500 Hz. (Qualysis, Sävedalen, Sweden) with 15 markers fastened on the lower extremities (both troch. majors, both superior iliac crests, both lateral knees, both medial knees, both lateral malleolus, both medial malleolus, both lateral metatarsal-phalangeal joints and I. medial metatarsal-phalangeal joint).

Computation of maximal linear velocity of the kicking foot's lateral markers (distal foot, ankle, knee and hip) together with the maximal angular velocity of joint movements (knee-, hip-extension and hip rotation) and their timing. All calculations were performed in Matlab 7.0 (The Mathworks Inc., MA, USA). Electromyography (Musclelab, Ergotest Technology AS, Langesund, Norway) was used to record muscle activity of m. vastus lateralis, m. vastus medialis and m. rectus femoris of the kicking leg during the kicks.

To examine the effect of warming up with and without ER a paired T-Test was used. The level of significance was accepted at $P < 0.05$ and all data are expressed as mean \pm SD. Statistical analysis was performed using SPSS 18.0 for windows (SPSS, inc., Chicago, IL).

RESULTS: A significant 3.3% higher velocity ($p = 0.009$) was found at the kicking foot's toe (Fig. 1) and knee marker when conducting the warming up with ER compared to the one without ER (table 1). In addition 2.5% higher linear velocity was found for the knee marker ($p = 0.026$), while only a trend was found for the linear velocities of the hip ($p = 0.059$) and ankle ($p = 0.092$).

Table 1: Effect of kicking with elastic resistance on different parameters in kicking performance. *Significant difference without ER to with ER ($p < 0.05$). Timing is displayed as impact - occurrence.

Parameter	Without ER		With ER	
	Peak	Timing	Peak	Timing
Hip marker (m/s)	3.29 \pm 0.55	0.647 \pm 0.29	3.47 \pm 0.69	0.706 \pm 0.37
Knee marker (m/s)	7.16 \pm 0.96	0.580 \pm 0.28	7.34 \pm 1.07*	0.628 \pm 0.36
Ankle marker (m/s)	13.29 \pm 1.34	0.495 \pm 0.28	13.51 \pm 1.63	0.546 \pm 0.37
Foot (m/s)	17.35 \pm 1.98	0.491 \pm 0.28	17.93 \pm 2.26*	0.541 \pm 0.37
Hip rotation (rad/s)	10.98 \pm 2.09	0.246 \pm 0.11	11.03 \pm 1.99	0.257 \pm 0.11
Hip extension (rad/s)	4.72 \pm 1.18	0.174 \pm 0.08	5.08 \pm 1.77	0.212 \pm 0.11
Knee extension (rad/s)	30.13 \pm 4.54	-0.011 \pm 0.01	30.86 \pm 5.47	-0.019 \pm 0.01

About the muscle activity only a significantly higher M-RMS was found in m. rectus femoris (without ER: 104.96 \pm 80.13 M-RMS, with ER: 151.11 \pm 131.26, $p = 0.04$). A trend was found

in the increase of muscle activity in m. vastus medialis (without ER: 157.23 ± 66.76 M-RMS, with ER: 212.64 ± 151.59 , $p = 0.05$), but there were no significant changes found in m. vastus lateralis ($p = 0.36$).

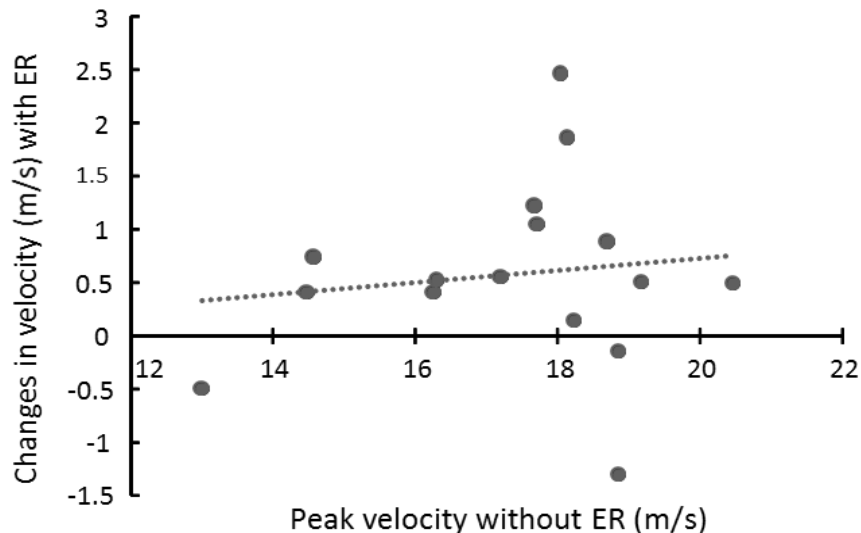


Figure 1: Effect of kicking with elastic resistance on kicking performance measured at the distal end point of foot in roundhouse kicks by the participants. The X-axis show peak velocity (m/s) recorded under testing after warmup without ER. The Y-axis show the difference in peak velocity (m/s) measured at toe marker from best test-kick after warmup without ER to best test-kick after warmup including ER.

DISCUSSION: The results in this study show that using a warming up protocol that includes kicking with elastic resistance positively affects kicking performance in the participating martial arts practitioners.

Even though there were not found any significant changes in terms of knee, hip extension and hip rotation, there were found two trends in terms of the hip ($p = 0.08$) and knee ($p = 0.06$) extensions timing. The overall results in timing indicates that the peak values of the kicking parameters occurred sooner after initiating the kick after including ER in the warming up protocol, thus leading to a better kicking performance.

The improvements in kicking performance were compliant with the theory of neural enhancements. Increased recruitment of higher order motor units (Chiu, et al., 2003; Güllich & Schmidtbleicher, 1996), a better synchronisation of the involved motor units and a reduced pre-synaptic inhibition (Aagard, et al., 2002; Aagard, 2003) could be the cause for a faster kick and reaching peak parameter values faster.

The increased kicking velocity could have been caused by physiological enhancements. The physiological enhancements involves a shorter path for myosin heads (Tillin & Bishop, 2009), increased supply of ATP (Hodgson, et al., 2005), heightened sensitivity for Ca^{2+} (Szczena, et al., 2002), thus increasing the rate of cross-bridging and a greater muscular contraction velocity which could cause the increased kicking velocity. However, due to equipment limitation it was not possible to measure such physiological enhancements. Therefore we cannot conclude whether or not such physiological enhancements occurred or had an effect on the participant's kicking performance.

Changes in pennation angle is thought to provide a greater transmission of power from the muscle to the moving structure (Tillin & Bishop, 2009). The increased kicking velocity recorded

in this study could have benefitted from a greater transmission of power from the muscle to the moving structure. The tensile strength of the muscle tendons could be decreased during a warmup and thusly counteract any increase gained from a greater transmission of power (Kubo, et al., 2001).

Advantages by including kicking with elastic resistance as part of a warming up strategy could be to increase short term performance in a competition environment for certain combat sports. Elastic tubing is very portable and including them as part of a warm up routine is very feasible. Even so, before this method of enhancing performance in a competition environment takes place, more research should be conducted.

CONCLUSION: This study shows that a warming up strategy that includes kicking with ER caused a positive effect in the kicking performance for trained martial arts practitioners. The forethought effects of PAP could have caused the 3.3% increase in the kicking-foot's distal velocity. The increased muscle activity indicates that the PAP effect could have been present after kicking with ER. Such effects are beneficially to include kicking with ER as part of a pre-competition warming up protocol.

REFERENCES:

- Aagard, P., 2003. Training induced changes in neural function. *Exerc. Sport Sci. Rev.*, 2(31), pp. 61-67.
- Aagard, P. et al., 2002. Neural adaptations to resistance training: Evoked V-wave and H-reflex responses. *J. Appl. Physiol.*, Issue 92, pp. 2309-2318.
- Batista, M. A., Ugrinowitsch, C., H., R. & al., e., 2007. Intermittent exercise as a conditioning activity to induce postactivation potentiation. *J Strength Cond Res*, pp. 837-840.
- Baudry, S. & Duchateau, J., 2007. Postactivation Potentiation in a human muscle: effect on the rate of torque development of tetanic and voluntary isometric contraction. *J Appl Physiol*.
- Behm, D. G. et al., 2004. Conflicting effects of fatigue and potentiation on voluntary force. *J Strength Cond Res*, pp. 365-72.
- Bergmann, J., Kramer, A. & Gruber, M., 2013. Repetitive hops induce postactivation potentiation in triceps surae as well as an increase in the jump height of subsequent maximal drop jumps. *PLoS One*.
- Chiu, L. Z. et al., 2003. Postactivation potentiation responses in athletic and recreationally trained individuals. *J. Strength Cond. Res.*, 4(17), pp. 671-677.
- Güllich, A. & Schmidtbleicher, D., 1996. MCV-induced short-term potentiation of explosive force. *Güllich, A.; Schmidtbleicher, D.*, 4(11), pp. 67-81.
- Hodgson, M., Docherty, D. & Robbins, D., 2005. Post activation potentiation: underlying physiology and implication for motor performance. *Sports Medicin.*, 7(35), pp. 585-595.
- Jakubiak, N. & Saunders, D. H., 2008. The Feasibility and Efficacy of Elastic Resistance Training For Improving the Velocity of the Olympic Taekwondo Turning Kick. *Journal of Strength and Conditioning Research*, Jul, pp. 1194-1197.
- Kubo, K., Kanehisa, H., Kawakami, Y. & Fukunaga, T., 2001. Effects of repeated muscle contractions on the tendon structures in humans. *Eur J. appl. Physiol.*, Volume 84, pp. 162-166.
- Mangus, B. C., Takahashi, M., Mercer, J. A. & al., e., 2006. Investigation of vertical jump performance after completing heavy squat exercises. *J Strength Cond Res*, pp. 497-600.
- Miarka, B., Del Vecchio, F. B. & Franchini, E., 2011. Acute effects and postactivation potentiation in the Special Judo Fitness Test. *J Strength Cond Res*, 2(25), pp. 427-431.
- Rahimi, R., Boroujerd, S. S., Mozafari, A. A. & Faraji, H., 2009. The effects of different rest intervals between sets on the training volume of female athletes. *I. J. Fitness*, 5 issue 1, pp-61-67.

RESEARCH ON DIFFERENT SIZES OF PLATFORM'S EFFECTS ON THE ATHLETES' LEAVING PLATFORM SPEED IN THE FREESTYLE SKIING AERIAL SKILL PROJECT

Hou Boyi¹ and Wang Xin²

Graduate School, Shenyang Sport University, Shenyang, China¹
Sport Science College, Shenyang Sport University, Shenyang, China²

The freestyle skiing aerial skill is an advantage project to win medals at the winter Olympic Games for China. This research applies the mathematical model method, combining theory with experiment, with the help of the athletes' leaving platform speed calculation software, to research and Analysis different sizes of platforms' effects on the athletes' leaving platform speed. The research result indicates that: the increasing of the platform height will decrease the leaving platform speed, and the decreasing range is related to the changing range. In order to ensure the specific actions' required leaving platform speed, it can be solved through adjusting the sliding distance and the speed of changing postures.

KEY WORDS: mathematical model method, calculation software, integral operation, sliding distances, transition zone distance, platform size.

INTRODUCTION: China began to carry out the freestyle skiing aerials project from the 1980s. Since the project focused primarily on skills, flexibility and agility which are consistent with the sporting characteristics and physical characteristics of Chinese people, The freestyle skiing aerials has been an important breakthrough for Chinese players winning the gold medal in the Winter Olympics. The action of the freestyle skiing aerials is composed of four parts (skiing stage, jumping stage, tuck dive stage and landing stage). which are connecting and interacting with each other. One of the key factors that determine the success of the action is to control the jumping height, that is to control the leaving the platform speed.

Freestyle skier first glide at an accelerating speed in ascertains loping and slide, then jump up from the platform with different height sand complete the air movement. The difference of the size of the platform has an influence on the leaving the platform speed. This study starts from three aspects of the skiing distance, the distance of transition zone and the size of curve segment to analysis the influence on the leaving the platform speed by the size of the platform .

METHODS: The study takes the national team athletes of free style skiing aerial as the object. Firstly, the freestyle skiing athletes need to speed up sliding on a slope with certain gradient, and then jump up from different highs of platforms and accomplish aerial actions. As shown in figure 1, according to the athletes' postures changing, the sliding stages can be divided into: Start (S1), Squat Down Sliding (S2-S3), Squat Sliding (S4), Straight Up (S5-S6), Straight Up Sliding (S7), Horizontally Sliding Arm Lifting (S8-S9). It can be divided into two stages according to the change of curvature radius and air resistance (S10-S11), as shown in figure 1 . Each stage brings in different air resistance changing equation separately to calculate.

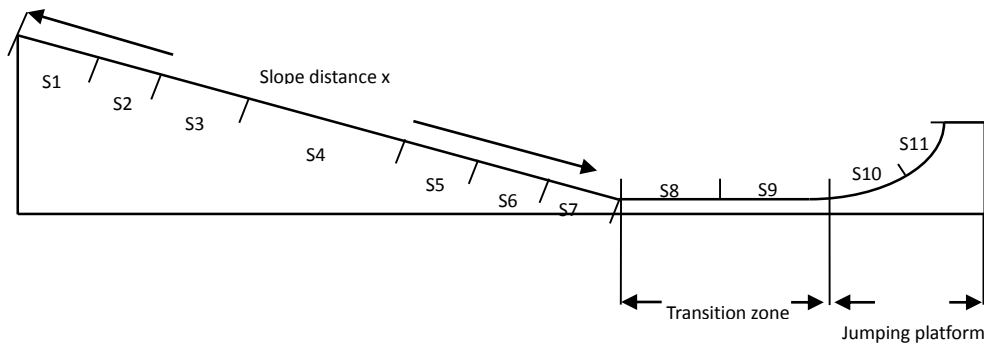


Figure 1: The athletes sliding stage dividing schematic diagram

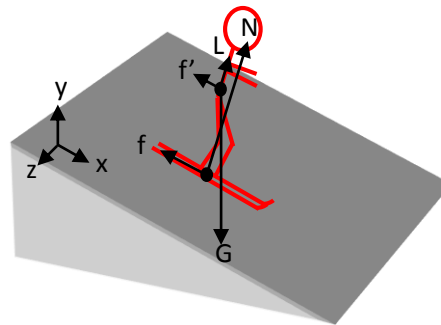


Figure 2: The figure of skiers' stress in straight segment

Considering the differences between the slope and the platform's geometrical structure, to calculate the athletes' leaving platform speed accurately, the mathematical equation is divided into two parts: one part is the straight line sections, which starts from the slope to the transition zone, where the athletes move on the surface with certain gradient or no gradient, with integral operation to select displacement as the step length; the other part is from the athletes' moving into the platform's radius to the moment of leaving the platform, because in this process, the athletes need to do circular motion on radius with certain curvature, selecting the change of angle as the step length.

In the software, the calculation of leaving platform speed's control equation uses Euler to do the calculation of two segments' ordinary differential equations. Assuming that $f(x,y)$ in the $y=f(x,y)$ ($a \leq x \leq b$) is sufficiently smooth, expand $y(x_{i+1})$ at point x_i by Taylor. So we get

$$\begin{cases} y_{i+1} = y_i + K \\ K = hf(x_i, y_i) \end{cases}$$

According to figure2, the motion equation of direction which is along the slope of approach is as follows.

$$\frac{dv}{dx} \Rightarrow \int_{x_0}^x F(x) dx = \int_{v_0}^v mvdv \Rightarrow v(x) \text{ Formula 1}$$

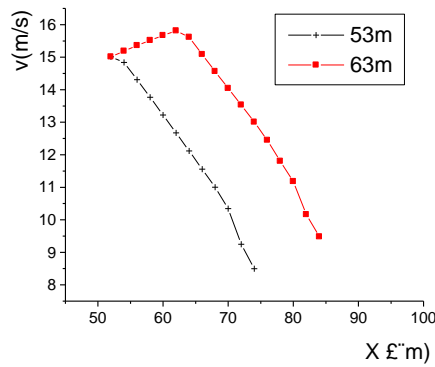
$$\int_0^x (f + f' + G_x + N_x) dx = m \int_{v_0}^v v dv \text{ Formula 2}$$

According to formula1, there is $dv = \frac{\sum F}{mv_i} \cdot dx$, When Δx is very small, there is $dv \approx \Delta v = K \cdot \Delta x$, so $dv = f'(x_i) \Delta x$, $f'(x_i) = \frac{\sum F}{mv_i}$. According to equation of *Taylor* expansion, the equation of

speed is $\begin{cases} v_{i+1} = v_i + h \frac{\sum F}{mv_i} \\ v_0 = 0.8 \end{cases}$

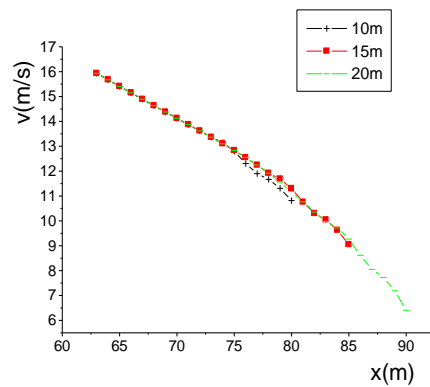
Curve equation's calculation method is the same, here is a little.

RESULTS:This study analyses the effects of sliding distance, the transition zone distance and the platform sizes changing on the leaving platform speed. The results are as follows.



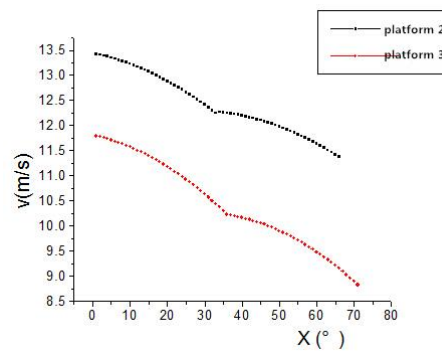
X said the sliding distance

Figure 3: Different sliding distances and athletes sliding speed changing figure



X said the sliding distance

Figure 4: The influence of the transition zone distance to the leaving platform speed



X said the radian angle

Figure 5: The influence of the platform sizes changing to the leaving platform speed

DISCUSSION:The former researches indicate that:the sliding velocity and the sliding distance are in direct proportion, and the sliding speed affects the athletes' gravity leaving platform speed. According to the characteristics of projectile motion, when the athletes leave platform, the gravity vertical speed affects the jump height, and with the higher gravity vertical speed while leaving platform, the athletes' jumping height is higher, the jumping time is relatively prolonged, and the athletes can accomplish much more difficult motions. According to input

ifferent sliding distance, this paper finds that the increasing of the sliding distance will increase the leaving platform speed, as shown in figure 3. When the sliding distance increases by 10m, the leaving platform speed will increase by 1m/s, which will improve the jumping height.

The transition zone is a section of straight line zone, where the athletes should complete the speed controlling and preparation before going to the platform. But because there's no slope in this section, gravity will not play the role of acceleration, instead, the air resistance and friction will decrease the sliding speed. So this section's distance will directly affects the speed of going onto the platform, then affects the speed of leaving platform. As shown in figure 4, when the transition distance increases from 10m to 20m, the speed's decreasing range is obvious which indicates the changing of this section's size influences largely on the leaving platform speed.

As shown in figure 5, under the same sliding distance, the jumping speed from platform 2 is higher than platform 3. That is because the curvature radius and the height of platform 3 are both higher than platform 2, which leads to the increasing of resistance work, and the speed decreasing function is also increasing accordingly.

CONCLUSION: The research results show that when the slip distance increases 10m, the leaving platform speed increases 1m/s. When the length of transition zone increases from 10m to 15m and 20m, the leaving platform speed drops from 11m/s to 9m/s and 6m/s. When the slip distance is same as the transition zone length, the jumping speed from platform 2 is 2m/s higher than from platform 3. With the increasing of radian angle of platform, the leaving platform speed decrease. When the radian angle increases 5 degree, the leaving platform speed decreases 0.2m/s.

REFERENCES:

- Ma Yi, Yan red, Wu Zhihai, et al. The related factors influencing the Freestyle Aerial movement difficulty analysis J. *Journal of Shenyang Sport University*, 2010, 29 (1): 8-16.
- Tong Yongdian, Yan red, Liu Ping, et al. The athletes of Freestyle Skiing Aerials landing stability of the main influence factors of J. *Journal of Shenyang Sport University*, 2003, 22 (4): 15-17.
- Wang Xin, Ma Yi, HaoQingwei, et al. Freestyle Skiing Aerials Technical Diagnosis System Research (J). *Journal of Shenyang Sport University*, 2011, 30 (2):4-7.
- Yan Hongguang, Lou Yantao, Wu Songlin. The Freestyle Aerial action technology of biomechanics principle of J. *Journal of Shenyang Sport University*, 2010, 29 (1) 12-16.
- Zheng Kai, Zheng Fei. The project of Freestyle Skiing Aerials help sliding distance and speed control for J. *Journal of Shenyang Sport University*, 2006, 25 (5): 118-119.

Acknowledgement

This work was financially supported by the National Natural Science Foundation (11102120).

THE ESTABLISHMENT OF MATHEMATICAL MODEL OF THE TAKE-OFF SPEED OF AERIALS OF FREESTYLE SKIING

Wang Xin¹, Fu Yanming¹ and Zhao Le²

School of Sports Kinetics, Shenyang Sport University, Shenyang, China¹
Sport Science College, Shenyang Sport University, Shenyang, China²

The take-off speed of freestyle skiing aerials is one of the key factors which can decide the success. However, the take-off speed depends on snow quality, circumstance condition, in-run slope angle, in-run distance, air resistance and skiers' action. By using sports biomechanics, mathematical model and numerical simulation method and combining theory with experiment, this study sets up a mathematical model of outside circumstance and skiers' self-adjustment, simulates the changes of inside and outside stress in each stage of sliding, calculates the parameters intuitively and then forms into speed values. The setup of this model can provide scientific guidance for ensuring necessary take-off speed for specific actions.

KEY WORDS: freestyle skiing aerials, take-off speed, mathematical model method, calculation software, integral operation.

INTRODUCTION: The movement structure of the freestyle skiing aerials consists of in-run, take-off, soaring and landing^[1]. And one of the key factors that determine the success of the action is the control of the soaring height, which involves the control of take-off speed^[2]. This paper focuses on the air resistance simulation and skiers' internal regulation, using the simulation technology to reveal the effect of pedaling acceleration and lifting arm of freestyle skiing of aerials skiers on supporting force^[3-4]. The simulation technology has been widely applied to the study of sports events at home and abroad for its advantages of fast computation and the reduction of the experiments. This paper also explores methods by which the reaction force value measured in laboratory is directly loaded on computer software to simplify the simulation calculation process.

METHODS: The research object is Chinese women's freestyle skier Xu Mengtao whose total score ranks the first in the world, and Jia Zongyang, the champion of men's freestyle skiing aerials in the 24th Universiade. We establish three-dimensional solid model of skiers according to the theory of reverse model and 3D laser scan. By adopting the module insert / merge and inherited functions of 3D virtual design in pro/ENGINEER, we establish the space model of skiers' flow around field. Finally, the air resistance and lifting value will be computed in the software of Adina. By adopting the method of laboratory simulation, we measure the supporting counter force of different stances to pedal and lift arm of skiers. Finally, we select the mathematical calculation software of Matlab to calculate the take-off speed and establish equation of the take-off speed control to calculate the take-off speed.

RESULTS: Forces skiers get on the in-run slope are all written in function that force changes as the location of the in-run slope changes, according to the integral expression of Newton's second law:

$$\frac{dv}{dx} \Rightarrow \int_{x_0}^x F(x) dx = \int_{v_0}^v mvdv \Rightarrow v(x) \text{ Formula 1}$$

As shown in figure 1, skiers put on weight on the in-run slope. While x is the in-run distance, v is the skiers' running speed, α is the inclination angle of ski track, G is gravity, N is supporting force, f' is air resistance, f is friction force, L is lift force. Skiers do the regulatory action in the sliding process, namely that the change of body stance will be a force on surface, in turn, snow surface also gives human a force N , N can be decomposed into force N_x which parallels to the snow surface, force N_y which perpendiculars to the snow surface and force N_z along the body axis (influence on in-run speed direction is so small as to ignore).

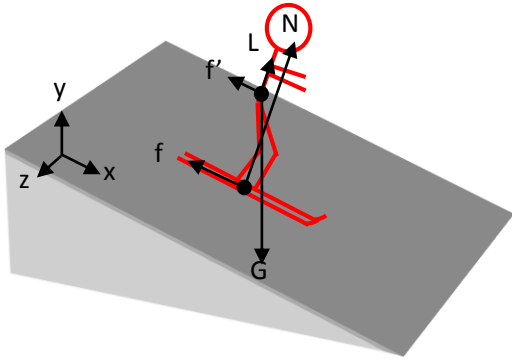


Fig.1The figure of skiers' stress in straight segment

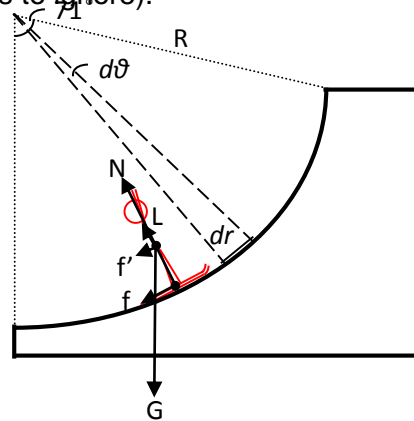


Fig.2The figure of skiers' stress in curve segment

According to Formula 1, the motion equation along the slope on the in-run slope is as follow:

$$\int_0^x (f + f' + G_x + N_x) dx = m \int_{v_0}^v v dv \text{ Formula 2}$$

Bodies of skiers have kept upright before entering the arc zone of platform, and they basically go up onto the platform maintaining this posture. In view of the fact that this posture doesn't get changed, and meanwhile simplifying the calculation, this process ignores the influence that the variation of supporting counter-force of human body has on the speed of leaving platform. Considering skiers always slide on the curving surface, the radius of curvature is regarded as a fixed value, and the equation of velocity of leaving platform adopts the theorem of kinetic energy to calculate. The equation is shown as Figure 2:

$$W_{A-B} = \int_A^B (f + f' + G_x) \cdot dr = \int_0^\alpha (f + f' + G \sin \alpha) \cdot R d\alpha \text{ Formula 3}$$

Air has a huge influence on the action effect of freestyle skiers. The control equation of the flow field around a player is turbulent model, and finite element method can be used to solve this equation. Adopting mesh generation on the established flow field space model (it is divided into more than 8 units), as shown in Figure 3. Considering the relatively large velocity gradient of the boundary layer, which is close to the surface of skiers and complex skiers' surface, the grids of skiers' surface are specially encrypted, as shown in Figure 4.

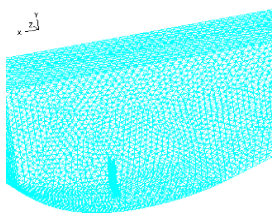


Fig.3Turbulent model of mesh

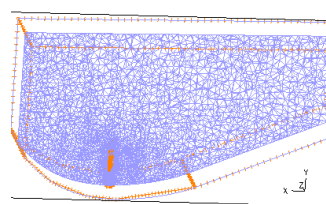


Fig.4 Encrypted grids on skiers' surface

$$f' = \frac{1}{2} \rho C_k A (V + V_f \cos \theta)^2 \text{Formula4}$$

$$L = \frac{1}{2} \rho C_s A (V + V_f \cos \theta)^2 \text{Formula5}$$

During the whole movement process, due to the windward area of skier's body is variable on the in-run slope, and the sliding speed of human body is variable in the in-run process, the calculation equations according to the resistance and lift force of air are, In this equation, C_k is resistance coefficient, ρ is air density, V_f is wind speed, θ is wind direction angle, and C_s is lift force coefficient. Regarding the influence of wind on the auxiliary sliding speed, the most important factor is wind speed. Through smoothly simulating calculating software to calculate the resistance coefficient and lift force coefficient of human body in different position, and then calculate the values of the resistance and lift force of the air when skiers slide thrusting against the ground in different wind directions and postures. Regulation force is the force influenced by variable postures of skiers themselves, namely the force that generated by skiers' changing postures. In order to fix the values of supporting counter force in different postures, the fitting function of the value of supporting counter force and the and the size of the joint angle is established according to the joints which have primary influence in different stages. In the software, the calculation of leaving platform speed's control equation uses Euler to do the calculation of two segments' ordinary differential equations. Assuming that $f(x,y)$ in the $y'=f(x,y)$ ($a \leq x \leq b$) is sufficiently smooth, expand $y(x_{i+1})$ at point x_i by Taylor. So we get $\begin{cases} y_{i+1} = y_i + K \\ K = hf(x_i, y_i) \end{cases}$. According to figure2, the motion equation of direction which is along the slope of

approach is as follows. According to formula1, there is $dv = \frac{\sum F}{mv_i} \cdot dx$, When Δx is very small,

there is $dv \approx \Delta v = K \cdot \Delta x$, so $dv = f'(x_i) \Delta x$, $f'(x_i) = \frac{\sum F}{mv_i}$. According to equation of Taylor

expansion, the equation of speed is $\begin{cases} v_{i+1} = v_i + h \frac{\sum F}{mv_i} \\ v_0 = 0.8 \end{cases}$. Curve equation's calculation method is

the same, here is a little.

CONCLUSION: To sum up, the air resistance, friction coefficient, jumping, sliding distance, posture changes will affect the speed. This paper uses numerical simulation method to demonstrate the whole process of the external environment and skiers' self-regulation, and then to quantitatively simulate the force that skiers get during the whole process, which can help athletes and coaches adjust the body posture and help increase sliding distance. We should ensure a reasonable pace vacated, flight time for different actions and the quality of the ground. Analysed from kinematics, aerial action of freestyle skiing is enable athletes to gain vertical velocity on the air. When the vertical velocity is increased, the flight height is bigger, the movement completed is relatively better, according to the scoring criterion of judgment reflecting the high floating principle. The pre-efficient determined slide aid scheme will help coaches and athletes reduce the number of the venue and get good grades.

REFERENCES:

Ma Yi, Yan red, Wu Zhihai, et al. The related factors influencing the Freestyle Aerial movement difficulty analysis. *Journal of Shenyang Sport University*, 2010, 29 (1): 8-16.

Tong Yongdian, Yan red, Liu Ping, et al. The athletes of Freestyle Skiing Aerials landing stability of the main influence factors. *Journal of Shenyang Sport University*, 2003, 22 (4): 15-17.

Xin Wang, Yi Ma, Qing-weiHao, Kinematic Analysis on Chinese Female Athletes' bFdF Action in Freestyle Skiing Aerialse, *International Journal of Advancements in Computing Technology*, 2012,11 (4): 147-150.

Yan Hongguang, Lou Yantao, Wu Songlin. The Freestyle Aerial action technology of biomechanics principle of J. *Journal of Shenyang Sport University*, 2010, 29 (1) 12-16.

Acknowledgement

This work was financially supported by the National Natural Science Foundation (11102120).

SHOT PERFORMANCE USING ANCHORED LONG PUTTING CLUBS

Ian Kenny and Ian Sherwin

Biomechanics Research Unit, University of Limerick, Limerick, Ireland

The study purpose was to measure putting outcome performance when different length putters were used with an anchoring mechanism. 72 skilled golfers each executed a total of 60 putts using standard, belly and long putters from two distances. Putting mechanics were assessed using SAM PuttLab™. From 1.83 m (6 ft) participants holed 80.3% of putts with a standard length putter, dropping to 78.6% and 75.3% for belly and long-handled putters. At 3.66 m (12 ft) participants holed 51.7% of putts with a standard length putter, and 50.8% and 46.9% for belly and long-handled putters. Shot performance showed no significant differences between clubs. There were significant ($p < 0.05$) between-club differences for swing time, putter head rotation and putter face impact spot. While anchoring may reduce putter head rotation it does not sufficiently limit rotation.

KEY WORDS: golf, performance, putter length, putting.

INTRODUCTION: The aim of the putting stroke is to start the ball with the intended speed on the intended line (Karlsen, 2010). A statement (Associated Press, 28th November 2012) by both governing bodies of golf the USGA and the R&A Ltd. introduced the possibility of a ban on using an anchoring mechanism while putting but made it very clear that the ban did not apply to the equipment, only the manner in which it is being used. As it stands the rules of the game will not allow the ban to come into play until January 2016. The proposal is to introduce Rule 14-1(b) which will read, "In making a stroke, the player must not anchor the club, either 'directly' or by use of an 'anchor point' (Figure 1). There were no empirical data offered during the statement to suggest that putters which use an anchoring mechanism (the belly putter and the long putter) made golf easier or improved performance. A good technique is crucial to create confidence in this area of the game and the ability to create a stable posture and pivot point is essential if the putter is to be returned consistently from the point of address to the moment of impact (Hurrion and Hurrion, 2008). The aim of the current study was to examine putting outcome performance and establish if there is a performance advantage to be gained by using an anchored putter.

ANCHORING THE CLUB—UNDERSTANDING RULE 14-1b

The USGA and The R&A, golf's governing bodies, have adopted changes to Rule 14-1 of the Rules of Golf that prohibit anchoring the club in making a stroke. The new Rule will go into effect on January 1, 2016, in accordance with the regular four-year cycle for changes to the Rules of Golf.

WHAT CHANGES?
The new entry—*Rule 14-1b*—prohibits strokes made with the club or a hand gripping the club held directly against the player's body or with a forearm held against the body to establish an anchor point that indirectly anchors the club.

WHAT THE RULE SAYS
In making a stroke, the player must not anchor the club, either "directly" or by use of an "anchor point."

NOTE 1:
The club is anchored "directly" when the player intentionally holds the club or a gripping hand in contact with any part of his body, except that the player may hold the club or a gripping hand against a hand or forearm.

NOTE 2:
An "anchor point" exists when the player intentionally holds a forearm in contact with any part of his body to establish a gripping hand as a stable point around which the other hand may swing the club.

PERMITTED
CLAW
CROSS-HANDED
LONG PUTTER NOT ANCHORED

PROHIBITED
MID-LENGTH PUTTER ANCHORED AGAINST STOMACH
ANCHORED LONG PUTTER

REVIEW AND TIMETABLE
Between 2011 and 2012: Golf's governing bodies begin observing a dramatic increase in the use of anchoring at all levels of the game.
February 2012–February 2013: The USGA announces it is taking a "fresh look" at the anchored strokes; review continues throughout 2012. In November, the proposed Rule is announced. Prior to final action, the USGA and The R&A accept questions and comments.

Figure 1: Extract from proposals for the new anchoring rule in golf (R&A Ltd, 2014).

METHODS: Seventy-two healthy golfers (62 male, 10 female) participated ranging in age from 15 to 75. Participants were free from injury and held a current Golfing Union of Ireland (GUI) Handicap across the full spectrum from category 1 (≤ 5 handicap) to the top of category 5 (≤ 28 handicap). Seventy one of the seventy two participants were habitual standard length

putter users. All participants were right handed and were recruited through club notice boards, weekly newsletters and word of mouth. Approval for the use of human participants was obtained from the university review board of research compliance. Participants were informed of the experimental risks and signed an informed consent document before the investigation. All putting clubs and balls used in the study were of premium standard and supplied by Titleist Golf™. The specifications for each of the putters are listed in Table 1.

Table 1
Technical specifications of the putters used in the study

Putter	Loft (°)	Lie (°)	Length (m / inch)	Total mass (kg)	Neck
Standard	4	71	0.887 (34)	0.55	Single Bend
Belly	4	71	1.092 (43)	0.70	Single Bend
Long	4	79	1.321 (52)	0.85	Double Bend

The current study was conducted outdoors thus creating an ecologically sound natural environment for participants. The putt was straight and flat and thus did not require the participants to read the green. The reading from the Stimpmeter was 9.5 – 10.0. Putting parameters were recorded with a three-dimensional kinematic system (SAM PuttLab™, Science and Motion GmbH, Mainz, Germany) (Marquardt, 2007; Karlsen, Smith & Nilsson, 2008; Sones et al., 2012). Each participant was allowed to warm-up in a self-selected manner with a familiarisation practice period of ten minutes. No tuition was given. Calibration was achieved by lining up putts and as required using a laser device to align the putter head with the hole. This provided a relative calibrated start position for all golfers. Each participant was then asked to perform ten putts with each club from both distances. The order in which the putters were used was random as was the order from which distance the participant started. Belly and long putter clubs were used with an anchoring mechanism. Measures of backswing time (BSTIME), forward swing time from beginning of the forward swing to impact with the ball (TIMP), putter face angle at impact (FACEIMP), putter face rotation angle from the beginning of the forward swing to impact (ROTIMP) and horizontal putter impact spot (SPOTIMP) were recorded. In addition performance outcome measures data for successful and unsuccessful putts were amalgamated. Descriptive statistics and inter-putter variance was statistically analysed using a one-way analysis of variance (ANOVA) with a Bonferroni post-hoc test applied to any measures that showed significant variance. Significance level was set at 0.05.

RESULTS: Shown in Table two are the total number of putts holed and the percentage of successful putts with each putter, for all categories of golfer handicap, for short 1.83 m (6 ft) putts, and 3.66 m (12 ft) data are shown in Table three. Golfers were found to be most successful with the standard length putter from both distances. Table 4 illustrates the mean and standard deviation for all subjects using the three different putters from both distances, for the measures previously described. There was no significant club difference for FACEIMP for any of the putters. However significant differences were observed between clubs for all the other variables.

Table 2
Performance outcome scores for all participants from 1.83 m (6 ft) with three different putting clubs

All handicap categories from 1.83 m (6 ft)	TOTAL	%
Total successful putts with standard putter out of 720	578	80.3
Total successful putts with belly putter out of 720	566	78.6
Total successful putts with long handled putter out of 720	542	75.3
Total successful putts out of 2160	1686	78.1

Table 3
Performance outcome scores for all participants from 3.66 m (12 ft) with three different putting clubs

All handicap categories from 3.66 m (12 ft)	TOTAL	%
Total successful putts with standard putter out of 720	372	51.7
Total successful putts with belly putter out of 720	366	50.8
Total successful putts with long handled putter out of 720	338	46.9
Total Successful Putts out of 2160	1076	49.8

Table 4
Descriptive measures (mean \pm SD) for three putting clubs at two shot distances

Putter	BSTIME (ms)	TIMP (ms)	FACEIMP ($^{\circ}$)	ROTIMP ($^{\circ}$ /sec)	SPOTIMP (mm)
STANDARD (both distances)	604.12 \pm 135.87 ^a	277.7 \pm 59.89 ^b	0.23 \pm 3.37	4.9 \pm 3.04 ^d	1.03 \pm 8.44 ^a
BELLY (both distances)	621.29 \pm 137.28 ^a	283.02 \pm 60.71 ^c	0.25 \pm 2.9	4.96 \pm 2.83 ^d	-0.25 \pm 8.72 ^a
LONG (both distances)	634.04 \pm 126.52 ^a	290.55 \pm 62.34 ^{b c}	0.33 \pm 3.06	4.33 \pm 2.52 ^d	1.09 \pm 8.66 ^a
STANDARD 1.83 m	590.00 ^b \pm 139.70	277.72 \pm 62.03 ^b	0.29 \pm 3.31	4.36 \pm 2.58 ^b	2.11 \pm 6.72 ^f
BELLY 1.83 m	599.25 \pm 135.83	279.73 \pm 63.55 ^c	0.44 \pm 2.89	4.22 \pm 2.50 ^c	-0.07 \pm 8.29 ^f
LONG 1.83 m	609.93 \pm 126.39 ^b	290.46 \pm 69.89 ^{b c}	0.60 \pm 3.17	3.74 \pm 2.16 ^{b c}	1.03 \pm 9.13
STANDARD 3.66 m	618.24 \pm 130.54 ^{f b}	277.69 \pm 57.72 ^a	0.18 \pm 3.42	5.44 \pm 3.35 ^b	0.11 \pm 8.53
BELLY 3.66 m	643.33 \pm 135.28 ^f	286.32 \pm 57.59 ^a	0.06 \pm 2.93	5.69 \pm 2.94 ^c	-0.44 \pm 9.13 ^c
LONG 3.66 m	658.15 \pm 122.07 ^b	290.64 \pm 53.81 ^a	0.06 \pm 2.92	4.92 \pm 2.71 ^{b c}	1.14 \pm 8.17 ^c

^a between clubs $p < 0.05$, post-Hoc 1v2, 1v3

^b between clubs $p < 0.05$, post-Hoc 1v3

^c between clubs $p < 0.05$, post-Hoc 2v3

^d between clubs $p < 0.05$, post-Hoc 1v3, 2v3

^e between clubs $p < 0.05$, post-Hoc 1v2, 2v3
1=STANDARD 2=BELLY

^f between clubs $p < 0.05$, post-Hoc 1v2
3=LONG

DISCUSSION: The purpose of the present study was to examine putting outcome performance using different length putting clubs used with an anchoring mechanism. No significant club differences existed for overall shot performance. Significant differences were noted for backswing time (BSTIME), forward swing time (TIMP), putter face rotation from the beginning of the forward swing to impact (ROTIMP) and horizontal impact spot (SPOTIMP). Sones et al. (2012) found that using an anchored putter will not change your stroke and that the stroke performance with a standard putter will be the same as that with a belly putter and vice versa. Overall, results from the current study would suggest that is not the case, however, when the data are separated by distance there was no difference in backswing time between the standard putter and belly putter on a 1.83 m (6 ft) putt but there was a difference on a longer putt of 3.66 m (12 ft). Swing tempo ratio however, was not affected.

Pelz (2000) established that face angle contributes to 83% of the effect on the putt line but also not hitting the ball out of the sweet spot will have an adverse effect on the speed and distance control of the ball. This effect can be minimised by consistently hitting the ball in the same spot on the clubface. Both putter head path rotation through impact (ROTIMP) and putter face impact location (SPOTIMP) are important factors when trying to hit the ball out of the 'sweet spot'. The results of the current study showed that there was a significant difference in ROTIMP and SPOTIMP between the standard and belly putter and the belly and long putter. While an anchoring mechanism may reduce putter head rotation via reduced degree-of-freedom of the wrists, it does not sufficiently limit rotation. MacKenzie et al (2010) and Karlsen et al (2008) showed that while impact location may vary, it does not have a large influence on short putt success from four metres.

Participants in the current study were successful 78.06% of the time from 1.83 m (6 ft) irrespective of which putter they used. This is compared to a 75.45% on the PGA Tour from the same distance for the top thirty golfers in 2014. For longer 3.66 m (12 ft) putts, on average the participants in this study were successful 49.8% of the time from this distance compared to 35.4% on the PGA Tour top thirty over a similar distance of 3.05m (10ft) to 4.57m (15ft). As in the case of the shorter putt (1.83 m, 6 ft) players were more successful with the standard putter (51.7%) than the other two putters, 50.8% and 49.6% for the belly and long putters respectively.

CONCLUSION: For a large cohort of different handicap golfers not accustomed to using longer putters, using an anchored putter will not necessarily provide a scoring advantage over using a standard putter without an anchoring system. All trials showed more successful putts with the standard putter. This study tested seventy two golfers on a one-off test and no training or tuition was given to the participants. Further study is needed to test what effect a training programme may have on all golfers. Experimenting with different types of putter and grips would be useful in finding a putting method and style that suits each individual golfer. Results showed that all golfers, regardless of which putter used, coped with changes in putter face impact location and rotation angle by very consistent swing tempo and putter face angle at impact. Anchoring does not seem to provide a putting performance advantage.

REFERENCES:

- Hurrion, P.D., & Hurrion, R. D. (2008). An investigation into Weight Distribution and Kinematic Parameters during the Putting Stroke. In *Science and Golf V: Proceedings of the World Scientific Congress of Golf*, 31, 232-238.
- Karlsen, J. (2010). Performance in golf putting, (Unpublished doctoral thesis). Norwegian School of Sport Sciences, Norway.
- Karlsen, J., Smith, G., & Nilsson, J. (2008). The stroke has only a minor influence on direction consistency in golf putting among elite players, *Journal of Sports Sciences*, 26, 243-250.
- MacKenzie, S. J., Evans, D. B. (2010). Validity and reliability of a new method for measuring putting stroke kinematics using the TOMI system. *Journal of Sports Sciences*, 28, 891-899.
- Marquardt, C. (2007). The SAM PuttLab. Concept and PGA Tour data. *Annual Review of Golf Coaching 2007: International Journal of Sports Science & Coaching*, 2, 101-114.
- Pelz, D. (2000). *Putting bible: The complete guide to mastering the green*. New York, NY: Doubleday.
- Sones, T, Filmlalter, M, DeNunzio, D., & Chwasky, M. (2012). Belly vs Short. *Golf Magazine*, 54(1), 81-88.
- The R&A Ltd.* (2014). *Rules and amateur status*. Retrieved from <http://www.randa.org/en/Rules-and-Amateur-Status.aspx> .

Acknowledgement

The authors express thanks to Titleist for supplying test clubs.

A SIMPLE METHOD TO MEASURE EXTERNAL FORCE, POWER OUTPUT AND EFFECTIVENESS OF FORCE APPLICATION DURING SPRINT ACCELERATION

Jean-Benoit Morin

Laboratory of Human Motricity, Education Sport and Health, University of Nice
Sophia Antipolis, France

The aim of this applied session was to introduce and show a recently validated simple field method to determine individual force, velocity, power output properties and effectiveness of force application onto the ground during a sprint running acceleration. This method requires the use of a radar device (or several timing gates), and models the horizontal, vertical and resultant force an athlete develops over sprint acceleration using a macroscopic inverse dynamic approach. Low differences in comparison to force plate data support the validity of this simple method to determine force-velocity relationship and maximal power output, as well as the index of effectiveness of force application onto the ground. Its validity and ease of use make it an interesting tool for sprint training and performance optimization, in a specific field context of practice.

KEY WORDS: acceleration, power output, ground reaction force, mechanical effectiveness.

INTRODUCTION: Sprint running is a key factor of performance in many sport activities (track and field events, soccer, rugby, etc.). Sprint performance implies large forward acceleration, which is directly depending on the capacity to develop and apply high amounts of horizontal external force onto the ground at various speeds over the sprint acceleration (Morin et al., 2011). The overall capability of athletes to produce external horizontal force during sprint acceleration is very well described by the linear force-velocity (F-V) relationship (Morin et al., 2012; Rabita et al., 2015). This macroscopic relationship describes the mechanical limits of the entire neuromuscular system during sprint propulsion and is well summarized through the maximal force (F_0) and velocity (V_0) this system can develop, and the associated maximal power output (P_{max}). Furthermore, the slope of the F-V relationship determines the individual F-V mechanical profile, i.e. the ratio between force and velocity qualities, which has recently been shown to determine explosive performances, independently from the influence of P_{max} (Samozino et al., 2012). These parameters are a complex integration of numerous individual muscle mechanical properties, morphological and neural factors affecting the total external force developed by sprinters lower limbs, but also of the technical ability to apply/orient the external force effectively onto the ground (Morin et al. 2011, 2012). Consequently, determining individual F-V characteristics and P_{max} specifically during sprint propulsion is of great interest for coaches and sport practitioners, and could be an objective functional assessment of muscular capability for sprint acceleration, in both training and injury management context. However, such evaluations hitherto required to test athletes on motorized instrumented sprint treadmills measuring force, velocity and power output very accurately, or to use track-imbedded force plates and complex experimental design (Morin et al. 2012; Rabita et al., 2015). This technical limitation made such measurements impossible to most scientists and sport practitioners. A simple method that accurately measures the main external mechanical outputs of sprint acceleration (F-V relationships, P_{max} and effectiveness of force application) in field conditions could therefore be interesting and useful to generalize such evaluations for training or scientific purposes. Such a simple method has been recently presented and validated against reference force plate measurements (Samozino et al., 2015), and the aim of this applied session was to show how to use this method, from data collection to data processing and results interpretation.

METHODS: The method presented requires completing a single all-out sprint starting from a null velocity position (starting-blocks or standing crouched position, depending on subjects'

preference and specialization). The sprint distance must be long enough to allow for maximal or almost (>95%) maximal running speed to be reached. This distance depends on subjects skills and ranges approximately from 30 to 60 m. In the applied session, a 40-m distance was used. Running speed was measured with a radar device (Stalker ATS pro II, RadarSales, Minneapolis, USA) at a sampling frequency of 47 Hz (Figure 1). During such a running acceleration, the velocity-time curve has been shown to consistently follow a mono-exponential function: $V(t) = V_{\max} \cdot (1 - e^{-t/\tau})$, with V_{\max} the maximal velocity reached and τ the acceleration time constant. For more accuracy in $V(t)$ derivation, the radar curve was fitted with such an exponential function using the least square regression method. Then, the horizontal acceleration (a) of the body center of mass as a function of time can then be expressed after derivation of $V(t)$ over time as: $a(t) = (V_{\max}/\tau) \cdot e^{-t/\tau}$. The net horizontal external force (F_H) was then modeled over time as: $F_H(t) = m \cdot a(t) + F_{air}$, with F_{air} the aerodynamic friction force to overcome during sprint running computed from running velocity and an estimation of runner's frontal area and drag coefficient (Arsac et al., 2002).

In the vertical direction, during such an acceleration, the runner's body center of mass position goes up from the starting position to the standing running position, and then does not change from one complete step cycle to another. Since this initial upward movement is overall smoothed through a relative long time/distance (~40 m, Cavagna et al., 1971), we considered that the mean net vertical acceleration of the CM over each step was almost null throughout the sprint acceleration phase. Consequently, applying the fundamental laws of dynamics in the vertical direction, the mean net vertical GRF (F_V) applied to the runner's center of mass over each complete step can be modeled over time as equal to body weight: $F_V(t) = mg$, where g is the gravitational acceleration ($9.81 \text{ m} \cdot \text{s}^{-2}$).

Morin et al. (2011) proposed that the technical ability of force application during running acceleration could be quantified over each support phase or step cycle by the ratio (RF in %) of F_H to the corresponding total resultant GRF (F_{RES} , in N), and over the entire acceleration phase by the slope of the linear decrease in RF when velocity increases (D_{RF} , see Morin et al. 2011 and Rabita et al. 2015): $RF = (F_H/F_{RES}) \cdot 100 = F_H / [(F_H^2 + F_V^2)^{0.5}] \cdot 100$.

For more accuracy (linear decrease in RF as speed increases, after the initial rise in center of mass position during the first few steps), D_{RF} was computed from F_H and F_V values modeled for $t > 0.3 \text{ s}$.

Last, mechanical power output in the horizontal direction (P) was computed as $P(t) = F_H(t) \cdot V(t)$, and from these force-, velocity- and power-time expressions, we determined the linear F-V and second degree polynomial P-V relationships, and compute F_0 , V_0 and P_{\max} for the subjects tested.

DISCUSSION: The main advantage of the method presented during this applied session is that it makes possible to accurately measure the main macroscopic output of sprint running performance from a few input variables that are pretty simple to obtain in field conditions of practice. This method makes possible to estimate GRFs in the sagittal plane of motion during one single sprint running acceleration from anthropometric (body mass and stature) and spatiotemporal (split times or instantaneous running velocity) data. Furthermore, this model can then be used as a simple method to determine the F-V and P-V relationships and the associated variables, as well as the mechanical effectiveness of force application parameters (RF and D_{RF}). The concurrent validity and the reliability of this method have been clearly demonstrated by a direct comparison to track-imbedded force plate measurements (for full details, see Samozino et al., 2015), and the devices required are pretty cheap and easy to use compared to the only existing alternative, i.e. track-embedded force plates. In addition, to date no data has been published on direct measurements of ground reaction forces over 40-m sprints. Such data have only recently been approached using a multiple sprint study design (Rabita et al., 2015).

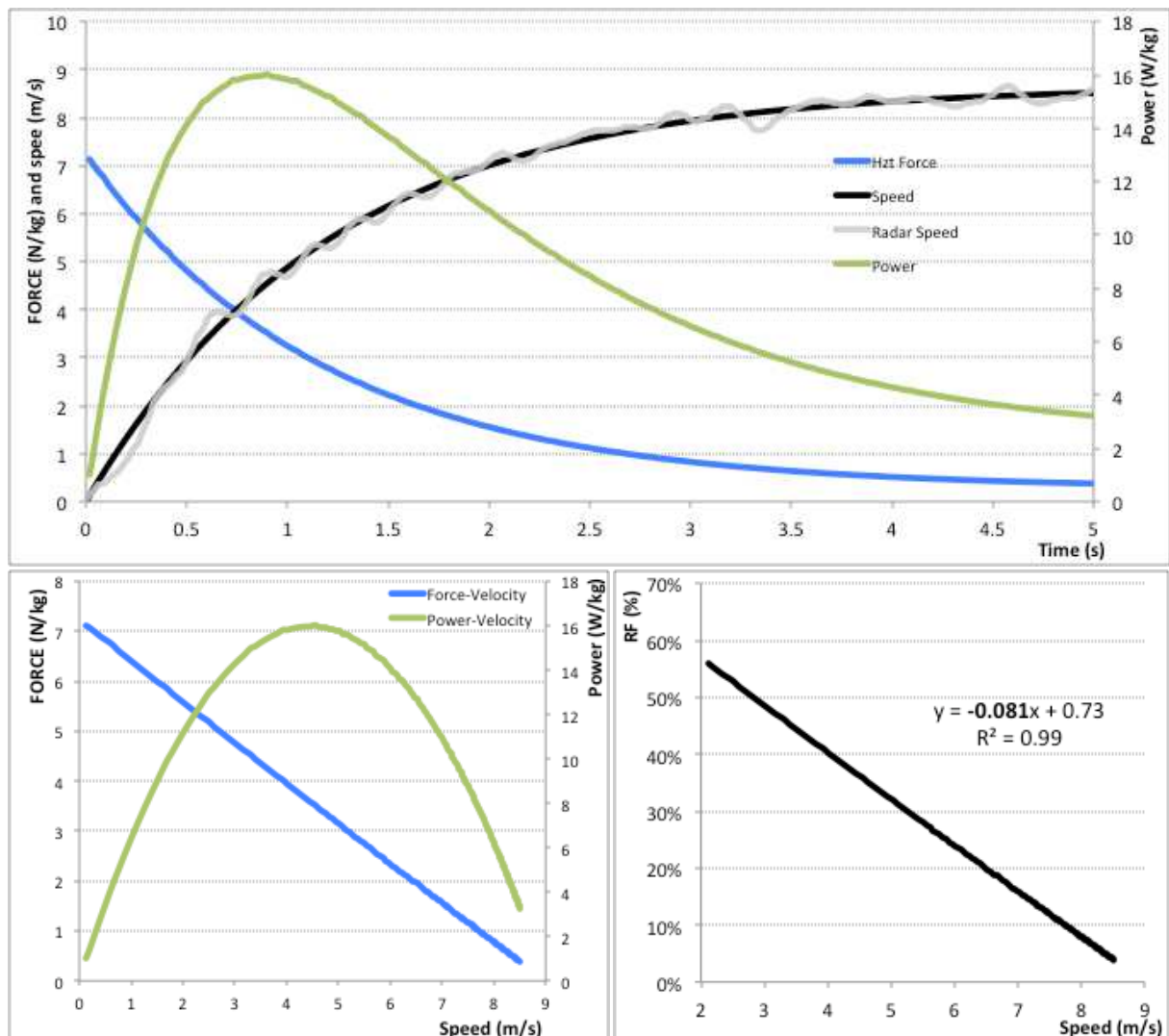


Figure 1: Typical computations using the method presented (data for a 20 years old physically active subject, 72 kg, not sprint specialist). The instantaneous running speed was measured with a radar device (47 Hz, upper panel, grey trace) from start to maximal speed. Then, the speed-time curve was modeled with a mono-exponential equation (upper panel, black trace), and instantaneous horizontal net ground reaction force (upper panel, blue trace) and corresponding mechanical power (upper panel, green trace) were computed. The lower left panel shows the force-velocity (blue trace) and power-velocity (green trace) relationships. The lower right panel shows the linear decrease in the ratio of force with increasing speed. The D_{RF} for this individual is -0.081.

Although it allows computation of variables that were hitherto impossible to obtain in such conditions (i.e. sprint acceleration mechanical outputs and effectiveness of ground force application over an entire sprint acceleration), this method has limitations. For instance, it does not consider the inter-step variability, or other important variables such as ground impulse or rate of force development. Furthermore, it does not help better understand the determinants of F_0 , V_0 and other integrative variables described. Therefore, further research is needed to go further into the details of the important features of these F-V and P-V profiles in sprinting, with potential improvements of performance (through training) and injury prevention (through a more accurate understanding of the mechanical key features of the acceleration capability).

In conclusion, the simple field method presented in this applied session allows sport scientists and practitioners to accurately measure the main sprint acceleration mechanical outputs, draw and explore the force-velocity and power-velocity relationships, and investigate the effectiveness of force application onto the ground. This might have direct applications in the field of performance analysis, training, rehabilitation and injury prevention, in all the sports that include sprint accelerations.

REFERENCES:

- Arsac, L.M., & Locatelli, E. (2002). Modeling the energetics of 100-m running by using speed curves of world champions. *Journal of Applied Physiology*, 92, 1781-1788.
- Cavagna, G.A., Komarek, L., & Mazzoleni, S. (1971). The mechanics of sprint running. *Journal of Physiology*, 217, 709-721.
- Morin, J-B., Edouard, P., & Samozino, P. (2011). Technical ability of force application as a determinant factor of sprint performance. *Medicine and Science in Sports and Exercise*, 43, 1680-1688.
- Morin, J-B., Bourdin, M., Edouard, P., Peyrot, N., Samozino, P., & Lacour, J-R. (2012). Mechanical determinants of 100-m sprint running performance. *European Journal of Applied Physiology*, 112, 3921-3930.
- Rabita, G., Dorel, S., Slawinski, J., Saez de villarreal, E., Couturier, A., Samozino, P., & Morin, J-B. (2015). Sprint mechanics in world-class athletes: a new insight into the limits of human locomotion. *Scandinavian Journal of Medicine and Science in Sports*. In press.
- Samozino, P., Rejc, E., Di Prampero, P.E, Belli, A., & Morin, J-B. (2012). Optimal force-velocity profile in ballistic movements. *Altius: citius or fortius? Medicine and Science in Sports and Exercise*, 44, 313-322.
- Samozino, P., Rabita, G., Dorel, S., Slawinski, J., Peyrot, N., Saez de Villarreal, E., & Morin, J-B. (2015). A simple method for measuring power, force, velocity properties and mechanical effectiveness in sprint running. *Scandinavian Journal of Medicine and Science in Sports*, in press.

Acknowledgements

We are very grateful to Dr Pierre Samozino (Université de Savoie-Mont Blanc) and all the other co-authors who collaborated to design and validate the method presented during this applied session.

THE APPLICATION OF FUNCTIONAL DATA ANALYSIS TECHNIQUES FOR CHARACTERIZING DIFFERENCES IN ROWING PROPULSIVE-PIN FORCE CURVES.

John Warmenhoven¹, Richard Smith¹, Conny Draper¹, Stephen Cobley¹, Andrew Harrison², Norma Bargary³.

Exercise and Sports Science, University of Sydney, Sydney, Australia.¹

Physical Education and Sport Sciences, University of Limerick, Limerick, Ireland.²

Department of Mathematics and Statistics, University of Limerick, Limerick, Ireland.³

The pattern of propulsive force (measured at the pin), represented by force-time and force-angle graphs, typically differs among rowers. How the pattern differs according to competition level and gender has not been identified. Functional data analysis (FDA) techniques were used on force-time and force-angle data to identify the main modes of variance in curves representing thirty eight rowers of different competition levels (domestic, underage international and open international) and different gender. Stepwise discriminant function analysis showed strong classification of rowers using force-time and force-angle graphs and strong classification of female rowers. Male rowers, Underage rowers and Open International rowers showed weaker classification. Despite this, FDA provided useful information for the assessment of rowing performance.

KEY WORDS: principal components analysis, shape, waveform, on-water.

INTRODUCTION: The idea of a rowing technique ‘signature’ was first proposed by researchers in the nineteen seventies, and was associated with execution of the pulling force on the oar handle (Ishiko, 1971). A force signature is usually represented graphically with force either plotted against time (Smith & Spinks, 1995) or against the horizontal angle of the oar (Spinks, 1996); and rowers have been qualitatively identified by their distinctive shape on such graphs. However, empirical research analysing the specific importance of shape characteristics and their relationship with performance is currently limited. Yet the use and manipulation of ‘signatures’ to enhance performance is feasible. Two strategies for investigating differences in the shape of force-time and force-angle profiles are ‘Functional Principal Components Analysis’ (*fPCA*) and ‘Bivariate Functional Principal Components Analysis’ (*bfPCA*), from the Functional Data Analysis (FDA) family of statistical techniques (Ramsay, 2006). The benefits of *fPCA* and *bfPCA* for assessing trends in biomechanical variables have already been highlighted for use on vertical jump performance (Ryan, Harrison & Hayes, 2006; Harrison, Ryan & Hayes, 2007). In rowing the shape of the force-time curve could be analysed using *fPCA*, and the force-angle profile could be analysed using *bfPCA*. In the present study, data obtained on thirty eight athletes were processed to assess whether force trends in continuous data can be used to discriminate between rowers, and whether they can predict competition level and gender.

METHODS: Subjects: Following institutional ethical approval, data from thirty eight subjects were analysed (11 male, 27 female). The rowers consisted of highly trained heavyweight and lightweight scullers. Athletes were classified as Domestic (D) ($n = 20$), Australian International Underage (IU) ($n = 7$) or Australian International Open (IO) ($n = 11$) athletes.

Testing and Data Processing: Athletes were directed to row at four stroke rates in 250m steps (20, 24, 28, 32 Str min^{-1}), separated by one minute of light rowing. Ten strokes from the 32 Str min^{-1} data only were analyzed. The drive and recovery phases were identified using the horizontal angle of the oar (Smith & Loschner, 2002), and only the drive phase was analysed for this study. A linear length normalization strategy using an interpolating cubic spline was applied, normalizing each curve to 100% of the drive phase. An amplitude normalization (AN) technique was also applied, ensuring that variability described in the curves was only reflective of shape characteristics independent of amplitude. For AN, force was converted to a percentage relative

to each curve's maximum value. Similarly, horizontal oar angle was normalized to a percentage relative to the length of each drive phase. Both normalization formulas are below:

$$Force_{Norm(i)} = \left(\frac{Force_{(i)}}{Force_{(Maximum)}} \right) \times 100(\%) \quad \quad \quad Angle_{Norm(i)} = \left(\frac{Angle_{(i)}}{Angle_{(Maximum)} - Angle_{(Minimum)}} \right) \times 100(\%)$$

The horizontal oar angle normalization strategy is expressed as a relative percentage of the drive phase length, but still preserves important information on where the oar is relative to the boat. An average curve created from each participant's ten strokes was used for further analysis.

fPCA and bfPCA: For fPCA, B-spline basis functions were used for creation of force-time curves. The smoothing parameter was selected using a generalized cross validation (GCV) procedure and from these curves the functional principal components were derived. Each force-time curve was weighted by each of the first five functional principal components (fPCs), with resulting scalar averages referred to as fPC scores. For bfPCA, B-spline basis functions were used for force-time and angle-time curves. The smoothing parameter was again selected using a GCV procedure. A composite function was derived from the inner product of the bivariate functions. The composite function was then used to extract a set of bivariate functional principal components (bfPCs) and corresponding bfPC scores (Ramsay, 2006).

Discriminant Analysis: fPC and bfPC scores were input to separate stepwise discriminant function analyses (SDFA) for classification according to competition level and gender. The smallest Mahalanobis distance (D2) procedure was used in each case using prior allocation probabilities to account for the different sample sizes in each comparison.

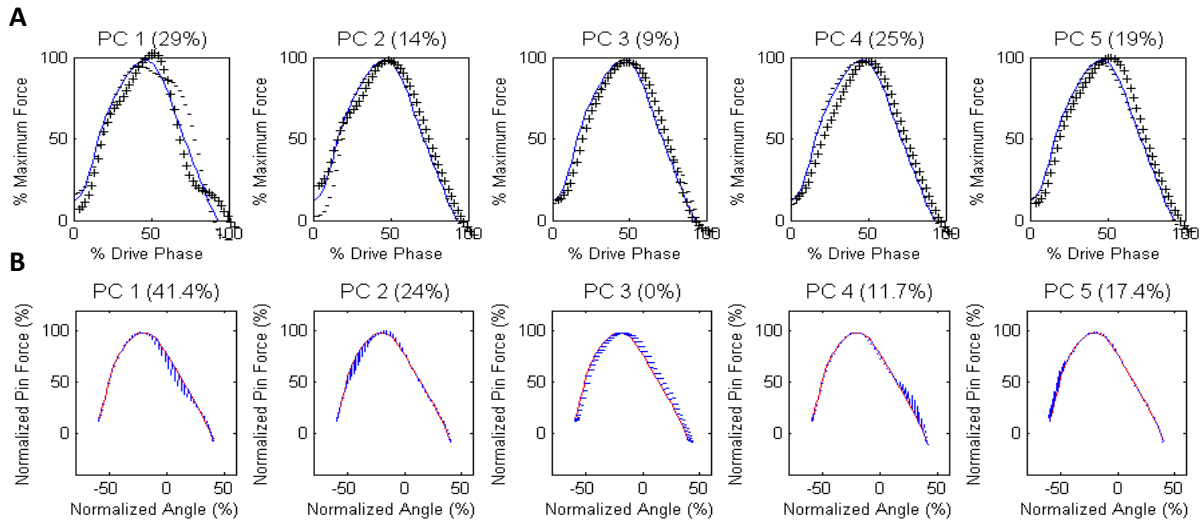


Figure 1. The first five varimax rotated fPCs (A) and bfPCs (B). For fPCs, the blue line represents mean force-time, the '+' line represents positive scorers who are +2SD and the '-' line represents negative scorers who are -2SD from the mean function. For bfPCs, the red line represents the mean force-angle function and the blue lines represent positive scorers +2SD from the mean function.

RESULTS: The corresponding percentage contribution for each fPC and bfPC to the total variability in all curves are shown in Figure 1. Mean scores for fPCs and bfPCs are in Table 1.

SDFA for competition levels using fPCA: fPC2 had the greatest discriminating power for the first step ($p < 0.001$), demonstrating a change in the pattern of force production in the first half of the drive phase. In the second step, fPC4 was identified ($p = 0.017$) showing a greater rate of

force development early in the drive phase for negative scorers, and in the third step *fPC3* was identified ($p = 0.017$), showing greater force production leading into the finish.

SDFA for competition levels using *bFPC*: Scores on *bFPC2* had the greatest discriminant power for the first step ($p = 0.002$), demonstrating a lower rate of force development leading into maximum force, but a better ability to maintain a higher force closer to square-off for positive scorers. In the second step, *bFPC4* was also identified ($p < 0.001$), showing a greater ability to produce force at the end of the drive phase.

SDFA for gender using *fPCA*: *fPC5* ($p < 0.001$), *fPC3* ($p < 0.001$) and *fPC4* ($p < 0.001$) were discriminating variables for classification, with each identified in separate steps.

SDFA for gender using *bFPC*: *bFPC1* ($p < 0.001$) and *bFPC4* ($p < 0.001$) were discriminating variables for classification, with each identified in separate steps. *bFPC1* showed a reduction in force production after reaching maximum force for positive scorers. The results of the discriminant analyses using *fPC* and *bFPC* scores for force-time and force-angle data as predictors of competition level and gender are shown in Table 1.

Table 1. *fPCA* and *bFPCA* mean (SD) scores for competition level and gender (A). Percentages of correct classification of *fPCA* (B) and *bFPCA* (C) for competition and gender.

(A) Competition Level <i>fPCA</i> and <i>bFPCA</i> scores				Gender <i>fPCA</i> and <i>bFPCA</i> scores			
		<i>fPCA</i>	<i>bFPCA</i>			<i>fPCA</i>	<i>bFPCA</i>
<i>D</i>	PC1	-3.4 (43.4)	-7.5 (52.1)	<i>F</i>	PC1	9.2 (34.8)	14.9 (43.7)
	PC2	-10 (26.9)	-2.4 (37.5)		PC2	2.7 (24.1)	-6.6 (38.9)
	PC3	0.2 (19.6)	-6.5 (24.1)		PC3	-5.1 (21.1)	0.7 (24.5)
	PC4	3.6 (35)	-2.3 (21.1)		PC4	-6.8 (34.3)	4.5 (22.5)
	PC5	4.7 (31.1)	-10.7 (31)		PC5	-11.3 (29.8)	3.6 (26.8)
<i>IU</i>	PC1	8.2 (24)	15.6 (35.3)	<i>M</i>	PC1	-22.6 (43.2)	-36.4 (46.3)
	PC2	24.4 (27.2)	-25.3 (32.4)		PC2	-6.6 (34.5)	16.2 (38.2)
	PC3	-15.5 (16.2)	-2 (23.1)		PC3	12.5 (18.8)	-1.8 (22.8)
	PC4	-26.3 (28.9)	13.8 (19.9)		PC4	16.6 (39.1)	-11.1 (23.5)
	PC5	-13.6 (27.8)	27.9 (28.5)		PC5	27.8 (20.1)	-8.9 (39.9)
<i>IO</i>	PC1	1 (41.9)	3.76 (53.1)				
	PC2	2.6 (17.9)	20.5 (39.2)				
	PC3	9.5 (24)	13.1 (19)				
	PC4	10.1 (38.7)	-4.6 (27.9)				
	PC5	0 (36.6)	1.8 (22.1)				

(B) Competition Level <i>fPCA</i> - % Classified				Gender <i>fPCA</i> - % Classified			
	<i>D</i>	<i>IU</i>	<i>IO</i>		<i>F</i>	<i>M</i>	
<i>D</i>	87.5	2.5	10.0	<i>F</i>	90.7	9.3	
<i>IU</i>	50.0	35.7	14.3	<i>M</i>	27.3	72.7	
<i>IO</i>	36.4	9.1	54.5				

(C) Competition Level <i>bFPCA</i> - % Classified				Gender <i>bFPCA</i> - % Classified			
	<i>D</i>	<i>IU</i>	<i>IO</i>		<i>F</i>	<i>M</i>	
<i>D</i>	85.0	5.0	10.0	<i>F</i>	92.6	7.4	
<i>IU</i>	42.9	57.1	0.0	<i>M</i>	27.3	72.7	
<i>IO</i>	45.5	9.1	45.5				

DISCUSSION: The purpose of this paper was to see if FDA-analysed force-time and force-angle data from single scullers could be used to discriminate between their competition level and gender. If the analysis was successful it could be a method of identifying the 'ideal' force-angle shape characteristic of competition-winning scullers. Knowing the shape of the force-

angle profile is critical for the development of strength and conditioning strategies (Korner and Schanitz, 1987). In the present study *fPCs* and *bPCs* discriminated best between domestic and international open rowers. These results initially suggested that increased force near the start and the end of the drive phase may not be as important as increased force when the horizontal oar angle is closer to zero degrees, especially indicated by *bPC2*. Despite this, both *fPC* and *bPC* scores provided high correct classification percentages for domestic rowers but comparatively weaker percentages of classification for international underage and open rowers. It is possible that the skill in applying force to the oar is quite similar at lower performance levels, but international underage and open rowers have subsequently learned to adapt the shape of their force signatures with experience and potentially 'individualize' these shapes to fit other key performance characteristics. Both *fPC* and *bPC* scores also provided high correct classification percentages for gender, particularly for female rowers. Female rowers demonstrated a better ability to develop force early in the stroke and maintain force leading into the release, but males demonstrated a greater ability to maintain a higher force production closer to the oar angle equaling zero degrees. As a result of these differences it is advisable to assess shape characteristic differences independent of gender, given that gender effects in the present study may have masked the discriminating ability of FDA at higher competition levels. Importantly, this preliminary investigation into shape differences has also been able to show the use of *bPCA* in particular as a novel method for assessment of the force-angle profile, something which has traditionally been assessed qualitatively. It is known that the shape of the force/angle profile has reflected the seat that the rower occupies in a crewed boat (Smith and Loschner, 2002; Roth, Schwanitz, Pas & Bauer, 1998). The FDA method described here provides a quantitative analysis of curve shape that can clearly isolate and define time segments where changes can be made to better approximate an elite performance. The importance of segments of the force curves suggested by the *f/bPCA* analysis provides a strong evidence base for discussions with coaches and athletes about how to increase performance in on-water rowing.

REFERENCES:

- Harrison, A. J., Ryan, W., & Hayes, K. (2007). Functional data analysis of joint coordination in the development of vertical jump performance. *Sports Biomechanics*, 6(2), 199-214.
- Ishiko, T. (1971). Biomechanics of rowing. In J. a. W. Vredenburg, J. (Ed.), *Biomechanics II, International Series on Biomechanics* (Vol. 2, pp. 249-252). Eindhoven, Netherland. Baltimore, MD: University Park Press.
- Körner, T., & Schwanitz, P. (1987). *Rudern*. Sportverlag.
- Ramsay, J. O. (2006). *Functional data analysis*. John Wiley & Sons, Inc.
- Roth, W., Schwanitz, P., Pas, P., & Bauer, P. (1993). Force-time characteristics of the rowing stroke and corresponding physiological muscle adaptations. *International Journal of Sports Medicine*. 14, S32-S34.
- Ryan, W., Harrison, A., & Hayes, K. (2006). Functional data analysis of knee joint kinematics in the vertical jump. *Sports Biomechanics*, 5(1), 121-138.
- Smith, R. M., & Loschner, C. (2002). Biomechanics feedback for rowing. *Journal of Sports Sciences*, 20(10), 783-791.
- Smith, R. M., & Spinks, W. L. (1995). Discriminant analysis of biomechanical differences between novice, good and elite rowers. *Journal of sports sciences*, 13(5), 377-385.
- Spinks, W. (1996). Force-angle profile analysis in rowing. *Journal of Human Movement Studies*, 31(5), 211-233.

Acknowledgement

The authors would like to acknowledge the International Society of Biomechanics in Sport as this project was supported by an ISBS Student Mini Research Grant for 2014.

COMPARISON OF TWO PEDALING SENSORS, ICRANKSET AND SRM, AGAINST A STANDARD REFERENCE SENSOR

**Julien Bernard, Arnaud Decatoire and Patrick Lacouture
Institute Pprime, CNRS & University of Poitiers, Poitiers, France**

Our aim was *i)* to validate the I-Crankset sensor (I-CS) with a reference torque sensor (RTSL) for the calculation of crankset torque, power and work outputs and *ii)* to compare I-CS with the SRM sensor, a popular device. SRM and I-CS sensors were mounted simultaneously on a test bench instrumented with the RTSL used to validate I-CS. The protocol included multiple sets of 30 pedaling cycles in three conditions to explore various solicitations. Torque magnitudes, angular velocity and power output were compared using the coefficient of multiple correlation inter-protocol. The results showed a good validity of both the I-CS and SRM for all the conditions in comparison to RTSL for torque's measurements and power's calculations, even if an average angular velocity is used by SRM. But this one showed its limitations when calculating the work output.

KEY WORDS: powermeter, SRM sensor, I-Crankset sensor, validation, cycling.

INTRODUCTION: In the last decade, several measurement systems have been designed to evaluate the crankset torque and power output during pedaling. These tools are used by cyclists and coaches both during training and competition sessions. SRM (Schöberer Rad Meßtechnik, Julich, Germany) and I-CS (SENSIX Society, Poitiers, France) are two interesting systems that cyclists can install on their own bike on the road or during laboratory testing. Many authors proposed validation studies of cycling powermeters [eg PolarS710 (Millet, 2003), PowerTap (Bertucci, 2005), SRM (Paton, 2001)]. But no study has validated the I-CS. This newer mobile cycling powermeter measures the forces and torques produced at the right and left pedals together with pedals' orientation and then calculates the resultant torque and power output at the crankset. To our knowledge, no study has compared torque obtained with powermeter to reference torque sensor's measurements. The aim of this study was to assess the validity of the I-CS with a RTSL [Eaton Corporation, Troy Michigan, USA] and to compare it to the SRM.

METHODS: Subject One subject took part in this study since the aim of this work was to validate a measurement chain. The validation should be independent of the subject, of his level of practice and of his technique. Before the tests, the cyclist was verbally informed of the objectives of the study. He gave written his consent. The test bench was composed of several elements (Figure 1).

Instrumentation: The chainring (A) was used to connect the ergocycle to the bench through a chain. The RTSL (C) was installed on the axis (B), and finally a flywheel (D) used to modify the resistive load through a mechanical braking device (E) compound tray to put additional masses. The cyclist had to produce a pedaling torque to overcome that resistive load. The SRM uses a technology based on strain gauges to measure the torque and calculates an average angular velocity for each revolution of the chainring. The I-CS calculates torque and instantaneous angular velocity from measurements of instrumented pedals (six load components and optical encoders positioned on the crankset axis). After calibration procedure, precision of the RTSL was 1 Nm. All the signals are acquired at 200 Hz. We recorded a synchronization signal from the acquisition system of the I-CS in order to synchronize all the measuring devices. Thus, for each cycle and for each acquisition system, we had the same number of acquisitions.

Protocols The rider adjusted the cycle ergometer (saddle and handlebar positions) according to his personal preference. The validation protocol was implemented to realize

multiple pedaling conditions included in three conditions presented in table 1. Verbal instructions were given to the cyclist and feedback of mechanical power and cadence were displayed on the "Power Control" SRM bicycle computer.

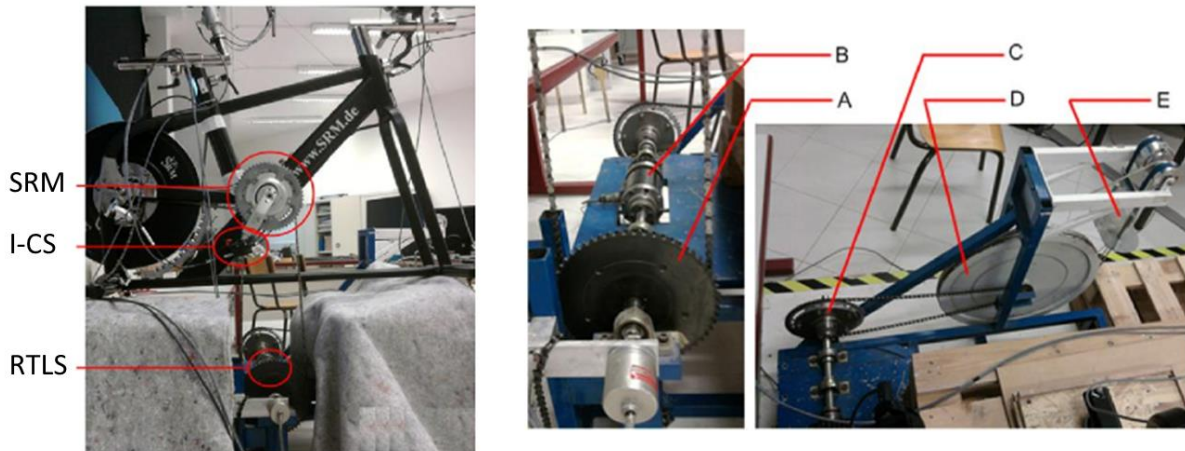


Figure 1: Test bench description: SRM sensor, instrumented pedals by I-CS sensor, RTSL (B), chainrings (A,C), flywheel (D) and mechanical braking device (E).

Table 1: The pedaling conditions. The C1 was obtained with both fixed pedaling cadence and resistive load; C2 with a fixed pedaling cadence and an increasing resistive load and C3 with a fixed resistive load and an increasing pedaling cadence.

Conditions	C1	C2	C3
Resistive load	26 Nm	18 to 30 Nm	42 Nm
Pedaling cadence	80 rpm	80 rpm	56 to 90 rpm

Statistical analysis: For each condition, the same analysis was performed on torque, angular velocity and power output obtained from the different systems. The pedaling cycles, once normalized were compared using a coefficient of multiple correlation inter-protocol (CMC_{ip}) proposed by Ferrari (2010). The CMC_{ip} is designed to appreciate the similarity of the measures given by various sensors in a single acquisition of the same parameter. In our case, the CMC_{ip} compared two by two the values obtained for the three parameters for each cycle. A CMC_{ip} close to 1, indicates that values obtained by two devices are significantly identical while a value less than 0.95 indicates no possible conclusion on significant similarity of the measured values.

RESULTS: Torque comparison: The signals are compared pairwise; the torque produced by the RTSL is compared with those given by I-CS and SRM. Then the data from the I-CS and SRM are also compared (Figure 2). Table 2 reports the average values of the CMC_{ip}^{Torque} obtained for the comparison of the torque measured for the three systems and for the three conditions. All the values are very close to 1.

Angular velocity comparison: Similarly to the torque, we calculated $CMC_{ip}^{Velocity}$ for the angular velocities measured by SRM and I-CS. By the way it is design, the SRM determines a constant value of angular velocity averaged over the cycle (see dashed line of second graph of figure 2). By calibration, RTSL and I-CS give the same instantaneous cranks' angular velocity thus resulting to $CMC_{ip}^{Velocity}$ equal to 1. In contrast, there is no similarity for the angular velocity between I-CS and SRM sensors; result confirmed by the complex values of $CMC_{ip}^{Velocity}$ (not reported here).

Mechanical power output comparison: Table 2 also shows the values of CMC_{ip}^{Power} for the mechanical power output. Whatever the systems used and whatever the conditions, CMC_{ip}^{Power} values averaged over all cycles are greater than 0.95.

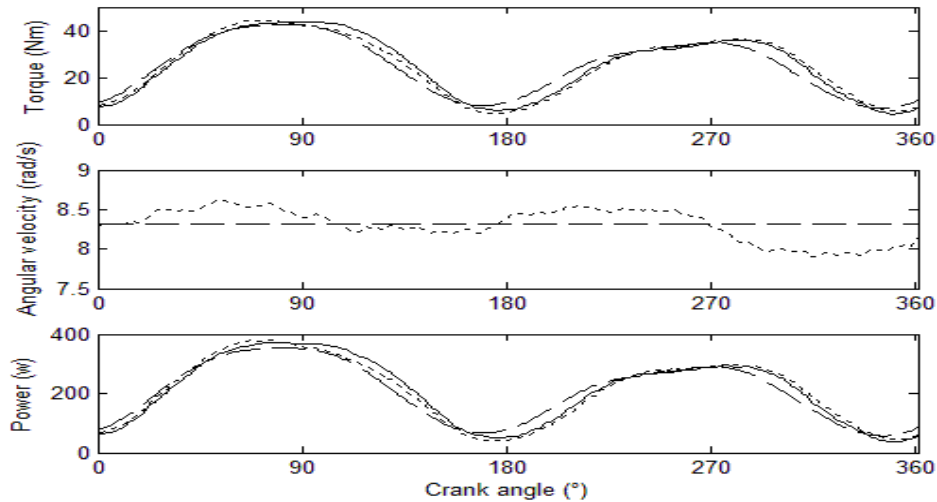


Figure 2: Representation of one cycle for the torque, angular velocity and power obtained with RTSL (solid line), I-CS (dotted line) and SRM (dashed line). The cycle starts at 0° with the left pedal in the top dead center.

Table 2: Average values of the CMC_{ip}^{Torque} and the CMC_{ip}^{Power} obtained for all cycles measured by the different sensors and the different pedaling conditions.

	C1		C2		C3	
	Torque	Power	Torque	Power	Torque	Power
I-CS versus RTSL	0.99	0.99	0.99	0.99	0.99	0.99
SRM versus RTSL	0.98	0.98	0.98	0.98	0.98	0.98

Mechanical work output comparison: Table 3 shows the difference of cumulative output work over thirty cycles between I-CS versus RTSL and SRM versus RTSL. The differences are also expressed as the percentage of the total cumulated work. To analyze the influence of the angular velocity, we integrated power output over time to calculate the work output in using *i*) the torque and angular velocity measured by SRM and *ii*) the SRM's torque multiplied by I-CS's angular velocity. These results are presented at the last lines of table 3.

Table 3: Total difference of cumulative work output over thirty cycles between I-CS and RTSL

sensors and SRM and RTSL sensors. * Work calculated with $W = \int [\tau_{SRM} \cdot \bar{\omega}_{SRM}] dt$ and

calculated with ** $W = \int [\tau_{SRM} \cdot \omega_{I-CS}] dt$ with τ_{SRM} is torque measured by SRM, $\bar{\omega}_{SRM}$ is average angular velocity measured by SRM and ω_{I-CS} instantaneous angular velocity measured by I-CS.

	C1		C2		C3	
	Work (J)	(%)	Work (J)	(%)	Work (J)	(%)
I-CS versus RTSL	1.63	0.03	74.27	1.88	117.44	1.56
SRM versus RTSL*	46.25	0.98	45.72	1.16	396.77	5.26
SRM versus RTSL**	38.42	0.81	39.37	1.00	108.28	1.44

DISCUSSION: In this study, the parameters analyzed were torque, angular velocity, power and work outputs generated at the crankset. In figure 2, we note that the variations of the torque and power output given by the three sensors are similar but not for the angular velocity. This result is confirmed by the CMC_{ip} values (table 2). Consequently, I-CS and SRM sensors were validated with the RTSL for the measures of torque and power output whatever the conditions. Thus, the powers calculated by I-CS and SRM were similar although the angular velocities were not. Apparently, changes in angular velocity do not seem to have much influence on the power's calculation. However, table 3 shows that considering average angular velocity affects work's calculation, especially for C3. The error in percent was 5.26% for the SRM sensor against 1.2% for I-CS. Also, for this condition (C3), SRM sensor was less accurate than I-CS compared to the reference sensor. For the other conditions (C1, C2) calculated precisions were included in those announced par the manufacturers (>1% for I-CS and 1% for SRM). Thus, when pedaling with variable angular velocity, the power output measured by SRM was not enough accurate to calculate work output. The integration of power over time accumulated small differences between the powers measured by SRM and I-CS. If these differences measured at each instant were not significant ($CMC_{ip} > 0.95$), it was necessary to take into account when calculating the work as part of an energy study of the pedaling motion.

However, the error in % was reduced to 1.44% when the torque measured by SRM was multiplied by the instantaneous angular velocity measured by I-CS. For the C1 and C2 conditions, the results were also better. Also, for C3 condition, SRM sensor was less accurate than I-CS compared to the reference sensor.

CONCLUSION: Our study demonstrated that I-CS is a valid powermeter and compared well with a standard reference sensor and the SRM irrespective the pedaling cadence and the resistive load. It can be used as a valid torque/power/work evaluation system with the advantage of being able to differentiate the right and left legs contributions in the overall torque and power output at the crankset. These differentiated measures are necessary input data to initiate the inverse dynamics procedure, in order to proceed to energetic analysis of the cyclist. Finally, if some studies have shown a good accuracy of the SRM, these authors were limited to the comparison of powers calculated while the assessment of energy expenditure required to compute the work. In this case, we showed that the SRM sensor is not suitable; pedaling velocity measured by the SRM is not enough accurate especially when it varies significantly.

REFERENCES:

- Ferrari, A., Cutti, A.G. & Cappello, A. (2010). A new formulation of the coefficient of multiple correlation to assess the similarity of waveforms measured synchronously by different motion analysis protocols. *Gait & Posture*. 31, 540-542.
- Millet, G.P., Tronche, C., Fuster, N., Bentley, D.J. & Candau, R. (2003). Validity and reliability of the polarS710 mobile cycling powermeter. *International Journal of Sports Medicine*. 24: 156-161.
- Bertucci, W., Duc, S., Villerius, V., Pernin J.N. & Grappe, F. (2005). Validity and reliability of the PowerTap Mobile cycling powermeter when compared with the SRM device. *International Journal of Sports Medicine*. 26: 868-873.
- Paton, C.D. & Hopkins, W.G. (2001). Tests of cycling performance. *Sport Medicine*. 31: 489-496.

KINEMATIC ANALYSIS ON SERVE TECHNIQUE OF WORLD'S ELITE FEMALE TENNIS PLAYER

Jun Guo, Jihe Zhou

Graduate Student Faculty, Chengdu Sport University, Sichuan, Chengdu, China

The purpose of this study was to obtain the kinematic parameters on serve technique of WTA (Women's Tennis Association) top two Serena Williams and Simona Halep. The study selected WTA top two players' first serve in 2014 China Open, which was held in Beijing, China. This paper makes analysis on serve technique between two elite players through the method of three-dimensional video analysis. The kinematic technical feature has been obtained through this study, resulting in not only providing referential statistics for the technical training of the players, but also enriching the technical theory of tennis.

KEY WORDS: toss, backswing, hitting, whiplash movement.

INTRODUCTION: In recent years the speed of the serve has increased considerably. For instance, the fastest serve speed of professional female players is 211km/h. Serve is the main mean of scoring to win the match, especially the first serve, which is an offensive weapon. The quality of the first serve indeed directly influences the set of serves for player and high quality first serves make difficult for opponent from the start. Therefore, it is the start of the game and the start of attack. A large number of documents shows that the statistics collected about kinematic research of first serve is mostly focused on training professional and amateur athletes. Besides, it is rare to collect data of world's elite tennis players by the application of 3D video analysis. Owing to the widespread application of first serve in tennis matches, this paper will explore WTA (Women's Tennis Association) top two players' serve technique by 3D video in 2014 China Open. The purpose of this study was to obtain the kinematic parameters on serve technique of world's elite female tennis players.

METHODS: *Three-dimensional video analytic method:* We use two JVC9800 cameras to record research objects serve technique in the game of 2014 China Open. The camera has a length of 1.25m, and their main axis angle is about 95°. One of them is located about 20m behind the player to the right. Another is placed in front of her about 20m to the right. 3D Signal TEC V1.0C software has been adopted for the analysis of the video recorded, and the study uses the 3D Signal TEC V1.0C software to analysis frame by frame. The Dempster's human model is used (21 joints, 16 links). The original data are smoothed by a low pass filter, which the cut off frequency is 8 Hz. Meanwhile, the process will be studied one motion after another with the purpose of obtaining reliable statistics. Furthermore, in order to satisfy the need of this research, three measuring points are added which cover the top of racket, the tennis and the projected angle of shoulder and hip.

RESULTS AND DISCUSSION: According to the technical characteristics of the tennis serve action, the paper divided the serve process into three stages: the tossing stage, the backward swing stage and swinging forward swing stage. Williams and Halep are using step up stance when serve, it can let player obtain a larger upward force from the ground. It is found that the higher the hitting point, the higher the successful rate. Through analyzing the important technology link of tossing, the average heights of the ball away hand of Williams and Halep are 1.70m and 1.58m respectively. Due to the player's height difference, the height of the ball away hand will be different. Relative researches showed that it is reasonable to throw the ball from head. The average height of tossing of Williams and Halep are 3.12m and 3.53m respectively. At the end of the first stage of tossing, Williams' left knee average angle is +108° and the right is +114°, Halep's left knee average angle is +113° and the right is +120°. The knees keep bending in a certain degree when serve, it will produce

linear momentum by bending to stretch up of knee, then transferred the ground reaction force to the trunk. The average angle between shoulder and hip of Williams is $+32^\circ$ and Halep is $+37^\circ$, their trunk with a great range of rotating, therefore, it can save more energy for hitting (Cristina & Enrique, 2009). Williams and Halep's right elbow bend degree is reasonable at the end of this stage. Williams' right elbow average angle is $+87^\circ$ and Halep is $+90^\circ$. In backward swing stage, Williams' left knee average angle is $+175^\circ$ and the right is $+173^\circ$ at the end of this stage, Halep's left knee average angle is $+177^\circ$ and the right is $+176^\circ$ at the end of this stage. Williams' stretch range of left and right knee is $+68^\circ$ and 59° respectively, Halep's stretch range of left and right knee is $+64^\circ$ and 56° respectively. We found that it is considered that players' stretch range of knee should increase moderately, through rapid extending of lower limbs to obtain more energy (Duane, 2006). Athletes keep larger right shoulder joint angle at the end of backward swing stage, it can increase the working distance (Williams & Schmidt, 2006). Williams' right shoulder average angle is $+82^\circ$ at the end of this stage and Halep's right shoulder average angle is $+76^\circ$. The research shows that reasonable elbow flexion can have good effect to final acceleration. At the end of backward swing stage, Williams and Halep's right elbow average angle is $+61^\circ$ and 67° respectively. In swinging forward swing stage, the average hitting height of Williams and Halep are 2.61m and 2.55m respectively. The hitting height is 1.49 times to Williams' height and Halep is 1.52 times to her height. Relative researches showed that world's elite tennis players' hitting height is 1.50 times to their height. By analysing the difference from the highest point of ball to the hitting point, Williams' difference is 0.46m and Halep is 0.91m. In contrast, Williams' difference is 0.45m smaller than Halep, small difference is beneficial to players' judgment, in order to insure the success of serve and reduce mistakes. Because serve is a typical whiplash movement, therefore the maximum speed of body segments are present from lower to upper limbs in turn in the stage of swinging forward swing. The calculation results show that, while hitting the ball, the average speed of Williams' right shoulder joint is 2.56m/s, the right elbow joint is 3.68m/s, the right wrist joint 6.40m/s and the head of racket is 22.30m/s. The average speed of Halep's right shoulder joint is 2.39m/s, the right elbow joint is 3.49m/s, the right wrist joint 5.60m/s and the head of racket is 20.60m/s.

CONCLUSION: The paper shows that serve is a typical whiplash movement. Through the analysis and discussion of Williams and Halep's serve, we found that the kinematic parameters have reference value. Williams and Halep's main indications are as follow:

(1) In contrast, Williams has high stability in tossing. With a good tossing, player can make the ball has stable movement route. Moreover, it will make sufficient preparation for hitting. In addition, two elite players' trunk with a great range of rotating when backswing, it can save more energy for hitting.

(2) In back forward swing stage, the data showed that two elite players' left and right knee stretching in large range, through rapid extending of lower limbs to obtain more energy. At the end of back forward swing stage, two elite players' right shoulder keep a large angle, it can let players have a larger range movement and form a good initial state for next action. In swinging forward swing stage, two elite players have higher hitting height. The higher hitting height, the higher success rate of serve. Williams' difference from the highest point of ball to the hitting point only 0.46m, small difference is beneficial to players' judgment, in order to insure the success of serve and reduce mistakes. Through the speed of two elite players' body segments in swinging forward swing stage, we found that the speed of shoulder, elbow, wrist and the head of racket are increase gradually, it is accord with the technical principles of whiplash movement.

REFERENCES:

Duane, K. (2006). *Biomechanical Principles of Tennis Technique* (pp 77-85). Perth: Racquet Tech Press.

Cristina, L. & Enrique, N. (2009). Kinetic Energy Transfer during the Tennis Serve. *Journal of Human Sport and Exercise*, 4(Suppl. 2), 114-128.

Williams, S. & Schmidt, R. (2006). An upper body model for the kinematical analysis of the joint chain of the human arm. *Journal of Biomechanics*, 39, 10-15.

BIOMECHANICS OF SURFING: DEVELOPMENT AND VALIDATION OF AN INSTRUMENTED SURFBOARD TO MEASURE SURFBOARD KINETICS

K. Lestrade^{1,2,3}, S. Guérard^{1,3}, P. Lanusse^{2,3}, Ph. Viot^{1,3}

Arts et Metiers ParisTech, I2M UMR 5295 CNRS, 33400 Talence, France¹
Université de Bordeaux, IMS UMR 5218 CNRS, 33405 Talence, France²
Bordeaux INP, I2M UMR 5295 / IMS UMR 5218 CNRS, 33405 Talence, France³

The purpose of this study was to investigate the different relations between the actions of a surfer and the kinematic behaviour of his surfboard. An instrumented surfboard has been designed with a force platform synchronized with an inertial measurement unit and acquisition system. An experimental campaign has been carried out *in situ*, where different waves have been surfed to validate the device. Results revealed that measured efforts of the surfer and kinematics of his surfboard are consistent regarding the expected behaviour. Instrumented surfboards will help coaches by giving them a new performance analysis tool. It will also provide an experimental database for the development of numerical models about interactions Surfer/Surfboard/Wave.

Acknowledgments: We thank the Regional Council of Aquitaine, which granted this work.

KEY WORDS: Motion analysis, Dynamic solicitation, Instrumented Surfboard.

INTRODUCTION: In surfing, a system allowing for the quantitative analysis of the movements of an athlete to execute a given figure doesn't exist at the present time. A lot of sports use simulation and scientific approaches to understand interactions between a sportsman and his equipment. Recently, in some sports like tennis, baseball or golf, on-board instrumentation has been used to assess precisely the material performance and the athlete's training (Nathan & Faber, 2011; Andrew, Chow & Knudson, 2003). In order to develop a surf simulator to study the relations between a given figure and the biomechanical response of the surfer, interindividual variability to execute a given movement and to optimise actions of the person aiming at better performances, surfing trajectories have to be reproduced in controlled environment. In 2011, as part of the SurfSens project (now abandoned), Tecnalía initiated instrumentation of a surfboard using sensors with the main objectives of improving the characteristics of a surfboard (Letamendia, 2011) but they didn't identify direct interactions with the surfer.

The purpose of this study was to provide an instrumented surfboard to identify, record and analyse *in situ* the interactions Surfer/Surfboard/Wave. First, we identified all the experimental devices to measure all the data defining the interactions Surfer/Surfboard/Wave. Secondly, the complex and indefinite oceanic environment to design a reliable experimental surfboard and to instrument it with all the necessary measuring tools has been taken into account. Finally, an experimental campaign was organized *in situ* whose results will be presented.

METHODS:

1. Identification of measuring tools.

The interactions between the surfer and the surfboard can be measured with a 6-component force platform. Such a force sensor gives access to the six components of resulting force and moment applied on the platform. The force platform (O2-A1, Sensix, Poitiers, France) has been designed from specifications defined by preliminary tests about dimensions and measuring ranges on each axis. Specific behaviour of this platform, based on the results of Boucher (2005) allows large measuring ranges with small volume: respectively (5000N, 5400N, 14500N, 560Nm, 650Nm, 750Nm) for (Fx, Fy, Fz, Mx, My, Mz). The conditioner is

located inside the platform in order to facilitate and reduce the acquisition system. Interactions between the surfboard and the wave can be identified by analysing the dynamic behaviour of the surfboard: angular velocities and longitudinal accelerations of the surfboard using a 3-axis gyroscope (ITG3200, InvenSense, San Jose, California) and a 3-axis accelerometer (ADXL345, Analog Devices, Norwood, USA). An acquisition system equipped with an analog-digital converter (Arduino Mega2560 card, Arduino, Torino, Italy) and a microSD shield (microSD Shield, SparkFun Electronics, Niwot, USA) have been used to synchronize the three measurement devices: force platform, accelerometer, and gyroscope.

2. Complex environment to implement an instrumented surfboard

Design of the surfboard was the subject of a specific work in collaboration with a professional surfer and surfboard shaper. A board has been created to accommodate all measurement tools without losing manoeuvrability and reactivity. The force platform has been placed in the surfboard (Figure 1) under the front foot of the rider which corresponds, in surfing, to the predominant foot and is directly correlated to the behaviour of the surfboard. To obtain a reliable measurement of the mechanical actions, it was necessary to have quasi-direct contact between foot and sensor. As the latter is not waterproof, some experiments have been done in laboratory conditions to find a sufficiently tight and resistant fabric (Seaguard Flex 5400, Dickson, Wasquehal, France) to protect the sensor from the marine environment without degrading the measurements.

All the electronic components (accelerometer, gyroscope, acquisition system, battery) have been placed on top of the surfboard in a waterproof case connected to the force sensor (Figure 1). It was designed with a switch for triggering and activating the manual stop at the beginning and the end of the wave. *In situ* data acquisition was started (manual activation by the surfer) when the surfer was lying down and could see a wave coming. The acquisition ended when the surfer finished surfing the wave and was no longer on the surfboard (manual stop). Frequency of the acquisition was chosen at 50Hz. The 12 measuring tensions were stored on an SD card associated to a time measurement. Moreover, a video camera was placed on the beach filming the surfer on the wave: it was used to analyse the behaviour of the surfer, his surfboard and some characteristics about the wave (size and direction). Another on-board video camera (GoPro Hero3, GoPro, California, USA) was on the top of the board (Figure 1b), filming front foot positions on the force platform.

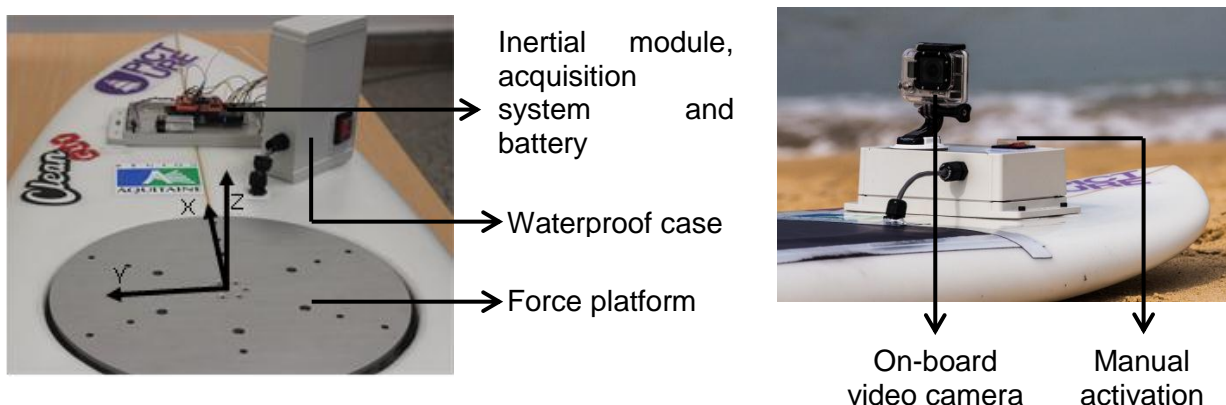


Figure 1: Photos of the instrumented surfboard

3. Data Processing

Data processing was done in several steps. First, all the stored tensions were converted into physical values ([N], [Nm], [$\text{m}\cdot\text{s}^{-1}$], [$\text{m}\cdot\text{s}^{-2}$]) and reduced to the basis $(\vec{X}, \vec{Y}, \vec{Z})$. Vertical force F_z was analysed numerically to identify the four main actions of the surfer once the acquisition is triggered: the first one is to wait for the wave sitting on the board: $F_z = 0$. The second is the paddling to catch the wave: the surfer is lying on his surfboard, only his chest is in contact with part of the sensor, therefore the range of F_z corresponds to 40 to 60% of bodyweight.

Then there is the surfing phase beginning with a take-off corresponding to a significant F_z -peak linked to the first contact between the foot and the sensor. The last phase corresponds to the surfer when he gets off the surfboard (end of the wave or fall): $F_z = 0$.

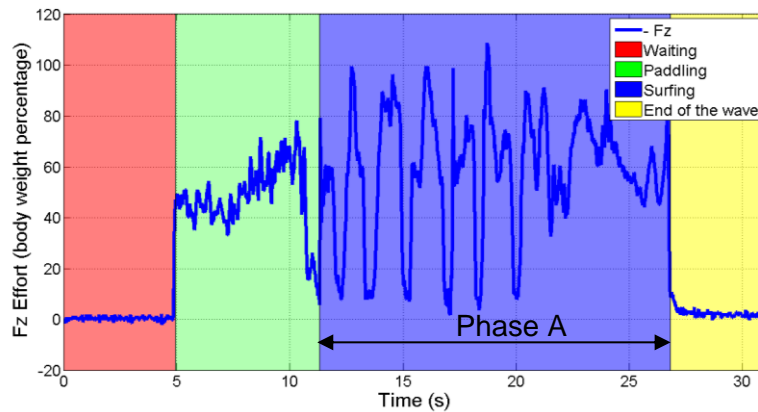


Figure 2: Example of F_z raw efforts saved on a wave with a 50Hz frequency.

The most interesting part is the "Surfing" phase (referred as phase A in Figure 2) where the surfer is generating an action with his body to point his surfboard on the wave. Instantaneous position of the centre of pressure (COP) was calculated considering that the resulting free moments along the X and Y axes are equal to zero (Besser, Kowalk & Vaughan, 1993). Finally, video cameras were synchronized manually during post processing to keep only parts corresponding to phase A using the time of contact between the foot and force sensor.

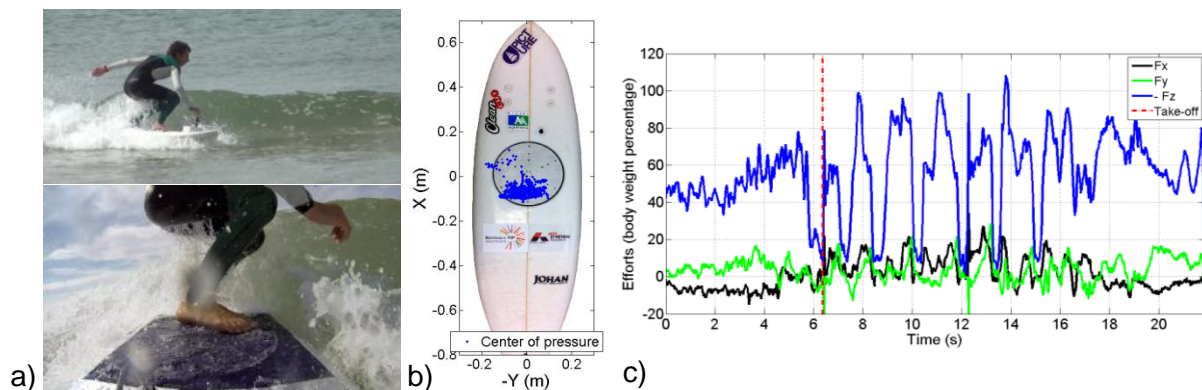


Figure 3: Synchronized experiment data on one wave: a) onshore and in-board videos, b) COP and c) forces on each axis.

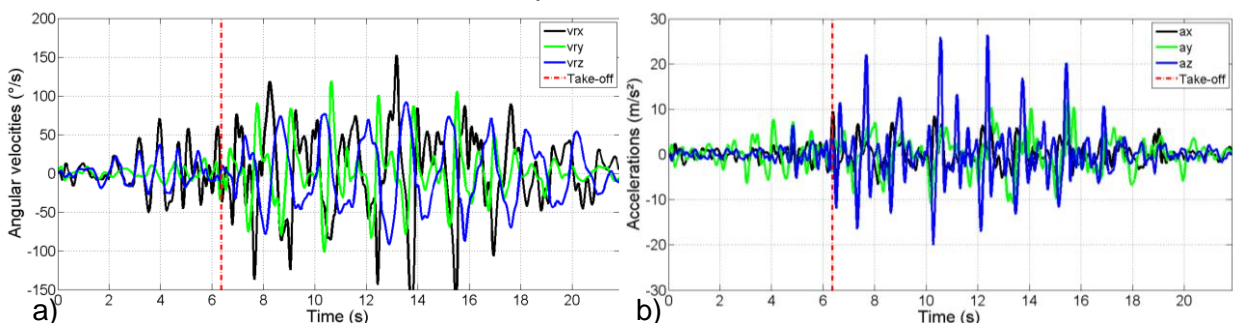


Figure 4: Example of synchronized experiment data on one wave: angular velocities (a) and longitudinal accelerations (b) on each axis.

RESULTS: The objective of this project was to develop an experimental device to evaluate interactions Surfer/Surfboard/Wave during the progression of a surfer on a wave. The easiest

way to show that such a system is successful is to present the results of a test with a professional surfer. Figures 3 & 4 are an example of raw data analysed to check the validity of the device. Firstly, instantaneous positions of the COP during «Surfing» phase (Figure 3.a) are consistent with the real front foot position recorded with the on-board camera. In this example, the athlete performed a "Speed generation" on the wave, which corresponds to several flexion-extension movements of the surfer. During the "Speed generation" phase, a professional surfer should put almost all of his body weight on his front foot during the flexion-extension phase. Conversely, he must have almost no support during the reduction phase. On figure 3c, the graph shows as a function of time the evolution of efforts between the rider and his surfboard expressed in percentage of body weight of the surfer. It perfectly illustrates this concept of « speed generation ». Figure 4 presents the evolution of angular velocities (Figure 4a) and longitudinal accelerations (Figure 4b) along the three axes (\vec{X} , \vec{Y} , \vec{Z}). To check their validity, high frequencies of these signals have been filtered. After integration, instantaneous surfboard movements on the wave have been directly analysed. For example, after filtering and integration of data from Figure 4, the evolution of instantaneous positions on the vertical axis Z is a sinusoid of amplitude 45cm. This is consistent with the behaviour of the surfboard noticed with the onshore camera on this wave of 50cm, which oscillated between the top and bottom of the wave due to the « speed generation » action of the surfer.

DISCUSSION: As part of a surfing simulator project with a hexapod, equipped with multi-axis force plates, a database is built up for the development of a numerical model characterizing connections between actions of a surfer and the dynamic behaviour of the surfboard. The development of the simulator based on the hexapod will require a control of the trajectory of the moving platform from the forces generated by the user. From a biomechanical point of view, the associated technologic and scientific challenges are numerous: the study of training, practice and balance rehabilitation. Several studies in the literature have been done to evaluate the physiological properties of the human body and their dependencies to experimental protocol (Knuesel, Geyer & Seyfarth, 1983). However, for all the used protocols, movements carried out by the subjects were elementary (one solicitation direction and one level of solicitation). The use of the hexapod and its instrumentation could allow to find the links between the parameters of a complex disturbance (degree of freedom, range of movement, speed, acceleration) and the biomechanical response of the human body.

CONCLUSION: There is a real demand from coaches and athletes to have technical tools allowing them to analyse their actions and their equipment's behaviour. This instrumented surfboard is the first complete interactions Surfer/Surfboard/Wave analysis tool and potentially offers surfers and coaches a way of improving their level of performance and their way of training.

REFERENCES:

- Andrew, D.P., Chow, J.W. & Knudson, D.V. (2003). Effect of ball size on player reaction and racket acceleration during the tennis volley. *Journal of Science and Medicine in Sport*. 6(1), 102-112.
- Besser, M., Kowalk, D. & Vaughan, C. (1993). Mounting and calibration of stairs on piezoelectric force platforms. *Gait Posture*, 1, 231–235.
- Boucher, M. (2005). *Limites et précision d'une analyse mécanique de la performance sur ergocycle instrumenté* (Thesis in French). Université de Poitiers, Poitiers.
- Knuesel H., Geyer, H. & Seyfarth, A. (2005). Influence of swing leg movement on running stability. *Human Movement Science*, 24(4), 532-543.
- Letamendia, A. (2011, March 11). SurfSens project. *Wired Magazine*. Retrieved from <http://www.wired.co.uk/news/archive/2011-03/04/surfsens-future-of-surfing>
- Nathan, A.M., Smith, L.V. & Faber W.L. (2011). Reducing the effect of the ball on bat performance measurements. *Sports Technology*, 4, 19-28.

ACUTE EFFECTS OF TRAINING ON HURDLE CONFIGURATION DURING SPRINT HURDLE MOTION

Kazuhito Shibayama¹, Norihisa Fujii² and Michiyoshi Ae²

Faculty of Sport Science, Sendai University, Japan¹

Faculty of Health and Sport Sciences, University of Tsukuba, Japan²

Here we assessed the acute effects of training in hurdle configuration on sprint hurdle motion in five male hurdlers. We compared the hurdlers' motion between the pre- and post-training conditions for three different types of training programs. Our results showed that a short-interval training program was effective in reducing the duration of all four step, particularly that of the 2nd step. On the other hand, a long-interval training program particularly influenced the characteristics of the 3rd step without improving the overall four steps. Thus, a long-approach training was effective in adjusting the ground reaction force in the support phase of the 4th step, necessary to appropriately clear the hurdle.

KEY WORDS: Motion analysis, training, interval.

INTRODUCTION: Faster hurdlers have great speed, power, and coordination abilities. Training exercises to boost coordination usually involve changing the speed and rhythm of the hurdle motion (Bompa, 1999). In general, hurdle manuals recommend changing the hurdle configuration, such as the distance between the hurdles and their height, for effective training; however, not many studies have comprehensively assessed the effect of this type of training programs. Step frequency is expected to increase during hurdle races; therefore, understanding the effects of changing hurdle configuration on sprint hurdle motion, particularly regarding the step frequency, is essential to evaluate the effectiveness of this type of training programs.

Set against this background, we assessed the acute effects of training in hurdle configuration on sprint hurdle motion.

METHODS: Five male hurdlers (Height: 1.77 ± 0.06 m; body mass: 67.4 ± 7.2 kg; PB: 15.44 ± 0.75 s) participated in this study. First, we recorded the athlete's motion between the 3rd and the 4th hurdle prior to specific training in regular hurdle configuration (pre-trial; length from start to 1st hurdle (approach): 13.72 m, length of interval: 9.14 m). Then we recorded the same motion in regular hurdle configuration after three training programs:

1. Short-interval training (SI; length of approach: 13.72 m, length of interval: 8.64 m)
2. Long-interval training (LI; length of approach: 13.72 m, length of interval: 9.64 m)
3. Long-approach training (LA; length of approach: 20 m, length of interval: 9.64 m)

The order of the training programs was randomized per subject. Motions in regular hurdle configuration in pre- and post-trials during four steps (1cycle) were recorded using a high-speed VTR camera (EX-F1, CASIO, Japan). In addition, we used a motion analyzer (Frame-DIAS-II ver.3, DKH, Japan) to digitize the position of 25 body landmarks and calibration marks in the projected images. Next, we calculated the position of the two-dimensional coordinates based on the calibration marks. These data were subsequently smoothed using a butterworth low-pass filter with optimal cut-off frequencies, which were determined using the residual error method proposed by Wells & Winter (1980). Figure 1 shows the classification of the movement phases. We analyzed the following kinematic parameters: the duration of each phase, vertical velocity of the center of gravity (CG), step length, and angular velocity of the thighs. In addition, we assessed whether the differences between the pre- and post-training conditions were statistically significant using a Wilcoxon rank-sum test for paired values ($p < 0.05$).

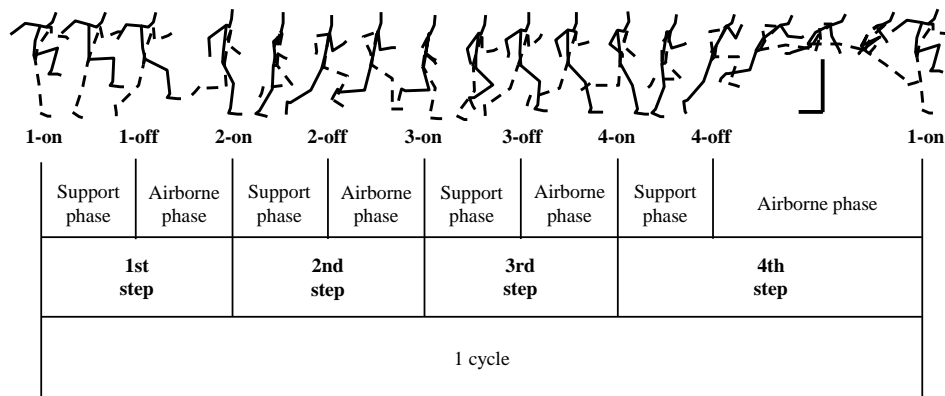


Figure 1 Movement phases during four steps in hurdle motion (1cycle).

RESULTS: Table 1 shows the durations of each phase during 1cycle motion for pre- and post-training conditions (SI, LI, and LA). The durations of 1cycle and the airborne phase in the 2nd step for SI were shorter than those for pre-training condition. The duration of the airborne phase of the 3rd step for LI was shorter than that for pre-training condition. On the other hand, the duration of the airborne phase of the 4th step was shorter after LA than that during pre-training condition. Figure 2 shows the ratio of “step length of each step” to “step length of the 1cycle motion” for pre- and post-training conditions. For SI, this ratio increased during the 4th step compared with the pre-training value, whereas the step length of the 3rd step decreased for LI compared with that of pre-training value.

Table 1 Duration of 1cycle, and the support and the airborne phases for each training program.

Variables [mean(SD)]	CT	1st step		2nd step		3rd step		4th step	
		ST	AT	ST	AT	ST	AT	ST	AT
pre	1.28 (0.06)	0.12 (0.02)	0.05 (0.01)	0.16 (0.02)	0.13 (0.01)	0.15 (0.02)	0.08 (0.01)	0.15 (0.01)	0.45 (0.03)
SI	1.25 (0.06)	0.12 (0.01)	0.05 (0.01)	0.15 (0.02)	0.12 (0.01)	0.14 (0.02)	0.07 (0.01)	0.15 (0.01)	0.44 (0.03)
LI	1.29 (0.05)	0.13 (0.01)	0.04 (0.01)	0.16 (0.02)	0.13 (0.02)	0.15 (0.02)	0.07 (0.01)	0.15 (0.02)	0.46 (0.04)
LA	1.25 (0.03)	0.12 (0.01)	0.05 (0.01)	0.16 (0.01)	0.13 (0.02)	0.14 (0.02)	0.07 (0.01)	0.15 (0.01)	0.43 (0.02)
Significant difference	pre > SI	n.s.	n.s.	n.s.	pre > SI	n.s.	pre > LI	n.s.	pre > LA

Unit : [s]

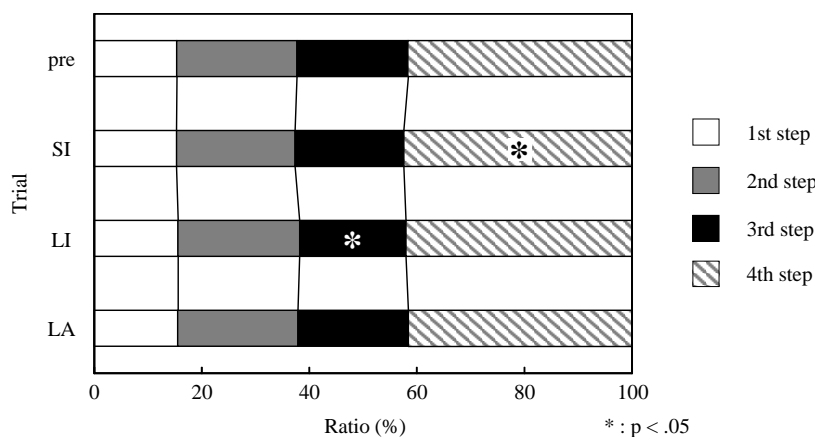


Figure 2 Step length for each step to 1-cycle step length ratio.

Figure 3 shows the changes in vertical velocity of CG for each step for pre- and post-training conditions. Although CG vertical velocity did not significantly differ for pre- and post-training conditions, mean CG vertical velocity during the 4th step was smaller after training than at pre-training condition. Figure 4 shows the average angular velocity patterns of the lead leg thigh during 1cycle motion at pre- and post-training conditions. For SI, the angular velocity of the lead leg thigh during the airborne phase of the 2nd step was smaller than that during pre-training condition.

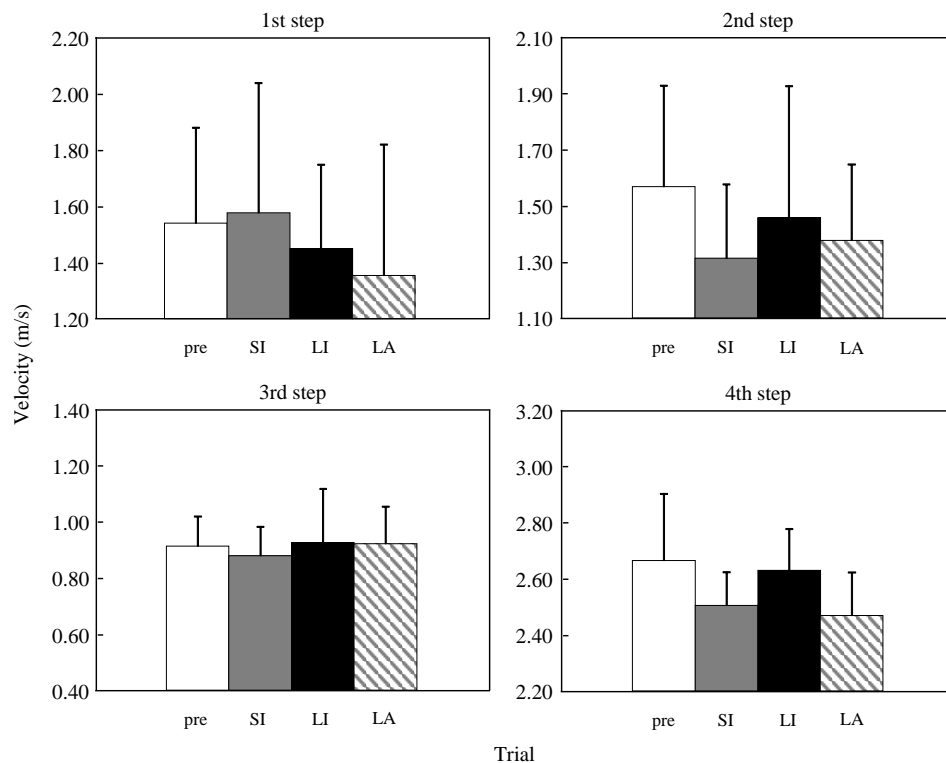


Figure 3 Changes in vertical velocity of CG for each step.

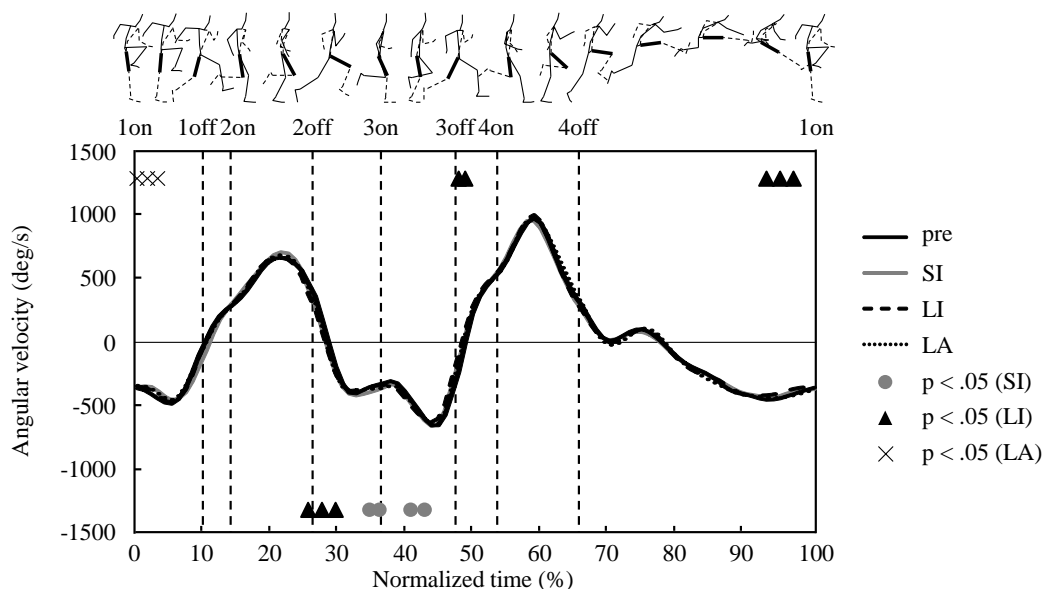


Figure 4 Average angular velocity patterns of the lead leg thigh during 1cycle motion.

DISCUSSION:

1. Short-interval training effect: 1cycle duration decreased due to a reduction in the duration of the airborne phase of the 2nd step. A shorter airborne phase during this step is achieved by active landing with the lead leg. These results are similar to those previously reported by Shibayama et al. (2011), who discussed the characteristics common to fast hurdlers. Thus, short-interval training arises as effective in reducing the duration of a full cycle, particularly by influencing the 2nd step.

2. Long-interval training effect: Although 1cycle duration did not significantly differ between the pre- and post- training conditions for this program, the mean duration decreased following LI training. In addition, the duration of the airborne phase of the 3rd step decreased. The main reason is the increase in the ratio of step length in 1st step and 2nd step. In general, it is important to keep the distance between the take-off point and the hurdle in a constant range. As a result, LI training alters the characteristics of the 3rd step without significantly improving a 1cycle motion.

3. Long-approach training effect: The duration of the airborne phase of the 4th step decreased due to small changes in CG vertical velocity during the support phase of this step. However, the duration of the support phase in this step did not significantly differ between the pre- and post-training conditions. The change in momentum is directly related to the impulse obtained during the support phase; consequently, LA training is effective in adjusting the ground reaction force during the support phase of the 4th step to clear the hurdle successfully.

CONCLUSION: Our results suggested that short-interval training was the most appropriate to reduce the duration of a 1cycle motion. In addition, long-approach training appeared effective in improving the take-off motion when approaching the hurdle. Long-interval training was not suitable for improving a 1cycle motion.

REFERENCES:

- Shibayama, K., Fujii, N. & Ae, M. (2011) Kinematic study of 1-cycle motion in elite 110 m hurdlers: Focusing on relations between running velocity, leg length and motion. *Japan Journal of Physical Education Health and Sport Sciences*, 56: 75-88. (in Japanese)
- Bompa, T. O. (1999) *Periodization: Theory and Methodology of Training*, 4th edition. Kendall/Hunt: IA.
- Wells, R.P. & Winter, D.A. (1980) Assessment of signal noise in the kinematics of normal, pathological and sporting gaits. *Human locomotion*, 1: 36-41.

MEASURING BILATERAL ASYMMETRY IN A LONG-TERM ATHLETE MONITORING

Kimitake Sato

Department of Exercise and Sport Science, Center of Excellence for Sport Science and Coach Education, East Tennessee State University, USA

The purpose of this lecture is to provide examples of how biomechanical testing methods are used to analyse bilateral asymmetry from a long-term athlete monitoring program. This lecture includes the results of bilateral asymmetry data to examine the physical status of both highly competitive and recreational athletes. Athlete monitoring is a vital component of achieving a successful athletic career. It is important to understand how the magnitude of bilateral asymmetry is potentially detrimental to performance. The bilateral asymmetry data has been analysed to understand physical demands of athletes in various sports. Different types of jumping, landing, and isometric tests have provided data showing effectiveness of the tests in displaying the athlete's physical characteristics. Bridging the gap between science and practice is mentioned in the lecture.

KEYWORDS: tests, sports, symmetry.

INTRODUCTION: Athlete monitoring is an important way of tracking the progress that athletes make throughout their careers. From the scientific view point, monitoring athletes with selected physiological and biomechanical variables provides a sense of how training stimulates the physical conditioning towards to a competition phase (Hornsby, 2012). Additionally, monitoring data can be summarized and analysed through statistical methods such as single-subject design analysis and trend analysis to give athletes and coaches observation-based information on how evaluating overall training volume can better prepare the athletes. Within athlete monitoring, some tests can be used as a diagnostic evaluation (Knapik et al., 1991; Nadler et al., 2001). Simple measurements such as body composition, hydration, jumps, and other tests can be done frequently to keep track of athlete's physical condition. At the same time, some diagnostic tests are done to better predict athletic performance, return to play decision, and/or a risk of injury (Knapik et al., 1991; Nadler et al., 2001; Johnston, 2014).

Bilateral asymmetry research has been done mainly in clinical settings with pathological issues comparing the functionality of bilateral movements (Panariello et al., 1994; Thein et al., 1998). In recent years, this idea has been used for athletic populations to evaluate aforementioned information (Bailey et al., 2014; Sato et al., 2012). Although having abnormal functionality such as a certain level of asymmetry from kinetic and kinematic data in bilateral tasks receives attention, asymmetry measures in athletic populations do not receive the same attention in the existing literature and most importantly not for practical use.

Therefore, the purpose of the lecture is to provide information on how bilateral asymmetry testing methods are being used to evaluate athletes in a long-term athlete monitoring program. The lecture consists of methodological procedures, data outcome, and data interpretation in quantitative and qualitative perspectives.

METHODS: Typical participants in these studies are competitive to recreational level athletic populations. Many studies being mentioned in this lecture are based on the athlete monitoring data from National Collegiate Athletic Association (aka, NCAA) Division I athletes (Bailey et al., 2014; Chiang, 2014; Hornsby, 2012; Johnston, 2014; Sato et al., 2012; Sha et al., 2014). The long-term athlete monitoring program at East Tennessee State University is completed through a collaborative effort between the Department of Exercise and Sport Science, Center of Excellence for Sport Science and Coach Education, and the Department of Athletics, called the Sport Performance Enhancement Consortium (SPEC). SPEC athletes go through a battery of testing, which includes the following: hydration, body composition, two types of jumps (static and counter-movement) with unloaded and loaded conditions, and isometric mid-thigh pull

(IMTP). Depending on sports, additional tests such as agility and distance-specific sprints are also examined.

All of the jump tests are done on dual force plates (RoughDeck HP; Rice Lake, WI) and athletes are positioned so that their midline is along the center line of two force plates. The force plates measure ground reaction force (GRF) simultaneously at the same sampling frequency of 1,000 Hz. The two types of jumps, static jump (SJ) and counter-movement jump (CMJ), are done using unloaded (0 kg) and loaded (11 and/or 20 kg) conditions. Force data such as peak force (raw and scaled), time specific forces (50, 90, 200, and 250 ms), rate of force development (RFD), peak power, and impulse are considered for the performance measures (Bailey et al., 2013; Chiang, 2014; Johnston, 2014; Sha et al., 2014). The IMTP are done on identical force plate setups to measure GRF variables from both sides to consider similar data to the jumps. Agility tests are another test protocol with potential for asymmetry identification (Chiang, 2014). It is important to note that this asymmetry consideration is based on limb-dominancy and/or preference. As a measure of performance, the tests are timed using infrared timing gates (TC Timing System, Brower Timing Systems, Draper, UT) and as a measure of foot contact time using an OptoGate system (Microgate, Balzano, Italy). Top-speed sprints are also considered between the limbs using 3-dimensional (3D) motion capture systems (Nexus 1.8.5, Vicon, UK) to identify potential limb kinematic asymmetry. Specific measurements such as joint and segment kinematics between both sides of limb are considered (Sha et al., 2014).

From a rehabilitative perspective, a closed-chain task such as jumps have been examined and utilized as a “return-to-play” decision making tool (Johnston, 2014). Athletes who are coming back from surgery or injury are expected to produce movement compensations. For example, when conducting the jump test during the rehabilitative phase, push-off and landing GRF measures from both sides are a good indication how athlete uses uninjured and injured side differently. Excessive magnitudes of asymmetry indicate the presence of compensation, and it is expected that the magnitude of asymmetry decreases as the rehabilitation progresses.

There are several ways to calculate asymmetry from the literature (Bell et al., 2008; Sato et al., 2012). In order to keep the data coach-friendly for practical use, a typical method being used for the asymmetry calculation is to identify variables with a symmetry index (SI) score. Statistical analysis to answer research questions consists with correlation to associate how strength predicts the level of asymmetry, and how asymmetry in strength can be a carryover to sport-related tasks such as jumping, landing, sprinting, and agility (Bailey et al., 2014; Chiang et al., 2014). Other methods are to compare groups of population to identify if the level of asymmetry matters in certain sport-related tasks (Bazyler et al., 2014; Sato et al., 2012). Cohen’s *d* was used to describe the relevance of differences (Cohen, 1992). Other alternative statistics such as single-subject design and trend analysis are used for tracking the injured athlete for monitoring purpose to determine the return to play (Johnston, 2014).

RESULTS: As results of aforementioned studies, figures and tables are shown below.

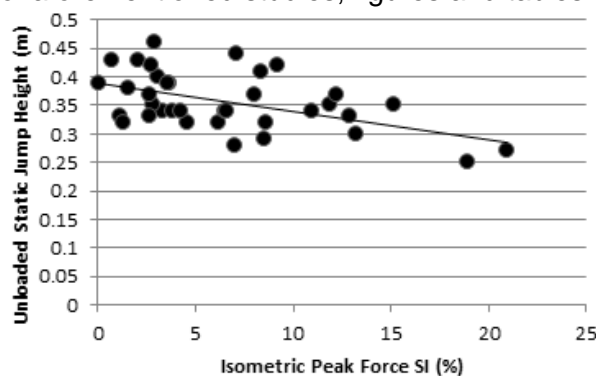


Figure 1: Correlation value of $r = -.52$ for the relationship between static jump height (m) and a magnitude of isometric mid-thigh pull symmetry index score (%), (from Bailey et al., 2013).

Table 1.

The relationships between isometric mid-thigh pull force symmetry index score and change of direction symmetry index score, (from Chiang, 2014).

	IPF	F50	F90	F250
3m acceleration	-0.13	0.00	0.12	-0.20
Partial time	0.12	0.42*	0.60**	0.20
Total time	0.03	0.23	0.38	0.23

Note: * $p < 0.05$, ** $p < 0.01$,

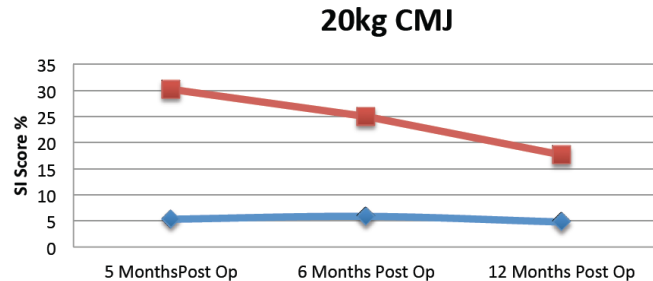


Figure 2: Descriptive comparison on 20kg countermovement jump landing force asymmetry, red square = injured side, blue diamond = uninjured side, (from Johnston, 2014).

DISCUSSION: Overall, based on the various approaches to examine the influence of bilateral asymmetry in sport tasks, there is some justification to the notion that high magnitude of asymmetry may become detrimental to athletic performance such as jumping (propulsion and landing force asymmetry) (Bailey et al., 2013; Johnston, 2014). This supports the idea that individuals with high asymmetry from specific tests can be categorized into a “watch-list”, and should receive attention from athletic trainers, strength coaches, and sport scientists to reduce the level of asymmetry in order to improve the jump-related performance. The results also can be used as a monitoring tool to determine if the certain training is effectively stimulating decreases in the magnitude of asymmetry. Specifically concerning injury, this can be used when athletes are in the rehabilitation process. Making the “return-to-play” decision based on a single field test or an isokinetic symmetry evaluation may not be adequate. Previous evidence has shown that an athlete may return to full symmetry in one assessment method, while still compensating during jump performances (Johnston, 2014). From an athlete monitoring standpoint, when tracking SI scores or any variable of a single athlete, data analysis may become mostly visual (see Figure 3).

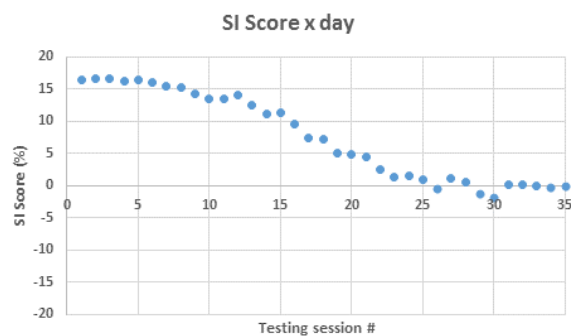


Figure 3: Example of visual nature of the analysis athlete monitoring data.

At the same time, strength training tends to reduce the magnitude of bilateral asymmetry in isometric force production measured by isometric squat tasks (Bazyler et al, 2014). It is important to note that this applies to healthy athletes who are relatively weak. Therefore, if relatively weaker individuals possess strength asymmetry, strength training may help reduce the asymmetry as they become stronger. Especially when considering the data from Bailey et al. (2014), relatively weak individuals who possess large magnitude of asymmetry could benefit from strength training to minimize the strength asymmetry.

On the other hand, agility and change of direction tasks from collegiate athletes showed a weak relationship between the magnitude of bilateral strength asymmetry and the modified version of the 505 change of direction task (Chiang, 2014). Even though this notion may be

speculative, sprint performance from collegiate sprinters at peak velocity phase also showed no relationship between strength asymmetry and sprint performance, nor limb characteristic asymmetry (Sha et al., 2014).

It is important to acknowledge that there are some tasks that influence of asymmetry is minimal or non-existent to the task performance. This may mean that coaches should be more attentive to excessive levels of asymmetry in certain tasks and physical characteristics and less attentive in others. Further investigation is certainly necessary.

CONCLUSION: Concerning a performance standpoint, when considering to measure bilateral asymmetry, certain tests have become useful to the understanding of how to improve performance. But at the same time, some tasks are not heavily influenced by presence of asymmetry and may not necessitate evaluation or correction. Thus, further research is warranted to determine which tasks are sensitive to asymmetry and which are not.

REFERENCES:

- Bailey, C., Sato, K., Alexander, R., Chiang, C.Y., & Stone, M.H. (2013). Isometric force production symmetry and jumping performance in college athletes. *Journal of Trainology*, 2(1), 1-5.
- Bailey, C., Sato, K., Alexander, R., Chiang, C.Y., Stone, M.H. (2014 accepted). Force production asymmetry in male and female athletes of differing strength levels. *International Journal of Sport Physiology and Performance*.
- Bell, D.R., Padua, D.A., & Clark, M.A. (2008). Muscle strength and flexibility characteristics of people displaying excessive medial knee displacement. *Archives of Physical Medicine and Rehabilitation*, 89, 1323-1328.
- Chiang, C.Y. (2014). Lower body strength and power characteristics influencing change of direction and straight-line sprinting performance in Division I soccer players: An exploratory study. Electronic Theses and Dissertations.
- Cohen, J. (1992). A power primer. *Psychological Bulletin*, 112(1), 155-159.
- Hornsby, W.G. (2013). A systematic approach to the monitoring of competitive weightlifters. Electronic Theses and Dissertations. Paper 1189. <http://dc.etsu.edu/etd/1189>
- Johnston, B.D. (2014). Exploring the use of a jumps protocol as a return-to-play guideline following anterior cruciate ligament reconstruction. Electronic Theses and Dissertations. Paper 2336. <http://dc.etsu.edu/etd/2336>
- Knapik, J.J., Bauman, C.L., Jones, B.H., Harris, J.M., & Vaughan, L. (1991). Preseason strength and flexibility imbalances associated with athletic injuries in female collegiate athletes. *American Journal of Sports Medicine*, 19, 76-81.
- Nadler, S.F., Malanga, G.A., Feinberg, J.H., Prybicien, M., Stitik, T.P., & DePrince, M.S. (2001). Relationship between hip muscle imbalance and occurrence of low back pain in collegiate athletes: a prospective study. *American Journal of Physical Medicine and Rehabilitation*, 80(8), 572-577.
- Panariello, R.A., Cherry, S.I., & Parker, J.W. (1994). The effect of the squat exercise on anterior-posterior knee translation in professional football players. *American Journal of Sports Medicine*, 22, 768-773.
- Sato, K., & Heise, G.D. (2012). Influence of weight distribution asymmetry on the biomechanics of a barbell back squat. *Journal of Strength and Conditioning Research*, 26(2), 342-349.
- Sha, Z., Bailey, C.A., McInnis, T.C., Sato, K., & Stone, M.H. Using kinetic isometric mid-thigh pull variables to predict D-I male sprinters' 60M performance. In: Sato, K., Sands, W.A., & Mizuguchi, S. (eds.), eProceedings of the 32nd Conference of the International Society of Biomechanics in Sports, 2014: Volume 1: pp 389-392.
- Thein, J.M., & Brody, L.T. (1998). Aquatic-based rehabilitation and training for the elite athletes. *Journal of Orthopedic and Sports Physical Therapy*, 22(3), 653-660.

Acknowledgement

This lecture has been completed by the effort of research collaboration within the Center of Excellence for Sport Science and Coach Education at East Tennessee State University. Specifically, graduates from the program have contributed significantly in their theses and dissertations for this lecture.

A KINEMATICS ANALYSIS OF GIANT SWING BACKWARD AND DOUBLE SALTO BACKWARD STRETCHED DISMOUNT IN JINNAN YAO 'S UNEVEN BARS

Lu Zhong, Jihe Zhou and Shuai Wang

Chengdu Sport University, Chengdu, China 610041

Using 3D camera analytic method, the paper tests Jinnan Yao's (who won the gold medal in the female uneven bars final of the 45th World Gymnastics Championship in October 11th, 2014) technical movements of giant swing backward and double salto backward stretched dismount and make a kinematics analysis of the complete movements. The purpose of this study was to reveal the kinematic rules and technical features of the movements, in order to provide references of technical training for athletes. The results indicated that better performance was demonstrated if gymnast could increase the height of salto suspension, so that increase the flight time, in order to prepare landing.

KEY WORDS: uneven bars, giant swing backward, double salto backward stretched dismount, kinematic analysis.

INTRODUCTION: The movements named giant swing backward and double salto backward stretched dismount is one of the most frequently used dismounts through worldly outstanding gymnasts nowadays. It belongs to group D dismount action in the rule of international gymnastics. As it were, the key to win the competitions is not finishing that movements whether or not but how to complete the movements with high quality. This paper reveals the kinematics rules and technical feature of giant swing backward and double salto backward stretched dismount in uneven bars performed by Jinnan Yao through the sport biomechanics analysis, which conducts a kinematics analysis on the dismount by her, and further more obtains the kinematics characteristics of Jinnan Yao's dismount. All of that are in order to provide references of technical training for athletes.

METHODS: The main method is three-dimension camera analyze. We used two JVC9800 Synchronized cameras at the right side and back side of the game site. The shooting frequency is 50 frames per second. The record analysis used 3-DSignalTec system and series analysis. The anthropometric dummy is Japanese Songjingxiuzhi phantom (21 articulation points, 16 segments). It passed the original data filter and the cut off frequency is 8Hz.

RESULTS AND DISCUSSION: The actions of giant swing backward and double salto backward stretched dismount can divide into two phases, the first phase is to giant swing backward which starts with handstand statically, then turns to do giant swing backward, and ends with let go her hold from the high bar. According to the action feature of giant swing backward, it can divide into three processes including two circles giant swing acceleration process, giant swing continuing downswing process and giant swing continuing upswing process. The second phase starts within moments of letting go her finished hold from the high bar, and ends with having double salto backward somersault body straight until the buffering when falling to the ground and then stop. According the feature of the action, it can divide into two processes including double salto backward stretched process and landing and buffering process. Please see below, the technological analysis of the action structure's two phases.

Athletes starts with handstand statically and then turns to do giant swing backward, end with completed two circumference giant swing backward acceleration process. This process is prepared

for obtaining greater speed in the third circumference swing.

In the moment of from handstand statically to doing giant swing backward, the vertical distance of the center of gravity and the high bar surface is 0.90m. When the first circumference swing is over, which means the handstand on the bar of the third circumference swing moment, the resultant velocity of center of gravity is 2.6m/s after the acceleration of the two circles giant swing.

The process named giant swing continuing downswing process which means athletes starts with the third circumference handstand downswing backward and ends with being the sagging face of the bar. That is the motor process when the body center of gravity turns the highest to the lowest point. In this process, the potential energy of human body will transform to the kinetic energy, which is the energy for backward somersault.

With the body downswing, the whole body should unbend, and the head should be lower down, shoulder fully unfolded, to increase the gravity torques. The greater the gravity torques is, the greater the angular momentum will be and the strength to finish a wreath will be much greater. The round bar loopback ability is one of the main powers to complete the action. In the process of Jinnan Yao's body downswing, the humeral angle and the hip angle will decrease a few. But the two angles starts to increase again on the horizontal plane of the high bar. At this moment, the left and right humeral angles are 167° and 169°, and the hip angles are 173° and 175°. Besides, the center of gravity acceleration is 4.90m/s², which is profit from the backward vertical speed. By now, human body can obtain the greater moment of momentum, which is good for the action behind.

Human body will continue downswing at the moment passing the horizontal plane of the high bar, the humeral angle will increase, the shoulder joint will subsidence and the hip angle will increase obviously at that moment. When the body continues downswing reach to vertical position, the humeral angles increase to 198° and 201° and the hip angles increase to 168° and 170°, the center of gravity resultant velocity is 6.13m/s. The purpose of lowering the shoulders is to let the high bar become shape change, which is prepared for utilizing the elastic potential energy of high bar fully while finishing next process actions. Visibility, Jinnan Yao completes that process preferably.

The giant swing continuing upswing process starts with the upswing on the vertical plane under the bar, and ends with the releasing grip the bar moment. This process is for decreasing the loss of flip angle's speed and increasing the height of release grip.

When body has passed the vertical place under the bar, two legs must kick up energetically to create favourable muscle operating conditions. In order to finish this in the upswing process, the speed of left and right legs respectively accelerate obviously. At the same time that two legs upswing, the shoulder joint must keep down the stalk head and avoid lifting shoulders and head. Otherwise it will affect the speed at the top of the shoulder is rather small. In the moment, the humeral angle and the hip angle decrease obviously, which shortens the radius between the body center of gravity and bar axis to decrease the loss of palstance while body center of gravity rising.

When body is close to the horizontal plane of releases grip from the bar immediately and closes legs together, at that moment the angel means the included angle between the center of gravity to rod shaft and vertical plane down bar. At the moment while leaving the bar the kinematic velocity of two legs will decrease, that is the left and right kinematic velocity will decrease to 9.05m/s and 8.98m/s. Since two legs has braked before leaving the high bar and the shoulder joint is rushed forward, so it can avoid bumping bar by two legs in the double salto backward somersault body straight process after releasing grip. It takes 0.24s from vertical position under the bar to the moment while leaving the bar. Thus, too short time can lead to the lower center of gravity while leaving the bar. Whereas, Jinnan Yao's reversal palstance is about 3.26rad/s, and it is bigger than

other gymnasts, which is benefit for quickening the palstance while body overturning to backward after releasing grip from the high bar.

Beginning with the moment while leaving the bar, and ending with finishing backward somersault body straight for two circumferences, and that is double salto backward stretched process .In that process human body turns into without support condition and will be affected with the gravity mainly. Due to vertical velocity of gravity is far greater than horizontal velocity at the moment of away from the bar, the parabolic trajectory of body center of gravity is 0.001m/s^2 ---which is near zero when arriving at the highest center of gravity point. And then continuing arc backward by gravity .The vertical velocity of gravity accumulates slowly, and the moment legs landing it's 3.13m/s . Jinnan Yao's highest center of gravity point is 0.38m taller than asymmetrical bars' rod shaft, the vertical distance is 2.52m from the pad and the horizontal distance is 2.35m between the bar and the landing point. The flight time in the air is 1.24s from leaving the bar to landing. The basic condition of completing that action are height of arch, landing distance and flight time after leaving the bar .If the higher the height of arch, the father the landing distance and the longer the flight time will be ,the action can be better completed. However Jinnan Yao's center of gravity while leaving the bar is not that high, so it leads to the low height of arch.

To finish the backward somersault body straight for two circumferences must utilize not only the rotation angular velocity by body rolling the rod shaft while leaving the bar, but only the mechanics to change body's reversal radius so that it can quicken the reversal palstance while body rolling the horizontal axis. Therefore, make sure to brake legs immediately after leaving the bar, unbend the body, the upper body backward bending and head lifting, and the body is reverse-bow shape of a circle. At this moment, the lip angels increase obviously which are 215° and 218° when the center of gravity is in the highest. The upper arm will move from the upthrow position to the sides of body, the humeral angles decrease obviously. Thus, the radius of the whole body's longitudinal axis can decrease, it is benefit for increasing the reversal palstance while body rolling the horizontal axis. The reversal palstance of straight reversal for two circles is about 5.20rad/s . It's clear that her reversal palstance is kind of fast. When the reversal proceeds about $3/4$, the body start to unbend and the lip angels decrease step by step to prepare for landing .The left and right lip angels decrease to 128° and 130° while the moment legs landing.

The process, from the feet touch pads to landing buffer still, namely the landing buffer process, this process is to maintain the balance of the body.

Before landing legs stretched as far as possible to contact pads, thus create favorable buffering time and space for the landing buffer, after landing the knee and ankle bending buffer immediately retreat. If the moment when it land, the ground horizontal velocity of center of gravity is very big, the landing angle is also large, on the contrary, the gravity torque is smaller. Effect of heavy torque is insufficient to offset torque, the body will reach or was forced to change the original supporting point. When the gravity torque can make it brake in buffer process, which will waste forward or backward inertia torque, the focus now in support is arranged on the top of the stable boundary range, their vector and tends to zero or equal to zero, the body will stand still. However, the moment when Jinnan Yao landing on the ground, the horizontal velocity is 0.98m/s , the landing angle is 83° (the angle between the center of gravity of the body and landing instant connection with the formation of the ground).The body center of gravity toward the front side, the remaining of the horizontal velocity is also large, so Jinnan Yao landed a small step jump forward ,which indicated that the human body from high sky jumping and landing, not only the height determines the human body's impact force to the ground, the action of the sky jumping and landing also increase the impact force to the ground. If

the energy is not consumed before falling to the ground, the body will be hard to be balanced.

CONCLUSION: Through the kinematics analysis of double salto backward stretched dismount by Jinnan Yao ----the champion in the world, it is concluded that Jinnan Yao motion model is as follows: Giant swing backward phase: when the third circumference handstand downswing backward, the resultant velocity of center of gravity is 2.60m/s, and it is bigger than other gymnasts. Because Jinnan Yao took three circumferences giant swing backward. It takes 0.24s from vertical position under the bar to the moment while leaving the bar. Thus too short time can lead to the lower center of gravity while leaving the bar. Whereas, Jinnan Yao's reversal palstance is about 3.26rad/s, which is benefit for quickening the palstance while body overturning to backward after releasing grip from the high bar.

Double salto backward stretched dismount in uneven bars phase: time to let she go away from the poles, the flight time is 1.24s. The height of salto suspension is 0.38m, it is low. When body reach to the highest center of gravity point, the hip angles increase obviously and the humeral angles decrease obviously, the body is reverse-bow shape of a circle. Now the left and right humeral angles are 68° and 70° , the left and right hip angles are 215° and 218° . It is benefit for decrease the radius of the whole body's longitudinal axis, so that increasing the reversal palstance while body rolling the horizontal axis. The reversal palstance of straight reversal for two circles is 5.20rad/s. It's clear that her reversal palstance is kind of fast. When Jinnan Yao landing on the ground, the horizontal velocity is 0.98m/s. The body center of gravity toward the front side, the remaining of the horizontal velocity is also large, so Jinnan Yao landed a small step jump forward. Visibility, Jinnan Yao completed the double salto backward stretched dismount. But also can improve in the following aspects: to increase the height of salto suspension, so that increase the flight time, in order to prepare landing.

REFERENCES:

- L. Chen . (2007).The Athletics Analysis on Li Ya' s Reverse Suspense Straddle front Somersault to Re-grasp the Bar on Asymmetrical Bars. *Sport Science And Technology*,51-56.
- X.W. YAO.(2007) Kinematics Analysis of Actions of Upside Down - Salto Forward with Legs Together-Holding the Bar Again on Uneven Bars performed by Lin Li . *Journal of Beijing Sport University*,1707-1708.
- B.Yang.(1999)Elementary research of the dismount in Gymnastics:The skill and the training[J].*Journal of Chuxiong Teachers' College*, 120-124.

AN INVESTIGATION OF FULL BODY KINEMATICS FOR STATIC AND DYNAMIC THROW-IN IN PROFICIENT AND NON-PROFICIENT SOCCER PLAYERS WHEN THEY TRIED TO HIT A SPECIFIC TARGET.

Luis Carlos Hernandez Barraza¹, Chen Hua Yeow^{1,2}

Department of Biomedical Engineering, National University of Singapore,
Singapore¹

SINAPSE-Advanced Robotic Center, National University of Singapore,
Singapore^{1,2}

The purpose of this study was to identify the kinetic differences between proficient and non-proficient players during one ability: Throw-in. Twelve players were recruited from the local university to perform the experiment. Many studies have been conducted to explain the biomechanics of this ability, however there is about a lack of research, investigating the comparison between proficient and non-proficient players. The hypotheses of this study were that a) peak knee flexion angles would be higher for dynamic style for proficient and less proficient subjects, and b) peak vertical ground reaction force (GRF) would be higher for the dynamic style. Our results showed a markedly difference in the peak flexion angles for proficient players. The results may be useful to develop training strategies to help to the players to achieve precise throws.

KEY WORDS: Kinematics, comparison, hip flexion, peak angles.

INTRODUCTION: The throw-in is a method for restarting the game and can be used as an attacking manoeuvre near to the goal mouth. The farther a player can throw the ball, the larger the area in which his team mates may receive the ball and the greater the scoring opportunities. In soccer, there are several styles of throw-in, whereby static and dynamic styles are the most used styles during a game (Lees, 1998). In a static throw-in, the movement is performed with the feet side by side on the ground, while the dynamic throw-in the movement is performed some steps further back from the touch-line. Both styles are initiated by flexing the knees and taking the ball backwards with respect to the body, there is an upward extension of the knee joint and a marked pushing of the hips both forwards and upwards. This serves to prepare the upper body for the recoil that will propel the ball forwards. As the upper body starts to come forwards, there is a sequential unwinding starting with the hips, followed by the shoulders, elbows and, finally, the wrist and hands until ball release. Linthorne & Everret et al. (2006) studied the release angle that maximizes the distance attained in a long soccer throw in. The release angle was calculated as the mathematical expression for the relation between release speed and release angle. They found that using a low release angle the player released the ball with a greater release speed and concluded that the optimal release angle is about 30°. Currently, it is still not known how lower and upper extremity biomechanics affect the proficiency of a throw-in, for both static and dynamic styles. Therefore, the objective of this study was to investigate the differences between proficient and less proficient subjects during soccer throw-in (static and dynamic), through examination of the peak GRF, joint kinematics and kinetics. We hypothesized that: a) Peak knee flexion angles would be higher for dynamic style for proficient and less proficient subjects, and b) Peak vertical ground reaction force (GRF) would be higher for dynamic style.

METHODS: Twelve healthy male participants were recruited from the local university, with a mean age of 23 ± 2.0 years, height of 1.74 ± 0.08 m and weight 66.0 ± 8.7 kg. The exclusion criterion was a history of lower extremity injuries/diseases that might affect the throw biomechanics. All the participants signed informed consent before participation, in accordance with the university's Institutional Review Board. Anthropometric data such as, height, weight, shoulder off-set, elbow width, wrist width, hand width, knee width, ankle

width, leg length and inter-anterior superior iliac spine distance were acquired from the participants. To eliminate the effect of shoe type on the subject performance, all subjects wore the same F50 shoe model (ADIDAS, Germany) sizes from 9-11(USA). The study was carried out in a motion analysis laboratory. Two force plates (AMTI, UK), embedded into the floor, were used to determine GRF data at a sampling rate of 1000 Hz. A motion-capture system (Vicon Mx, Oxford Metrics, UK), consisting of six infrared cameras, was employed to collect kinematics data at a sample rate of 100 Hz. The force plates were synchronized to the motion capture system; both were calibrated according to the manufacturer's recommendation before the throw trials were conducted. Thirty five retro reflective markers (14-mm diameter) were attached to the participant's full body based on the Plug-In-Gait Marker set, to facilitate capture of the participants' soccer throw-in motion. One white board (170 x 190 cm) was placed from a distance of 5.5 m away from the throw point. The white board was divided in a grid of 5-cm-sized squares, with the purpose of quantifying the deviation (distance between hitting location of ball and actual target position) for "x" axis and "y" axis. One target (15-cm diameter) marked in black, was placed in the center of the board. The participants were instructed to perform a throw-in from a distance of 5.5 m away and they were asked to employ their natural throw-in style for dynamic and static task. In the case of static style, the participants threw the ball from a stationary position landing both feet on the force plate. For dynamic style, the initial position of the participant was two steps away from the force plate. Once he was told to start, the subject moved the two steps and once he was on the force plate, he threw the ball. The participants were given 5 min of practice and 5 min of rest before commencing the actual throw trial. A trial was considered successfully when the participant hit the white board. Three trials were conducted and the results were averaged from each set of three trials. All the trials were recorded using a standard video-camera (SONY, Japan) to determine the deviation of the ball respect the target. All the videos obtained during the trials were analyzed to calculate the spatial deviation from the impact location of the ball on the board to the actual target location, using tracking software (Tracker Video Analysis and Modeling Tool Open Source Physics, USA). Based on the deviation values obtained from the video analysis, the athletes were ranked, accordingly to the proficiency obtained. The top nine athletes were classified as proficient, while the bottom nine athletes were classified as less proficient. The software, Vicon Workstation 5.1 and Polygon 3.5, were used for data collection and processing respectively. The kinematics data were smoothed using a Woltring filter. The peak angle for the hip, knee, angle, shoulder, elbow and wrist during the two phases of soccer throw-in. The Throw-in phase was taken as the time between the subject's hands hold the ball and till the ball is launched. The recovery phase was taken at the event after the subject launched the ball till the subject recovered his start position. Two Factor (Style x proficient/non-proficient) ANOVA, followed by Holm-Sidak post-hoc testing, was used to compare the peak angle at Throw-in phase, and recovery phase. All significance levels were set at $p=0.05$.

RESULTS: The deviation results were the factors that allow us to classify the subjects in proficient or less proficient players. In the case of the proficient players, their deviation values were lesser by almost the half of the proficient players.

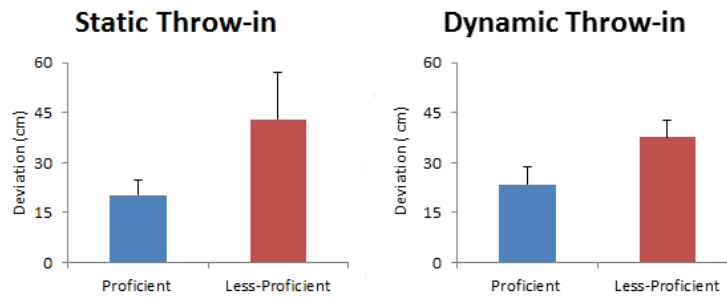


Figure 1: Comparison of the deviation for all the targets between the proficient and less-proficient players.

For the non-dominant side during the Throw-in phase, we found a higher ($p < 0.05$) hip flexion angles for dynamic style in proficient and less proficient players, and a higher knee flexion angle only in less proficient subjects. Moreover, during the recovery phase, we found a higher ($p < 0.05$) flexion angle in hip and knee joints in the less proficient players (Table 1). The peak vertical GRF was higher ($p < 0.05$) for the dynamic style for proficient players and less proficient players during the Throw-in phase (Table 2).

Table 1
Summary of mean (SD) of peak joint angles in non-dominant side between proficient and less proficient players for both throw-in styles, in sagittal plane. * Significant difference ($p < 0.05$)

Classification	Joint	Phase	Peak Joint Angles (Degrees)		P-value
			Static	Dynamic	
Proficient	Hip	Throw-in	10.52 (0.08)	34.35(11.9)	0.007*
Less Proficient	Hip	Throw-in	1.98(4.89)	45.62(11.73)	0.001*

DISCUSSION: The purpose of this study was to investigate the differences in dominant and dominant side biomechanics between proficient and less proficient subjects during two styles of soccer throw-in. Our key findings indicated that: (1) peak vertical GRF was higher at the non-dominant support leg for proficient players in both styles, (2) The hip plays an important role in determining throw proficiency for both styles, (3) The hip peak flexion is different in the two styles, in the case of the static throw in, the angle was higher for proficient players whereas in the case of the dynamic style, the value was lesser. During the throw-in phase and based on our results we found that the proficiency is related to exhibited a high value of ground reaction force for both styles. The ground reaction force allows to the subjects to have more impulse and therefore, to exert more accurate hits. The differences in the peak hip flexion angles could be because in the static throw in the proficiency is related to exert a small flexion angle around 10° , whereas in the case of dynamic style the proficiency is related to exert an angle of 30° . Kibler et al. (2006) studied the role of the core stability in sports, and his results showed that hip and pelvis are responsible for maintain body stability and that they are involved in almost all extremity activities such as running, kicking and throwing.

Table 2.
Summary of mean (\pm SD) peak vertical ground reaction forces (GRF) between proficient and less proficient subjects for non-dominant leg side, in static and dynamic throw-in. * Significant difference ($p < 0.05$).

Vertical GRF (BW units)				
Classification	Phase	Static	Dynamic	p-value
Proficient	Throw-in	0.62(0.05)	1.06(0.07)	0.001*
Less-Proficient	Throw-in	0.54(0.01)	0.87(0.04)	0.002*

CONCLUSION: Interestingly, our results only showed a significant difference in lower body kinematics. These results may suggest that the lower body plays a key role to make an accurate throw. Furthermore, the GRF could be an important parameter in the accuracy of hit a target, especially in the case of the dynamic style, because with high values of vertical GRF the player may help to propel the upper body and perform an accurate hit. The results found in the present study, may help to understand the biomechanics of the lower body and upper body in two different styles of throw-in. Moreover, the results could help to soccer players about the correct range of motion that they need to perform to achieve a precise throw. Additionally, the results could contribute to develop specific muscular training to increase the accuracy and distance of the throw-in skill during a soccer game.

REFERENCES:

- Lees, A., & Nolan, L. (1998). The biomechanics of soccer: a review. *Journal of sports sciences*, 16(3), 211-234.
- Linthorne, N. P., & Everett, D. J. (2006). Soccer: Release angle for attaining maximum distance in the soccer throw-in. *Sports Biomechanics*, 5(2), 243-260.
- Kibler, W. B., Press, J., & Sciascia, A. (2006). The role of core stability in athletic function. *Sports medicine*, 36(3), 189-198.

Acknowledgment

This work was funded by the Grant MOE ACRF-Tier 1(R397-000-143-133)

A KINEMATIC STUDY ON HOW TO KICK QUICKLY IN TAEKWONDO

Madoka KINOSHITA¹ and Norihisa FUJII²

Doctoral Program in Physical Education, Health and Sport Sciences,
University of Tsukuba, Tsukuba, Japan¹

Faculty of Health and Sport Sciences, University of Tsukuba, Tsukuba, Japan²

The purpose of this study was to evaluate techniques for increasing kicking speed in a Taekwondo roundhouse kick according to different target distance conditions. The results were summarized as follows: i) With short condition, there was no significant correlation between kicking speed and pelvic speed; ii) Good subjects attained greater extension angular velocity of the knee joint with individual kinematic chain technique regardless of different distance conditions; and iii) subjects changed motion of the support leg in order to adapt the translational motion according to different distance conditions. Taken together, our data suggest that coaches should pay greater attention to the support leg when adapting the technique for kicking distance as well as the motions of the pelvis and hip joint of the kicking leg when adapting the technique to increase kicking speed.

KEY WORDS: martial arts, kicking techniques, target distance, kinematic chain.

INTRODUCTION: Taekwondo is a form of Korean martial arts and has been an Olympic event since 2000. With the latest Taekwondo rules, Taekwondo athletes have to kick their opponents more accurately to score more points and win games. In competitions, athletes are required to adjust their distance to opponents while increasing kicking speed. The distance to opponents is defined as the relation between athletes, which can constantly change. According to previous studies, a roundhouse kick (RHK) is one of the kicks used most frequently in competitions. Some studies have presented techniques for both increasing kicking speed and decreasing kicking time (Kinoshita & Fujii, 2014; Kinoshita & Fujii, 2015), and the kinematic mechanisms of different target distances (Kim, Kwon, Yenuga, & Kwon, 2010). Kinoshita & Fujii (2014) stated that it is critical to have a greater extension angular velocity of the knee joint with effective patterns of both left rotation angular velocity of the lower torso and flexion angular velocity of the hip joint to kick at a faster speed and with a shorter time. Kinoshita & Fujii (2015) elucidated the possibility of a relationship between pelvic speed at the moment the toe leaves the floor and kicking speed. Kim et al. (2010) concluded that the adjustment to different target distances was mainly accomplished through pivot hip displacements of the support leg, hip flexion of the kicking leg, and left rotation of the pelvis; target distance mainly affected the reach control function of the pelvis and the linear balance function of the trunk. However, they did not clarify how to kick quickly according to different target distances. The purpose of this study was to evaluate techniques of increasing kicking speed in a Taekwondo RHK with kinematic data according to three different target distance conditions.

METHODS: Thirteen male Japanese Taekwondo athletes, who were also included in our previous studies (Kinoshita & Fujii, 2014; Kinoshita & Fujii, 2015), participated in this study after the informed consent. The participants had diverse skill levels. The experiment trial consisted of an RHK to a target with a preferred leg. The target height was the same as the participants' torso. There were three target distance conditions (Figure 1: Short; 0.68 ± 0.06 [m], Normal; 0.90 ± 0.07 [m], and Long; 1.15 ± 0.09 [m]). The target distance conditions were determined according to participants' leg lengths. The global coordinate system was defined as shown in Figure 1. The 3D coordinates of the reflective markers placed on body segments and the target were captured by a motion capture system (Vicon MX+, 250 Hz) and filtered with a Butterworth digital filter (12.5-25 Hz). The RHK was divided into three phases with four events as shown in Figure 1. The four events were as follows: STR, the instant that the

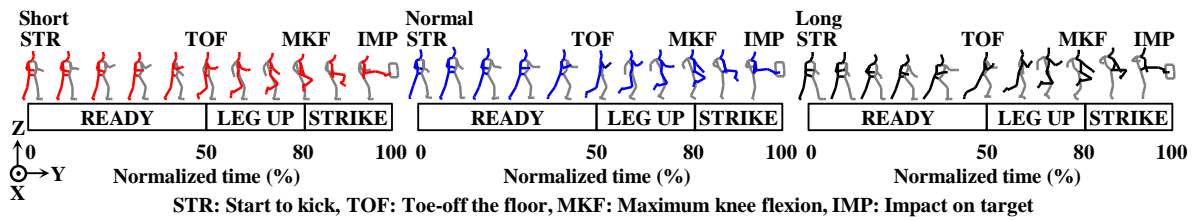


Figure 1: Motion of RHK in three different distance conditions.

speed of the body center of gravity surpassed 0.5 m/s; TOF, toe of kicking leg took off the floor; MKF, maximum knee flexion of the kicking leg; and IMP, impact on the target. To normalize a kicking motion, STR, TOF, MKF, and IMP were defined as 0%, 50%, 80%, and 100% time respectively. READY, LEG UP, and STRIKE phases were termed, respectively. The kinematics data were calculated to evaluate the movements of body segments and joints for increasing kicking speed according to different distances.

RESULTS: Figure 2 showed the average kicking speed at IMP according to three different distance conditions. In all conditions, kicking speed was almost 17 [m/s]. There was no significant difference in kicking speed among the three distance conditions. Figure 3 showed the relationship between kicking speed at IMP and pelvic speed at TOF in all subjects according to three distance conditions. With Normal and Long conditions there was a positive correlation between kicking speed and pelvic speed (Normal: $r=0.7250$, $p<0.01$ and Long: $r=0.7915$, $p<0.01$). With Short condition, there was no correlation between these parameters. All subjects could kick the target with the same kicking speed, regardless of distance conditions. Table 1 provided the kicking speed at IMP and pelvic speed at TOF in two representative subjects (Subj. A and B) and the average magnitude in all subjects. Both subj. A and B had a greater kicking speed in all conditions. Subj. B also had a greater pelvic speed in all conditions. On the other hand, subj. A had the lowest pelvic speed among all subjects with only Short condition. Figure 4 showed the angular velocities (pelvis: left rotation/right rotation; hip joint of kicking leg: flexion/extension; and knee joint of kicking leg: extension/flexion) of subj. A and B. Both subj. A and B had a greater extension angular velocity of the knee joint at IMP in all conditions. The patterns of angular velocities were similar with every condition among the individuals. This tendency was represented in all subjects (not shown here). Subj. A maintained greater flexion angular velocity of the hip joint

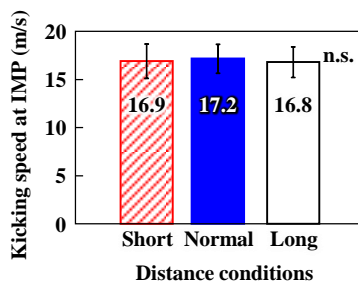


Figure 2: Average kicking speed at IMP.

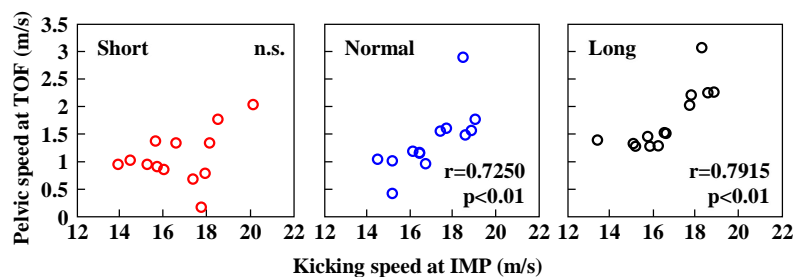


Figure 3: Kicking speed at IMP and pelvic speed at TOF in all subjects according to three distance conditions.

Table 1

Kicking speed and pelvic speed of selected subjects and average magnitudes

Conditions	Kicking speed (m/s)			Pelvic speed (m/s)		
	Subj. A	Subj. B	Mean	Subj. A	Subj. B	Mean
Short	17.9	18.3	16.9±1.8	0.2	1.4	1.1±0.5
Normal	19.0	19.2	17.2±1.5	1.6	1.8	1.4±0.6
Long	19.1	18.8	16.8±1.6	2.3	2.3	1.8±0.6

during the STRIKE phase and decreased the left rotation of the pelvis rapidly before MKF, regardless of distance conditions. On the other hand, subj. B decreased the flexion angular velocity of the hip joint rapidly before MKF and the left rotation of the pelvis at 90% time for all conditions. There were different angular velocity patterns for pelvis left rotation and hip joint flexion between the two subjects. Figure 5 illustrated the contribution ratio of motion of support leg, pelvis left rotation/right rotation, hip joint flexion/extension, knee joint flexion/extension, and other motions (pelvis flexion/extension and left bending/right bending, hip joint adduction/abduction and internal rotation/external rotation) to all kicking trajectories according to different distance conditions in subj. A, subj. B, and average magnitudes. The contribution of the support leg represented magnitude of the translational motion produced by the support leg. Both subj. A and B increased the ratio of the support leg to all kicking trajectories as with increasing target distance. subj. A decreased the ratio of hip joint flexion/extension while increasing the ratio of support leg. However, Subj. B decreased the ratio of pelvis left rotation/right rotation while increasing the ratio of the support leg.

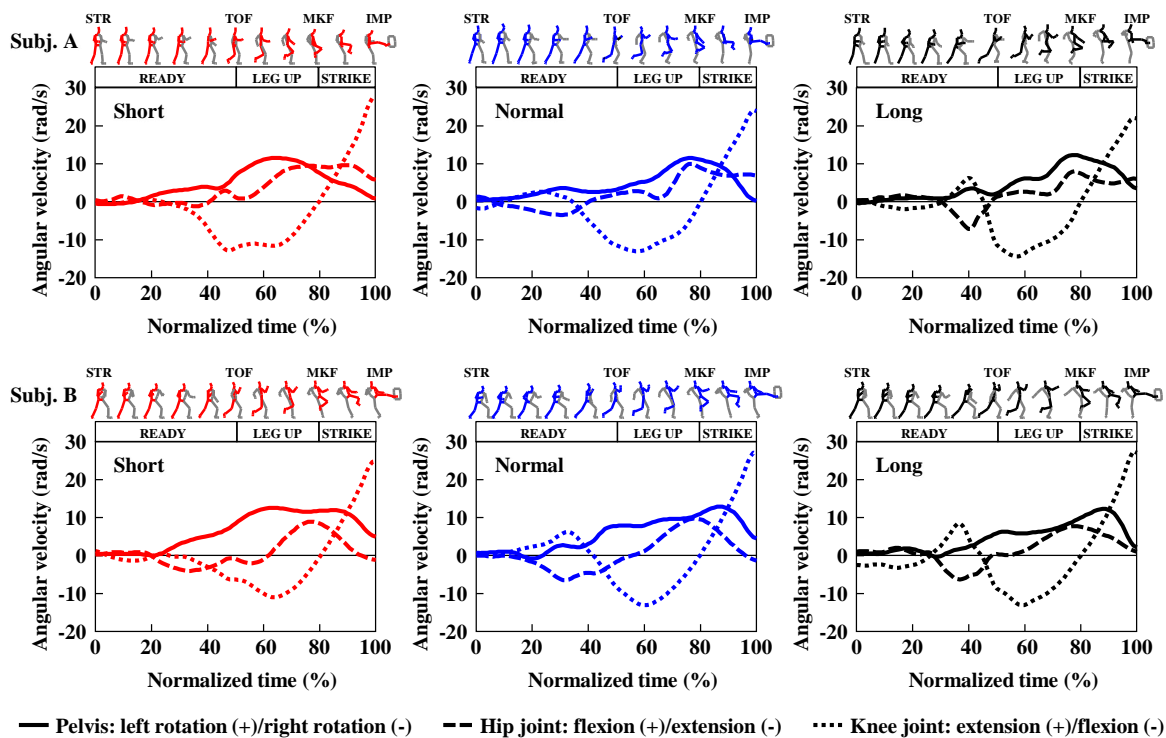
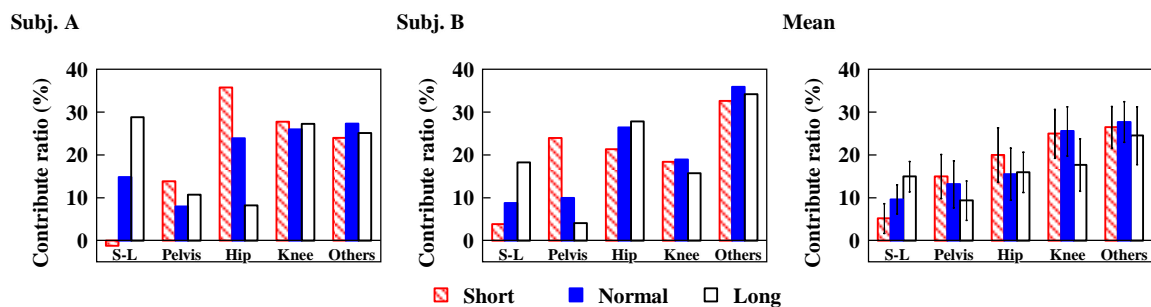


Figure 4: Angular velocities of pelvis left rotation/right rotation, hip joint flexion/extension, and knee joint flexion/extension according to distance conditions in subj. A and B.



S-L: Motion of support leg, Pelvis: Left rotation/Right rotation of pelvis, Hip: Flexion/Extension of hip joint in kicking leg
 Knee: Flexion/Extension of knee joint in kicking leg, Others: The other motions in pelvis and hip joint in kicking leg

Figure 5: Contribution ratio of motion in pelvis and lower extremities to all kicking trajectory according to distance conditions in subj. A, B and average magnitudes.

DISCUSSION: The purpose of this study was to evaluate techniques of increasing kicking speed according to the different target distance conditions. According to Figure 2, kicking speed was almost the same for all distance conditions. This result illustrated that the subjects who participated in this study had their own maximum kicking speed regardless of distance conditions. Kinoshita & Fujii (2015) elucidated the possibility of a relationship between pelvic speed at TOF and kicking speed with Normal condition. In this study, there was no significant relationship between kicking speed at IMP and pelvic speed at TOF only with Short condition, regardless of the same kicking speed in all conditions (Figure 2 and 3). This result demonstrated that the greater translational pelvic speed is related to kicking speed with Normal and Long conditions. In contrast, the pelvic speed was not always an important contribution in Short condition when subjects controlled rotational motion to increase kicking speed. Thus, it was possible to identify the techniques to increase kicking speed according to different distance conditions by comparing subj. A and B who could kick with high speed for all conditions and had different pelvic speeds with Short condition. Kinoshita & Fujii (2014) reported that it was necessary to increase the extension angular velocity of the knee joint of the kicking leg during STRIKE phase. Subj. A and B had a greater extension angular velocity of the knee joint of the kicking leg during STRIKE phase (Figure 4). However they kicked by utilizing different kinematic chains to increase angular velocity. The kinematic chain of subj. A was caused by the rapidly decreasing left rotation of the pelvis before MKF. The kinematic chain of subj. B was caused by the rapidly decreasing flexion of the hip joint before MKF and the rapidly decreasing left rotation of the pelvis at 90 % time. These motions might produce the moment of joint force related to the extension angular velocity of the knee joint in different ways. Thus, in the case of utilizing pelvis left rotation as the source of kinematic chain, pelvic speed at TOF does not play an important role in increase kicking speed, because greater flexion angular velocity of the hip joint compensates for kicking speed. Kim et al. (2010) stated motions of the support leg, hip joint, and pelvis were related to the adaption for distance conditions. The patterns of angular velocity were similar with every distance condition among all individuals, regardless of the kicking speed. According to Figure 4 and 5, subjects did not change the sequence motion of the kicking leg but changed the translational motion produced by the support leg. Thus, in order to improve kicking speed according to different distance conditions, athletes should first train for kicking quickly with a Normal distance condition as kicking by utilizing the good kinematic chain. After they acquire the technique for increasing kicking speed, coaches should pay more attention to the support leg in order to improve athletes' techniques for adapting to different distance conditions.

CONCLUSION: This study identified techniques for increasing kicking speed in a Taekwondo RHK according to different distance conditions. It is our view that coaches should pay more attention to the support leg when adapting the technique for different kicking distances and to the motions of the pelvis and hip joint of the kicking leg when adapting the technique to increase kicking speed.

REFERENCES:

- Kim, J. W., Kwon, M. S., Yenuga, S. S., & Kwon, Y. H. (2010). The effect of target distance on pivot hip, trunk, pelvis, and kicking leg kinematics in Taekwondo round house kick. *Sports Biomechanics*, 9, 98-114.
- Kinoshita, M. & Fujii, N. (2014). Biomechanics of Taekwondo roundhouse kick. *Biomechanism*, 22, 143-154. (in Japanese).
- Kinoshita, M. & Fujii, N. (2015). Biomechanical analysis of Taekwondo roundhouse kick focused on mechanical energy flow. *Journal of the Society of Biomechanisms Japan*, 39, 37-46. (in Japanese).

IDENTIFYING RELEASE FOR HIGH BAR SKILLS

Melanie Golding, Gareth Irwin, Ian Bezodis, Tim Exell and David G Kerwin

Cardiff School of Sport, Cardiff Metropolitan University, Cardiff, UK

The release from the high bar for both dismounts and release re-grasp skills is a compulsory part of any high bar routine. Despite the importance of the instant of release there is no definitive scientific method to identify this instant in high bar gymnastics. Various methods of release definitions were compared using automatic motion analysis (200Hz), visual images (200Hz) and bar force (1000Hz). A single elite gymnast performed 5 dismounts and 5 Tkachevs. Differences between bar force derivatives and motion analysis suggest the approach taken can influence the key release parameters. Differences between skills also highlights that a global release definition may not be appropriate and further research should consider skill specific definitions of release from the bar.

KEY WORDS: gymnastics, methodology, event definition

INTRODUCTION: The release is a key part of any high bar routine in Men's Artistic Gymnastics, despite this there is no definitive scientific method to identify the instant of release from the bar. The instant of release is the moment that the trajectory of the gymnast's mass centre is set and is unchangeable until re-grasp or landing (Hiley & Yeadon, 2003). It is important that the performance of the skill preceding release allows for the desired release parameters to be created leading to successful performance of a release re-grasp skill or dismount. Understanding of the instant of release is crucial as this determines the success of the performance of the flight element. Throughout the literature varying definitions have been employed utilising methods from visual cues (Kerwin, Yeadon & Lee, 1990; Hiley & Yeadon, 2005) to measures of grip radius (Harwood, Kerwin & Yeadon, 1991; Kerwin, Yeadon & Harwood, 1993; Kerwin & Irwin, 2010, 2011; Manning, Irwin, Gittoes & Kerwin, 2011) and contact switches (Gervais & Baudin, 1995). Kerwin et al. (1993) initially highlighted the importance of correct release identification when results that appeared mechanically impossible were reported showing the mass centre of the gymnast to be higher than the bar at release for a dismount (Kerwin et al., 1990). Previously, Gervais and Baudin (1995) considered release identification by comparing various methods, however the study was inconclusive and a criterion method of release identification has yet to be established. The importance of accuracy when identifying release was highlighted by Harwood et al., (1991) who stated that measured contributions to velocity and body position can change greatly with the error of one frame when identifying release. The instant of release is not easily identifiable and the impact of the choice of method to define release is still not well understood. The aim of this study was to quantify the effect of release definition on key parameters during the performance of flight elements on high bar.

METHODS: Data Collection: Ethical approval was gained from the University and informed consent given by the participant. A single subject design was adopted in order for differences to be attributable to the methodology and not individual differences. An elite male gymnast (age: 15 years; mass: 59.2 kg; height: 1.63 m) performed five dismounts (full twisting double straight, twisting occurred in the second somersault) and five straddle Tkachevs on a competition standard high bar. Kinematic data were collected using an automated motion analysis system (200 Hz) (CODAmotion, Charnwood Dynamics Ltd., Leicester, UK). Active markers were placed bilaterally on the fifth metatarsophalangeal joint (MTP), lateral malleolus, femoral condyle, greater trochanter, the estimate centre of rotation of the glenohumeral joint, lateral epicondyle of the elbow, ulna styloid process, centre of the bar and 0.5 m to the left and right of the centre of the bar. A video camera (Sony HVR-Z5E, Sony, Japan) was located near to the high bar upright to give a close up view of the gymnast's hands on the bar. The camera operated at 200 Hz with a shutter speed of 1/300 s.

Kinetic data were collected using a high bar instrumented with strain gauges (1000 Hz) outputting data as a voltage. Calibration of the high bar strain gauges was achieved through incremental loading and unloading of the bar with known loads and linear regression incorporating vertical and horizontal stiffness values (Kerwin & Irwin, 2006) was employed to predict vertical and horizontal bar forces from voltage outputs. Synchronisation of data accurate to 0.001 s was achieved using a trigger resulting in a voltage drop and incremental lighting of 20 light-emitting diodes in the field of view.

Data Analysis: The gymnast was assumed to be bilaterally symmetrical throughout the movement and was therefore analysed as planar model (Irwin & Kerwin, 2001). In order to obtain kinematic information for a planar gymnast the mid-points of the joints of the left and right were used throughout the analysis. A residual analysis (Winter, 2005) was used to identify an appropriate cut off frequency to filter the data; residuals were calculated using the toe, hip and wrist markers in both the y and z directions, resulting in a cut of frequency of 11 Hz. Whole body and segmental inertia parameters including centre of mass were calculated based on Yeadon's (1990) inertia model through a method of scaling. Circle angle, vertical velocity and horizontal velocity of the mass centre were identified as variables of interest due to them being key to the gymnast's trajectory during flight. The gymnast's circle angle was defined by the location of the total body mass centre and the location of the centre of the bar relative to the y axis; the gymnast was defined as 90° at handstand and 270° when under the bar. Grip radius was defined as the distance between the gymnast's mid wrists and the centre of the high bar (Irwin & Kerwin, 2008). Release was defined using methods from previous literature and also novel methods. A 1% increase in the maximum grip radius in the preceding longswing ($GR_{1\%}$) (Harwood et al., 1991; Kerwin et al., 1993). A 10% increase in the maximum grip radius in the preceding longswing ($GR_{10\%}$) (Kerwin & Irwin, 2010; Manning et al., 2011). Novel methods included a calculation of jerk using vertical (J_{FZ}), horizontal (J_{FY}) and resultant (J_{FR}) force at the bar. Peak force and oscillation of the force trace are identified; the peak in jerk between those points is then identified as release from the bar. Using a higher order kinematic variable allows for a potentially more robust measure to be employed to identify release. For further reference visual methods of release identification were employed; the first frame in which a clear space was visible between the bar and the gymnast's hands (HS) (Kerwin et al., 1990) and the frame before there was a clear space visible between the gymnast's hands and the bar (HS_{-1}) (Hiley & Yeadon, 2005).

RESULTS & DISCUSSION: Release times show that J_{FZ} consistently identifies release earlier than the other methods employed (Table 1). During dismounts methods utilising jerk identify release earlier than those utilising grip radius ($GR_{1\%}$, $GR_{10\%}$) or visual identification (HS , HS_{-1}), however during Tkachevs this changes. Release times reported for Tkachevs are earliest using J_{FZ} , however J_{FY} and J_{FR} identify release later than all other methods employed.

Table 1. Average release time (s) for dismounts and Tkachevs reported relative to J_{FZ} .

	Dismount		Tkachev	
J_{FZ}	0.000	± 0.000	0.000	± 0.000
J_{FY}	0.041	± 0.004	0.119	± 0.010
J_{FR}	-0.001	± 0.002	0.117	± 0.009
$GR_{1\%}$	0.127	± 0.002	0.071	± 0.010
$GR_{10\%}$	0.132	± 0.002	0.078	± 0.007
HS	0.129	± 0.005	0.082	± 0.016
HS_{-1}	0.124	± 0.005	0.077	± 0.016

As expected, circle angle is greater for Tkachevs than for dismounts as the gymnast releases later in order to travel backwards over the bar (Table 2). Release angles reported for Tkachevs were all greater than 360° allowing the gymnast to travel back over the bar to re-grasp. Circle angles between 401° and 409° reported for the female Tkachev (Manning et al.,

2011) compare favourably to those reported by methods using horizontal and resultant jerk (J_{FY} , J_{FR}).

Previously Kerwin et al. (1990) found the gymnast's centre of mass to be higher than the height of the bar during dismounts, this highlighted that the instant identified as release may not be correct. If a gymnast released the bar when their mass centre was higher than the height of the bar this would result in a trajectory of the mass centre travelling towards the bar rather than away from the bar as in a dismount (Kerwin et al., 1993). Kerwin et al. (1990) defined release as the instant there was a clear space between the gymnast's hands and the bar (HS) with 50 Hz video of the whole gymnast. The same method was employed here with 200 Hz video zoomed in on the gymnast's hands and values below 360° for circle angle are reported. This provides some support for the suggestion from Gervais and Baudin (1995) that a close up view of the hands may provide a better estimate of release.

The earlier release times identified by methods using jerk (J_{FZ} , J_{FY} , J_{FR}) during dismounts resulted in greater vertical velocities, however differences in horizontal velocities are less clear with greater standard deviations reported compared to methods utilising grip radius ($GR_{1\%}$, $GR_{10\%}$) and visual cues (HS , HS_{-1}). Hiley and Yeadon (2003) reported average vertical velocities of 4.83 m·s⁻¹, which reports lower values than methods employing jerk to identify release and higher values than those using grip radius ($GR_{1\%}$, $GR_{10\%}$) and visual identification (HS , HS_{-1}). Horizontal velocities reported are greater than the average reported by Hiley and Yeadon (2003) for dismounts as 1.27 m·s⁻¹ and Arampatzis and Brüggemann (1999) who reported horizontal velocities of 0.82 m·s⁻¹.

Table 2. Release parameters for dismounts and Tkachevs when using each of the methods of release identification (mean ± SD).

	Circle Angle (°)		Vertical Velocity (m·s ⁻¹)		Horizontal Velocity (m·s ⁻¹)	
	Dismounts	Tkachevs	Dismounts	Tkachevs	Dismounts	Tkachevs
J_{FZ}	309 ± 0.5	379 ± 2.4	5.1 ± 0.06	3.2 ± 0.10	1.6 ± 0.13	-1.2 ± 0.15
J_{FY}	323 ± 0.9	401 ± 4.0	5.0 ± 0.06	2.0 ± 0.12	1.4 ± 0.12	-1.9 ± 0.12
J_{FR}	309 ± 0.5	401 ± 3.9	5.1 ± 0.06	2.0 ± 0.14	1.6 ± 0.13	-1.9 ± 0.12
$GR_{1\%}$	353 ± 0.9	393 ± 2.9	4.1 ± 0.04	2.3 ± 0.19	1.5 ± 0.10	-1.7 ± 0.10
$GR_{10\%}$	355 ± 1.0	394 ± 2.9	4.1 ± 0.04	2.3 ± 0.18	1.5 ± 0.10	-1.8 ± 0.10
HS	354 ± 1.7	395 ± 3.8	4.1 ± 0.05	2.3 ± 0.14	1.5 ± 0.10	-1.8 ± 0.12
HS_{-1}	352 ± 1.8	394 ± 3.8	4.2 ± 0.05	2.3 ± 0.14	1.4 ± 0.10	-1.8 ± 0.13

Across methods Tkachevs consistently displayed greater standard deviations indicating greater variability across trials, therefore, variability in Tkachevs may be due to variation in performance of the skill rather than variation in the method used to define release.

Images taken from high speed video (200 Hz) of the hand show what is happening at the instant of release from the high bar; Figure 1 shows that using J_{FZ} and J_{FR} to identify release the gymnast is still pulling down on the high bar, these methods report average circle angles of 43°-46° less than methods using grip radius ($GR_{1\%}$, $GR_{10\%}$) and visual identification (HS , HS_{-1}). Visually grip radius methods ($GR_{1\%}$, $GR_{10\%}$) and visual identification (HS , HS_{-1}) produced similar release times for dismounts and this was supported by similar circle angles, vertical and horizontal velocities of the mass centre (Table 2).

J_{FY} and J_{FR} (Figure 2, b; c) identify release when the gymnast is clearly off the bar; this method reported a greater circle angle than other methods where the gymnast still has some contact with the bar. J_{FR} appeared to identify release early during a dismount, however when considering a Tkachev the same method identified release much later; the gymnast is no longer in contact with the bar. This highlighted that the skills being performed needs to be taken into consideration, the gymnast may release the bar in different ways for different skills and therefore a different method of release identification may be more appropriate.

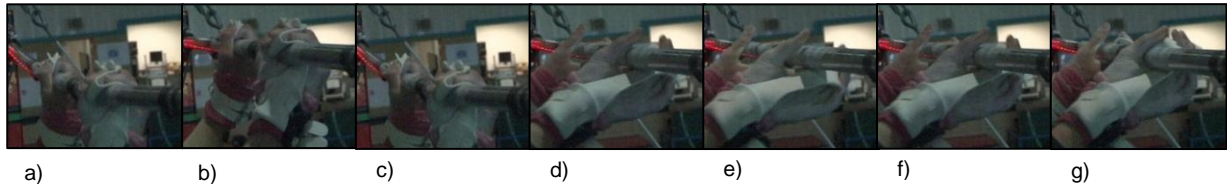


Figure 1. Images of the hand at release using varying methods of release identification during a dismount; a) J_{FZ} , b) J_{FY} , c) J_{FR} , d) $GR_{1\%}$, e) $GR_{10\%}$, f) HS , g) HS_{-1} .

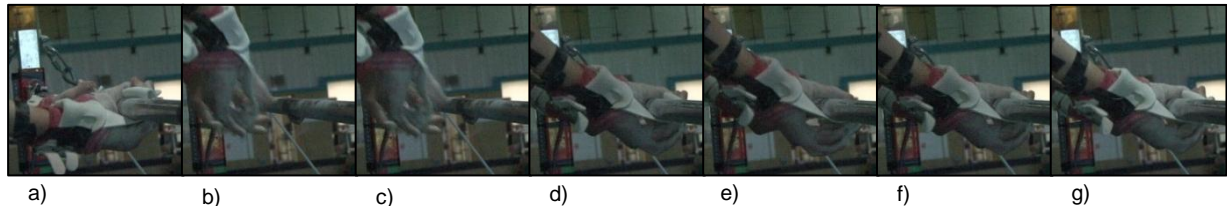


Figure 2. Images of the hand at release using varying methods of release identification during a Takchev; a) J_{FZ} , b) J_{FY} , c) J_{FR} , d) $GR_{1\%}$, e) $GR_{10\%}$, f) HS , g) HS_{-1} .

CONCLUSION: High-speed video provides valuable insight into the validation of different methods employed to identify release from the high bar. This study highlighted that there are variations in skills and release definition and therefore a definition employed may need to be skill specific. A global release definition may not be appropriate and further research should investigate skill specific definitions of release from the bar.

REFERENCES:

- Arampatzis, A. & Brüggemann, G.-P. (1999). Mechanical energetic processes during the giant swing exercise before dismounts and flight elements on the high bar and uneven parallel bars. *Journal of Biomechanics*, 32, 811-820.
- Gervais, P. & Baudin, J. P. (1995). The identification of release on the horizontal bar. In: T. Bauer ed. *Proceedings of the 13th International Symposium on Biomechanics in Sport*. Ontario, Canada, 147-150.
- Harwood, M. J., Kerwin, D. G. & Yeadon, M. R. (1991). Release mechanics in the triple tucked backward salto dismount from high bar. *Proceedings of the XIII International Congress of Biomechanics*, Perth, Australia, 73-74.
- Hiley, M. J. & Yeadon, M. R. (2003). The margin for error when releasing the high bar for dismounts. *Journal of Biomechanics*, 36, 313-319.
- Hiley, M. J. & Yeadon, M. R. (2005). The margin for error when releasing the asymmetric bars for dismounts. *Journal of Applied Biomechanics*, 21, 223-235.
- Irwin, G. & Kerwin, D. G. (2001). Use of '2D-DLT' for the analysis of longswings on high bar. In: *Proceedings of Oral Sessions, XIX International Symposium on Biomechanics in Sport* (edited by J. R. Blackwell), pp. 315-318.
- Irwin, G. & Kerwin, D. G. (2008). Musculoskeletal work preceding the Tkachev on uneven bars. *Proceedings of the 26th International Symposium on Biomechanics in Sport*. Seoul, Korea, 191-194.
- Kerwin, D. G., Yeadon, M. R. & Lee, S-C. (1990). Body Configuration in Multiple Somersault High Bar Dismounts. *International Journal of Sport Biomechanics*, 6, 147-156.
- Kerwin, D. G., Yeadon, M. R. & Harwood, M. J. (1993). High Bar Release in Triple Somersault Dismounts. *Journal of Applied Biomechanics*, 9, 279-286.
- Kerwin, D. G. & Irwin, G. (2006). Predicting high bar forces in the longswing. *Sports Engineering*, 9, (2), 115.
- Kerwin, D. G. & Irwin, G. (2010). Musculoskeletal work preceding the outward and inward Tkachev on uneven bars in artistic gymnastics. *Sports Biomechanics*, 9, (1), 16-28.
- Kerwin, D. G. & Irwin, G. (2011) Kinetic analysis of toe-on Tkachev on uneven bars. *Portuguese Journal of Sport Sciences*, 11, (2), 283-286.
- Manning, M. L., Irwin, G., Gittoes, M. J. R. & Kerwin, D. G. (2011). Influence of longswing technique on the kinematics and key release parameters of the straddle Tkachev on uneven bars. *Sports Biomechanics*, 10, (3), 161-173.
- Winter, D. A. (2005). *Biomechanics and motor Control of Human Movement* (3rd edition). Chichester: Wiley.
- Yeadon, M. R. (1990). The simulation of aerial movement. Part II: A mathematical inertia model of the human body. *Journal of Biomechanics*, 23, 67-74.

BIOMECHANICS OF TECHNIQUE SELECTION IN WOMEN'S ARTISTIC GYMNASTICS: FROM THEORY TO PRACTICE

Michelle Manning^{1,2}, Gareth Irwin², David G. Kerwin² and Marianne J.R. Gittoes²

School of Life Sciences, Kingston University, Kingston Upon Thames, UK¹
Cardiff School of Sport, Cardiff Metropolitan University, Cardiff, Wales, UK²

This research aimed to determine effective technique selection for the female longswing through four themes: contemporary trend (T1), biomechanical conceptual (T2), musculoskeletal (T3) and energetic (T4) approaches. 3D video data at two elite competitions provided high ecological validity. T1 identified the straddle Tkachev as the ideal vehicle with three distinct preparatory techniques (arch, pike, straddle) preceding it. Significant joint kinematic differences were not replicated in release parameters (T2) although joint kinetics highlighted greater physical demands in the pike (T3), with an energetics effectiveness score highlighting the arch as a technique promoting skill development (T4). Increasing knowledge and understanding allows coaches to optimise technique selection.

KEY WORDS: coaching, skill development, longswing, effective technique.

INTRODUCTION: Technique selection is a central feature of coaching when developing effective skill learning. In gymnastics many skills can be performed with different techniques and knowing which is best is the biggest challenge for coaches at all levels. The mindset of the coach is key to the technique selection process and the development of the gymnast (Irwin et al., 2005). Coaches observe skills as a series of body shapes and movement patterns that cause biomechanical changes that are often unobservable to the coach's eye. Effective coaching practices therefore require mechanical knowledge and understanding of the desired skills in order to develop technique and keep in line with the rapidly developing sport. The female longswing is a key skill that directly links to the development of more complex skills (Hiley & Yeadon, 2007). Although the backward longswing has received a high amount of research focus, variations in longswing technique have not. Previous researchers have highlighted the importance of the shoulder and hip joints in the success of the longswing; the varying movement patterns at these joints and resultant mechanics therefore require further investigation. Manning et al. (2011) identified that three distinct longswing techniques preceding the straddle Tkachev had varying joint kinematic characteristics during the previously defined functional phases (shoulder hyperflexion to extension and hip hyperextension to flexion; Irwin & Kerwin, 2005). However, a significantly earlier initiation of the shoulder and hip functional phase in the arch longswing did not significantly influence the key release parameters; therefore it was not apparent as to why one technique would be selected over another. Analysis into the musculoskeletal demands of each technique would provide coaches with insight into a scientific criterion to add to the technique selection process. Furthermore, previous researchers have established the importance of considering the biomechanical energetic input from gymnasts and their interaction within the gymnast-high-bar energy system (Arampatzis & Brüggemann, 2001). Providing coaches with information on the overall energy cost of each technique assists in gymnast preparation, technique development and technique selection. Therefore this research aimed to increase the knowledge and understanding of the biomechanics underpinning female longswing techniques to determine effective technique selection, with the overall aim to demonstrate the important link between theory and the underlying processes of practice.

METHOD: Data Collection: Data were collected from the qualification rounds at the 2000 Olympic Games (OG) and 2007 World Championships (WC). Video image data were obtained from two 50 Hz video cameras (Sony Digital Handycam VX1000E). Initially each of the 82 qualification routines from OG and 117 from WC were recorded with the age ($17.7 \pm$

2.8 years), height (1.54 ± 0.07 m) and body mass (45.12 ± 6.88 kg) of the elite gymnasts by IOC and FIG approved researchers respectively prior to the competition. The methods followed a thematic approach; from Theme 1: *Contemporary trend analysis* where eighteen successfully executed straddle Tkachev recordings were selected for the subsequent three themes. Images of calibration objects at OG consisted of a single calibration pole with five equally spaced (1.0 m) spheres (0.1 m diameter) at six pre-measured locations giving 30 known coordinates. At the 2007 WC two static (1 m x 1 m x 3 m) cuboids giving 48 known coordinates provided the calibrated volume encompassing the analysed preparatory longswing. The origin was defined as the centre of the high bar in its neutral bar position.

Data Processing: Theme 1: *Contemporary trend analysis* incorporated identification of release and re-grasp skills performed and the preparatory longswings preceding these skills. Longswing techniques were defined through visual inspection of shoulder and hip movement patterns consisting of degree of shoulder extension and hip flexion, location of movement (above or below the low bar) and presence of hip abduction. Calibration and movement frames for the 18 straddle Tkachev trials used within Theme 2-4 were digitised (Vicon Peak 9.0, UK) with calibration images consisting of ten frames for each camera and movement data comprising of the preparatory longswing, straddle Tkachev and re-grasp. Gymnast circle angle was defined as 90° when the gymnast was in a handstand position and continued to 450° as the gymnast returned to handstand. All movement data were analysed between a circle angle of 135° and release. The left and right fifth MTP, ankle, knee, hip, shoulder, elbow, wrist, centre of the gymnast's head and the centre of the high bar for each movement frame were digitised from each camera view. Data were time synchronised using the methods of Yeadon and King (1999) and a 12-parameter three-dimensional (3D) direct linear transformation (Marzan & Karara, 1975) was used to reconstruct the 3D coordinate data. Reconstructed 3D coordinate data were filtered with a low pass digital filter with a cut off frequency of 8 Hz. Customised segmental inertia parameters for each gymnast were calculated using Yeadon's inertia model (1990), limb lengths determined from the video data and the height and mass of each gymnast. A four segment planar representation of the gymnast was constructed by averaging the digitised coordinate data for the left and right sides of the body.

Data Analysis: Theme 2: *Biomechanical conceptual approach* analysed the functional phases defined by Irwin and Kerwin (2005) as maximum shoulder flexion to extension and maximum hip extension to flexion. Corresponding joint kinematics were also reported together with release parameters consisting of angle of release, horizontal and vertical velocity of the gymnast's mass centre (CM) and angular momentum about the gymnast CM and bar. The instant of release was defined using a linear coordinate separation between the virtual mid-wrists and centre of the high bar (Manning et al., 2011) and occurred once the distance exceeded 10% of the maximum value obtained during the preceding longswing. Angular momentum (L) of each segment about its CM and of each segment about the whole body CM were summed over the four segments to determine L about the gymnast's CM. L values were further normalised (L_n and $L_{n_{bar}}$) by dividing by the product of 2π and the moment of inertia in the anatomical position (SS/s). Theme 3: *Biomechanical musculoskeletal approach* incorporated a two dimensional (2D) inverse dynamics analysis to calculate internal joint forces (IJF) and moments (JM) at the knees, hips, shoulders and high bar. Known zero forces at the toes were used with Newton's second laws of linear and angular motion to calculate net joint forces. Joint powers (JP) were calculated as the product of the previously defined JM and joint angular velocities to determine the nature of the muscle action occurring around the joint centres. The time integral of JP was calculated in determining joint work (JW) with JW at the shoulder, hip and knee joints summed to calculate total JW. Total JW represented gymnast energy contribution to the gymnast-high-bar total energy system. Theme 4: *Biomechanical energetics approach* determined longswing effectiveness by calculating the change in total energy (En_{Tot}) between a circle angle of 135° and release and dividing by change in gymnast energy (En_{Gym}) producing a biomechanical energetic effectiveness score.

Statistical Analysis: Having met assumptions of normality (Shapiro-Wilkes) and homogeneity of variance (Levene's test), differences between discrete variables for the arch, straddle and pike longswings were quantified with an Analysis of

Variance ($p \leq 0.05$) with continuous data differences quantified by a percentage Root Mean Squared Difference.

RESULTS & DISCUSSION: *Contemporary trend analysis* (Theme 1): The straddle Tkachev was identified as the most frequently performed release and re-grasp skill from a backward preceding longswing across both competitions (53%). Of the backward longswings performed where negotiation of the low bar was required on the downswing, the arch (19%), straddle (35%) and pike (31%) longswings were the most distinct techniques employed. Building on from Theme 1 and the work of Manning et al. (2011) Theme 2: *Biomechanical conceptual approach* investigated the joint kinematics and key release parameters providing coaches with more in-depth knowledge of these varying techniques to perform the same skill. Significantly earlier initiation of the shoulder and hip functional phases in the arch technique ($p < 0.05$), coupled with significantly greater hip extension ($p < 0.05$) at the functional phase initiation than the pike technique. However, differences in joint kinematics were not reflected in key release parameters, in agreement with the findings reported by Manning et al. (2011). Therefore the selection criteria of one technique over another remained unclear and Theme 3 followed: *Biomechanical musculoskeletal approach*.

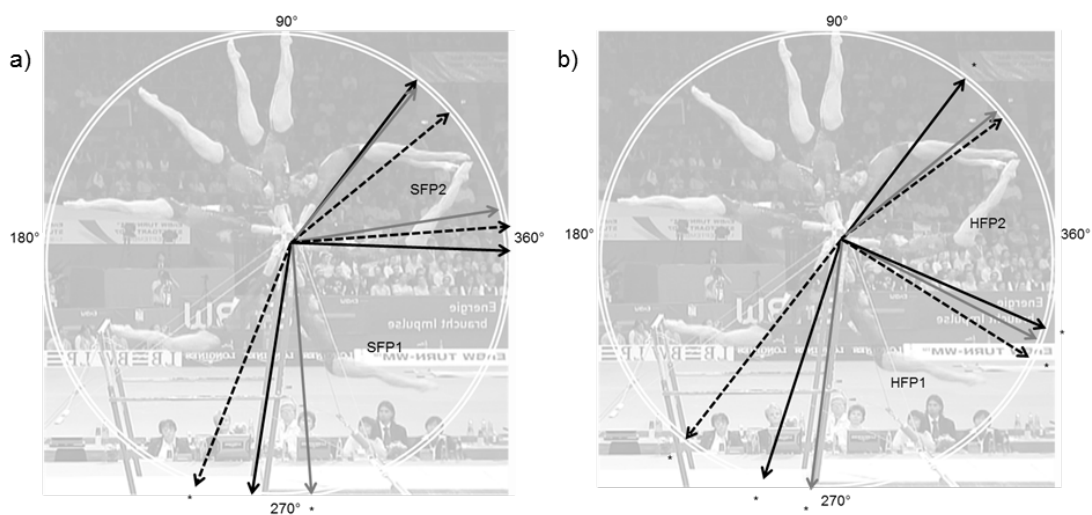


Figure 1: Dartfish™ image of a) shoulder (SFP) and b) hip (HFP) functional phases (1 & 2) for the arch (dashed), straddle (black) and pike (grey) longswing. * Denotes significant difference ($p \leq 0.05$).

Theme 3 highlighted that the pike longswing had significant greater physical demand placed at the gymnast's hips with a significantly earlier concentric action to initiate the second functional phase with greater work contribution during this period. Similarly at the shoulder joint the pike longswing executed a greater shoulder flexion joint moment to prepare the gymnast for release. The physical requirement inferred by Theme 3 of the pike longswing provides coaches with understanding of prescribing specific physical preparation activities compared to the comparative longswing techniques. Building on Themes 1-3, Theme 4: *Biomechanical energetics approach* applied a novel effectiveness score to further investigate the gymnastics energetic contribution to the total gymnast-high-bar energy system. For each longswing technique En_{Tot} decreased as the gymnast negotiated the low bar with the gymnast adding to the system through muscular action (En_{Gym}) on the ascent. The arch longswing was highlighted as the technique that over came the energy deficit during the descent phase, had an increase in energy to successfully complete the straddle Tkachev and has 23% of energy remaining in reserve (Figure 2). Compared to the pike technique that utilised all their gymnast energy to overcome the deficit in energy due to energy lost in the

descent phase, the arch longswing is potentially the key technique for the development of more complex skills or combinations of skills.

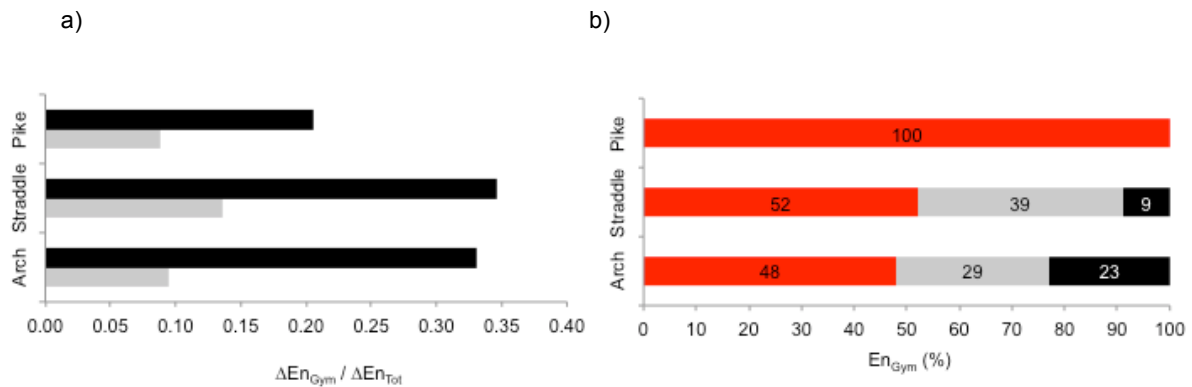


Figure 2: a) Increase in normalised gymnast energy (black) and total energy (grey). b) Percentage of gymnast energy utilised to overcome deficit in total energy (red) and increase total energy (grey) with remaining gymnast energy (black).

CONCLUSION: The thematic approach has allowed the research findings to emerge in a meaningful and ecologically valid manner. The findings can be directly linked to enhancing coaching knowledge and providing further insight into the trends in elite gymnastics competition and identified varying techniques to perform the Tkachev (Theme 1). Biomechanical analyses provided knowledge of the techniques performed developing coaches' conceptual understanding of these skills and providing insight into the underlying mechanisms controlling these skills (Theme 2). The pike longswing was identified as requiring varying physical preparation to the contrasting techniques (Theme 3) with potential development opportunities also highlighted with the arch longswing having excess energy to develop more complex versions and combinations of skills (Theme 4). Coaches have access to knowledge that they can employ to optimise the technique selection process with potential to customise technique selection to the needs of individual gymnasts.

REFERENCES:

- Arampatzis, A., & Brüggemann, G.P. (2001). Mechanical energetic processes during the giant swing exercise before Tkatchev exercise. *Journal of Biomechanics*, 34, 505-512.
- Hiley, M.J., & Yeadon, M.R. (2007). Optimisation of backward giant circle technique on the asymmetric bars. *Journal of Applied Biomechanics*, 23, 301-309.
- Irwin, G., Hanton, S., & Kerwin, D. G. (2005). The conceptual process of skill progression development in artistic gymnastics. *Journal of Sports Sciences*, 23, 1089-1099.
- Irwin, G., & Kerwin, D.G. (2005). Biomechanical similarities of progression for the longswing on high bar. *Sports Biomechanics*, 4, 163-144.
- Manning, M.L., Irwin, G., Gittoes, M.J.R., & Kerwin, D.G. (2011). Influence of longswing technique on the kinematics and key release parameters of the straddle Tkachev on uneven bars. *Sports Biomechanics*, 10, 161-173.
- Marzan, G.T., & Karara, H.M. (1975). A computer program for direct linear transformation solution of the collinearity condition and some applications of it. In *Proceedings of the Symposium on Close-Range Photogrammetric Systems*, 420- 476. Falls Church VA: American Society of Photogrammetry.
- Yeadon, M.R. (1990). The simulation of aerial movements. Part II: A mathematical inertia model of the human body. *Journal of Biomechanics*, 23, 67-74.
- Yeadon, M.R., & King, M.A. (1999). A method for synchronising digitised video data. *Journal of Biomechanics*, 32, 983-986.

**BIOMECHANICAL ANALYSIS OF SAVING MOTION FOR SOCCER
GOALKEEPERS FOCUSED ON THE FUNCTION OF LOWER EXTREMITIES**
Naoki Numazu¹, Norihisa Fujii²

Doctoral Program in Physical Education, Health and Sport Sciences, University of
Tsukuba, Tsukuba, Japan¹
Faculty of Health and Sport Sciences, University of Tsukuba, Tsukuba, Japan²

The purpose of this study was to clarify the function of the lower extremities during the saving motion of a goal keeper (GK). Eleven male university GKs dived toward a ball thrown 3.5 m ahead. Three-dimensional (3D) coordinates and ground reaction forces were obtained with a 3D motion capture system (250 Hz) and 2 force platforms (1000 Hz). The novel findings in this study are summarized as follows: (1) hip extension of the contralateral side leg to the ball is an important motion in the Pre phase and (2) exertion of extension torque at the hip in the early Transition phase has an important role for controlling backward leaning of the thigh during the saving motion.

KEY WORDS: soccer, goal keeper, saving motion, hip extension torque.

INTRODUCTION: In addition to scoring a goal, preventing the opponent from scoring is a key factor for winning a soccer game. One of the roles of the goalkeeper (GK) is to prevent goals. The GK dives toward the ball kicked by opponents to save a goal. According to previous studies, during the take-off phase of the saving motion, the contralateral side (CS) leg controls the magnitude of power, and the ball-side (BS) leg controls both the magnitude and the direction of power to dive directly towards the ball, depending on the ball height (Matsukura and Asai, 2013). Furthermore, Matsukura and Asai (2013) also reported that extension torque at the knee and ankle in CS leg is important to accelerate the center of gravity (CG). However, the function of the hip joint in the CS leg is unclear. Therefore, the purpose of this study was to clarify the function of the lower extremities, especially the CS hip joint, during the saving motion of a GK.

METHODS: Eleven male university GKs (height 1.78 ± 0.04 m, body mass 70.9 ± 5.6 kg) volunteered for the present study. This study was approved by the University of Tsukuba Ethics Committee. Figure 1 shows an overview of the experimental set-up of the present study. We asked the subjects to stand at the specified position on the force platforms and, after a preparatory motion, to dive toward a ball thrown 3.5 m ahead. We asked subjects to jump lightly as a preparatory motion before the saving motion. The throwing direction of the ball (leftward or rightward) was instructed randomly. The global coordinate system was defined as follows: the Y (anteroposterior)-axis was the direction from the subject to the thrower, the Z (longitudinal)-axis was the vertical axis, and the X (mediolateral)-axis crossed with the Y- and Z-axes at a right angle. Ground reaction forces (GRFs) of both legs were obtained with 2 force platforms (9287B, 9287C, Kistler) at 1000 Hz. Three-dimensional (3D) coordinates of 47 reflective markers on a body and 4 reflective markers on a ball were collected using a motion analysis system (Vicon MX+, Vicon) at 250 Hz. GRFs and 3D coordinates were time-synchronized in the motion analysis system. One trial in which each subject showed the best rightward save was selected for further analysis. For these analyses, we defined the right leg as the BS leg and the left leg as the CS leg. 3D coordinates of the markers were smoothed using a fourth-order Butterworth low-pass-digital-filter at cut-off frequencies based on the residual method of Wells and Winter (1980). The cut-off frequencies ranged from 8 to 25 Hz. The ball center was estimated from the reflective markers on the ball using the least-square method. Figure 2 shows the motion events and phases for saving motion as follows. OFF: defined as the instant at which CS or BS leg leaves the ground in the preparatory motion; STR: defined as the instant of 0.4 s to OFF; CSon: defined as the instant at which the CS leg touches the ground after the preparatory motion; CSoff: defined as the instant at which the CS leg leaves the ground after CSon; BSon: defined as the instant at

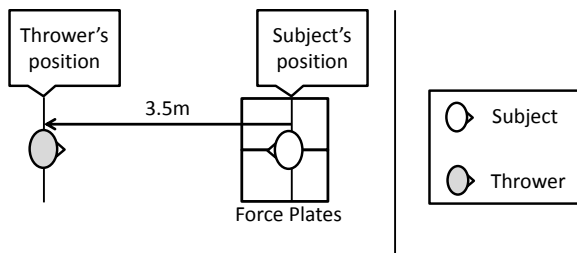


Figure 1 Experimental set up (over view)

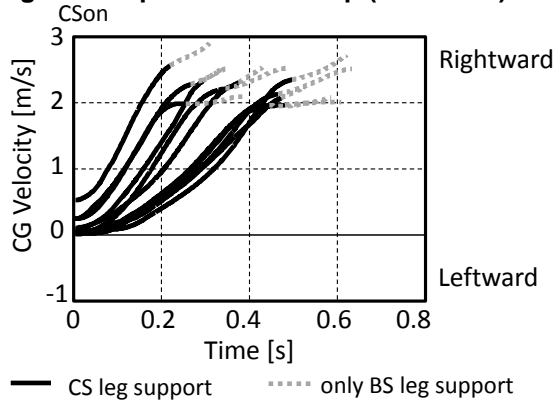


Figure 3 CG velocity during Saving phase

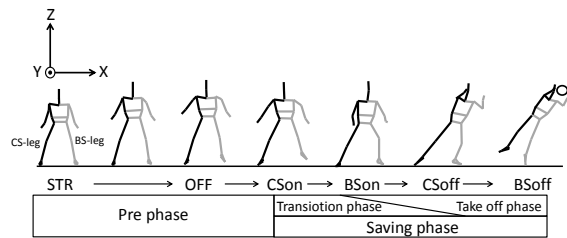


Figure 2 Analysis phases and events

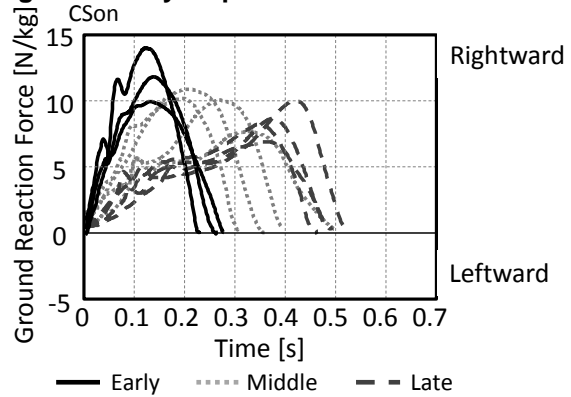


Figure 4 Group selection

which the BS leg touches the ground after the preparatory motion; and BSoff: defined as the instant at which the BS leg leaves the ground after Bson. Figure 3 shows CG velocity in the mediolateral direction of all subjects during the Saving phase. Average CG velocity of all subjects at BSoff was 2.48 ± 0.29 m/s. All subjects achieved the greatest CG velocity in the CS leg support phase (solid line). Since it is considered that the CS leg has an important role in the saving motion, we focused on the function of the CS leg. We divided the Saving phase into two phases as follows: the Transition phase was Cson to CSoff, and the Take-off phase was Bson to BSoff. To normalize the Pre phase and the Transition phase, we defined 0–100% in each phase. Kinematic and kinetic data were calculated to evaluate the function of the CS leg in the Pre and Transition phases.

RESULTS: In previous studies, GKs motion continuously changed from the preparatory motion to the saving motion (Isokawa, Sakuma, Togari, Ohashi, and Suzuki, 1986). In addition, Nunome, Asai, Ikegami, and Sakurai (2002) reported the average ball velocity of the instep kick was 28.0 ± 2.1 m/s. This indicates that shots from the penalty area (16.5 m from the goal) can reach the goal about 0.5 s. Hence, the GK must shorten the movement time during the saving motion. Therefore, we defined the motion that GK translates continuously from the preparatory motion to the saving motion as a “good saving motion”. We classified all subjects into three groups (Early, Middle, and Late) based on the ground time during the Transition phase and timing of peak GRF in the CS leg. Figure 4 shows the mediolateral component of GRF in the CS leg of all subjects during the Transition phase. Figures 5-a and 5-b show the mean of joint torques about the flexion/extension axis of the hip and knee in the CS leg for the Early and Late groups during the Transition phase (a: Early, b: Late). In the hip joint, the Early group exerted a larger extension torque than the Late group (0–50%). In the knee joint, the Late group exerted the extension torque for a longer time during the Transition phase, and the peak value was lower than the Early group. Figures 6-a and 6-b show the mean of joint angles about the flexion/extension axis of the hip and knee in the CS leg for Early and Late groups during the Transition phase (a: Early, b: Late). In the hip joint, the Early group continued to extend during the Transition phase; in contrast, the Late group flexed the hip joint for 0–50% of the Transition phase, then extended the hip joint. Comparing the timing of extension of the hip joint with the knee joint, the hip joint was extended earlier than the knee joint in the Early group. In the Late group, the hip and knee joints extended at the same time.

Pre phase

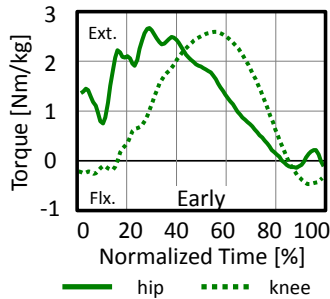
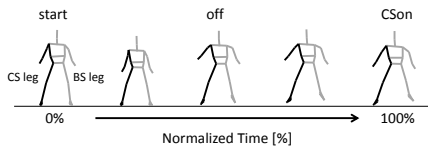


Figure 5-a Joint torques of hip and knee in the CS leg for Early group during the Transition phase

Transition phase

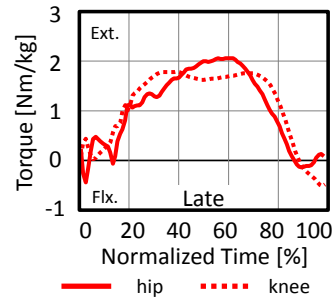
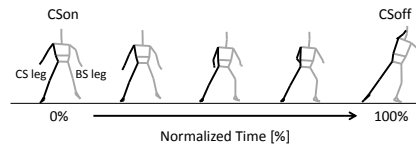


Figure 5-b Joint torques of hip and knee in the CS leg for Late group during the Transition phase

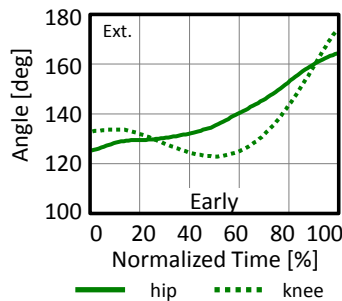


Figure 6-a Joint angles of hip and knee in the CS leg for Early group during the Transition phase

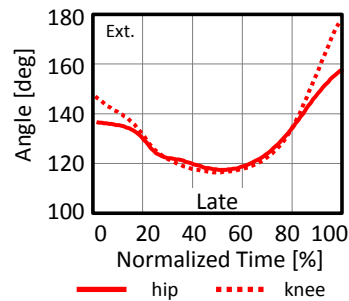


Figure 6-b Joint angles of hip and knee in the CS leg for Late group during the Transition phase

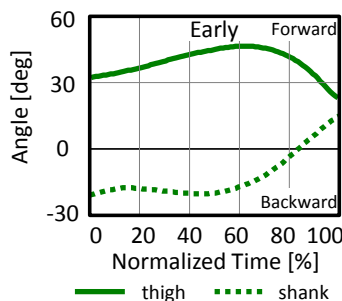


Figure 7-a Segment angles of thigh and shank in the CS leg for Early group during the Transition phase

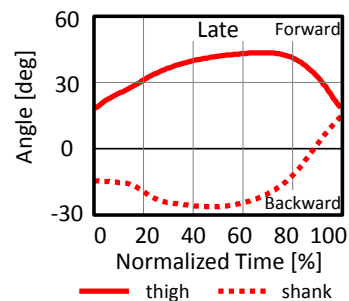


Figure 7-b Segment angles of thigh and shank in the CS leg for Late group during the Transition phase

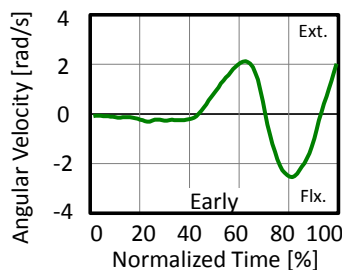


Figure 8-a Joint angular velocities of hip and knee in CS leg for Early group during Transition phase

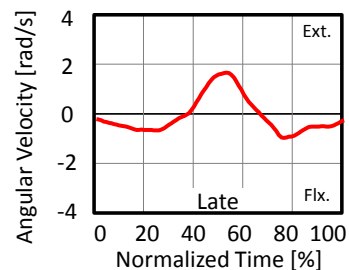


Figure 8-b Joint angular velocities of hip and knee in CS leg for Late group during Transition phase

Figures 7-a and 7-b show the mean of forward/backward lean angles of the thigh and shank in the CS leg for the Early and Late groups during the Transition phase (a: Early, b: Late). In the

thigh, the Early group stayed in the backward leaning position for 0–50% of the Transition phase, but the Late group continued to lean backward for 0–50% of the Transition phase, after which both the Early and Late groups changed to a forward leaning position. In the shank, both the Early and Late groups continued to lean forward for 0–70% of the Transition phase and stayed in a forward leaning position during the Transition phase. Figures 8-a and 8-b show the mean of joint angular velocities about the flexion/extension axis of the hip in the CS leg for the Early and Late groups during the Pre phase (a: Early, b: Late). In the terminal Pre phase (90–100%), the Early group increased the extension angular velocity, while the Late group recorded the flexor angular velocity.

DISCUSSION: According to previous studies, in a rebound jump, grounding in a flexed leg position and minimizing eccentric extension torque at the hip were important to obtain a large impulse with a shorter foot contact time (Zushi and Takamatsu, 1996). At CSon, the Late group had a more extended position than the Early group. It is assumed that this is one of the reasons that the foot contact time of the Late group was longer than that in the Early group. Furthermore, exertion of eccentric hip extension torque indicates that the hip joint is flexing and that hip joint torque is extending. Kinematically, it is assumed that the thigh leaning backward accompanies hip and knee joint flexion when grounding. Therefore, the thigh leaning backward increases foot contact time. Kinetically, it is assumed that extension torque at the hip helps prevent the thigh from leaning backward when grounding. Thus, exerting extension torque at the hip in the early Transition phase is important to obtain the larger impulse in a shorter time. In the previous study, Matsukura and Asai (2013) reported that extension torque at the knee and ankle in the CS leg is important to accelerate CG during the saving motion of a GK. In addition, we revealed that exerting extension torque at the hip is also important in the early Transition phase. Moreover, as shown in Figure 8-a, the Early group showed increased extension angular velocity in the terminal Pre phase (90–100%). This may help hip extension in the early Transition phase. In addition, grounding with extension of the hip joint may help prevent the thigh from leaning backward in the Transition phase. Hence, it is assumed that extending the hip joint in the preparatory motion during the saving motion of a GK is also important to obtain the large impulse in a shorter time.

CONCLUSIONS: The purpose of this study was to clarify the function of the lower extremities, especially the hip joint in the CS leg, in the saving motion. The new findings in this study are summarized as follows: (1) hip extension of the CS leg is an important motion in the Pre phase, and (2) exertion of extension torque at the hip in the early Transition phase has an important role for controlling backward leaning of the thigh in the saving motion. These findings might be useful to improve a GK's saving motion.

REFERENCES:

- Isokawa, M., Sakuma, H., Togari, H., Ohashi, J., & Suzuki, S. (1986): Motion analysis of goal keeper on saving (in Japanese). *Japanese Journal of Sports Sciences*, 11, 55-64.
- Nunome, H., Asai, T., Ikegami, Y., & Sakurai, S. (2002): Three-dimensional kinetic analysis of side-foot and instep soccer kicks. *Medicine and Science in Sports and Exercise* 34, 2028-2036.
- Matsukura, K. & Asai, T. (2013): Characteristics of force exerted by soccer goalkeepers during diving motion (in Japanese). *Japan Journal of Physical Education, Health and Sport Sciences*. 58, 277-296.
- Wells, R. P. & Winter, D. A. (1980): Assessment of signal and noise in the kinematics of normal, pathological and sporting gaits. *Human Locomotion*, 1, 92-93.
- Zushi, K. & Takamatsu, K. (1996): Factors to shorten the contact time in rebound drop jump -With special reference to work done by the lower limb joints and anticipation of the landing - (in Japanese). *Japan Journal of Physical Education, Health and Sport Sciences*. 40, 29-39.

ADDING MASS TO THE SHOE DOES NOT AFFECT BALL VELOCITY IN A SOCCER PENALTY KICK

Nicholas P. Linthorne, Stephanie Cripps, and Jake A. Byrne

Brunel University, Uxbridge, Middlesex, United Kingdom

The aim of this study was to identify the optimum shoe mass that maximizes ball velocity in a soccer instep penalty kick. Two players performed 20–30 maximum-effort penalty kicks while wearing football shoes with lead weights attached to the base of the shoe (total mass: 0.26 – 0.81 kg). The kicks were recorded by a video camera at 100 Hz and a biomechanical analysis was conducted to obtain measures of ball projection velocity and kinematics of the kicking leg. We found that ball velocity was insensitive to shoe mass (at least for the range of shoe mass tested). An important contributing factor to the observed relationship was that the velocity of the kicking foot at ball impact decreased as the mass of the shoe increased. Our result indicates that players should not change their shoes before taking a penalty kick.

KEYWORDS: collision, football, kinematics.

INTRODUCTION: Attaining a high ball velocity is very important in a penalty kick. The faster the player can kick the ball, the less time the goalkeeper has to react to the shot and so the better the chance of scoring a goal. Most players prefer lightweight shoes for field play so as to perform more rapid acceleration runs and to minimize the aerobic demands of running. However, calculations using a collision model of kicking (Daish, 1972) led us to believe that a player might increase ball projection velocity in a penalty kick by changing to a heavier shoe. Our calculations suggest that there might be an optimum shoe mass that is determined by the interplay between the advantage of increased striking mass in the foot-ball collision and the disadvantage of decreased foot velocity when swinging a heavier kicking leg.

The effect of shoe mass on ball velocity in a maximal instep kick was previously investigated by Moschini and Smith (2012). They used video analysis to examine 10 experienced male players who performed kicks while wearing shoes of mass 0.18, 0.26, and 0.36 kg. A heavier shoe reduced foot velocity at impact, but ball velocity was the same for all three shoe conditions. Moschini and Smith used inferential statistics (t-tests) to identify statistically significant differences in group mean values between shoe conditions. However, a single-subject intervention analysis is also an appropriate methodology, especially when studying relatively complex systems such as human movement (Bates, 1996). We suggest that a study of the responses of an individual participant, using a greater range of shoe masses, should lead to a precise knowledge of the form and magnitude of the relationship between shoe mass and ball velocity.

The aim of the present study was to quantify the relationship between shoe mass and the projection ball velocity of the ball in a simulated full-instep penalty kick. Our hypothesis was that there would be an inverted-u relationship, with a clear optimum shoe mass that produces the greatest ball projection velocity.

METHODS: This study used an experimental research design in which the mass of the shoe was systematically varied. Two experienced intercollegiate soccer players volunteered to participate in the study (female participant: 21 years, 1.65 m, 78 kg; male participant: 23 years, 1.91 m, 86 kg). The study adhered to the tenets of the Declaration of Helsinki and was conducted in accordance with procedures approved by our institutional ethics committee. The participants were informed of the protocol and procedures prior to their involvement, and written consent to participate was obtained.

The participants performed 20–30 simulated penalty kicks in still air conditions in an outdoor football facility. The kicks were performed on a 3G artificial grass surface using a FIFA-approved size 5 match ball that was inflated to the regulation pressure. The participants wore tight-fitting clothes and their own football shoes (female participant, Adidas Predator II X;

male participant, Nike CTR360 Trequartista III FG). Colour-contrasted markers were placed on the participant's skin or clothing directly over the joint centres of the shoulder (glenohumeral joint), hip (major trochanter), knee (lateral epicondyle of femur), ankle (lateral malleolus of fibula), and toe (lateral aspect of distal head of fifth metatarsus). Lead weights were attached to the base of the kicking shoe, giving a total shoe mass of between 0.29 and 0.81 kg for the female participant, and between 0.26 and 0.76 kg for the male participant. The participants used a constant run-up length of three steps (about 3 m), and the run-up and kicking action of the kicking leg were in the plane of the flight of the ball. The participants performed maximum-effort kicks while attempting to achieve maximum ball speed. The order of shoe mass was randomized and an unlimited rest interval was given between kicks to minimize the effects of fatigue on performance.

A JVC GR-DVL9600 video camera (Victor Company of Japan, Yokohama, Japan) operating at 100 Hz was used to record the movement of the ball and the participant during the kicks. The video camera was mounted at right angles to the kick direction and the movement space was calibrated with three vertical poles that were placed along the line of the kicking plane. An Ariel Performance Analysis System (Ariel Dynamics, Trabuco Canyon, CA, USA) was used to digitize the motion of the participant's kicking leg and the centre of the ball in the video images. Each trial was digitized from one step before the kick to at least 10 frames after the ball broke contact with the foot. The coordinates of the participant and ball were calculated from the digitized data using the two-dimensional direct linear transform (2D-DLT) algorithm. Joint coordinate data were smoothed using a second-order Butterworth digital filter with a cut-off frequency of 10 Hz for the horizontal direction and 12 Hz for the vertical direction, and the velocities of the joint markers were calculated by numerical differentiation of the coordinate data.

The projection velocity of the ball was calculated using unfiltered ball displacement data from images immediately after the ball broke contact with the foot. The horizontal component of the ball velocity was calculated as the first derivative of a linear regression line fitted to the ball displacement data, and the vertical component of the ball velocity was calculated as the first derivative of a quadratic regression line (with the second derivative set equal to -9.81 m/s^2) fitted to the ball displacement data (Nunome, Ikegami, Kozakai, Apriantono, & Sano, 2006). The uncertainties arising from the fitted curves indicated that the uncertainty in ball velocity was about 0.3 m/s ($\pm 95\%$ CI).

The participant's kicking technique was quantified with measures of foot velocity at impact, rotational range of motion of the thigh, knee angle at maximum knee flexion, maximum angular velocity of the thigh, and angular velocities of the thigh and shank at impact (Ball, 2009; Linthorne & Patel, 2011; Moschini & Smith, 2012). We also measured the angles of the knee and hip joints and the angle to the horizontal of the shank and thigh segments at the instant of impact. The horizontal velocity of the hip at touchdown of the support leg was taken as a measure of the participant's run-up velocity. In this study the greatest source of uncertainty in the kick technique variables arose from the sampling frequency of the video camera (Hay & Nohara, 1990). The uncertainties were: foot velocity, 1.5 m/s; run-up velocity, 0.3 m/s; segment angle or joint angle, 7 deg; and segment angular velocity or joint angular velocity, 60 deg/s.

The ball velocity and kicking technique variables (y) were plotted as a function of the mass of the shoe (m). A straight line, $y = bm + c$, and an inverted-u function, $y = y_{\text{opt}} - a(m - m_{\text{opt}})^2$, were fitted to the data (Linthorne & Patel, 2011). The most appropriate curve for the data was decided by examining the distribution of the residuals and with calculations of Akaike's Information Criterion (Motulsky & Christopoulos, 2004).

RESULTS: For ball velocity, we could not reliably distinguish between a linear relationship and an inverted-u relationship as the best fit to the data. Neither participant exhibited a clear optimum shoe mass (Figure 1a). The curvature of the inverted-u fit was zero (female, $a = 8 \pm 11 \text{ m/s per kg}^2$; male, $a = 10 \pm 13 \text{ m/s per kg}^2$; $\pm 95\%$ CI), and the gradient of the linear fit was zero (female, $b = -0.7 \pm 1.7 \text{ m/s per kg}$; male, $b = -1.6 \pm 3.3 \text{ m/s per kg}$). For the inverted-u fit, the difference in ball velocity between the calculated optimum shoe mass (female, $m_{\text{opt}} =$

0.50 ± 0.12 kg; male, $m_{opt} = 0.44 \pm 0.14$ kg; ±95% CI) and the participant's normal shoe mass was not substantially different from zero (female, 0.5 ± 2.2 m/s; male, 0.3 ± 1.3 m/s; ±95% CI). Across all kicks the average ball velocity was 20.5 ± 0.5 m/s (mean ± SD) for the female participant and 21.6 ± 0.5 m/s for the male participant.

The participants displayed the characteristic whip action of the kicking leg, where the thigh angular velocity at impact was close to zero and the shank angular velocity reached a maximum at close to the instant of impact (Figure 1b). Most of the kick technique variables (run-up velocity, maximum thigh angular velocity, thigh angular velocity at impact, thigh and shank angle at impact) were independent of shoe mass. However, as shoe mass increased, the participants had a reduced range of motion in the knee joint during the swing of the kicking leg (because the minimum knee angle increased), and showed a linear decrease in shank angular velocity at impact. The decrease in shank angular velocity was reflected by a decrease in foot velocity (Figure 1a).

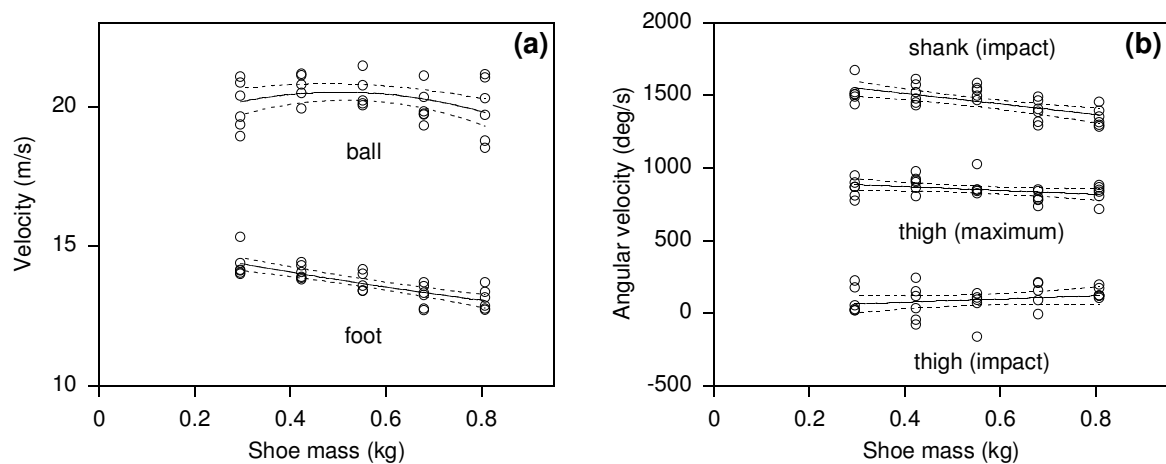


Figure 1: Plot (a) shows that the projection velocity of the ball was insensitive to shoe mass (female participant). Plot (b) shows that the maximum thigh angular velocity and the thigh angular velocity at impact were not affected by the mass of the shoe, but shank angular velocity at impact decreased with increasing shoe mass. The decrease in shank angular velocity was reflected by a decrease in foot velocity. The solid lines are the regression fits and the dashed lines show the 95% CI of the regression curve.

DISCUSSION: Kicking involves the transfer of momentum from the player to the ball. According to the collision model proposed by Daish (1972), the projection velocity of the ball is determined by the impact velocity of the player's foot, the effective mass of the player's foot, and the amount of energy that is dissipated during the collision. Our calculations with this model indicate that shoe mass should increase ball velocity at a rate of 0.5 – 5.5 m/s per 1 kg increase in shoe mass, depending on the strength of the mechanical coupling of the foot to the lower leg. However, these calculations are for a constant foot velocity at impact. Increasing the mass of the shoe reduces the foot velocity the player is able to generate in the swing. Several studies have found that ball velocity decreases at a rate of about 1.3 m/s per 1 m/s decrease in foot velocity (Bull Anderson, Dörge, & Thomsen, 1999). Overall, there should be an optimum shoe mass that is determined by the interplay between the advantage of increased striking mass in the foot-ball collision, and the disadvantage of decreased foot velocity when the swinging a heavier kicking leg.

The rate of decrease in foot velocity observed in the present study (2.6 m/s per 1 kg increase in shoe mass) should have produced a rate of decrease in ball velocity of about 3.4 m/s per kg. However, in the present study we found that ball velocity was independent of shoe mass. This result indicates that increasing the effective striking mass in the foot-ball collision produces an increase in ball velocity of about 3.4 m/s per kg. A rate of increase in ball velocity of this magnitude indicates that the mechanical coupling of the foot to the leg is relatively weak. The effective striking mass (1.4 kg) calculated from the collision model is

similar to the actual combined mass of the foot and the shoe (1.5 kg), and thus indicates there is little or no contribution to the effective striking mass from the shank or thigh segments.

In this study we did not monitor the location of the impact point of the ball on the foot. However, changes in ball velocity are expected to be small (less than about 1.5 m/s) for changes in impact position of less than 5 cm (Ishii, Yanagiya, Naito, Katamoto, & Maruyama, 2012). In this study we did not monitor the position of the support leg, movements of the upper body, or 3D motions of the kicking leg out of the plane of the flight of the ball. Therefore, we cannot exclude the possibility that the observed relationship between shoe mass and ball velocity was affected by systematic changes in these factors.

A limitation of our study is the use of only two participants, and so the results we obtained might be idiosyncratic. However, we observed measures of kicking technique that were similar to those obtained in other studies of male and female players (Ishii et al., 2012; Nunome et al., 2006; Sakamoto & Asai, 2013; Shinkai, Nunome, Isokawa, & Ikegami, 2009). Therefore, it appears likely that the results from the present study would apply to other adult male and female players of similar standard.

CONCLUSION: We found that ball velocity in an instep penalty kick is insensitive to the mass of the shoe (at least for shoes with mass between 0.26 and 0.81 kg). This result suggests that players should not change their shoes before taking a penalty kick.

REFERENCES:

- Ball, K. (2007). Biomechanical considerations of distance kicking in Australian Rules football. *Sports Biomechanics*, 7, 10–23.
- Bates, B. T. (1996). Single-subject methodology: An alternative approach. *Medicine and Science in Sports and Exercise*, 28, 631–638.
- Bull Anderson, T., Dörge, H. C., & Thomsen, F. I. (1999). Collisions in soccer kicking. *Sports Engineering*, 2, 121–125.
- Daish, C. B. (1972). *The physics of ball games*. London: English Universities Press.
- Hay, J. G., & Nohara, H. (1990). Techniques used by elite long jumpers in preparation for takeoff. *Journal of Biomechanics*, 23, 229–239.
- Ishii, H., Yanagiya, T., Naito, H., Katamoto, S., & Maruyama, T. (2012). Theoretical study of factors affecting ball velocity in instep soccer kicking. *Journal of Applied Biomechanics*, 28, 258–270.
- Linthorne, N. P., & Patel, D. S. (2011). Optimum projection angle for attaining maximum distance in a soccer punt kick. *Journal of Sports Science and Medicine*, 10, 203–214.
- Moschini, A., & Smith, N. (2012). Effect of shoe mass on soccer kicking velocity. In E. Bradshaw & A. Burnett (Eds.), *Scientific Proceedings of 30th Annual Conference of Biomechanics in Sports* (pp. 150–153). Melbourne: Australian Catholic University.
- Motulsky, H., & Christopoulos, A. (2004). *Fitting models to biological data using linear and nonlinear regression*. Oxford: Oxford University Press.
- Nunome, H., Ikegami, Y., Kozakai, R., Apriantono, T., & Sano, S. (2006). Segmental dynamics of soccer instep kicking with the preferred and non-preferred leg. *Journal of Sports Sciences*, 24, 529–541.
- Sakamoto, K., & Asai, T. (2013). Comparison of kicking motion characteristics at ball impact between female and male soccer players. *International Journal of Sports Science and Coaching*, 8, 63–76.
- Shinkai, H., Nunome, H., Isokawa, M., & Ikegami, Y. (2009). Ball impact dynamics of instep soccer kicking. *Medicine and Science in Sports and Exercise*, 41, 889–897.

GENERATING AND APPLYING KNOWLEDGE IN SPORTS BIOMECHANICS: EXAMPLES FROM ROWING AND RUNNING

Richard Smith

The University of Sydney, Sydney, Australia

Sometimes new knowledge, gleaned from our biomechanics experiments, is surprising, even counter-intuitive. Some examples from rowing and footwear biomechanics research illustrate this phenomenon. A study of ergometer rowing reveals a flexion moment at the knee joint while it is extending during the drive phase with implications for strength and conditioning. On-water rowing measurements of rower power output underline the importance of recovery phase technique. Observations of multi-segment foot motion while running have exposed the barefoot as a flexible power generator, raising questions about the efficacy of footwear. These experiences, surprising at their time, were signs of pushing the envelope and fine tuning of our models.

KEY WORDS: joint power, energy, range of motion, specificity, footwear

INTRODUCTION: Biomechanics enables us to ascribe cause and effect between elements of the execution of a movement and its outcomes. It provides the conceptual framework for understanding the mechanisms of sport movements and thence to improve performance, minimise injury and suggest novel techniques and improvements to equipment. It is rare for biomechanical analysis to be at the instigation of paradigm shifts in technique such as the somersault long jump and the Fosbury Flop. More often biomechanics contributes incrementally to small gains in performance. This paper is a glimpse at the experience of these processes by one sports biomechanist through rowing and footwear research.

Case One: Ergometer rowing

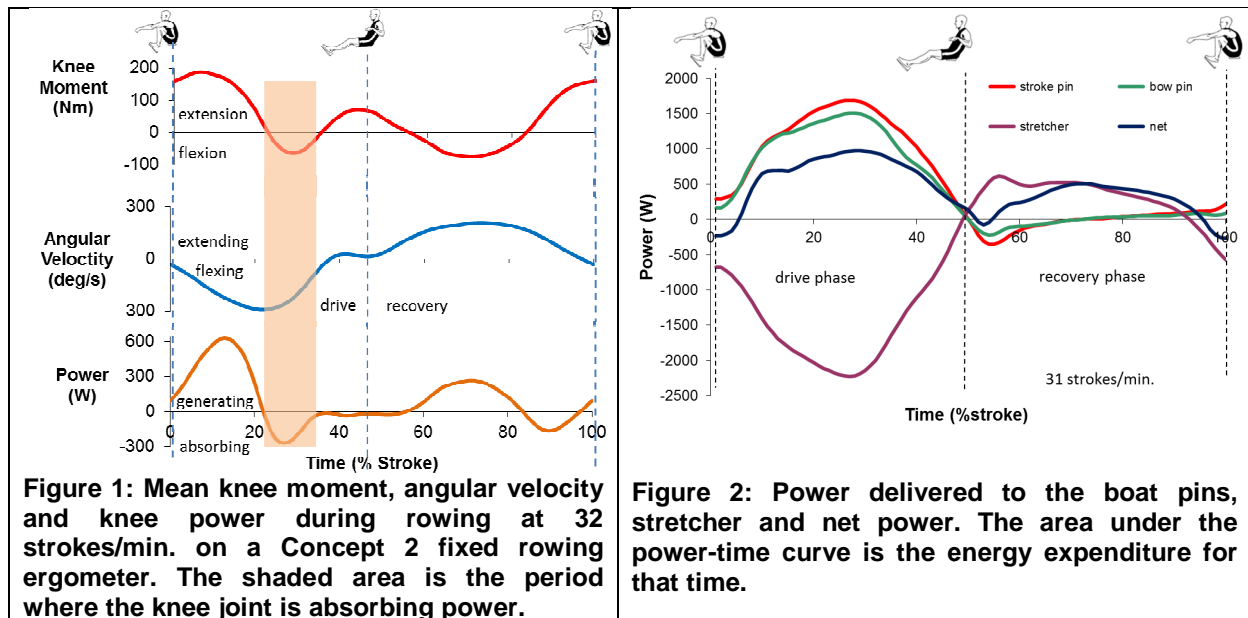
BACKGROUND: Rowing takes place recreationally and competitively on ergometers. To maximise performance it is helpful to understand the mechanisms of power production. Joint powers, developed during execution of the task, describe the relative contribution of the major muscle groups to total external power output, their implications for strength and conditioning and, with further modelling, insight into the causes of pain or injury (Greene, Sinclair, Dickson, Colloud, & Smith, 2013).

METHODOLOGY: Fifteen injury-free elite male rowers (age 25.2 ± 4.4 years, height 1.915 ± 0.072 m and body mass 91.0 ± 7.4 kg) volunteered to participate in this study approved by the Human Ethics Review Committee of the University of Sydney. Rowers were asked to warm up for 5 min then perform 1 min rowing at 80 % maximal power at 32 strokes/min on a Rowperfect rowing simulator equipped with handle and stretcher force transducers.

The 3D trajectories of fifty two retroreflective markers were tracked by a nine camera motion capture system synchronised with the recording of simulator force transducer outputs at 100 Hz. Toe, ankle, knee and hip joint centres were calculated from this data. The force and filtered (5 Hz) joint centre data were input to a nine segment, sagittal plane, inverse dynamics model of the rower (Winter, 1979).

RESULTS: The mean joint energy per drive phase generated by the rowers was 479 ± 24 J (hip), 231 ± 16 J (knee), 211 ± 18 J (lumbar), 125 ± 8 J (shoulder) and 108 ± 5 J (ankle). The knee joint absorbed energy during the drive phase between 23% and 36% of the stroke due to the knee moment becoming a flexion moment for this period (Figure 1). Inspection of the emg record for muscles crossing the knee supported this finding in that the rectus femoris and vastus lateralis muscles were highly activated after the catch but passed through a minimum while the hamstrings' activation reached a maximum in this same 23% – 36% period.

DISCUSSION AND CONCLUSION: It is counter-intuitive that the knee joint should be exerting a flexion moment in the middle of the drive phase of rowing. However, consider that at this point in the stroke almost all body weight is supported by the feet of the rower. Thus there is a large external extension moment applied to the knees until the knees are fully extended. This explanation was supported by observation of activity in muscles crossing the knee extensor muscles. The same pattern of muscle activation was found for rowing on-water by (Fleming,



Donne, & Mahony (Fleming, Donne, & Mahony, 2014). This pattern is clearly different to the pattern observed in the dead lift, a common strength training activity for rowers. A more specific activity for rower's lower limb muscles should be introduced into the strength training program.

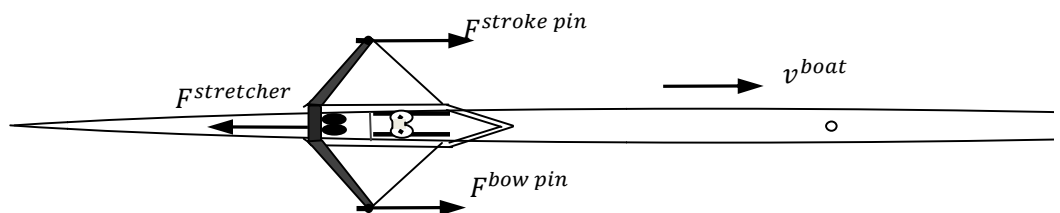
Case Two: On-water rowing

BACKGROUND: In the case of a single sculler the forces applied to the boat in the propulsive direction by the rower are:

$$F^{boat} = F^{bow\ pin} + F^{stroke\ pin} + F^{stretcher} + F^{seat}$$

$$= F^{bow\ pin} + F^{stroke\ pin} + F^{stretcher}$$

neglecting the seat force as it is on wheels.



Then the power delivered to the boat by the rower will be:

$$p^{boat} = F^{boat} \cdot v^{boat} = F^{bow\ pin} \cdot v^{boat} + F^{stroke\ pin} \cdot v^{boat} + F^{stretcher} \cdot v^{boat}$$

The purpose of this experiment was to examine the power delivered to a single scull throughout the whole stroke.

METHODOLOGY: For this case study a world champion female sculler rowed an instrumented single scull at 32 strokes per minute. Scull velocity was measured with a magnetic turbine and pickup coil, pin force with multi-component force transducers, stretcher force with strain gauge transducers, and oar angle with servo potentiometers. This information was sampled at 100 Hz

for twenty consecutive strokes. Power delivered to the boat by the rower was calculated as the product of boat velocity and the pin and stretcher forces.

RESULTS: Immediately after the catch for 5% of the stroke the rower was absorbing power from the stretcher at a greater rate than was delivered to the pins via the oars. From that time on power was delivered to the boat until a peak of 974 W was reached during the drive phase. After another minimum at the finish of the drive phase power was again delivered to the boat during the recovery reaching a peak of 505 W before the rower again absorbed power from the boat leading up to the next catch. The total energy delivered to the boat was 816 J/stroke. Thirty percent of this energy was delivered during the recovery phase (Figure 2).

DISCUSSION AND CONCLUSION: The on-water observation that 30% of the power of power delivered to the boat was during the recovery phase has focussed attention on movement technique during the recovery phase. Certainly the rower is expending the great majority of rower-generated energy during the drive phase. However, most of this energy is absorbed by the rower's body during the drive phase due to the stretcher reaction force. Hence the perception of the rower is that little energy is transferred to the boat by comparison during the recovery phase. Focussing on recovery technique can optimise the 'run of the boat' during this phase in which the boat velocity reaches a maximum.

Case Three: Foot dynamics during running

BACKGROUND: The foot is a complex structure with 26 bones and wide range of other tissues active and 'passive'. The myth still abounds that "... as the subtalar joint supinates, the midtarsal joint's motion decreases until it eventually locks the forefoot on the rearfoot in preparation for its rigid lever function during the propulsive phase of gait."

METHODOLOGY: Ten healthy males (height $1.78 \pm 0.12\text{m}$, weight $74 \pm 2.1\text{kg}$, age 24 ± 7 yrs, shoe size US 10 ± 2) gave their informed consent to participate in the study and ran overground through the data collection area of the laboratory. The 3D trajectories of 18 retroreflective markers (skin-mounted for both conditions) were tracked by a ten camera motion capture system synchronised with the recording of ground reaction force data at 200 Hz. The forefoot was modelled by the navicular and metatarsal head markers (Wrbaski & Dowling, 2007) and the rearfoot by a three-marker wand attached to the calcaneus.

RESULTS: The dorsi-plantarflexion range of motion of the midfoot joint was comparable with ankle dorsi-plantarflexion (Figures 3 and 4) in the barefoot condition while shoe-wearing made a

Table 1. Energy expenditure (J) after heel rise in the sagittal plane during running.

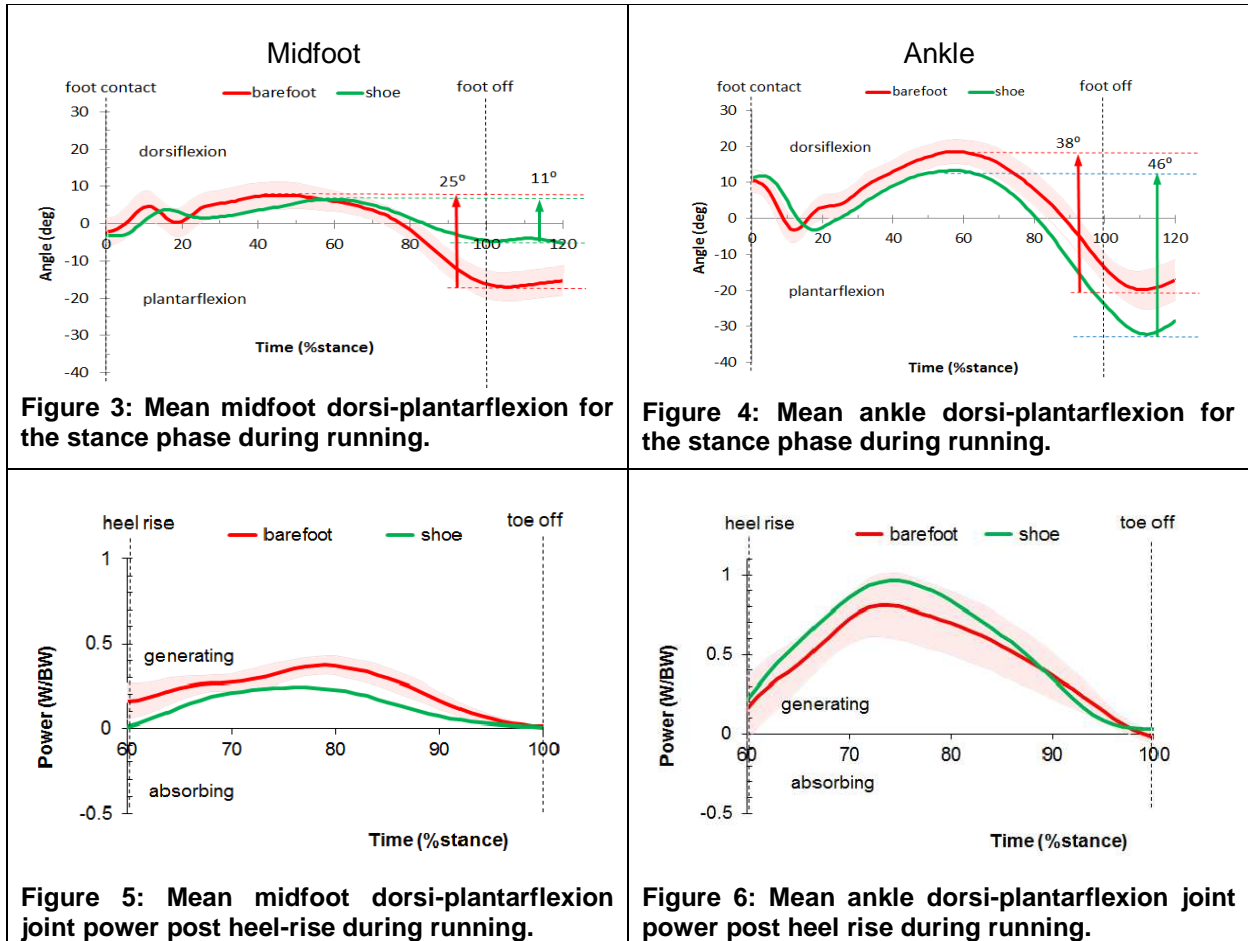
		Footwear	
		Barefoot	Shod
Joint	Midfoot	24	14
	Ankle	50	58
	Total	74	72

differential change to these angles. After heel rise (~60% stance phase), the peak power from the midfoot joint in the sagittal plane during running (0.37 W/BW) was reduced by 30% when wearing shoes ($p < 0.001$) (0.23 watts/BW) (Figure 5). On the other hand, the power at the ankle joint when wearing shoes (0.73 W/BW) was increased by 22% ($p = 0.043$) compared with the power developed

when barefoot (0.60 W/BW) (Figure 6). The total amount of power from this region remained relatively constant between the footwear conditions (Table 1).

DISCUSSION AND CONCLUSION: The wide range of motion exhibited by the midfoot joint during propulsion while generating a significant fraction of total power output suggests that a single segment model of the foot during running oversimplifies lower limb function during running. If the function of footwear is to facilitate movement that mimics barefoot gait while providing comfort and protection for the foot, then the prevailing paradigm for footwear needs to change. For example, a traditional Oxford style school shoe has a relatively rigid upper and sole

which often has “arch support”. The long term effects such a shoe has on movement function should be studied in comparison with a shoe that allows barefoot action.



Acknowledgements

The author would like to thank all supporters and collaborators in these experiments, the Australian Research Council, Australian Institute of Sport, NSW Institute of Sport, ASICS, Croker Oars, Professional Officers: Ray Patton and Tim Turner, and all the experiment participants.

REFERENCES:

Fleming, N., Donne, B., & Mahony, N. (2014). A comparison of electromyography and stroke kinematics during ergometer and on-water rowing. *Journal of sports sciences*, 32(12), 1127-1138.

Greene, A. J., Sinclair, P. J., Dickson, M. H., Colloud, F., & Smith, R. M. (2013). The effect of ergometer design on rowing stroke mechanics. *Scandinavian journal of medicine & science in sports*, 23(4), 468-477.

Winter, D. A. (1979). *Biomechanics of Human Movement*. New York: John Wiley and Sons.

Wrbaski, N., & Dowling, J. J. (2007). An investigation into the deformable characteristics of the human foot using fluoroscopic imaging. *Clinical biomechanics*, 22(2), 230-238.

THE EFFECTS OF COMPRESSION SHORTS ON MUSCLE OSCILLATION AND LONG JUMP PERFORMANCE.

Russell Peters¹, Neal Smith², and Mike Lauder².

Newman University, Birmingham, UK¹.
University of Chichester, Chichester, UK².

Compression garments were used to explore their effect on athletic performance and muscle oscillation during a 3-step long jump task. The study consisted of a 3 dimensional kinematic analysis (Vicon Motus 9.2) with force data collected by a Kistler force platform. Ten male subjects performed 6 jumps under 2 conditions, bare leg (control condition) and with the compression shorts. Two-tailed paired samples T-test were conducted to discover significant changes in the measures of Muscle Oscillation (MO), Peak Vertical Ground Reaction Force (PVGRF), Peak Horizontal Ground Reaction Force (PHGRF) and Jump Length. The findings of the study suggest that long jump performance can be increased (.18m) while wearing compression shorts, although the legs ability to disperse force may be reduced by the garment.

KEY WORDS: acceleration, wobbling mass, jump length

INTRODUCTION: In the current competitive sporting domain athletic equipment and apparel is constantly evolving to improve sport and exercise performance (Duffield and Portus, 2007). Often modern athletic clothing is worn simply as a fashion garment; however, the literature suggests that compression clothing may provide vital performance benefits (Doan et al., 2003). Another suggested benefit of compression garments is focusing the direction of the muscle fibres increasing the number recruited during a contraction. This is done by reducing muscle oscillation which can hinder the alignment of muscle fibres when moving, reducing the function of the muscle (Kraemer et al., 1998). This suggests that reducing the oscillation of a muscle could help improve technique and maximise the ability for a muscle to recruit fibres, which in turn would enhance performance (McComas, 1996). However, the concept of reducing muscle oscillation and making the segments of the body more rigid may not be totally beneficial. It has long been discussed in the area of computer simulation that the human body is not constructed of solely rigid. A segment also comprises of skin, adipose tissue, muscle and connecting tissue (Challis and Pain, 2008) and is what Gruber et al. (1998) describes as 'wobbling mass'. Challis and Pain (2008) believe that the wobbling effects of these tissues are a functional mechanism within the musculoskeletal system that may reduce the overall acceleration and distribution of load.

The 3 step running long jump was selected to test the effectiveness of the compression garment. The rationale for using this activity is that the long jump has been extensively researched in recent times and many of the factors effecting performance have been identified (Graham-Smith and Lees, 2005). The goal of a long jumper is to obtain vertical velocity of the centre of mass while retaining as large a horizontal velocity as possible (Muraki et al., 2008). Due to the recent increase in popularity of compression garments there is a need to establish the effect of these on a dynamic movement that involves a substantial impact. Therefore, the aim of the study is to explore the effect of the compression garment on athletic performance and its influence on muscle oscillation during the take-offs phase of a long jump. A secondary aim of the study was to investigate how the compression garments affect the force and load experienced during the task.

METHODS: Ten males (age: 25.30 ±5.66 years; mass: 76.14 ±10.00Kg; height: 1.82 ±0.54) volunteered for the study. All were free from injury and able to perform the task efficiently with no health problems. Informed consent was obtained and the subjects were free to withdraw from the study without prejudice at any time. The study had received university ethical clearance.

Subjects performed 6 3 step long jumps under 2 conditions, bare leg (control condition) and compression shorts. The compression shorts used were Adidas's PowerWeb shorts and for the control condition ordinary gym shorts were used with the shorts of the limb being filmed taped to above the hip leaving the leg bare for analysis. Lower-body jump performance kinematics and kinetic data were recorded using 6 camera Vicon Motus system sampling at 250Hz and a Kistler 9851 piezoelectric force plate (Kistler, Hook, UK) sampling at 500Hz respectively. Three retro- reflective spherical markers (19mm in diameter) were used to measure the muscle oscillation. The markers were attached to the dominant leg and marker 2 was placed between the greater trochanter and lateral condyle of the knee. The girth was measured and then marker 1 and 3 were placed 12.5% to the posterior and anterior side of marker 2. This measurement system allowed there to be control over marker placement as anatomical landmarks were unable to be used. Acceleration data were chosen to analyse muscle oscillation as it provided greater sensitivity with regard to the movement velocity associated with the jump studied during this investigation.

All data acquisition was conducted on the same day with several familiarisation trials prior to performance. The participants were asked to perform the jump with their normal technique as powerfully as possible. To aid the analysis the movement was broken down into braking (eccentric) and propulsion (concentric) phases of the jump for analysis. The point at which the phases were divided was at the instant of maximum knee flexion as suggested by Muraki et al. (2008) as during the first half of the takeoff the joints in the leg are flexing and then extend for the second phase. The main measures taken were Muscle Oscillation (MO), Peak Vertical Ground Reaction Force (PVGRF), Peak Horizontal Ground Reaction Force (PHGRF) and Jump Length. To establish whether there were any significant differences two-tailed paired sampled *t*-tests were used on the means with the statistical significance set at $p \leq 0.05$.

RESULTS AND DISCUSSION: There was a statistically significant difference in distance jumped ($t(9) = 3.972, P < 0.003$) with table 1 showing that on average the subjects were able to jump 5.8% (0.18m) further with the compression garments compared to when the subject performed the jump under the bare leg condition. The findings are supported by the literature with Kraemer et al. (1998) noting an enhancement in athletic performance, specifically in the increase in repetitive jump power. This was further supported by Doan et al. (2003) who found that while wearing compression shorts the subjects were able increase their jump height by 0.24m compared to a controlled condition. This does suggest that wearing compression garments a person's performance can be increased.

Table 1: Means and Standard Deviations for Distanced Jumped and percentage difference.
* represents significant.

	Bare Leg Condition	Compression garment condition	% difference of compression garment compared to bare leg.
Distance Jumped	2.73 ± 0.22	*2.92 ± 0.33	5.8%

There was a significant difference in muscle oscillation peak accelerations between the conditions during the braking phase at the anterior marker ($t(9) = 3.012, P < 0.015$) and the posterior marker ($t(9) = 4.641, P < 0.001$), although there was no significant difference at the mid-thigh marker ($t(9) = 1.034, P > 0.328$). During the propulsion phase only the posterior marker was statistically significant ($t(9) = 7.321, P < 0.000$) with the mid-thigh marker ($t(9) = 1.162, P > 0.275$) and the anterior marker ($t(9) = 1.650, P > 0.133$) not significant. Although there was no significant difference at a number of the marker positions there was a percentage decrease in muscle oscillation during all compression garment trials compared to the bare leg condition. The most enlightening of these results is the reduction in oscillation at the posterior marker, which was significantly reduced by 60.4% at the braking and 72.7% at the propulsion phase. During the propulsion phase the quadriceps is the prime mover generating the explosive force for take-off, leaving the hamstrings to stabilise the body. Therefore, if the oscillation of the hamstring is reduced in this phase it possibly aids the performance of the quadriceps as greater propulsion force can be generated from a stable base (Kraemer et al., 1998).

The average data for the ground reaction force during the take-off phase can be seen in table 2. The largest peak occurred during the initial impact with a smaller second peak occurring before the propulsion phase. The results for the peak VGRF were significant ($t(9) = -3.373, P > 0.008$) and the subjects experienced on average 23.4% more force during the peak impact while wearing the compression garment. This result suggests that the force experience by the body is increased by wearing the compression garments, which could have negative aspects with unaccustomed force linked to an increase risk of injury. This is supported by Speed et al. (1996) who investigated stress fractures of the tibia. He found that increasing the force to which the body had become accustomed to lead to the development of fatigue stress injury.

Table 2: Means and Standard Deviations for Maximum Peak Ground Reaction Force (GRF). * represents significant ($P < 0.05$).

	Bare Leg Condition	PowerWeb condition	% difference of compression garment compared to bare leg.
Peak Vertical GRF (BW)	2.9 ± 0.5	3.8 ± 0.7	23.4%
Peak Horizontal GRF (BW)	0.8 ± 0.3	0.7 ± 0.2	5.3%

Although still greater than the bare leg condition the peak HGRF (5.3%) was not statistically significant ($t(9) = 1.209, P > 0.257$). the research has suggested that more force transferred to the ground, utilising as much of the horizontal approach speed as possible, is linked to a further distances being jumped (Muraki et al., 2008). This could be the possible explanation for the increase in the performance measure in the compression garment condition.

CONCLUSION: The results suggest compression shorts appear to increase jump length performance. This could due to the reduction of muscle oscillation, although the present study found that not all of the marker peak accelerations were reduced compared to a control condition there was still reductions in areas such as the posterior marker. However, the study has highlighted that this reduction in oscillation may have a negative aspect when wearing

the compression shorts. This may be due to the garment restricting the muscles ability to disperse energy, which could lead to higher forces being experienced.

REFERENCES:

Challis, J. and Pain, M. (2008). Soft Tissue Motion Influences Skeletal Loads During Impacts. *Exercise and Sport Science Review*, 36(2), 71-75.

Doan, B., Kwon, Y., Newton, R., Shim, J., Popper, E., Rogers, R., Bolt, L., Robertson, M. and Kraemer, W. (2003). Evaluation of a lower-body compression garment. *Journal of Sport Sciences*, 21 (8), 601-610.

Duffield, R. and Portus, M. (2007). Comparison of three types of full body compression garments on throwing and repeat-sprint performance in cricket players. *British Journal of Sports Medicine*, 41, 409-414.

Graham-Smith, P. and Lees, A. (2005). A three dimensional kinematic analysis of the long jump take-off. *Journal of Sports Sciences*, 23, 891-903.

Gruber, K., Ruder, H., Denoth, J. and Schneider, K. (1998). A comparative study of impact dynamics: wobbling mass model versus rigid body model. *Journal of Biomechanics*, 31, 439-444.

Kraemer, W.J., Bush, J.A., Bauer, J.A., Newton, R.U., Duncan, N.D., Volek, J.S., Denegar, C.R., Canavan, P., Johnston, J., Putukian, M. and Sebastianelli, W. (1998). Influence of a compression garment on repetitive power output production before and after different types of muscle fatigue. *Sports Medicine, Training and Rehabilitation*, 8 (2), 163-184.

McComas, A.J. (1996). Skeletal muscle. *Form and function*, Human Kinetics, Champaign, IL.

Muraki, Y., Ae, M., Koyama, H. and Yokozawa, T. (2008). Joint torque and power of the takeoff leg in the long jump.

Speed, C., Fordham, J. and Cunningham, J. (1996). Simultaneous bilateral tibial stress fractures in a 15-year old milkman. *Journal of Rheumatology*, 35, 905-907.

KINETIC AND KINEMATIC ANALYSIS OF THE LEG POSITIONING IN THE FREESTYLE TRACK START IN SWIMMING

**Sergio Carradori, David Burkhardt, Suzanne Sinistaj, William R. Taylor
and Silvio Lorenzetti**

Institute for Biomechanics, ETH Zurich, Zurich, Switzerland

In swimming competitions, the track start is an important part of the race. The aim of this study was to assess and compare the relative positioning of the dominant leg in the preferential freestyle track start. The data was collected using the (Kistler) Performance Analysis System for Swimming (PAS-S) that includes a force measurement and motion analysis system. The results taken from 15 high level competitive swimmers showed that 67.7 % of the subjects naturally position their dominant leg in front. Starting with the dominant leg in front (6.67 ± 0.24) was significantly ($p < 0.001$) faster than in the rear position (7.25 ± 0.23). However swimmers had faster starts when using their preferential track start. Detailed analysis of the swimming start and the footedness allows coaches and athletes to train the fastest starting technique.

KEYWORDS: swimming track start, start position, dominant leg, footedness.

INTRODUCTION: In swimming competitions the track start is an important part of the race (J. Cossor & B. R. Mason, 2001). Many scientific studies analyzing the swimming start have been performed in recent years, with investigators generally using either force platforms (Murrell D, 2012) or optical measurement systems (Nomura T, 2010; Takeda T, 2010) alone. Force platforms have also been utilized in the starting platform in combination with vision assessment systems (above and below the waterline) to analyze performance variables for starting performance (Honda KE, 2010; Takeda T, 2010; Vantorre J, 2010). In addition, Cossor JM (2010) used wireless accelerometers. In the study of Hardt, Benjanuvatra and Blanksby (2009) the relationship between lower limb asymmetry and stance preference in the swimming track start was explored. The majority of the participants produced better performances using the preferred track start stance, rather than the dominance of either limb in the forward or rear position. The conclusion was that further investigation is required to identify factors that predict the lateralized behavior of the track start.

The start position of the athletes is normally chosen based on the subjective feeling of the athletes. A detailed analysis of start performance based the athlete's footedness that includes force data for each foot, however, remains to be undertaken. Therefore, the aim of this study was to (1) identify the preferential positioning of the dominant leg in the freestyle track start, to (2) compare the preferred track start using the normal limb configuration (T_n) with the non-preferential track start opposite (T_o), and to (3) compare the track start with the dominant leg in the front position against the dominant leg in rear position. The results should enable athletes to improve their start performance and help coaches to identify the best start variant.

METHODS: 13 male and 2 female healthy, high-level swimmers (age: 20 ± 3 years, height: 1.85 ± 0.09 m, weight: 74 ± 11 kg, performance: 767 ± 88 FINA points) of the Swiss Swimming Training Base (SWTB) in Tenero participated in this study, which was approved by the local ethics committee. The study included a subjective component with 2 questionnaires, as well as 2 objective measurements using the new (Kistler) Performance Analysis System for Swimming (PAS-S) (Type 9691A) and the (Kistler) Quattro Jump (Type 9290AD).

The swimmers performed 10 track starts in a random order. Five track starts were performed with their preferential leg positioning T_n and 5 starts with the opposite variant T_o . Kinetic and kinematic data of the start and the first 15 meters were collected using PAS-S, a performance measurement system consisting of an instrumented starting platform with two force platforms and instrumented starting grips, as well as a corresponding vision system with four cameras (three underwater, one above). The measurement system had been

previously assessed for reproducibility after mounting and remounting (Sinistaj S. 2015). The dominant leg was identified in each subject using single leg jump performance and a footedness questionnaire.

The time after 15 m (t_{15m} [s]), the time from the start signal until the leave of the block (Block time [s]), entry meters [m] and the peak power [W/kg] were assessed using the PAS-S system. The horizontal/total momentum [Ns], the maximal horizontal force of the front plate and back plate [BW] and the maximal “negative” force of the grab bar [BW] were determined using MATLAB (Figure 1).

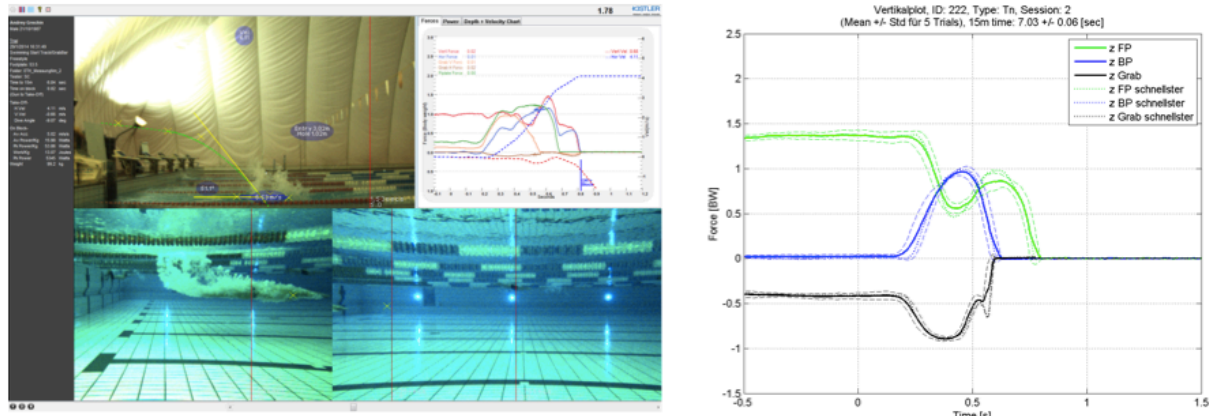


Figure 1: Video Sequence of the Analysis Software of PAS-S and horizontal force plots of MATLAB.

In order to objectively determine the footedness, the athletes performed single leg jumps on Quattro Jump and the maximal forces were measured. As predicting parameter of the leg dominance, the peak power has been determined, like it is chosen at the Swiss Olympic medical centers, Tschopp M. (2003). Furthermore, the first questionnaire was the footedness questionnaire also used in the study of Hardt et al. (2009) to determine the footedness of the athletes. The second questionnaire was a common questionnaire for further information of their swim capabilities.

To compare the two types of start, t-tests were performed. All the statistical analysis was performed in SPSS (version 22, SPSS Inc., Chicago). The t-test procedure was conducted with the chosen means of the parameters and corrected by the Bonferroni adjustment ($p < 0.05$ or $p < 0.00625$). Using descriptive statistics, the answers of the footedness questionnaire were compared with the maximum force of the jumps and the performance of their track start performance.

RESULTS: All 15 athletes completed the test protocol. In the preferential start T_n , 10 of the 15 subjects (66.7 %) positioned their dominant leg towards the front (Table 1). The comparison between the subjective answers of the footedness questionnaire and the objective measured parameters of the Quattro Jump showed that 7 of 15 (46.6 %) swimmers don't recognize their peak power leg as take-off leg.

**Table 1
Comparison of the subjective and objective variables to identify the dominant leg.**

Swimmer	335	222	441	445	442	223	331	111	224	333	225	332	334	411	443
Footedness Questionnaire	100% Right	100% Right	100% Right	100% Right	100% Right	71.4% Right	33.3% Right	100% Right	20% Right	45.4% Left	100% Right	100% Right	100% Right	85.7% Right	100% Right
4 Jump Peak Power	Right	Right	Right	Right	Right	Right	Right	Left	Left	Left	Left	Left	Left	Left	Left
Dominant leg position	Front	Front	Front	Front	Front	Front	Front	Front	Front	Front	Rear	Rear	Rear	Rear	Rear

By comparing T_n to T_o following results have been found. T_n showed a significantly better start performance compared to T_o in time to 15 m, block time, momentum and back plate maximum force. The peak power, the entry meters, front plate force and the grab bar values were similar.

Table 2
Comparison of track start normal (T_n) and track start opposite (T_o) parameters.

		Dependent Paired Samples T-Test				
		Preferential Track Start (T_n)		Opposite Track Start (T_o)		p-value
1	Time to 15m [s]	6.87	± 0.36	7.08	± 0.36	0.000 *
2	Block Time [s]	0.76	± 0.05	0.82	± 0.05	0.000 *
3	Entry Meters [m]	2.67	± 0.27	2.66	± 0.24	0.696
4	Peak Power [W/kg]	56	± 7	53	± 6	0.124
5	Momentum [Ns]	343	± 71	329	± 68	0.000 *
6	Front Plate max. [BW]	0.72	± 0.10	0.66	± 0.08	0.026
7	Back Plate max. [BW]	0.96	± 0.12	0.85	± 0.06	0.000 *
8	Grab Bar max. [BW]	-1	± 0.14	-0.92	± 0.18	0.020

* significant after Bonferroni = $p < 0.00625$

For the self-chosen T_n , 10 swimmers placed their dominant leg in the front position while 5 swimmers preferred their dominant leg in the rear position (Table 3). Swimmers with the dominant leg in the front position were significantly faster to the 15 meter distance. However, all the other parameters regarding the forces, times and distance were similar between the leg positions.

Table 3
Comparison of swimming parameters T_n of the Dominant Front and Dominant Back parameters.

		Independent Paired Samples T-Test				
		Dominant Leg Front (n = 10)		Dominant Leg Rear (n = 5)		p-value
1	Time to 15m [s]	6.67	± 0.24	7.25	± 0.23	0.001*
2	Block time [s]	0.77	± 0.03	0.75	± 0.07	0.681
3	Entry Meters [m]	2.77	± 0.24	2.47	± 0.23	0.040
4	Peak Power [W/kg]	58	± 8	52	± 3	0.156
5	Momentum [Ns]	371	± 64	286	± 48	0.023
6	Front Plate max. [BW]	0.72	± 0.11	0.71	± 0.07	0.839
7	Back Plate max. [BW]	0.98	± 0.11	0.93	± 0.16	0.447
8	Grab Bar max. [BW]	-1.01	± 0.14	-0.97	± 0.14	0.614

*significant after Bonferroni = $p < 0.00625$

DISCUSSION: For the first time, a start block allowing the detection of the force for each foot during track start was used to compare the start performance dependent on the athlete's footedness. 2/3 of all swimmers placed their dominant leg in front for the start although nearly half of the athletes were unable to recognize their peak power leg.

Our results show that the preferential technique T_n is highly stabilized and reproducible by swimmers as it is always the faster variant, in agreement with earlier findings of Hardt and co-workers (2009). Prior research into swimming starts has shown that "what one does most, one does best" (Pearson et. al 1998). Starts in the non-preferred position T_o were slower in the block time and swim time but they also exerted less force on the back plate, and thus generated lower body momentum.

By comparing the dominant leg in front with the dominant leg in the rear position, it was possible to demonstrate all start parameters were similar. However, the athletes with the

dominant leg in rear position showed a greater time to 15m. This is probably caused by the longer propulsion time from the block with the stronger leg. Due to the fact that the number of subjects was low and not well distributed, further studies to confirm these findings are required.

Although it was reported by Hardt et al., 2009 that the front limb produces more force than the rear limb in the propulsive phase, our results indicate that the maximum force is larger for the rear foot. By analyzing the time after 15 m, not only the start performance on the block is important but the behavior in entering and gliding in the water are also considered. Here, the higher momentum is in line with a larger maximum force of the rear leg (rather than the front leg), shows the importance of a leg specific measurement of the force.

CONCLUSION: Performing track start in the preferential start position showed the best start performance. However, it also seems to be beneficial for the track start, that the dominant leg is in front. This might indicate that for novice swimmers, an objective footedness test might help the athlete and the coach to identify the best start position.

REFERENCES:

- Cossor, J. M., Slawson, S. E., Justham, L. M., Conway, P. P., & West, A. A. (2010). The development of a component based approach for swim start analysis. *Biomechanics and Medicine in Swimming XI*, 11, 59-61.
- Hardt, J., Benjanuvattra, N., & Blanksby, B. (2009). Do footedness and strength asymmetry relate to the dominant stance in swimming track start? *Journal of sport sciences*, 27(11), 1221-1227.
- Honda, K. E., Sinclair, P. J., Mason, B. R., & Pease, D. L. (2010). A biomechanical comparison of elite swimmers start performance using the traditional track start and the new kick start. *Biomechanics and Medicine in Swimming XI*, 11, 94-96.
- Kishimoto, T., Takeda, T., Sugimoto, S., Tsubakimoto, S. & Takagi, H. (2010). An Analysis of an Underwater Turn for Butterfly and Breaststroke. *Biomechanics and Medicine in Swimming XI*, 11, 108-109.
- Murrell, D., & Dragunas, A. (2012). A Comparison of Two Swimming Start Techniques from the Omega OSB11 Starting Block. *WURJ: Health and Natural Sciences*, 3(1), 1-6.
- Nomura, T., Takeda, T., & Takagi, H. (2010). Influences of the back plate on competitive swimming starting motion in particular projection skill. *Biomechanics and Medicine in Swimming XI*, 11, 135-137.
- Puel, F., Morlier, J., Mesnard, M., Cid, M., & Hellard, P. (2011). Three dimensional kinematic and dynamic analysis of the crawl tumble turn performance: the expertise effect. *Computer Methods in Biomechanics and Biomedical Engineering*, 14(sup1), 215-216.
- Pearson, C. T., McElroy, G. K., Blitvich, J. D., Subic, A., & Blanksby, B. (1998). A comparison of the swimming start using traditional and modified starting blocks. *Journal of Human Movement Studies*, 34, 49-66.
- Sinistaj, S. (2015). *Kinematische und kinetische Analyse von Rückenstartvarianten* (Unpublished master's thesis). Universität Salzburg, Austria.
- Takeda, T., Takagi, H., & Tsubakimoto, S. (2010). Comparison Among Three Types of Relay Starts in Competitive Swimming. *Biomechanics and Medicine in Swimming XI*, 11, 170-172.
- Tschopp, M. (2003). *Manual Leistungsdiagnostik Kraft. Qualitätsentwicklung Sportmed. Swiss Olympic*. Magglingen: BASPO.
- Vantorre, J., Seifert, L., Fernandes, R. J., Vilas-Boas, J. P., & Chollet, D. (2010). Biomechanical influence of start technique preference for elite track starters in front crawl. *The Open Sports Sciences Journal*, 3, 137-139.

Acknowledgement:

Many thanks to the Kistler Instrumente AG, which provided the measurement system (PAS-S) with the force and video system.

DOES FORCEFUL EXTENSION OF THE SUPPORT LEG DURING THE KICKING STRIDE ENHANCE MAXIMAL INSTEP KICK PERFORMANCE IN A SKILLED SOCCER PLAYER?

Simon Augustus and Neal Smith

Centre for Applied Sport and Exercise Sciences, University of Chichester,
Chichester, UK.

The purpose of this study was to apply a technique intervention to the maximum instep kick to increase performance. A carefully constructed intervention was based on evidence from motor learning studies. A single semi-professional player undertook a single subject design to investigate the effectiveness of the intervention, and analyse the mechanisms which underpin the technical improvements. Kinetic and kinematic data was collected pre and post intervention. Ball speed ($26.9 \pm 1.3\text{m}\cdot\text{s}^{-1}$ to $29.2 \pm \text{SD } 0.9\text{m}\cdot\text{s}^{-1}$) and knee extension velocity increased following the intervention. The mechanisms presented display a greater active contraction of support leg musculature led to increased energy transfer across the pelvis, and a greater subsequent passive energy transfer through the kicking limb.

KEY WORDS: power, pelvis, technique intervention.

INTRODUCTION: The maximal instep kick of a stationary ball is the most analysed soccer technique within current biomechanical literature (Lees, Steward, Rahnema & Barton, 2009). Previous research has highlighted a biomechanical understanding of the maximal instep kick is important as it is the most commonly used technique when attempting a direct shot at goal (Lees, Asai, Andersen, Nunome and Sterzing, 2010; Inoue, Nunome, Sterzing, Shinkai and Ikegami, 2014) and there is large body of research that describes the kinematic, kinetic and electromyographic characteristics of the maximal instep kick (see Kellis & Katis (2007) or Lees *et al.* (2010) for a review). Subsequently, the independent motion of the kicking leg as a multi-segment open kinetic chain that rotates around the pelvis in a proximal-to-distal fashion to maximise shank angular and linear velocity at ball contact as described by Putnam (1991) is well established (Nunome, Ikegami, Kozakai, Apriantono and Sano, 2006).

Less attention has been paid to the function of the support leg during the kicking stride, despite evidence to suggest the proximal-to-distal sequencing of the kick emanates not from the kicking leg hip and thigh (Putnam 1991, 1993) but from support leg action (Lees *et al.*, 2009; Inoue *et al.*, 2014). Extension of the support leg during the kicking stride might serve to displace the support leg hip vertically; initiating an interactive moment which decelerates the pelvis and facilitates swing of the kicking leg through to ball impact. To date however, the highlighted research has been purely descriptive, with no recommendation of how these mechanisms might be altered to elicit an increase in performance. It is therefore proposed that manipulation of technique accordingly might enhance overall kicking performance (i.e. increased ball velocity) and inform how coaches might improve kicking technique. However, before this hypothesis can be reliably tested, it is necessary to effectively elicit the desired changes of technique within the kicker. The aim of this case study was therefore to assess the effectiveness of a technique adjustment intervention designed to produce forceful extension of the support leg and subsequent vertical displacement of the support leg hip during the kicking stride of the maximal instep kick.

METHODS: The single male participant (age 22 years, height 1.80m, weight 80.5kg) was a semi-professional, and right dominant.

Due to the exploratory aim and scope of the investigation, a single subject design case study was used. Data was collected over two separate sessions one week apart. A total of 20

kicking trials were collected; ten to establish a representative baseline of the participant's normal kicking technique (NORMAL) and ten to assess the immediate influence of the technique adjustment intervention (INTERVENTION). All kicks were performed with the right foot.

The intervention was designed using aspects of Carson and Collin's (2011) Five-A model for technical refinement in skilled performers. During the initial awareness phase, the aim was for the participant to call into consciousness the differences between current (NORMAL) versus desired new (INTERVENTION) techniques. The adjustment phase then aimed to modify the technique and internalise the change to the extent that it was no longer in conscious awareness.

All kicks were performed in a carpeted laboratory with the participant's preferred (right) foot using a ball of standard size and pressure. The only instruction given was to strike the ball as forcefully as possible into the centre of a catching net placed 4m away, so to allow the participant to approach the ball in the way most comfortable to them for the specific kick conditions. The ball was placed so that the support (left) foot landed on a Kistler 9281B force plate (Kistler Instruments, Hook, UK) which collected GRF data at 1000Hz during the kicking stride. The trials were also captured with a 10-camera motion analysis system (250Hz) (Vicon Nexus 1.7.1, Vicon Motion Systems, Oxford, UK) and a Casio Exilm EX-FH20 Digital camera (CASIO Computer Co. Ltd, Tokyo, Japan) (210Hz) that was used solely to provide qualitative feedback during the intervention process. The participant wore their usual Astroturf soccer shoes and compressive shirt, shorts and socks for all trials.

Prior to both data collection sessions, 22 passive reflective markers (14mm diameter) were attached to selected lower limb anatomical landmarks with double sided tape and a static trial captured to ascertain the relative positions of these markers. Marker clusters (consisting of three markers) were also attached to the left and right thigh and shank to determine the orientation of these segments relative to the anatomical markers during the kicking trials. Anatomical markers were removed following collection of the static trials; as was the right foot 2nd metatarsal marker so it did not influence foot to ball contact. Finally, one additional marker was cut into hemispheres and placed over opposing poles of the ball.

The raw marker displacements were filtered using a quintic spline (predicted mean square error 30, chosen as per residual analysis conducted on a similar data set and by visual inspection of the current data set) within the Vicon Nexus software and the synchronised force and 3D motion data were exported to the Visual 3D software package (V5, C-Motion, Rockville, USA) for further analysis.

The kicking motion was defined by four key events. Support foot touchdown (SFTD) was the instance the force plate began to measure a signal above 10N during the kicking stride, left hip joint low (LHLOW) was the instance where the calculated left hip joint centre was lowest in the global Z (vertical) plane, support leg extension (EXT) was the instance that the support leg knee began to exhibit an extension angular velocity and ball contact (CONTACT) was the instance that the kicking foot first contacted the ball. Subsequently, three key phases were identified based on support leg action during the kicking stride. Absorption Phase occurred between SFTD and LHLOW, Reversal Phase between LHLOW and EXT and Extension Phase between EXT and CONTACT. To allow for direct comparison between conditions, trials were time normalised between the instances of SFTD (0%) and CONTACT (100%). The variables chosen to represent the kicking motions were the support and kicking leg knee and hip joint power scalar, net joint moment (flexion/extension), joint contact forces (compressive/tensile), angular velocities (flexion/ extension) and angles (flexion/ extension).

RESULTS AND DISCUSSION: Peak ball velocity was consistently greater (Mean $29.2 \pm \text{SD } 0.9\text{m}\cdot\text{s}^{-1}$) during the INTERVENTION trials than the NORMAL ($26.9 \pm 1.3\text{m}\cdot\text{s}^{-1}$). These values are consistent with those found elsewhere in the literature (Nunome *et al.*, 2006; Lees *et al.*, 2009; Inoue *et al.*, 2014) and it is argued that kicking performance was enhanced during the INTERVENTION condition. Furthermore, kicking knee angular velocity (extension) at CONTACT increased from $1870 \pm 78 \text{ deg}\cdot\text{sec}^{-1}$ in the representative NORMAL trial to $2036 \pm 105 \text{ deg}\cdot\text{sec}^{-1}$ in the INTERVENTION trial.

The absorption phase lasted for 43% of the total kicking action in the NORMAL trial compared to only 36% in the INTERVENTION trial. During this phase the support leg hip and knee flex (as shown by flexion angular velocities and compressive joint contact forces) to absorb GRFs. However, for both techniques the support leg knee is generating power (extension) during this phase and is also counteracting this flexion action with an extension joint moment throughout the phase. When performing the INTERVENTION technique the participant exhibited larger extension moments and compressive joint forces to resist support leg flexion that in the NORMAL trials. It could be argued that the INTERVENTION technique allowed the participant to minimise knee flexion (flexion angular velocity is larger throughout this phase in the NORMAL trial), allowing the support leg to reverse these flexion actions sooner during the kicking stride and increase the potential for greater extension in the subsequent phases of the kicking action.

The INTERVENTION trial was characterised by a longer (36%) reversal phase compared to the NORMAL trial (27%). In the support leg, peak hip and knee flexion angular velocity occur in the as these joints slow and prepare for extension in the final phase of the kick. Peak flexion angular velocity in the INTERVENTION trials ($224 \text{ deg}\cdot\text{sec}^{-1}$) was less than half that of the NORMAL trials ($515 \text{ deg}\cdot\text{sec}^{-1}$), providing further support for the notion that the greater support knee extensor moment seen throughout the kicking action in the INTERVENTION trial served to limit knee flexion. Furthermore, support leg hip reaches peak compressive joint contact force during the reversal phase for both conditions and a greater compressive joint contact force is exhibited in the INTERVENTION trial ($30.5\text{N}/\text{Kg}^{-1}$) compared to the NORMAL trial ($21.9\text{N}/\text{Kg}^{-1}$).

During the extension phase the support leg knee was extending more rapidly during the INTERVENTION trials and extension angular velocity at CONTACT was $213.3 \text{ deg}\cdot\text{sec}^{-1}$ compared to $93.1 \text{ deg}\cdot\text{sec}^{-1}$ in the NORMAL trial, suggesting that the intervention had elicited the desired changes to the participant's kicking technique. The pronounced support leg hip and knee extension in the final Extension Phase of the kicking stride during the INTERVENTION condition may have served to lift the support leg hip vertically and promote the downward (extension) velocity of the shank towards the ball (Lees *et al.*, 2009; Inoue *et al.*, 2014).

CONCLUSION: The current data suggested that support leg extension contributed to proximal to distal movement pattern displayed by the participant by promoting the passive energy transfer from the support to the kicking leg. It can be argued that the mechanisms that caused this were enhanced when support leg extension was exacerbated using the INTERVENTION technique, leading to a greater transfer of energy across the pelvis segment, greater tensile joint forces in the kicking leg which increased passive energy transfer and resulted in consistently higher kicking knee extension velocity at CONTACT and a subsequent peak ball velocity. The 5 A model (Carson and Collins, 2011) intervention provided successful intervention in altering technique and increasing performance outcomes during maximum instep kicking in soccer.

REFERENCES:

- Carson, H.J. & Collins, D. (2011). Refining and regaining skills in fixation/ diversification stage performers: the Five- A Model. *International Review of Sport and Exercise Psychology*, 4 (2), 146-167.
- Inoue, K., Nunome, H., Sterzing, T., Shinkai, H., & Ikegami, Y. (2014). Dynamics of the support leg in soccer instep kicking. *Journal of sports sciences*, 32 (11), 1023-1032.
- Kelis, E. & Katis, A. (2007). Biomechanical characteristics and determinants of instep soccer kick. *Journal of Sports Science and Medicine*, 6, 154-165.
- Lees, A., Asai, T., Andersen, T.B., Nunome, H., & Sterzing T. (2010). The biomechanics of kicking in soccer: A review, *Journal of Sports Sciences*, 28(8), 85-817.
- Lees, A., Barton, G., & Robinson, M. (2010). The influence of Cardan rotation sequence on angular orientation data for the lower limb in the soccer kick, *Journal of Sports Sciences*, 28 (4), 445-450.
- Lees, A., Steward, I., Rahnama, N., & Barton, G. (2009). Understanding lower limb function in the performance of the maximal instep kick in soccer. In T. Reilly & G. Atkinson (Eds.), *Proceedings of the 6th International Conference on Sport, Leisure and Ergonomics* (pp. 149-160). London: Routledge.
- Nunome, H., Ikegami, Y., Kozakia, R., Apriantono, T., & Sano, S. (2006). Segmental dynamics of soccer instep kick with the preferred and non-preferred leg. *Journal of Sports Sciences*, 24, 529-541.
- Putnam, C.A. (1991). A segment interaction analysis of proximal-to-distal sequential segment motion patterns, *Medicine and Science in Sports and Exercise*, 23, 130-144.
- Putnam, C.A. (1993). Sequential motions of body segments in striking and throwing skills: descriptions and explanations. *Journal of Biomechanics*, 26, 125-135.

SPRINT ACCELERATION BIOMECHANICS

Steffen Willwacher

Institute of Biomechanics and Orthopaedics, German Sport University
Cologne, Germany

Sprint start performance (SSP) is of prime importance in short sprint races. The purpose of this workshop was to present a method for the evaluation of SSP in a typical training environment. For this purpose, starting blocks, instrumented with 3D force sensors in the front and the rear block were utilized in combination with high-speed video cameras and light barriers. Performance related parameters could be extracted immediately from the captured force signals. Individual values were compared to a large reference database. Comparisons were made to reference values of athletes with similar sprint performance capacity. Optimisation potentials in technical and strength related aspects of SSP were highlighted for each start, based on the actual overall sprinting performance level of the athlete.

KEY WORDS: sprint start performance, force measurement, sprint mechanics

INTRODUCTION: The importance of sprint start performance (SSP) is inversely related to the distance of the sprinting race. Particularly in 100 m sprint races (outdoors) or even more in 60 m sprint races (indoors) SSP is of critical importance for overall race time. Consequently, analysing SSP has frequently drawn the attention of researchers in the past (e.g. Harland, Kyröläinen & Komi, 2006, Bezodis, Salo & Trewartha, 2010, Mero, Kuitunen, Taboga, Grabowski, di Prampero & Kram, 2014 Bezodis, Salo & Trewartha, 2015) For the coach on the track it is important to know which biomechanical parameters are related to SSP in order to optimize the starting technique and related training programs (e.g. strength training, jumps, etc.). Force measurements in the starting blocks are of great importance in this context, as block reaction forces are directly linked to centre of mass acceleration of the athlete based on Newton's second law of motion. Two of the most basic parameters to describe starting performance are the average normalized horizontal block power (NAHBP, Bezodis, Salo & Trewartha, 2010) and the ratio of horizontal to resultant ground reaction force impulse (RHRI, Morin, Bourdin, Edouard, Peyrot, Samozino, & Lacour, 2012). Furthermore, using both feet to create propulsive impulse has been shown to be related to SSP (Willwacher, Herrmann, Heinrich & Brüggemann, 2013).

If these performance-related parameters are known, comparisons can be made between results of the individual athlete and reference values. In lots of cases these reference values are the results obtained from the best athletes in the sport, e.g. world record holders or world and / or Olympic champions. Nonetheless, in young or developmental athletes this comparison might be less useful, as the anthropometric characteristics, strength and technical capacities of these athletes might be too different to derive valid inferences for the design of training programs. A comparison with respect to athletes of similar or slightly higher performance level might be more appropriate in this case.

METHODS: Instrumented starting blocks were used to collect block reaction forces separately for the front and the rear starting block. The details of these blocks are described in Willwacher, Küsel-Feldker, Zohren, Herrmann & Brüggemann (2013). Then, a substantial amount of parameters were immediately extracted from the force waveforms. The most important ones are NAHBP, RHRI, peak forces and impulses in the front and rear blocks and push times. In addition to the instrumented starting blocks, dual light barriers were used in order to collect 5 m and 10 m times. Furthermore, high-speed video cameras were used to qualitatively analyse the motion of the athletes in the sagittal and frontal planes of motion.

When calibrated, these videos could be used for the subsequent analysis of spatio-temporal or joint kinematical parameters.

The force parameter analysis was based on the linear regression analysis detailed in Willwacher et al. (2015). Regression lines were calculated between 100 m personal record times and selected force parameters in a dataset of 142 male and female athletes ranging from regional to world record level.

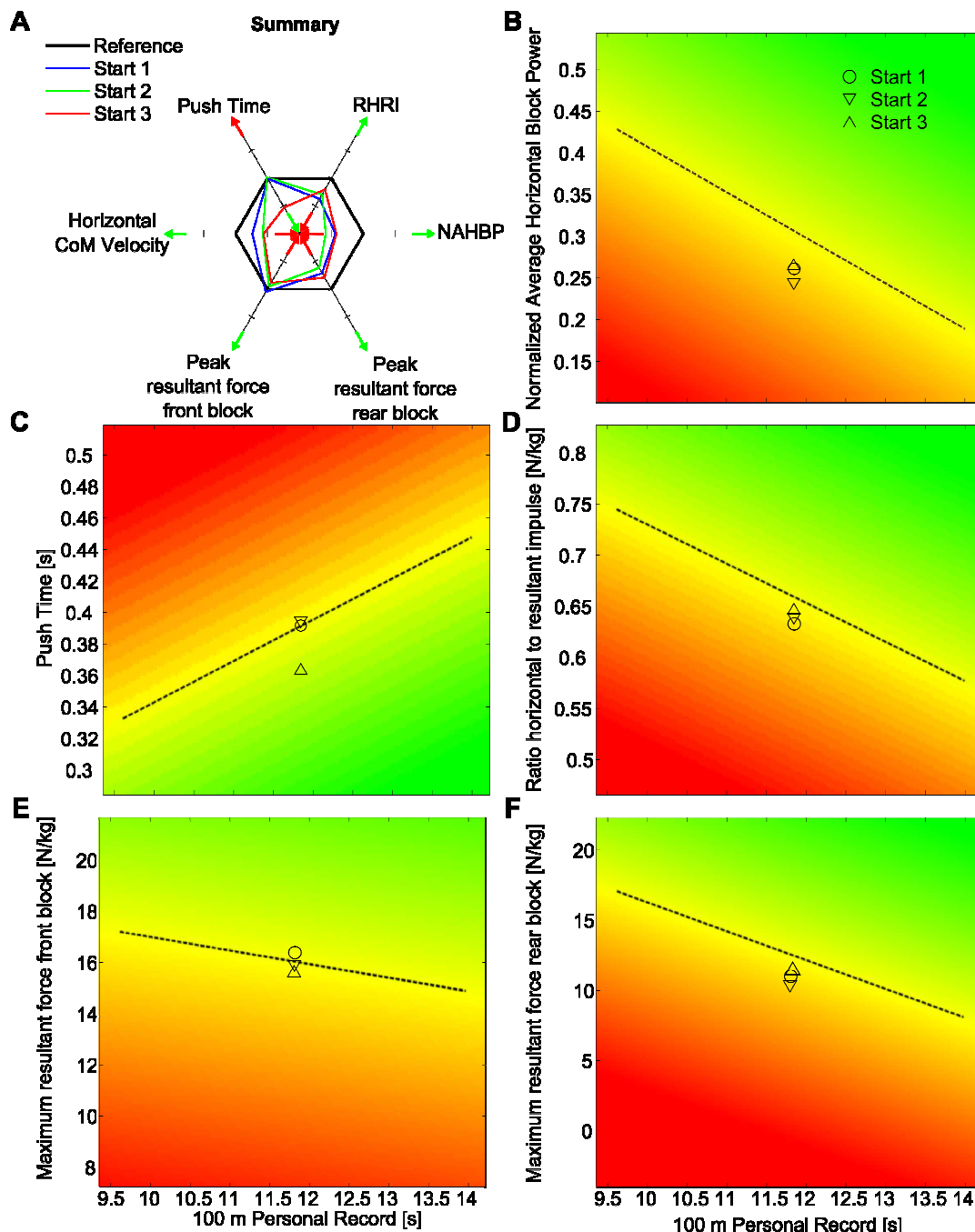


Figure 1: Graphical representation of block force characteristics of a regional level German decathlete. A summarizes the results of the specific parameters visualized in B – F. In A, the black line represents the average performance of an athlete with similar 100 m personal record time. For each start the z-normalized deviation from the average performance is represented in the radar chart.

The SSP of an individual athlete was evaluated by the distance of his or her results with respect to the linear regression line. A novel visual representation of the results has been developed in order to allow for a quick interpretation of the results. Therefore, the distance to the regression line was normalized to the standard deviation of the residuals in the linear regression model. Based on this normalized distance, a colour value was assigned to each point in the regression plot background, ranging from red (poor performance) to yellow (average performance) to green (excellent performance). Figure 1 displays an example of this graphical representation of a regional level German decathlete. In addition to the graphical representation, exact numbers of each individual start and the reference dataset are provided.

DISCUSSION: The proposed method to analyse SSP has several advantages. Firstly, it allows a direct feedback to the athlete, because the force parameters are available a few seconds after the athlete has left the blocks. Therefore, this method is highly valuable not only for performance diagnostics, but also for feedback training. The addition of high-speed video footage further helps to identify technical deficits of the athlete during the block phase and subsequent steps. The proposed methods allow for an immediate comparison of several starts, for example for the evaluation of different starting positions, different block separations, tilt angles or distances to the starting line. The potentially biggest strength of the approach is the comparison to a very large reference database, which includes starting performances of athletes ranging from regional level to the current world record holder and Olympic champion. The newly developed graphical representation eases the quick interpretation of the results. The comparison to athletes of a similar performance level further allows to draw conclusions with respect to the developmental stage of an individual athlete in different phases of the sprint race (start and acceleration phase, constant velocity phase or sprint endurance phase). The decathlete in figure 1 for example shows a below average SSP with respect to athletes of similar 100 m personal record time. This seems to be mostly related to a weak force production in the rear blocks (Fig. 1F), a too vertical oriented general force production (low RHRI, Fig. 1D), resulting in a low NAHBP (Fig. 1B). This implies that this athlete must perform relatively better in the constant speed phase of the 100 m race and / or in the speed endurance phase, because otherwise he would not be able to create his 100 m personal record time. Therefore, the results of this SSP analysis will help the coach in setting priorities in the training program of an individual athlete.

A severe limitation of the instrumented starting blocks used for the collection of the reference database (Willwacher et al., 2015) is that these blocks are very heavy and changing block settings takes a considerable amount of time. In order to make the proposed SSP analysis method feasible for on track performance diagnostics and feedback training, a more lightweight, easier to use version of instrumented starting blocks needs to be developed. In this process, care must be taken that the improvement of user friendliness does not come at the price of weak force signal detection quality.

REFERENCES:

- Bezodis, N. E., Salo, A. I. & Trewartha, G. (2010). Choice of sprint start performance measure affects the performance-based ranking within a group of sprinters: which is the most appropriate measure? *Sports Biomechanics*, 9, 258-269.
- Morin, J. B., Bourdin, M., Edouard, P., Peyrot, N., Samozino, P. & Lacour, J. (2012). Mechanical determinants of 100-m sprint running performance. *European Journal of Applied Physiology*, 112, 3921-3930.
- Willwacher, S., Herrmann, V., Heinrich, K. & Brüggerman, G. P. (2013). Start block kinetics: what the best do different than the rest. In T. Y. Shiang, W. H. Ho, P. C. Huang, and C. L.

Tsai (Eds.), Proceedings of XXXI International Conference on Biomechanics in Sports, Taipei, Taiwan.

Willwacher, S., Küsel-Feldker, M., Zohren, S., Herrmann, V. & Brüggemann, G.P. (2013). A novel method for the evaluation and certification of false start apparatus in sprint running. *Procedia Engineering*, 60, 124-129.

Willwacher, S., Herrmann, V., Heinrich, K., Funken, J., Potthast, W., Bezodis, I., Strutzenberger, G., Irwin, G. & Brüggerman, G. P. (2015). Sprint start kinetics: Comparison of amputee and non-amputee sprinters. Paper accepted for the presentation at the XXXIII International Conference on Biomechanics in Sports, Portiers, France.

Mero, A., Kuitunen, S., Harland, M., Kyröläinen, H., & Komi, P.V. (2006). Effects of muscle-tendon length on joint moment and power during sprint starts. *Journal of Sports Sciences*, 24(2), 165-173.

Bezodis, N.E., Salo, A.I., Trewartha, G. (2015). Relationships between lower-limb kinematics and block phase performance in a cross section of sprinters. *European Journal of Sport Sciences*. 15(2), 118-124.

Taboga, P., Grabowski, A.M., di Prampero, P.E., Kram, R. (2014). Optimal starting block configuration in sprint running: A comparison of biological and prosthetic legs. *Journal of Applied Biomechanics*. 30, 381-389.

REDUCING ACL INJURY RISK BY STANDING STILL WITH ZERO IMPACT PERCEPTUAL (ZIP) TRAINING!

Stephen Tidman¹, Brendan Lay¹, Alexis Brierty¹, Paul Bourke² & Jacqueline Alderson¹

School of Sports Science, Exercise & Health, University of Western Australia, Perth, Australia¹

iVEC @ UWA, University of Western Australia, Perth, Western Australia²

This study assessed novel zero-impact perceptual (ZIP) training, in which there is cognitive but no physical workload, in reducing biomechanical risk factors associated with anterior cruciate ligament injury. Tri-planar knee moments in amateur Australian rules footballers (n=16) were calculated during evasive sidestepping of 3D-projected opponents in 1-on-1, 2-on-2 and 3-on-3 game-based situations, pre and post intervention training. Video-only (VO) and Cueing (Q) training groups verbally evaded opponents in 8 sessions over 4 weeks. Cueing incorporated an additional task of counting visual cues within the scene. Training groups showed reductions in peak valgus and internal rotation moments, with greater reductions observed in Q training relative to controls. Results suggest that ZIP training can reduce ACL injury risk without impacting physical workload.

KEYWORDS: anterior cruciate ligament (ACL), injury prevention, perception, sidestepping.

INTRODUCTION: Workload management is a major consideration for sport science and medical staff involved in elite level sport in their efforts to reduce injury incidence (Rogalski, Dawson, Heasman, & Gabbett, 2013). Unfortunately, the containment nature of a risk minimisation management paradigm is restrictive and can serve to limit the time available for improving performance. Subsequently, specific skills and techniques not directly related to game performance (e.g. evasive sidestepping) may be overlooked when determining coaching priorities. Evasive sidestepping is a specific skill manoeuvre associated with anterior cruciate ligament (ACL) injury risk (Lloyd, 2011). *In-vitro* research has shown that the greatest ACL loads occur during a combination of applied internal rotation and anterior tibial force, with further increased load occurring when anterior tibial force is combined with valgus moments (Markolf et al., 1995). Further research has shown that knee valgus and internal rotation moments are increased when athletes have less time to plan a sidestepping manoeuvre (Besier, Lloyd, Ackland, & Cochrane, 2001). It is generally accepted that 'unplanned' scenarios are more representative of in-game scenarios where athletes must respond to a constantly evolving environment (Besier et al., 2001; Brown, Brughelli, & Hume, 2014). Current training methods focus on reducing injury risk by modifying technique (Dempsey et al., 2007b) or by training the neuromuscular system stabilising the knee during action through plyometric (Chappell & Limpisvasti, 2008) and/or strength training (Cochrane et al., 2010). Despite being effective in reducing risk factors, these methods often require significant levels of physical activity and may negatively impact on an athlete's physical workload allowance. Recent research has highlighted the need to investigate knee loads using stimuli that better represents the temporal and visuospatial demands found in competition (Lee, Lloyd, Lay, Bourke, & Alderson, 2013). Using 3D projected opponents Lee et al., (2013) observed that high-level footballers experienced lower peak knee valgus moments compared with low-level players, only when responding to a scene with multiple players. Lee et al (2010) suggested that previous research utilising non-specific stimuli such as light emitting diodes (Besier et al., 2001) and statically positioned mannequins (McLean & Lipfert, 2004) may not distinguish between high and low risk athletes as it may not account for an athlete's ability to perceive task-relevant information in a game-like environment. Historically, research investigating perceptual skill in athletes has focussed on expert-novice differences during anticipatory tasks. Experts exhibit superior performance in recognition and detection of objects within the visual field (M. Williams & Davids, 1995) and more appropriate visual search behaviours (Williams, Davids, Burwitz, & Williams, 1994) in sporting tasks. Additionally, experts have also shown an enhanced ability to pick up advance (early) cues in

postural orientation of opponents(Williams et al., 1994), allowing earlier response times. Given the disparity between high and low level players in perceptual ability and associated knee loads (Lee et al., 2013), current perceptual training methodologies have the potential to reduce injury risk. To date, perceptual training research has not directly investigated injury risk in sport. The purpose of this study was to explore the potential of ZIP training programs with a view to reduce knee loads associated with anterior cruciate ligament injury during an evasive sidestepping (SS) task.

METHODS: Sixteen community level footballers (mean Age: 24.87±3.38 yr, Height: 179.81±7.56 cm, Mass: 82.19±8.96 kg), participated in a 4-week video-only (VO, n=6)) or Cueing (Q, n=7) ZIP training program (2 x 15 minute sessions/week) or acted as controls (n=3). Participants were asked to verbally evade three-dimensional (3D) projected opponents in three scenarios. Scenarios depicted one opponent (1-on-1), one teammate and two opponents (2-on-2), and two teammates and three opponents (3-on-3) converging on the lab based participant. Forty-six trials per completed in each training session. VO and Q groups viewed identical scenarios throughout training. Visual cues (purple dots) were added to Q footage in information rich areas determined during pilot testing. Additional to verbal evasion, Q group were required to count cues (n =1-4) digitally added to scenario footage.

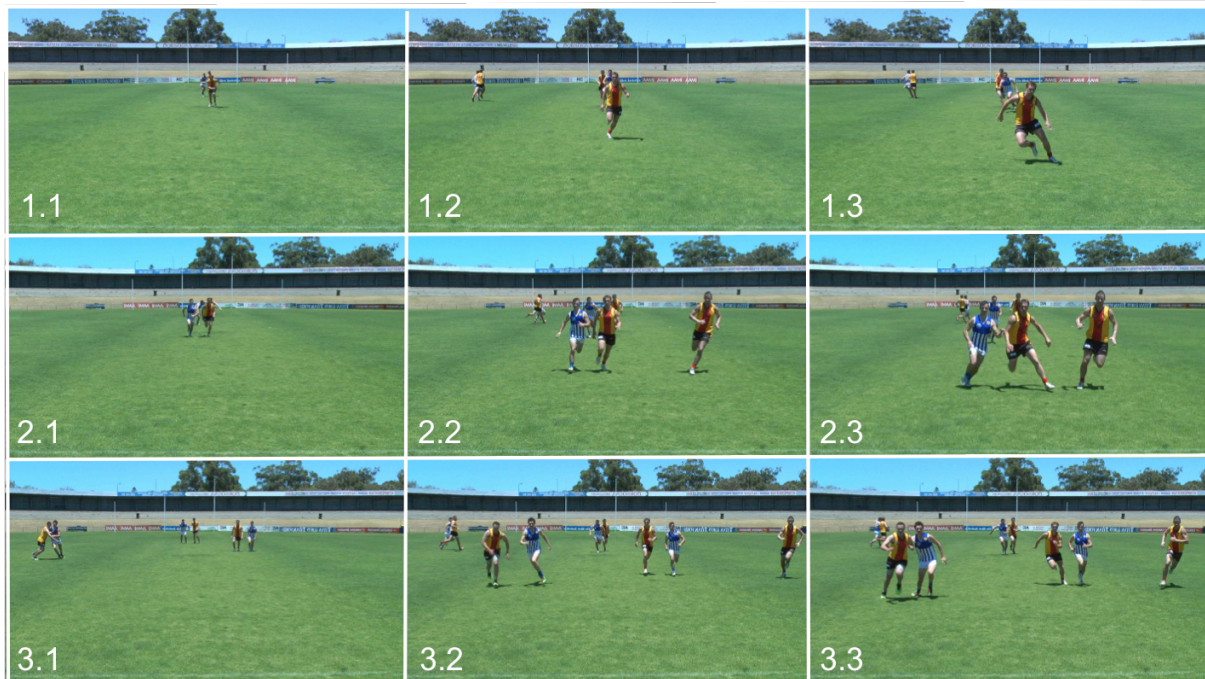


Figure 1: 2D representation of progression of 3D projected scenarios (1-on-1, 2-on-2 and 3-on-3) requiring sidestep/crosscut to the left from first frame (n.1) to approximate time of sidestep (n.3).

3D motion capture of each participant was captured using a previously published protocol (Lee et al., 2013) at baseline and post ZIP training. Players were instructed to 'run and carry' a football and evade oncoming opponents by sidestepping (SS) or crosscut manoeuvre at an angle of $45\pm 10^\circ$ from angle of approach. Thirty four retro-reflective markers were fitted as per the UWA lower-body marker set (Besier, Sturnieks, Alderson, & Lloyd, 2003). Marker trajectories were captured using a 22-camera Vicon MX/T40 system at 250 Hz (Oxford Metrics, Oxford, UK), and simultaneous ground reaction force (GRF) data at 2,000 Hz (AMTI, Watertown, MA). 3D kinematic and GRF data were low pass filtered using a 15 Hz zero-lag fourth order Butterworth filter. 15 Hz cut-off frequency was determined by residual analysis and visual inspection of kinematic data, and used for both kinematic and GRF to minimise knee joint kinetics artefact (Bisseling & Hof, 2006). Knee kinetics were calculated using established methods (Besier et al., 2003; Dempsey, Lloyd, Elliott, & Steele, 2007a;

Dempsey, Lloyd, Elliott, Steele, & Munro, 2009). Peak knee extension, valgus and internal rotation moments were analysed during weight acceptance (WA) of 3 successful SS in response to scenarios. SS were deemed successful if approach speed was 4.3-4.7ms⁻¹ and the correct direction was chosen. All knee moments were normalised to player body mass and height (Dempsey et al., 2009; Lee et al., 2013). One-way repeated measures ANOVA ($\alpha<0.05$), paired t-tests and Cohen's' d for effect sizes were calculated pre-post ZIP training, with one-way between groups ANOVA ($\alpha<0.05$) used to ensure no differences between groups at baseline.

RESULTS AND DISCUSSION: To date, no perceptual training methods have been utilised to reduce injury risk factors in sport. Historically, perceptual training has been successful in improving predictive and anticipatory performance in sporting tasks (Farrow & Abernethy, 2002; Jackson & Farrow, 2005). With time to plan a critical factor in knee injury risk (Brown et al., 2014), improving anticipatory and predictive performance may give an athlete more time to plan evasive action. Athletes who participated in ZIP training (VO and Q) showed overall reductions in peak knee moments associated with ACL injury, when compared with controls, suggesting ZIP training had a positive effect on reducing ACL injury risk. Prior to ZIP training, peak knee moments between groups were not significantly different. Peak knee valgus moments showed the greatest reductions post intervention, with notably greater reductions in Q (1-on-1 (p=0.49) and 2-on-2 (p=0.45) , 3-on-3 (d=1.05) compared to VO, (2-on-2 (d=0.84), 3-on-3 (d=0.89)). This combined with peak knee internal rotation reductions observed in Q (1-on-1 (p=0.034), 2-on-2 (d=0.73),3-on-3 (d=0.61)), suggests that Q was a more effective at reducing injury risk. It should be noted that the use of raw video footage without modification is easier to implement into a training environment and should not be overlooked as a potential training tool. These results highlight the potential benefit of orienting attention to information rich areas within the display that may be missed by adding visual cues.

Table 1
Peak Tri Planar Knee Moments during Weight Acceptance (Nm kg⁻¹ m⁻¹)

	1v1		2v2		3v3	
Valgus	Pre	Post	Pre	Post	Pre	Post
Control (C)	0.49±0.14	0.74±0.19*	0.40±0.07	0.82±0.18 ^a	0.56±0.21	0.74±0.04 ^a
Video-Only (VO)	0.44±0.28	0.40±0.09	0.47±0.21	0.29±0.22 ^a	0.48±0.31	0.26±0.16 ^a
Cueing (Q)	0.54±0.0.26	0.28±0.21*	0.51±0.0.22	0.29±0.0.25 ^a	0.40±0.25	0.11±0.0.30 ^a
Extension						
Control (C)	2.38±0.13	2.03±0.65 ^a	1.73±0.65	2.24±0.25 ^a	1.95±0.45	2.21±0.36 ^b
Video-Only (VO)	1.48±0.79	1.58±0.62	1.52±0.62	1.40±0.99	1.40±0.56	1.45±0.69
Cueing (Q)	1.52±0.55	1.30±0.32	1.49±0.32	1.34±0.63	1.34±0.81	1.31±0.68
Internal Rotation						
Control (C)	0.07±0.02	0.14±0.07	0.07±0.03	0.12±0.06 ^a	0.08±0.05	0.13±0.04*
Video-Only (VO)	0.06±0.04	0.06±0.03	0.05±0.04	0.07±0.04	0.06±0.05	0.06±0.03
Cueing (Q)	0.12±0.10	0.03±0.03*	0.08±0.03	0.05±0.05 ^b	0.08±0.09	0.04±0.02 ^b

* denote $p<0.05$, ^a denote strong *cohen's d* effect size ($d>0.8$), ^b denote moderate *cohen's d* effect size ($d>0.5$)

CONCLUSION: To our knowledge, this is the first demonstration of visual perceptual training's capability to reduce ACL injury risk. Traditional injury prevention training modalities such as plyometric, strength and technique modification training have been shown to be effective in reducing ACL injury risk but add to total player workload. These methods may

not be viable at an elite level if deemed to be too costly from a player workload perspective. Results suggest that zero impact perceptual (ZIP) training has the potential to provide coaches with a training platform that does not adversely impact player physical workloads, allowing for skills/techniques associated with injury to be trained without compromising performance goals. ZIP training also provides injured or rehabilitating players a low-risk, stable environment in which to continue training.

REFERENCES:

- Besier, T. F., Lloyd, D. G., Ackland, T. R., & Cochrane, J. L. (2001). Anticipatory effects on knee joint loading during running and cutting maneuvers. *Medicine & Science in Sports & Exercise*, 33(7), 1176–1181.
- Besier, T. F., Sturnieks, D. L., Alderson, J. A., & Lloyd, D. G. (2003). Repeatability of gait data using a functional hip joint centre and a mean helical knee axis. *Journal of Biomechanics*, 36(8), 1159–1168. doi:10.1016/S0021-9290(03)00087-3
- Bisseling, R. W., & Hof, A. L. (2006). Handling of impact forces in inverse dynamics. *Journal of Biomechanics*.
- Brown, S. R., Brughelli, M., & Hume, P. A. (2014). Knee Mechanics During Planned and Unplanned Sidestepping: A Systematic Review and Meta-Analysis. *Sports Medicine*, 44(11), 1573–1588. doi:10.1007/s40279-014-0225-3
- Chappell, J. D., & Limpisvasti, O. (2008). Effect of a Neuromuscular Training Program on the Kinetics and Kinematics of Jumping Tasks. *The American Journal of Sports Medicine*, 36(6), 1081–1086. doi:10.1177/0363546508314425
- Cochrane, J. L., Lloyd, D. G., Besier, T. F., Elliott, B. C., Doyle, T. L. A., & Ackland, T. R. (2010). Training Affects Knee Kinematics and Kinetics in Cutting Maneuvers in Sport. *Medicine & Science in Sports & Exercise*, 42(8), 1535–1544. doi:10.1249/MSS.0b013e3181d03ba0
- Dempsey, A. R., Lloyd, D. G., Elliott, B. C., & Steele, J. R. (2007a). The effect of technique change on knee loads during sidestep cutting. *Medicine & Science in Sports & Exercise*, 39(10), 1765–1774.
- Dempsey, A. R., Lloyd, D. G., Elliott, B. C., Steele, J. R., & Munro, B. J. (2009). Changing Sidestep Cutting Technique Reduces Knee Valgus Loading. *The American Journal of Sports Medicine*, 37(11), 2194–2200. doi:10.1177/0363546509334373
- Dempsey, A. R., Lloyd, D. G., Elliott, B. C., Steele, J. R., Munro, B. J., & Russo, K. A. (2007b). The effect of technique change on knee loads during sidestep cutting. *Medicine & Science in Sports & Exercise*, 39(10), 1765–1773. doi:10.1249/mss.0b013e31812f56d1
- Farrow, D., & Abernethy, B. (2002). Can anticipatory skills be learned through implicit video-based perceptual training? *Journal of Sports Sciences*, 20(6), 471–485.
- Jackson, R. C., & Farrow, D. (2005). Implicit perceptual training: how, when, and why? *Human Movement Science*, 24, 308–325.
- Lee, M., Lloyd, D. G., Lay, B., Bourke, P. D., & Alderson, J. (2013). Effects of Different Visual Stimuli on Postures and Knee Moments during Sidestepping. *Medicine & Science in Sports & Exercise*, 45(9), 1740–1748. doi:10.1249/MSS.0b013e318290c28a
- Lloyd, D. G. (2011). Rationale for Training Programs to Reduce Anterior Cruciate Ligament Injuries in Australian Football. *Journal of Orthopaedic and Sports Physical Therapy*, 31(11), 645–654.
- Markolf, K. L., Burchfield, D. M., Shapiro, M. M., Shepard, M. F., Finerman, G. A. M., & Slauterbeck, J. L. (1995). Combined knee loading states that generate high anterior cruciate ligament forces. *Journal of Orthopaedic Research*, 13(6), 930–935. doi:10.1002/jor.1100130618
- McLean, S. G., & Lipfert, S. W. (2004). Effect of gender and defensive opponent on the biomechanics of sidestep cutting. *Medicine & Science in Sports & Exercise*, 36(6), 1008–1016.
- Rogalski, B., Dawson, B., Heasman, J., & Gabbett, T. J. (2013). Training and game loads and injury risk in elite Australian footballers. *Journal of Science and Medicine in Sport / Sports Medicine Australia*, 16(6), 499–503. doi:10.1016/j.jsams.2012.12.004
- Williams, A. M., Davids, K., Burwitz, L., & Williams, J. G. (1994). Visual Search Strategies in Experienced and Inexperienced Soccer Players. *Research Quarterly for Exercise and Sport*, 65(2), 127–135. doi:10.1080/02701367.1994.10607607
- Williams, M., & Davids, K. (1995). Declarative Knowledge in Sport : A By-Product of Experience or a Characteristic of Expertise ? *Journal of Sport and Exercise Psychology*, 17, 259–275.

KINETIC AND KINEMATIC ANALYSIS OF THE BACKSTROKE START

Suzanne Sinistaj, David Burkhardt, Sergio Carradori, William R. Taylor
and Silvio Lorenzetti

Institute for Biomechanics, ETH Zurich, Switzerland

Race start technique in competitive swimming has developed considerably in recent years and is thought to be an important factor governing the outcome of a race. The purpose of this study was to measure the reliability of a new analysis system for swimming (PAS-S), as well as to analyse the backstroke start kinetics and kinematics and to compare the normal backstroke start with the backstroke start with a new start device. 16 high level competitive swimmers were examined in this study, which revealed that the measurements with the PAS-S are reliable. The analysis of the backstroke start showed the importance of a high preload force just before the start signal. Furthermore, if available, swimmers should use the new backstroke start device since the 15 m times were significantly faster even without considerable training with the new start device.

KEYWORDS: swimming start, backstroke start platform, kinetic analysis, kinematic analysis

INTRODUCTION: The start in competitive swimming has developed to become an important factor in the whole race outcome, with the start performance representing between 0.8% and 26.1% of the final race time (Mason & Cosser, 2001). Several changes in the rules and new starting blocks have led to changes in the starting technique, but studies that examine the backstroke start remain rare. Hohmann et al. (2008) searched for kinematic correlations between hands-off and feet-off, as well as between hands-off and hip entry. The authors were able to show that the 7.5m time is dependent on the maximal force on the wall plate directly before feet off. Furthermore, the data of Ngyuyen et al. (2014) demonstrated that the horizontal take off force had a high correlation with the starting time. For the ideal take off position, the hip position and a fast hip extension are important (Takeda et al., 2013). To our knowledge there are no studies measuring the forces on the grab bar.

Since 2014, a new backstroke start device can be used for the backstroke start. However, it remains unknown whether such a start device can provide an advantageous start time, and if so, by how much. Therefore the aims of this study were:

1. to test the new measurement system for its reliability.
2. to perform a kinetic and kinematic analysis of the backstroke start.
3. to compare the backstroke start with and without the start device.

METHODS: Fourteen male and two female high-level swimmers (age: 20 ± 3 years, height: 1.85 ± 0.09 m, weight: 74 ± 11 kg, performance: 767 ± 88 FINA points) of the Swiss Swimming Training Base (SWTB) in Tenero participated in this study, which was approved by the local ethics committee. With the Performance Analysis System for Swimming (PAS-S), a system for detailed analysis of different starting techniques in swimming, about 30 kinetic and kinematic parameters were measured. The PAS-S was developed by Kistler Instrumente AG (Winterthur). The starting block consisted of an instrumented starting platform with two force platforms and instrumented starting grips as well as a mountable turning plate and a corresponding vision system with four cameras (three underwater, one above). The swimmers were measured three times at intervals of one week. Between the first and the second week, the whole PAS-S including the starting block and the wall plate was dismantled and remounted. Between weeks two and three, only the camera system was dismantled and reinstalled. In each session, all swimmers performed five track starts and five backstroke starts in a random order. In the third session, the swimmers additionally performed five backstroke starts using the new backstroke start device. The raw data of the PAS-S then was processed using MATLAB (MathWorks Inc.). The raw data was filtered (low pass Butterworth filter) and offset corrected. With this data kinetic parameters were calculated. The reliability of the system was calculated a) to compare of the standard deviations from session one, two and three of one kinetic parameter (horizontal maximal

grab force) and one kinematic parameter (15m time) and b) with the comparison of the means of the 15m times from sessions one, two and three. All statistical analyses were undertaken in IBM SPSS Statistics (v22) with ANOVA. For the kinetic and the kinematic analyses two force plots were created, one for the horizontal forces of the force platforms and one for the vertical forces of the force platforms. In addition, correlations between several parameters were calculated. For the comparison between the normal start and the start with the backstroke start device, t-tests were used in SPSS.

RESULTS: No differences were found in the 15m times for the start types (Table 1). Furthermore, no differences were found between the means of the 15 m performance in sessions one, two or three (Table 2). The same results were found in the comparison of the standard deviations of the 15m times (Table 3) and the maximal horizontal grab forces (Table 4).

Table 1

15m times: means and standard deviations from trackstart and backstroke start in sessions one, two and three.

Starttype	Session 1	Session 2	Session 3	Overall
Trackstart (Tn)	6.68 ± 0.40	6.87 ± 0.36	6.88 ± 0.41	6.81 ± 0.39
Backstroke Start (Bn)	8.04 ± 0.56	8.33 ± 0.55	8.37 ± 0.56	8.25 ± 0.57

Table 2

Comparison of the means of the 15m times between session one, two and three (start 1=trackstart, start 2=backstroke start).

ANOVA

Mean time 15m

start	df	F	Sig.
1 between groups	2	1.268	0.292
in groups	42		
sum total	44		
2 between groups	2	1.579	0.218
in groups	42		
sum total	44		

Table 3

a) Comparison of the standard deviation of the 15m times between sessions one, two and three.

b) Comparison of the horizontal maximal grab force standard deviations between sessions one, two and three.

ANOVA

Standard deviation t 15m

ANOVA

Standard deviation maximal vertical Grabforce F

	df	F	Sig.		df	F	Sig.
between groups	2	1.590	0.210	between groups	2	0.478	0.622
in groups	87			in groupgs	87		
sum total	89			sum total	89		

Kinetic analysis of the grab forces showed the importance of a high preload force just before the start signal. Therefore it is important to ensure that after the start signal the horizontal grab force does not rise higher such that the swimmers can start faster (Figure 1). The same result was shown by the kinematic analysis, where a correlation was observed between the 15 m time and the time-on-block proportional to the time between the horizontal grab force maximum and the hands-off (Pearson = 0.645, p = 0.009). Furthermore correlations between the time-on-block to hands-off time and time-on-block to horizontal maximal grab force time were found.

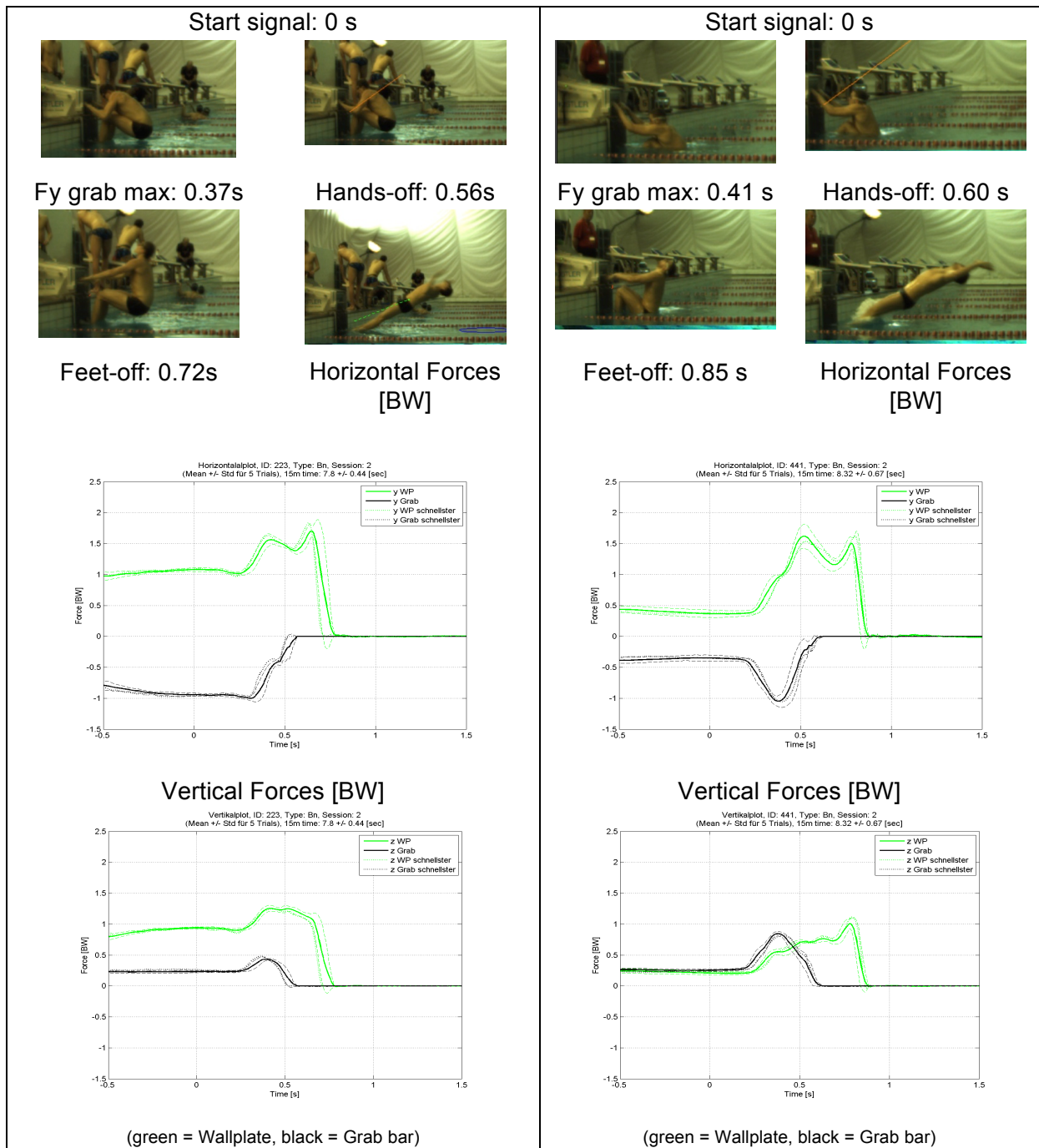


Figure 1: Comparison between a swimmer with a high preload (left) and one without (right).

The swimmers swam significantly faster, jumped further, entered the water in a better way (through a smaller hole) and dived deeper with the backstroke start device. There were no differences found in the time parameters hands-off and time-on-block between the start with the backstroke start device and the normal start in timing parameters (Table 5 and 6).

Table 5

15m times: means and standard deviations from backstroke start and backstroke start with start device.

Starttype	Time 15 m [s]
Normal Backstroke Start (Bn)	8.38 ± 0.58
Backstroke Start with Start Device (Ba)	8.31 ± 0.61

Table 6

P values of the comparison between Bn = Backstroke start normal and Ba = start with the backstroke start device. Significant values are highlighted.

Paar 1	Bn t 5m - Ba t 5m	0.002
Paar 2	Bn t 7.5m - Ba t 7.5m	0.001
Paar 3	Bn t 10m - Ba t 10m	0.003
Paar 4	Bn t 15m - Ba t 15m	0.011
Paar 5	Bn Time hands off - Ba Time hands off	0.654
Paar 6	Bn Time on block - Ba Time on block	0.590
Paar 7	Bn Entry metres - Ba Entry metres	0.000
Paar 8	Bn Entry Hole - Ba Entry Hole	0.012
Paar 9	Bn Max Depth - Ba Max Depth	0.001
Paar 10	Bn_Fz_grab_max - Ba_Fz_grab_max	0.000
Paar 11	Bn_Fz_grab_max_t - Ba_Fz_grab_max_t	0.081
Paar 12	Bn_Fy_graby_max - Ba_Fy_graby_max	0.041
Paar 13	Bn_Fy_graby_max_t - Ba_Fy_graby_max_t	0.907

DISCUSSION: For the first time, grab forces were measured separately in a backstroke start. The statistical calculations showed the reliability and resistance against mounting and dismounting of the PAS-S. This unique system has a huge potential for further scientific analysis of swimming starts and turns, as well as for the personal development of athletes. The results of this study have demonstrated that the better entry through a smaller hole into the water; with the backstroke start device the swimmer could generate a higher speed off the wall. The results confirm the findings of Takeda et al. (2013), who showed that a small entry hole into the water is important for a good starting time. Importantly, the time to 15 m was faster when using the backstroke start device. These clear benefits were surprising since the swimmers could only train once with this starting aid before the testing sessions. It is entirely possible that with more practice the advantages of the start device could even be even higher. No differences were found between the normal start and the start with the device in terms of the kinematic parameters. The take-off timing seems to be the same as with the normal backstroke start.

Further research, most notably for the force developments and changes on the wall plate are necessary to understand the backstroke start and the backstroke start device better before conclusions and training advice can be provided to coaches and swimmers.

CONCLUSION: The PAS-S is a suitable instrument for analysis of starts and turns in swimming. Kinematic analysis of elite swimmers has revealed that an ideal starting position right before the starting signal seems important for a fast backstroke start. Furthermore, if available, the swimmers should use the new backstroke start device since the 15 m times were significantly faster even without considerable training beforehand.

REFERENCES:

- Cossor, J., & Mason, B. (2001). Swim start performances at the Sydney 2000 Olympic Games. Poster presented at the Proceedings of XIX Symposium on Biomechanics in Sport.
- Hohmann et al. (2008). Biomechanical analysis of the backstroke start technique in swimming. *E-Journal Bewegung und Training*, 2(2008), 28-33
- Nguyen et al. (2014). Is starting with the feet out of the water faster in backstroke swimming? *Sports Biomechanics*. Last access 08.10.14: <http://dx.doi.org/10.1080/14763141.2014.885072>
- Takeda et al. (2013). Kinematic analysis of the backstroke start: differences between backstroke specialists and non-specialists. *Journal of Sports Science*, Vol. 32, No. 7, 635-641.

Acknowledgement

The authors would like to thank Kistler Instrumente AG (Winterthur) who provided the measurement system (PAS-S), including the force and video system.

DESIGN, VALIDATION AND APPLICATION OF AN UNOBTRUSIVE OAR FORCE-ANGLE MEASUREMENT SYSTEM

Timothy Turner¹, Franz Gravenhorst², Conny Draper³ and Richard Smith¹

The University of Sydney, Sydney, Australia¹

ETH Zurich, Zurich, Switzerland²

The University of Sydney, Sydney, Australia³

Feedback is necessary for the improvement of motor performance. Elite level athletes in particular require accurate and detailed kinematic and kinetic information for improvement. The purpose of this study was to design, build, validate and apply an unobtrusive oar force-angle measurement system for the evaluation of on-water rowing performance. Performance measurement systems must also meet the criteria of accuracy, unobtrusiveness, reliability, quality visualisation and affordability. Using high quality IMU and force measurement technology a system (RowIMU) was designed and built that met these criteria. Results for horizontal, vertical and feather angle of the oar and the normal handle force were obtained and reported. The system provided innovative and useful information for coaches and rowers.

KEY WORDS: rowing, performance, on-water.

INTRODUCTION: When learning motor skills, it is essential that the learner obtain appropriate feedback at each stage of development (Schmidt, 1988). Further, Newel, and Walter (1981), maintain that the provision of kinetic information feedback is preferable to mere knowledge of results and that feedback should occur as soon after performance as possible. More recently (Sigrist, Rauter, Riener, & Wolf, 2013) have shown that terminal visual feedback is the most effective because there was a focus on the internalization of relevant aspects of the task. However, concurrent feedback encouraged the correction of errors that were irrelevant to the task and thus hindered learning. Performance was much better in a concurrent visual and haptic feedback group during training with the feedback compared with nonfeedback trials. Training the three-dimensional movement using auditory feedback of the movement error was not practical for for most participants. The authors suggest that concurrent multimodal feedback in combination with terminal feedback may be most effective. The learning would be enhanced if the feedback strategy is adapted to individual skill level and preferences.

The systems developed by Smith and Loschner (2002) and Pilgeram and Delwiche (2006) are examples of many on-water systems for the provision of feedback to rowers. The advance of technology has facilitated increases in accuracy, unobtrusiveness, reliability, quality of visualisation and affordability and has the potential to provide the most effective feedback mode.

The aim of this project was to design and evaluate a rowing performance measurement system (RowIMU) that met these criteria.

METHODS: The RowIMU system consists of a narrow circuit board mounted in a water proofed enclosure which in turn is mounted inside a strain gauge equipped oar (Figure 1).

The circuit board contains an Invensense MPU-9050 tri-axial combined accelerometer, gyroscope and magnetometer as well as a TI LMP8358 precision strain gauge amplifier. The board also has a 32 bit ARM processor and Bluetooth connectivity.

The raw sensor data is acquired and processed to generate a complete dataset every 10 milliseconds. The dataset is composed of: the sample time, oar feather angle, oar elevation angle, oar (or yaw) angle and oar paddle force. This is streamed via the Bluetooth wireless protocol to a waterproof Smartphone attached to the rowing shell (Figure 2). The data from up to two oars can be collected simultaneously.

Sensors in the Smartphone compensate for yaw angle measurement errors due to rowing shell heading drift. The RowIMU application on the Smartphone allows test control and data display (Figure 3) as well as real time force/angle graphical feedback to the rower for technique monitoring (Figure 4). The dataset is saved both in the phone memory and in user online storage, for later detailed analysis.

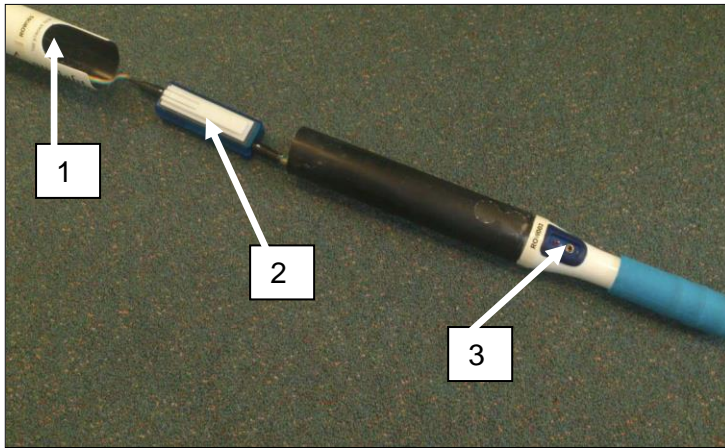


Figure 1. Dismantled Instrumented oar. Paddle with strain gauge force sensor (1). RowIMU module (2). On/Off switch, mode LED and charging port (3).

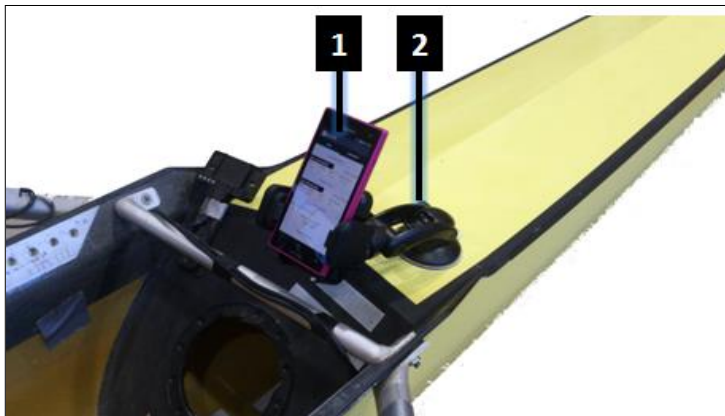


Figure 2. Smartphone (1) mounted on rowing shell (2).

The RowIMU was evaluated at an international rowing course with a sub-elite level female single sculler and two other male scullers. The oar force was pre-calibrated in the laboratory using known masses suspended from the handle (RMS error = 0.14%, $r = 0.999$, $p < .001$) and the oar angles gains calibrated against the laboratory motion analysis system (Cortex, Motion Analysis Corporation, USA) (RMS error = 0.03%, $r = 0.9997$, $p < 0.001$) (Figure 11).

On the course the IMU magnetometer was calibrated using a figure-of-eight movement of the oar in three dimensions. At the beginning of the test the oars were held in the square-off position while the IMU accelerometer and gyroscope were zeroed. The sculler then rowed for 500 m at a stroke rate of 26 strokes per minute with the RowIMU measuring and storing oar force, horizontal, vertical and feather angle of the oar. At the conclusion of the piece the data

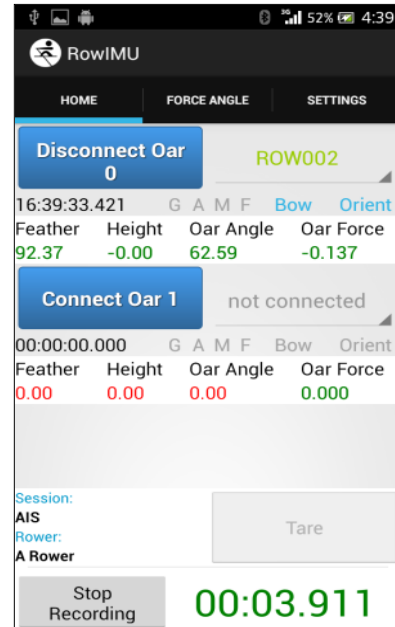


Figure 3. RowIMU application data monitor screen.

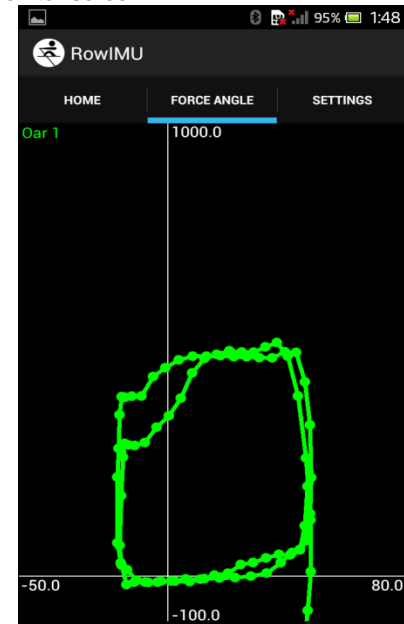


Figure 4. RowIMU application real time oar force angle display screen. (not a real stroke).

was transmitted to a cloud store. The data was downloaded to a laptop computer where rowing strokes were automatically detected, time normalised and averaged.

RESULTS: The RowIMU system was successful in measuring and storing the force and oar angle data and in providing a real-time display during on-water single sculling. An example of 21 successive strokes for one oar is displayed below for the horizontal oar angle (Figure 5), vertical angle (Figure 6), feather angle (Figure 7) and oar force (Figure 8). The catch is at 0 and 100 % of the stroke and the release or finish is at 40%.

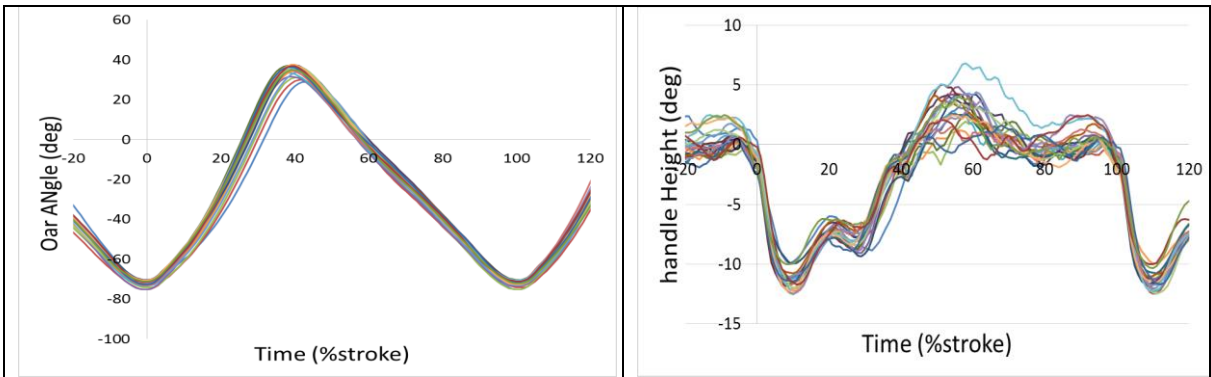


Figure 5: Horizontal oar angle

Figure 6: Vertical oar angle

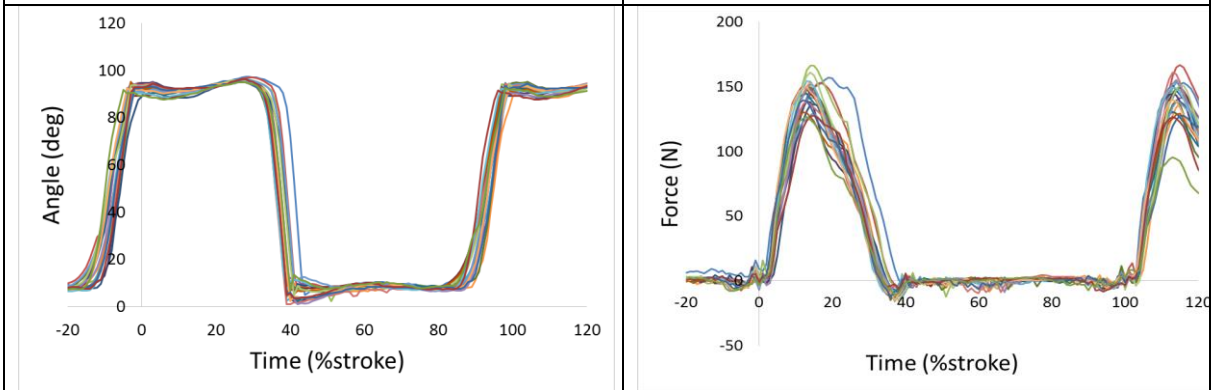


Figure 7: Feather angle

Figure 8: Normal handle force

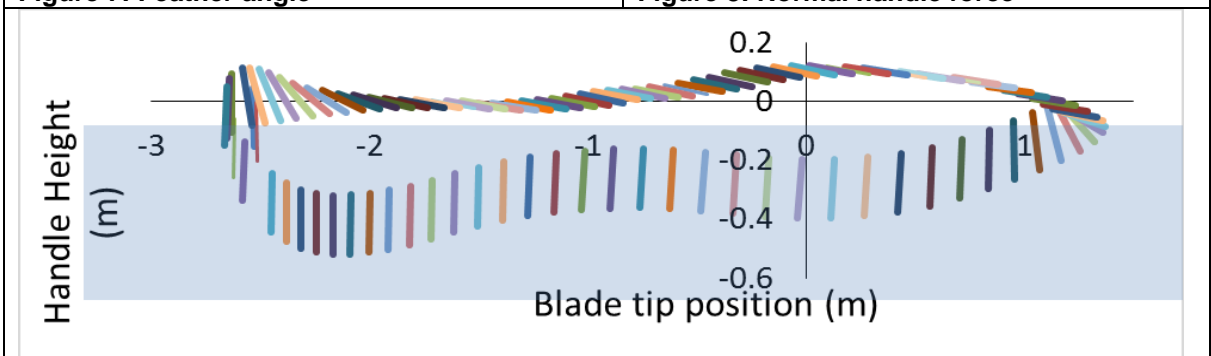
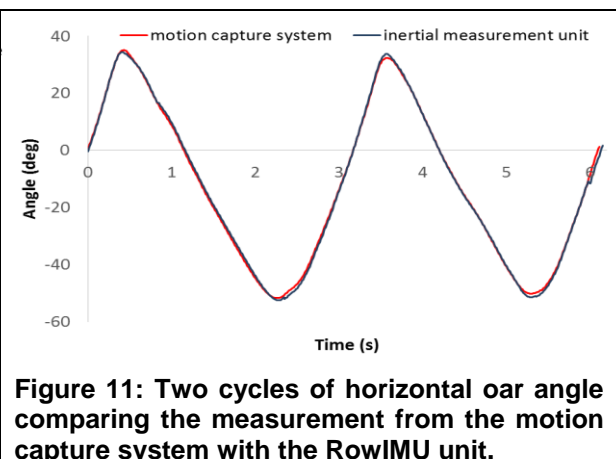
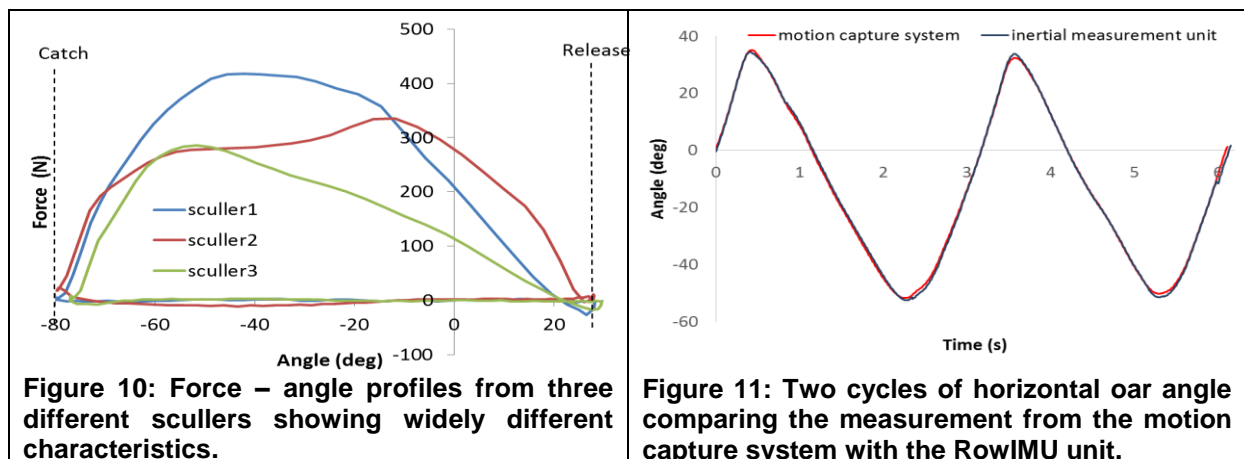


Figure 9: Visualisation of the orientation and position of the blade tip during one stroke. The blue background represents the water.

DISCUSSION: The RowIMU unit was easy and quick to set up on the course and was successful in measuring and storing the three oar angles and oar handle force. Importantly, the method used to calculate the oar angles in the RowIMU reports the true horizontal angle of the oar independently of the vertical and feather angle. Further, there is no need to mount custom gates on the boat pin in order to measure oar force as in other systems.



This is important for coaches who often mention the horizontal oar angle and its catch and release position as the most desired variables from a rowing performance measurement system. Differences in force angle profile are obvious when comparing force-angle profiles of different scullers (Figure 10).

An innovation in the visualisation of the data is the graph in Figure 9. This figure is a representation of the lateral view of the end of the blade every 10 ms as it would appear to the coach from their boat moving parallel to the scull. The horizontal and vertical position is calculated from the horizontal oar angle and the outboard length of the oar. From this graph the coach can discern the rower’s technique in getting the blade into and out of the water, the path of the blade in the water and the feathering during the recovery.

Obvious other visualisations are force-angle (Figure 10) and power-angle graphs. Performance variables available after data collection are average power and blade movement without force at the catch and finish.

CONCLUSION: The RowIMU system met the criteria set for its performance. It is unobtrusive, accurate, reliable and easy to use and provides useful information to coaches and rowers for the improvement of rowing performance. Work is also being done to characterise performance through the analysis of the force and angle data using functional data analysis to provide a more evidence based process for improving rowing performance.

REFERENCES:

- Newell, K. M., & Walter, C. B. (1981). Kinematic and kinetic parameters as information feedback in motor skill acquisition. *Journal of Human Movement Studies*, 7(4), 235-254.
- Pilgeram, K. C., & Delwiche, M. J. (2006). Device for on-the-water measurement of rowing output. *Sports Engineering (International Sports Engineering Association)*, 9(3), 165-174.
- Sigrist, R., Rauter, G., Riener, R., & Wolf, P. (2013). Terminal Feedback Outperforms Concurrent Visual, Auditory, and Haptic Feedback in Learning a Complex Rowing-Type Task. *Journal of motor behavior*, 45(6), 455-472. doi: 10.1080/00222895.2013.826169
- Smith, R. M., & Loschner, C. (2002). Biomechanics feedback for rowing. *Journal of sports sciences*, 20(10), 783-791. doi: 10.1080/026404102320675639

Acknowledgements:

Funding for the development of the RowIMU was provided by the Australian Institute of Sport.

IMAGE-BASED MEASUREMENT AND BIOMECHANICAL ANALYSIS OF THE KNEE JOINT DURING FUNCTIONAL ACTIVITIES

Tung-Wu Lu^{1,2*}, Cheng-Chung Lin¹ and Jia-Da Li¹

Institute of Biomedical Engineering, National Taiwan University, Taipei, Taiwan,
R. O. C.¹

Department of Orthopaedic Surgery, School of Medicine, National Taiwan
University, Taiwan, R. O. C.²

A new approach based on the integration of medical image-based measurement techniques, infrared stereophotogrammetry and finite element modelling (FEM) was developed for comprehensive subject-specific biomechanical analyses of the knee joint during weight-bearing functional activities including cycling. The medical image-based methods include digitally reconstructed radiograph (DRR) based 3D fluoroscopy methods, and a new slice-to-volume registration method using FLASH MRI for the real-time measurement of the 3D kinematics of the knee *in vivo*. With the new approach, the soft tissue artefacts associated with skin marker-based stereophotogrammetry and their effects on the calculated biomechanical variables were also investigated.

KEY WORDS: knee, kinematics, fluoroscopy, finite element modelling, MRI.

INTRODUCTION: The knee is one of the most commonly injured joints, making up about 55% of all sports injuries. Knowledge of the kinematic and force interactions between the force-bearing structures of the knee, including the articular surfaces, ligaments and muscles, during multi-joint functional activities is essential for a better understanding of the normal function of the joint and the mechanisms of injuries and diseases, as well as for the planning and evaluation of subsequent treatment. Skin marker-based stereophotogrammetry has been widely used in measuring inter-segmental motions and loads of human movement. However, such techniques are prone to soft tissue artefacts (STA) (Cappozzo et al., 1996; Tsai et al., 2009), which have significant effects on the calculated biomechanical variables (Tsai et al., 2011; Kuo et al., 2011). The detailed kinematics of the articular surfaces and the surrounding tissues cannot be measured simultaneously either. These limitations in measurements all contribute to the unsatisfactory predictions of the internal forces in the joint. Therefore, study of the force interactions within the knee *in vivo* remains a great challenge.

To bridge the gap, single-plane and bi-plane fluoroscopy-to-CT registration methods based on digitally reconstructed radiographs (DRR) and a similarity measure called Weighted Edge-Matching Score (WEMS) have been developed in our group for measuring 3D poses of the bone *in vivo* (Lu et al., 2008; Tsai et al., 2010). On the other hand, a new measurement technique for measuring 3D knee kinematics non-invasively and free from ionizing radiation will be helpful for future clinical applications (Lin et al., 2013).

The purposes of the current study was (1) to develop an approach based on the integration of the medical image-based techniques, infrared stereophotogrammetry and finite element modelling (FEM); (2) to measure non-invasively the 3D kinematics and arthrokinematics of the knee and ground reaction forces during functional activities including cycling; (3) to estimate the forces of the force-bearing structures of the knee during the tested activities; (3) to assess the STA and their effects on the calculated biomechanical variables; and (4) to develop a new slice-to-volume registration method using real-time MRI for non-invasive measurement of knee kinematics.

METHODS: A new measurement system was established by integrating a fluoroscope (Allura Xper FD20/20, Philips Medical Systems), 12 infrared cameras (Vicon Motion Systems Ltd, UK) and force plates/sensors (Advanced Mechanical Technology, Inc., USA). The integrated system was used to measure the movement of the knee and ground (or pedal) reaction forces in 13 young healthy subjects during isolated flexion/extension, sit-to-stand and stair-ascent and during cycling movements on an instrumented ergometer (Fig. 1a). Each subject was also CT and MR scanned to obtain the 3D volumetric data of the knee joint. The WEMS method was used to obtain the 3D poses of the femur and tibia which were used to derive the 3D kinematics of the knee joint (Fig. 1b). With the measured ground reaction forces, the forces and moments about the knee joint centre were calculated by considering the free bodies of the foot, shank and thigh using inverse dynamics analysis. Given the accurate kinematic data of the bones from the WEMS method and the 3D coordinates of the skin markers from VICON system, the STA of the markers (i.e., displacements of markers relative to the underlying bones) and its influence on the calculated biomechanical variables were also quantified.

A subject-specific FEM procedure of the knee (Fig. 1c) was developed validated *in vitro*, and used for the analysis of the stresses, strains, and forces of the ligaments during the test activities. For each model, the geometry of the bones and ligaments were reconstructed from subject-specific CT and MRI data; parameters for the constitutive equations were customized to the subject via a combined experiment and optimization approach; and the kinematic and boundary conditions data were obtained via the 3D motion experiments.

A new MRI-based method for real-time, 3D kinematic measurement of the knee was also developed by integrating a novel, 2D real-time MRI sequence (i.e., refocused FLASH) and a 3D MRI data set. The 3D MRI at fully extended position was used to reconstruct volumetric bone models. The 2D real-time MRI was acquired during isolated flexion/extension. The 3D bone pose at each instance was determined when the reformed images interpolated from the volumetric bone model best matched the corresponding real-time image (Fig. 1d). An *in vivo* validation study was carried out to evaluate the performance of the method, giving the validity and repeatability of its measurements.

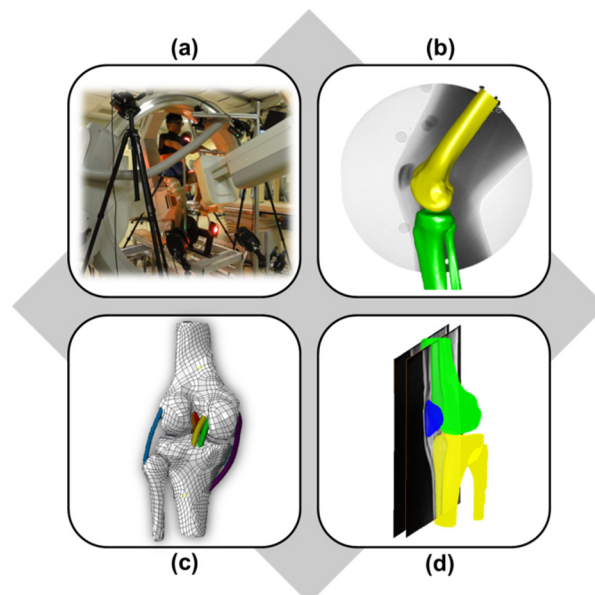


Figure 1: (a) *In vivo* measurement of knee kinematic and kinetic data during cycling using the integrated measurement system. (b) The fluoroscopy-to-CT registration method for the determination of 3D knee motion. (c) A subject-specific FEM model of the knee. (d) The new real-time MRI-based slice-to-volume registration method for non-invasive 3D knee kinematics.

RESULTS & DISCUSSION: The rigid-body kinematics (Fig. 2a) and arthrokinematics (Fig. 2b) of the knee during functional activities and cycling were measured for all subjects. The displacements of the skin markers relative to the underlying bones during all activities were also quantified and averaged across all subjects (Fig. 3a). The joint angles, shear forces and moments were underestimated and translations overestimated during cycling (Fig. 3b).

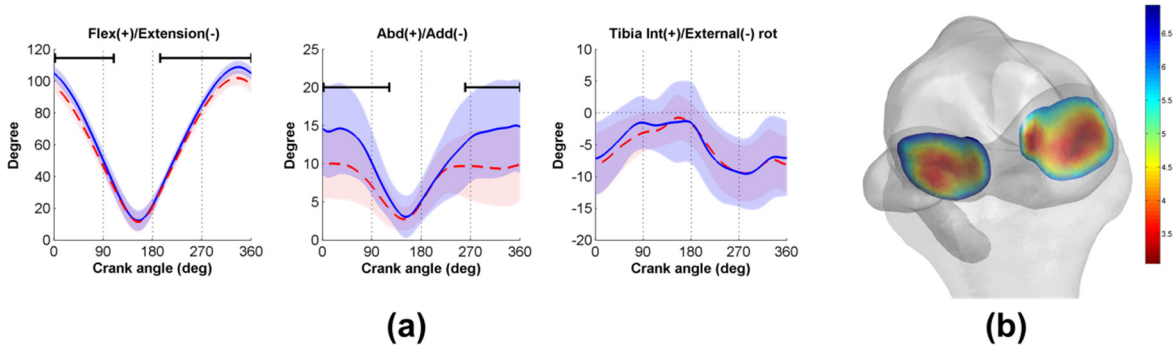


Figure 2: (a) The rotation angles of the knee during cycling using 3D fluoroscopy (blue lines) and motion capture system (red lines) (b) The colour map describing the relative distances between the femoral and tibial articular surfaces during cycling.

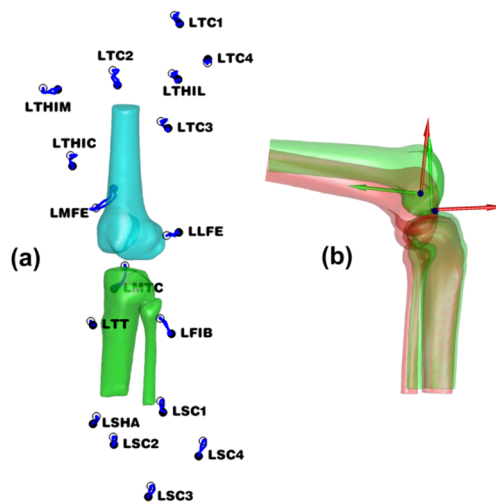


Figure 3: (a) The 3D displacements of the markers relative to the underlying bones. (b) The poses of femur and tibia obtained from the skin markers (red) and the true poses (green).

Finite element analysis of the knee joint and its surrounding soft tissues were performed. The resultant forces, stresses and strains of the cruciate and collateral ligaments during activities were obtained (Fig. 4). The PCL was found to transmit greater loads than the ACL during cycling, indicating a risk in PCL rehabilitation using cycling. Muscle activities played a crucial role in modulating the stresses and strains in the ligaments.

The new MRI-based slice-to-volume registration technique for 3D knee kinematics was shown to have sub-millimetre and sub-degree bias (means of errors) and precision (standard deviations of errors) for 3D poses of the femur and tibia, suggesting very good validity and reliability.

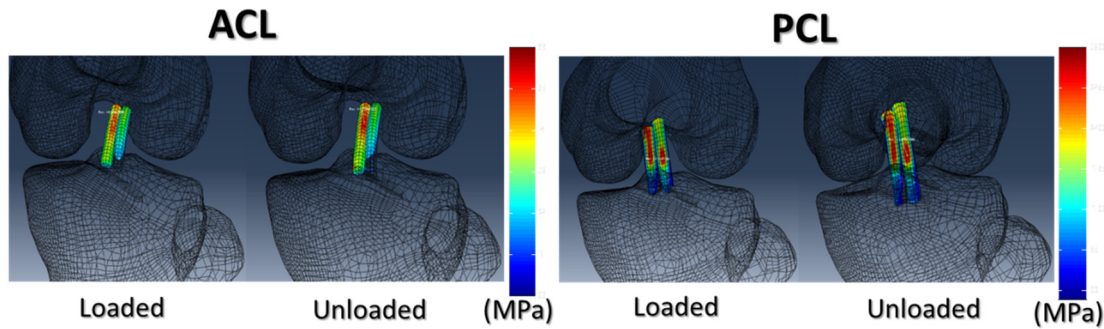


Figure 4: The principle stress patterns of the ACL (left) and PCL (right) at maximum knee flexion during cycling with and without external resistance.

CONCLUSION: A new integrated approach incorporating fluoroscopy-to-CT 3D measurement techniques, multi-camera motion capture system and finite element modelling techniques was developed and shown to be useful in the study of *in vivo* mechanical interactions between the force-bearing structures of the knee joint. The new approach provides a more comprehensive subject-specific biomechanical analysis of the knee during weight-bearing functional activities and exercises (e.g., cycling). The STA of the skin markers and their effects on the calculated biomechanical variables were quantified, which will be helpful for further improvement of modelling of the lower extremities in the field of 3D motion analysis. The new slice-to-volume registration method using the FLASH MRI for the real-time measurement of the 3D kinematics of the knee *in vivo* has been shown to be promising in future clinical applications and merits for further developments.

REFERENCES:

- Cappozzo, A., Catani, F., Leardini, A., Benedetti, M. G. & Della Croce, U. (1996) Position and orientation in space of bones during movement: experimental artefacts. *Clinical Biomechanics*, 11(2), 90-100.
- Kuo, M. Y., Tsai, T. Y., Lin, C. C., Lu, T. W., Hsu, H. C. & Shen, W. C. (2011) Influence of soft tissue artifacts on the calculated kinematics and kinetics of total knee replacements during sit-to-stand. *Gait and Posture*, 33(3), 379-384.
- Lu, T. W., Tsai, T. Y., Kuo, M. Y., Hsu, H. C. & Chen, H. L. (2008) In vivo three-dimensional kinematics of the normal knee during active extension under unloaded and loaded conditions using single-plane fluoroscopy. *Medical Engineering and Physics*, 30(8), 1004-1012.
- Lin, C.-C., Zhang, S., Frahm, J., Lu, T.-W., Hsu, C.-Y. & Shih, T.-F. (2013) A slice-to-volume registration method based on real-time magnetic resonance imaging for measuring three-dimensional kinematics of the knee. *Medical Physics*, 40(10), 102302.
- Tsai, T. Y., Lu, T. W., Kuo, M. Y. & Hsu, H. C. (2009) Quantification of three-dimensional movement of skin markers relative to the underlying bones during functional activities. *Biomedical Engineering - Applications, Basis and Communications*, 21(3), 223-232.
- Tsai, T. Y., Lu, T. W., Chen, C. M., Kuo, M. Y. & Hsu, H. C. (2010) A volumetric model-based 2D to 3D registration method for measuring kinematics of natural knees with single-plane fluoroscopy. *Medical Physics*, 37(3), 1273-1284.
- Tsai, T. Y., Lu, T. W., Kuo, M. Y. & Lin, C. C. (2011) Effects of soft tissue artifacts on the calculated kinematics and kinetics of the knee during stair-ascent. *Journal of Biomechanics*, 44(6), 1182-1188.

Acknowledgement

The authors gratefully acknowledge the financial support from the Ministry of Science and Technology of Taiwan. Thanks also to the assistance from Drs MY Kuo, HC Hsu, S Zhang, CY Hsu and TF Shih.

KINEMATIC ANALYSIS OF BASKET WITH 5/4 TURN TO HANDSTAND OF SHIXIONG ZHOU ON PARALLEL BARS

Wei Xie, Jihe Zhou, Shuai Wang
Chengdu Sport University, Chengdu, China

The basket with 5/4 turn to handstand on parallel bars is a representative movement of E group; in 1896 it is listed as the Olympic Games project. The parallel bars have been one of the Chinese men's gymnastics advantage projects since 1980s. From 1980 to 2011, China's elite athletes Li Yuejiu, Lou Yun, Li Jing, Huang Liping, Zhang Jingjin, Li Xiaopeng and Yang Wei won more than a dozen times world champion on the parallel bars in the world gymnastics competitions. China's athletes can keep long-term advantage of this project status and competitive strength, in addition to keep pace with the times innovation of difficult moves, there is another important reason is to continuously improve the leading trend of action quality.

KEY WORDS: Kinematic analysis, Shixiong Zhou, parallel bars.

INTRODUCTION: At present, only Chinese gymnast ShiXiong Zhou can complete this action in the world, in the final of the 2012 national gymnastics championships in the parallel bars, ShiXiong Zhou failed to complete the action very well. Therefore, in order to improve the quality of this action, it's necessary to analyze the action from both qualitative and quantitative aspects. We made a 3D camera resolution on ShiXiong Zhou at the game site, with the three-dimensional analysis we gained the kinematic parameters. Thus to analyze the reasons of errors, which provides theoretical and technical basis for the development and improvement of Chinese athletes.

METHODS: The whole process of the competition was recorded by two GC-PX10 video cameras (JVC, Japan) at 50 Hz from different angles (the included angle of the principal optic axes of two cameras was about 60 °). After the match, we put three-dimensional scale with 24 control points in filming area. We used 3-D Signal TEC V1.0C software, and built the coordinate system. In order to meet the research needs, we added the parallel bars as the 22 test points in Songjing Model (16 links, 21 joints). The original data was smoothed by low-pass filter with a cut off frequency of 6 Hz.

RESULTS AND DISCUSSIONS: In order to facilitate analysis the technical movement, this action can be divided into three stages by four events as follows (see figure 1).

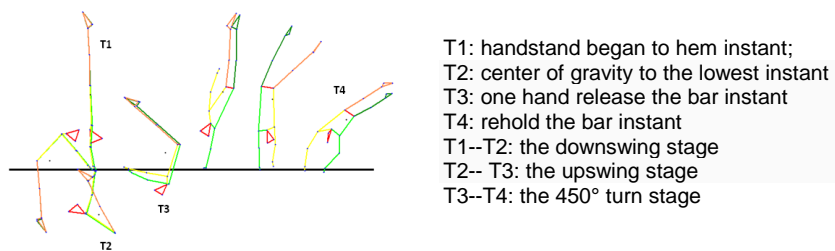


Figure 1: Schematic diagram of the stage division

The downswing stage: In the process of downswing, the shoulder angle first decreases, the minimum values of shoulder angle are 74.6 ° and 76.7 °, the hip angle and knee angle keep extension. Left hip angle is 174.5 ° and right hip angle is 173.7 °, left and right knee angle is 172.8 ° and 176.4 ° respectively. When the body center of gravity down to the horizontal plane, the horizontal distance from the body center of gravity to the bar is 0.57m. When the center of gravity down to the lowest position, the vertical distance from the body center of gravity and the holding point is 0.63 m, left and right shoulder angle are increased to 107.6 ° and 106.6 °, left

and right hip angle decreased to 26.8 ° and 31.1 °, knee angle decreases slightly, left and right knee angle are 170.6 ° and 171.2 °

To sink the shoulder Angle in order to increase the thick stick down force, its purpose is making thick stick down deformation, when the body upward movement can be done using the elastic potential energy of thick stick better behind the action. Due to the effect of gravity when the body to a vertical plane under bars, the speed center of gravity to the maximum 3.97 m/s. Handstand from the poles to the vertical plane under bars, run about 1.44 s, center of gravity hold rotate 180 °, the rotating angular velocity of 2.18 rad/s.

The upswing stage: When the body center of gravity close to the level before the bar surface, the shoulder angle are reduced to 92.1 ° and 93.8 °, left and right hip angle are increased to 85.9 ° and 87.2 °. The hip angle is too big, which shows the athlete hip extension too early, the range is too big, thus will affect the later twist action. The horizontal distance of the body center of gravity and the holding point is reduced to 0.47 m, 0.09m shorter than the bar after the horizontal surface of the body center of gravity and the holding point distance 0.56m. Body weight speed ratio under bars vertical surface velocity is up to 4.07m/s, which the vertical velocity to play the main role. When the body center of gravity around to the bar above the water level of about 23.1 °and 0.21m from the bar, the right hand released , left and right shoulder angle increased to 94.3 ° and 96.8 °, left and right hip angle increased to 116.1 ° and 117 °, left and right knee angle are 177.8 ° and 179.3°

The 450° turn stage: The body already has a 180° turn when the body center of gravity to the highest point, the left shoulder angle is 169.4 °, left and right hip angle are 168.1 ° and 164.3 °, left and right knee angle are 168.9 ° and 170.2 °, the height of center of gravity up to 0.979 m, the center of gravity speed is decreased to 0.71 m/ s, in the process of continue to complete the rest of 270 ° rotation, the body center of gravity does not fall on the supporting shaft, thus affected the handstand action. The left and right shoulder angle are 113.3 ° and 134.1 °, left and right hip angle are 163.1 ° and 174.2 °, left and right knee angle are 172.4 ° and 176.1 ° and the speed of body gravity is 2.01 m/ s.

CONCLUSION: According to the kinematics parameters from the three-dimension picture analysis, the athlete (Zhou) had completed the basket with 5/4 turn to handstand in the competition but the quality of the action needed to be improved. At the upswing stage, hip extension of the athlete is too early and exceeded, which makes a larger horizontal distance from the center of gravity to the supporting point when supporting by one arm, and this is the reason why the body has a lateral tilt.

REFERENCES:

J Yu, J Zhang.(2000). Artistic gymnastics advanced course, *Peoples Sports Publishing*.
XD Wang.(2009) Kinematic Analysis of Teng Haibin's Backward Giant Swing with twist 360° on Parallel Bars, *Journal of Beijing Sport University*,01.

Acknowledgement

This study is financed by China State Sports General Administration (Project No. 2014D015)

ACUTE EFFECTS OF FOREARM KINESIO TAPING ON MUSCLE STRENGTH AND FATIGUE IN HEALTHY TENNIS PLAYERS

Weijie Fu, Shen Zhang, Yu Liu

Key Laboratory of Exercise and Health Sciences of Ministry of Education,
Shanghai University of Sport, Shanghai, China

The aim of this study was to explore the acute effects of Kinesio taping (KT) applied over the wrist extensors and flexors on muscle strength and endurance. Fourteen participants completed 50 consecutive maximal concentric wrist extension and flexion repetitions at 60 °/s and 210 °/s in KT, placebo taping, and no taping conditions. There was no significant KT effect on the strength output (peak moment and peak / average power). KT reduced work fatigue and induced an increased regression of torque compared to no taping at 60 °/s. These findings provide preliminary evidences suggesting that KT may not be able to modulate strength production in healthy athletes immediately, but would have a significant positive effect on muscle fatigue resistance during repeated concentric muscle actions.

KEY WORDS: Kinesio taping, muscle strength, work fatigue, regression of torque

INTRODUCTION: In recent years, Kinesio taping (KT) has been widely applied in the prevention of various musculoskeletal conditions, especially in the fields of sports medicine and rehabilitation (Castro-Sanchez *et al.*, 2012; Griebert *et al.*, 2014). To date, the proposed mechanisms for the treatment of sports injuries and enhancement of performance with KT include 1) reducing inflammation and increasing range of motion by improving circulation of blood and lymph (Kase *et al.*, 1996; Yoshida & Kahanov, 2007), 2) relieving pain by decreasing the pressure on subcutaneous nociceptors (Adamczyk *et al.*, 2009; Álvarez-Álvarez *et al.*, 2014), 3) facilitating joint and muscle function by improving sensory feedback and muscle alignment / activation (Bassett *et al.*, 2010; Briem *et al.*, 2011). However, owing to the lack of clinical and experimental evidence, no clear scientific consensus has been reached yet with regard to the positive effect of KT on the improvement of athletic-based performance, especially on muscular strength and endurance.

The work by Fu *et al.* (2008) and Poon *et al.* (2014) suggested that KT does not enhance nor inhibit muscle strength during isokinetic knee extensions in healthy non-injured young athletes. These authors further suggested that previously reported muscle facilitatory effects using KT might be attributed to placebo effects. Moreover, a more recent meta-analysis showed that on average the application of KT to facilitate muscular contraction has no or only negligible effects on muscle strength (Williams *et al.*, 2012). There is, obviously, uncertainty concerning the beneficial effects of KT application for the improvement of muscular strength, and very few data are available in the literature regarding the effect of KT on continuous power outputs and endurance during repetitive exercise bouts, which further hinders our understanding of the potential mechanisms underlying KT effects (Beedie & Foad, 2009; Nakajima & Baldrige, 2013).

Based on the above observations, the purpose of this study was to examine the immediate effects of KT applied over the wrist extensors and flexors on muscle strength and endurance during isometric and isokinetic muscle actions at both low (60 °/s) and high (210 °/s) angular velocity. We hypothesized that a KT intervention would lead to an increase in wrist muscle strength as well as endurance performance.

METHODS: Fourteen trained male volunteers (age: 23.8 ± 1.4 years, height: 177.3 ± 4.0 cm, mass: 71.3 ± 6.5 kg) with a minimum of 3 years of experience in tennis events were recruited for this experiment. Three taping conditions were applied to each participant: 1) Kinesio taping (KT); 2) placebo taping (PT); 3) no taping (NT). The Kinesio Tex Tape (Kinesio Holding Company, Albuquerque, NM) was comprised of pure cotton fabric and waterborne

acrylic pressure-sensitive adhesives. The placebo tape was a common CaduMedi non-woven adhesive tape (T&G Healthcare Co. Ltd., China). The tapes were applied on the wrist flexors and extensors of the dominant arm.

Participants were asked to be in the laboratory on three separate days and complete strength testing in one of the three taping conditions, i.e., KT, PT, and NT, in each visit. During each visit, the participant was asked to complete two strength testing tasks using an isokinetic dynamometer (Contrex, PM1/MJ, CMV AG Corp., Switzerland). First, two sets of five seconds isometric MVCs of both the wrist extensors and flexors were measured at 0 ° angles of wrist extension. Subsequently, during the isokinetic testing session, participants performed one set of 50 consecutive maximal concentric wrist extensions and flexions at each of the two angular velocities (60 °/s and 210 °/s).

The variables for the wrist strength of the extensors and flexors normalized by body mass included 1) peak moment (PM, Nm/kg) during the isometric task; 2) peak moment (PM, Nm/kg), peak power (PP, W/kg), average power for the first five repetitions (AP, W/kg), and total work (TW, J/kg) during the isokinetic tasks. A work fatigue index (WF) and regression of torque (k) was chosen to reveal the decreasing trend of peak moment across the 50 repetitions and to evaluate the anti-fatigue ability of muscle during long duration tasks.

A 2 × 3 (velocity × condition) repeated measures analysis of variance (ANOVA) was used to examine the effects of the contraction velocities and taping conditions on muscle strength and fatigue performance. LSD post hoc tests were used to determine individual significant differences. The significant level was set at $\alpha = 0.05$.

RESULTS AND DISCUSSION:

Muscle strength: No significant differences were observed in peak moment of the wrist extensors and flexors among the KT, PT and NT during MVC trials. For the isokinetic strength testing, there were no significant differences in PM, AP, PP, and TW for both wrist extensors and flexors between the KT and NT conditions at both velocities (Table 1)

Table 1
The effect of Kinesio taping (KT), placebo taping (PT), and no taping (NT) on strength variables of wrist extensors and flexors during isokinetic muscle actions at 60 °/s and 210 °/s angular velocity.

Wrist muscles	Variables	60°/s			210°/s		
		KT	PT	NT	KT	PT	NT
EXT	PM (Nm/kg)	0.22±0.08	0.21±0.06	0.23±0.07	0.18±0.03	0.20±0.03	0.20±0.04
	AP (W/kg)	0.11±0.05	0.14±0.02	0.12±0.03	0.15±0.04	0.16±0.03	0.16±0.03
	PP (W/kg)	0.23±0.08	0.22±0.06	0.23±0.08	0.50±0.08	0.60±0.12	0.59±0.16
	TW (J/kg)	4.31±2.01	4.90±1.35	4.35±2.32	4.45±0.79	4.39±0.85	4.27±1.18
FLEX	PM (Nm/kg)	0.34±0.06	0.38±0.08	0.32±0.07	0.26±0.04	0.29±0.06	0.28±0.05
	AP (W/kg)	0.19±0.04	0.23±0.05	0.21±0.05	0.23±0.07	0.25±0.08	0.23±0.07
	PP (W/kg)	0.36±0.06	0.39±0.09	0.42±0.22	0.89±0.15	1.00±0.20	0.93±0.16
	TW (J/kg)	9.19±1.89	9.58±1.97	9.16±2.15	6.00±1.02	6.44±1.72	5.82±1.37

Note: EXT, wrist extensors; FLEX, wrist flexors; PM, peak moment normalized by body mass; AP, average power normalized by body mass; PP, peak power normalized by body mass; TW, total work normalized by body mass.

Work fatigue: At 60 °/s, KT showed a significant decrease in work fatigue (WF) of the wrist flexors compared to NT (Figure 1). No significant differences, however, were observed in the

wrist extensor WF among the three taping conditions. In addition, the WF of wrist muscles was not significantly different between the taping conditions at 210 °/s.

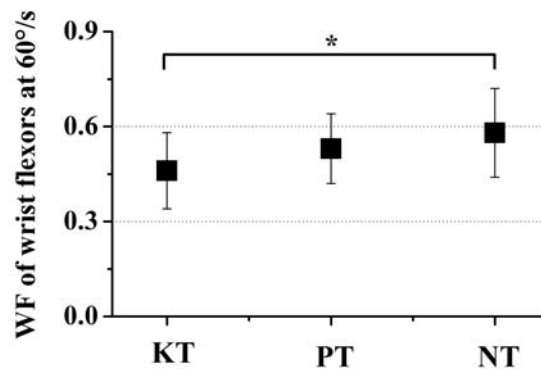


Figure 1: Effects of three taping conditions on work fatigue (WF) of the wrist flexors at 60 °/s.

Regression of torque: Compared to NT, a 19.98% increase was observed for KT in the slope of the curve k of the wrist flexors ($p < 0.01$) at 60 °/s (Figure 2). It is, however, noteworthy that the k in PT was also significantly higher compared to NT ($p < 0.05$). In addition, there was a trend for $k_{KT} > k_{PT} > k_{NT}$ in the wrist flexors at 210 °/s ($p < 0.1$). Meanwhile, for the wrist extensors, no significant taping effect was observed for the slope of the curve k at both velocities.

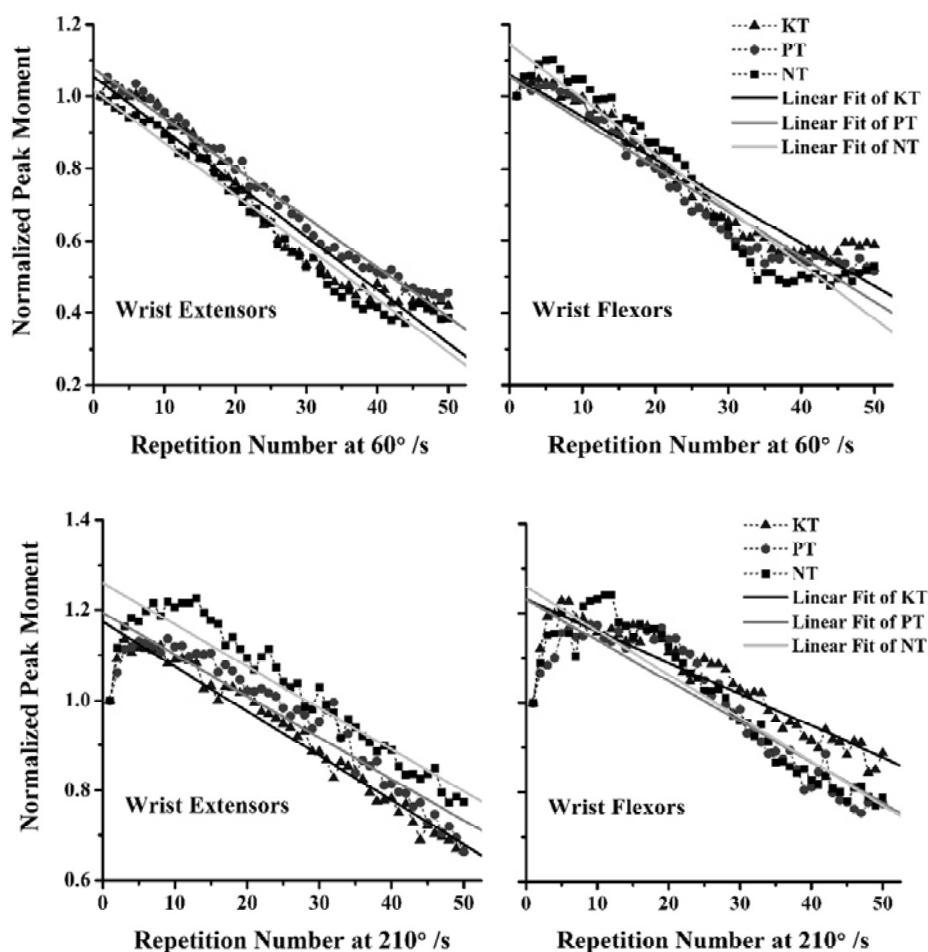


Figure 2: Effects of three taping conditions on the slope of the curve k of the wrist extensors and flexors at 60 °/s (upper) and 210 °/s (lower).

CONCLUSION: KT applied over the wrist extensors and flexors did not improve isometric and isokinetic strength, yielding no changes in normalized peak moment, peak power, average power, and total work. However, KT exerted on the wrist flexors reduced work fatigue and induced an increased regression of torque compared to no taping at 60 °/s. These findings provide preliminary evidences suggesting that KT may not be able to modulate strength production in healthy athletes immediately, but would have a significant positive effect on muscle fatigue resistance during repeated concentric muscle actions. Additionally, potential beneficial effects of PT on muscle endurance should not be ignored either.

REFERENCES:

- Adamczyk, A., Kiebzak, W., Wilk-Franczuk, M., & Sliwinski, Z. (2009). Effectiveness of holistic physiotherapy for low back pain. *Ortopedia, Traumatologia, Rehabilitacja*, 11, 562-576.
- Álvarez-Álvarez, S., José, F., Rodríguez-Fernández, A., Güeita-Rodríguez, J., & Waller, B. (2014). Effects of Kinesio® Tape in low back muscle fatigue: randomized, controlled, doubled-blinded clinical trial on healthy subjects. *Journal of Back and Musculoskeletal Rehabilitation*, 27, 203-212.
- Bassett, K. T., Lingman, S. A., & Ellis, R. F. (2010). The use and treatment efficacy of kinaesthetic taping for musculoskeletal conditions: a systematic review. *New Zealand Journal of Physiotherapy*, 38, 56-62.
- Beedie, C. J., & Foad, A. J. (2009). The placebo effect in sports performance: a brief review. *Sports Medicine*, 39, 313-329.
- Briem, K., Eythorsdottir, H., Magnúsdóttir, R. G., Palmarsson, R., Runarsdóttir, T., & Sveinsson, T. (2011). Effects of kinesio tape compared with nonelastic sports tape and the untaped ankle during a sudden inversion perturbation in male athletes. *The Journal of Orthopaedic and Sports Physical Therapy*, 41, 328-335.
- Castro-Sanchez, A. M., Lara-Palomo, I. C., Mataran-Penarrocha, G. A., Fernandez-Sanchez, M., Sanchez-Labraca, N., & Arroyo-Morales, M. (2012). Kinesio Taping reduces disability and pain slightly in chronic non-specific low back pain: a randomised trial. *Journal of Physiotherapy*, 58, 89-95.
- Fu, T. C., Wong, A. M., Pei, Y. C., Wu, K. P., Chou, S. W., & Lin, Y. C. (2008). Effect of Kinesio taping on muscle strength in athletes-a pilot study. *Journal of Science in Medicine and Sport*, 11, 198-201.
- Griebert, M., Needle, A., McConnell, J., & Kaminski, T. (2014). Lower-leg Kinesio tape reduces rate of loading in participants with medial tibial stress syndrome. *Physical Therapy in Sport*, 14, 2-9.
- Kase, K., Hashimoto, T., & Tomili, O. (1996). Development of kinesio-taping perfect manual. *Kinesiology Taping Association*, 117-118.
- Nakajima, M., & Baldrige, C. (2013). The effect of kinesio® tape on vertical jump and dynamic postural control. *International Journal of Sports Physical Therapy*, 8, 393-406.
- Poon, K., Li, S., Roper, M., Wong, M., Wong, O., & Cheung, R. (2014). Kinesiology tape does not facilitate muscle performance: A deceptive controlled trial. *Manual Therapy*, 14, 141-146.
- Williams, S., Whatman, C., Hume, P. A., & Sheerin, K. (2012). Kinesio taping in treatment and prevention of sports injuries: a meta-analysis of the evidence for its effectiveness. *Sports Medicine*, 42, 153-164.
- Yoshida, A., & Kahanov, L. (2007). The effect of kinesio taping on lower trunk range of motions. *Research in Sports Medicine*, 15, 103-112.

Acknowledgement

The authors would like to acknowledge supports for the study from the National Natural Science Foundation of China (11302131, 11372194), the Doctoral Fund of Ministry of Education of China (20123156120003), the Innovation Program of Shanghai Municipal Education Commission (14YZ125), and the Science and Technology Commission of Shanghai (14DZ1103500).

KINEMATICS ANALYSIS ON HANDSPRING SIDEWAYS STRETCHED SIDEWARD SOMERSAULT WITH 1 3/4 TURNS IN HORSE-VAULTING OF ZEPENG LUO

Xiuling Bian and Jihe Zhou

Chengdu Sport University, Chengdu, China

By using the 3D video analysis method, we have tested on the handspring sideways stretched side-ward somersault with 1 3/4 turns in Horse-vaulting (also known as Kasamatsu 360°) of Chinese elite athletes Zepeng Luo at the game site; obtain the relevant kinematics' parameters through analysis on the complete movement. The results show that: Zepeng Luo completed this action with high quality and advanced technology, but at the first flight, his legs were not fully close together.

KEYWORDS: horse-vaulting, Kasamatsu 360°, kinematics analysis.

INTRODUCTION: Horse-vaulting is one of advantage projects of China men's gymnastics team. The paper aims to use the three-dimension video to analyse the technology of Zepeng Luo at the game site of the 12th national games in 2013, and then get the kinematics parameters and summarize his skill features, so as to provide reference for the technical training of coaches and athletes.

METHODS: The main method is three-dimension video analyse. The whole process of the competition was recorded by two JVC cameras at 50 Hz from different angles (the angle of the two cameras was about 90°) (Figure1). And shooting frequency is 50 frames per second. The record analysis used 3-D SignalTec system and series analysis. We use Japanese Songjingxiuzhi phantom as the anthropometric dummy (22 articulation points, 16 segments). It passed the original data filter and the cut off frequency is 8 Hz. .

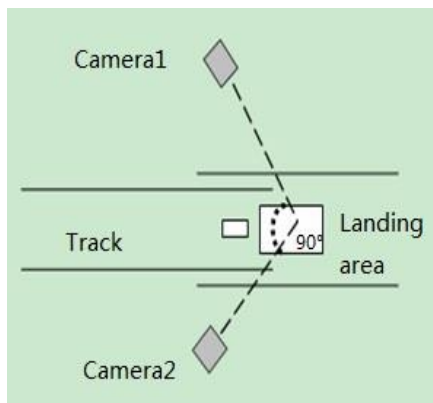


Figure1: Schematic diagram of cameras



Figure2: Game site photo

RESULTS AND DISCUSSION: In order to facilitate the analysis of the data, we divided the whole movement into four stages.

The run-up and pedal stage: In the run-up process (before feet touch the pedal) ,the flight height is 13cm, the maximum instantaneous horizontal velocity is 6.93 m/s, which can completely satisfy the needed to complete the action.

**Table1
Pedal stage kinematics parameters**

	Touch pedal moment	Leave pedal moment
horizontal velocity of cg (m/s)	6.01	4.42
vertical velocity of cg (m/s)	-0.52	3.13
shoulder Angle (°)	99	137
Hip angle (°)	119	146
knee angle (°)	153	175
ankle angle (°)	115	114
Pedal angle (°)	64	80

*cg: Body centre of gravity

Pedal angle: centre of gravity and foot-touching point connection with the horizontal angle

Pedal makes full preparations to get enough energy and it is the key technologies to complete the movement in the first flight (Wen, 2012). The jumping time is very short as 0.08 s. As seen from Table 1, during the pedal stage, horizontal velocity of cg decreased, but vertical velocity of cg increased significantly .this is because it is a brake take-off. This ensures the body to continue to move forward, and obtained a certain turnover speed.

The first flight and push hands stage: First flight time is 0.11s, horizontal velocity of cg is 3.97s, and vertical velocity of cg is 3.35s. Zepeng Luo's adnominal muscle tensioned, hip bent slightly before food leave the pedal. This will not only avoid reducing force transfer and can stretch the back muscles to help accelerate the legs swing. When he touching the horse, his left foot speed reached 8.37 m / s, right foot speed reached 10.57m/s. foot speed is not the same, indicates that the air control is not very good, his legs are not closed together. This is not allowed.

**Table2
Push hands stage kinematics parameters**

	Touch vaulting horse moment	Leave vaulting horse moment
horizontal velocity of cg (m/s)	3.75	3.18
vertical velocity of cg (m/s)	3.20	3.01
shoulder angle(°)	123	155
elbow angle (°)	100	160
hip angle (°)	140	162
foot speed(m/s)	8.58	11.34
horse angle (°)	43	80

*horse angle: Center of gravity and hand-touching point connection with the horizontal angle

After entering the first flight, it needs to turn 90° as quickly as possible. When the first hand touches the horse, elbow bend, this is the technical requirements of the operation.

The main purpose is to speed up the body's turn (Wen, 1989). The time of push hands stage is 0.23s, horse angle is 43°. The height of the centre of gravity from the vaulting horse is 50 cm. According to the mechanics principle, the higher the position of the centre of gravity is the better for hand pushing and second flight. Form Table 2, horizontal velocity of cg decreased, but vertical velocity of cg increased, the same as the first stage, it is a brake take-off.

The Second flight stage:

Table 3
Second flight kinematics parameters

The highest point of the centre of gravity				Flight time (s)	horizontal axis flip angular velocity (m/s)	Vertical axis flip angular velocity (m/s)
horizontal velocity (m/s)	vertical velocity (m/s)	distance from ground (m)	distance from vaulting horse (m)			
3.02	0.11	2.81	1.39	0.98	7.99	14.36

Table 3 shows the highest point of the centre of gravity distance from ground is 2.81m. Flight time is 0.98 s. All of these made a good preparation for landing stage.

Zepeng Luo turned left immediately after pushing away the horse, swivel power depends mainly on the head, shoulders, and arms hold flexing, driven to the chest to reduce the body vertical axis radius. According to the momentum conservation theorem ($K=mr^2\omega$). Radius is inversely proportional to the rotating angular velocity (Wen, & Li, 2004).

Near turn over 630 degrees, the hip angle reduces gradually, the arms move to the side of the body, The purposes have 3: one is to increase body vertical axis radius, reduce the rotating angular velocity; second is to reduce the horizontal axis rotation radius, to speed up the turnover velocity of the body; tree is to be prepared for the landing.

Landing stage: Landing is quite steady. It is illustrated that the landing process in accordance with the laws of mechanics and basic requirements. The landing angle is 58°, if the landing angle too large or too small, it will make the rotating torque and braking torque out of balance, causing the landing instability. Fall to the ground instantly, knee and ankle joints extended as far as possible, this helped to prolong the buffer time and reduce the impact force (Xu, 2001).

CONCLUSION: Zepeng Luo completed this action with high quality and advanced technology, but at the first flight, his legs were not fully close together.

1. At the run-up and pedal stage, the flight height is 13cm; the maximum instantaneous horizontal velocity is 6.93 m/s, which can completely satisfy the needed to complete the action. Pedal makes full preparations to get enough energy and it is the key technologies to complete the movement in the first flight.

2. First flight time is 0.11s, horizontal velocity of cg is 3.97s, and vertical velocity of cg is 3.35s. After entering the first flight, it needs to turn 90 ° as quickly as possible. When he touching the horse, the left and right foot speed is not the same, indicates that the air control is not very good, his legs are not closed together. This is not allowed.

3. At the Second flight stage, highest point of the centre of gravity distance from ground is 2.81m. Flight time is 0.98 s. All of these made good preparations for landing stage.

4. Landing is quite steady. The landing angle is 58°. Fall to the ground instantly, knee and ankle joints extended as far as possible, this helped to prolong the buffer time and reduce the impact force.

REFERENCES:

Wen, Y. X. (2012). Vaulting technique and modern teaching and training. *Journal of Beijing Sports University*, 40-60.

Wen, Y. X. (1989). Kinematics Analysis on Handspring Sideways Stretched Side-ward Somersault with 1 3/4 turns in Horse-vaulting of Ning Li. *China Sport Science and Technology*, 12, 21-30.

Wen, Y. X. & Li, J. (2004). Kinematics Analysis on Handspring Sideways Stretched Side-ward Somersault with 2 1/4 turns in Horse-vaulting of Aowei Xing. *Journal of Beijing University of Physical Education*, 1.

Xu, W. (2001). Kinematics Analysis on vaulting hand-side of the body 90°flip two and a half somersault tuck movement. *Sports Science*, 21 (4), 28-31.

DOSE FASTER HOPPING FREQUENCY IMPROVE RESPONSE TIME AND KICKING SPEED IN TAEKWONDO ROUNDHOUSE KICK?

Young-Kwan Kim, Hwi-Jung Jung and Ji-Yong Joo

Dept. of Physical Education, Chonnam National University, Gwangju, S. Korea

The purpose of this study was to investigate the effect of rhythmic hopping frequency on the response time and kicking speeds in Taekwondo roundhouse kick. Eleven elementary and middle-school athletes voluntarily participated in this study. They performed five roundhouse kicks at three different hopping frequencies (normal, 15% faster than normal, and 15% slower than normal) and no hop condition. Results indicated that the 15% slower hopping frequency induced a significantly longer response time than the 15% faster frequency. The 15% faster frequency resulted in faster maximum kicking speed than normal frequency did, while there was no difference in contact kicking speed. Partially the faster hopping frequency would be beneficial to kicking performance.

KEY WORDS: Taekwondo, roundhouse kick, response time, kicking speed, hopping, rhythm.

INTRODUCTION: Taekwondo sparring requires rapid response to an external stimulus and fast kicking velocity for winning a competition. This is because a shorter response time would increase the chance of successful kick and a faster kicking velocity may allow a kicker to give a strong impulse on an opponent.

In Taekwondo sparring most athletes practically use rhythmic hop as a preparatory motion while they are waiting for attacks and dodging in response to an opponent's action. Rhythmic hop consists of repetitive flexion and extension of ankle, knee, and hip joints simultaneously in place at a certain rhythm. Since rhythmic hop mechanically induces a prestretch potentiation of leg muscles (Aura & Komi, 1986; Bosco, Komi, & Ito, 1981) and functional stretch reflex (Melvill-Jones & Watt, 1971) in stretch-shortening cycle, it could be considered to affect the quality of the kicking movement to a certain extent.

Kim and Kim (2014) found that the rhythmic hop did not affect response time statistically but improved the kicking velocity significantly than no hop did. In addition, different instants of detecting an external stimulus in rhythmic hop for the back kick showed significantly different response times. They concluded that rhythmic hop is recommendable for the purpose of kicking velocity, but not for the purpose of response time.

However, there was no study on the effect of different hopping frequency deviated from normal hopping frequency on the kicking performance. Therefore, the purpose of this study was to investigate whether the change in hopping frequency from normal frequency affects the response time and kicking speed in Taekwondo.

METHODS: Eleven Taekwondo athletes consisting of five male athletes and six female athletes (age, 14.4 ± 1.4 years; mass, 43.5 ± 7.8 kg; height, 1.55 ± 0.07 m) voluntarily participated in this study. All of the participants have been practicing Taekwondo for more than four years and all have black belts of the 2nd Dan and above. Prior to experiment, the purpose and procedure of this study was explained to subjects. All subjects signed a consent form according to the rule of institutional review board (IRB) of the university.

Once subjects came to the laboratory, a sufficient time of stretching and warm-up was allowed. When they were ready for an experiment, nineteen reflective markers were placed on major anatomical positions of both legs. After capturing static posture, medial markers (knee and ankle) and toe markers (2nd and 5th metatarsophalangeal joints) were removed to facilitate the kicking motion. The virtual marker of toe was established by the mid-point of the medial and lateral markers (2nd and 5th metatarsophalangeal joints).

Motion capturing system, consisting of five CCD cameras (Osprey®, Motion Analysis Corp., Santa Rosa, CA, USA) with sampling rate of 200 Hz, was used to capture the trajectories of

reflective markers. A metronome (YCMTM-2000, Yongchang, Seoul, Korea) was used to set the rhythm of a designated hopping frequency. A hand-held pad (Adist 04, Adidas, Seoul, Korea), having one reflective marker on it, was used as the target. Movement of the marker was used to determine the onset of foot contact to the target. A force-plate (BP400600, AMTI®, Watertown, MA, USA) was used to determine the moment of the toe-off of kicking leg. An assistant held the target with one hand, and with the other hand, held a custom-made red light-emitting diode (LED) close to the target (Figure 1). A custom-made LED was designed to be a trigger for the participants to detect a cue signal for kicking (an external stimulus) and was synchronized with the motion data by the help of analog-to-digital board (NI USB 6525, National Instruments, Austin, TX, USA). The height of the target was adjusted according to the abdominal level of the participant and the distance of the target was the comfortable distance of each subject.



Figure 1: Experimental set-up for kicking task.

First, normal hopping frequency was determined by a preferred hopping frequency for 20 second. Each subject performed three trials of a 20-second natural hopping and the mean value of three trials was calculated as normal hopping frequency. Then a 15% faster and a 15% slower hopping frequencies than normal hopping were defined as faster and slower conditions of hopping frequency.

Each subject performed five trials of roundhouse kick as fast as possible immediately after seeing a LED blinking at four different conditions (normal, 15% faster, 15% slower, and no hop), respectively. The order of kicking conditions was decided by the counter-balanced design.

The response time was defined as the time interval from the onset of a LED blinking to foot contact to a target. It was divided into ground contact time (a LED blinking to toe-off) and kicking time (a toe-off to foot contact to a target). There were two kicking speed definitions. The maximum kicking speed was the maximum value of resultant linear velocity of the toe and the contact speed was the toe linear velocity at the moment of the contact. One-way repeated measures ANOVA was used to find statistical difference between conditions and performed in SPSS® 18.0. The significant level was set as .05.

RESULTS: The normal hopping frequency of all subjects was 2.87 ± 0.21 Hz. There was no main effect of change in hopping frequency on the response time, ground time, and kicking time (Table1). There was a significant difference on response time between 15% faster frequency (0.762 ± 0.056 s) and 15% slower frequency (0.808 ± 0.079 s). The slower hopping frequency was the longer response time of kicking except no hopping condition. The faster and slower hopping frequencies had same ground times but the faster hopping frequency induced a shorter kicking time than the slower hopping frequency.

Figure 2 indicates the change in maximum kicking speed and contact kicking speed according to changes in hopping frequency. There was no main effect of hopping frequency on maximum kicking speed and contact kicking speed. However, the 15% faster hopping frequency (9.43 ± 1.65 m/s) induced significantly faster maximum kicking speed than the 15% slower hopping frequency (9.12 ± 1.52 m/s) did ($p < .05$). The contact kicking speed was ranged from 6.0 m/s to 6.34 m/s, which was slower than the maximum kicking speed. The contact kicking speed of faster frequency (6.34 ± 1.32 m/s) was faster than that of normal frequency (6.13 ± 1.02 m/s) but it was no significance statistically.

Table 1
Response Time, Ground Time, and Kicking Time According to Change in Hopping Frequency
 (unit: second)

Frequency	Response Time		Ground Time		Kicking Time	
	M	SD	M	SD	M	SD
15% Faster	0.762*	0.056	0.222	0.075	0.542	0.111
Normal	0.800	0.099	0.200	0.040	0.605	0.130
15% Slower	0.808*	0.079	0.222	0.020	0.588	0.067
No Hop	0.768	0.050	0.227	0.023	0.545	0.038

* indicates significant difference between two groups ($p < .05$).

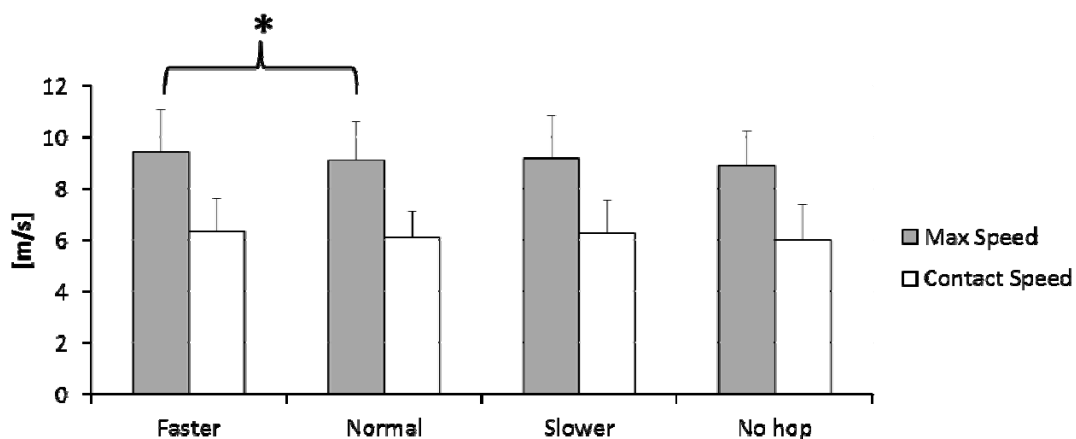


Figure 2: Comparison of maximum kicking speed and contact speed according to hopping frequency. * indicates significant difference between two groups ($p < .05$).

DISCUSSION: Almost athletes habitually perform rhythmical hopping as preparatory motions in Taekwondo sparring. Rhythmic hop was purposed to be ready for next movements such as attacking an opponent and dodging opponent's attack with controlling breathing and rhythm. However, the biomechanical effect of rhythmic hop was not well known to people. This study investigated the effect of hopping frequency on kicking performance.

Results demonstrated that there was no main effect of hopping frequency but there were significant differences between two groups for a couple of comparisons. The 15% faster hopping frequency reduced response time significantly than the 15% slower hopping frequency. All hopping conditions revealed no difference in response time statistically in comparison with no hop condition, which was agreed with Kim and Kim (2014) study.

Kim and Kim (2014) insisted that the rhythmic hop has advantage in kicking speed. This study demonstrated only difference in maximum kicking speed between 15% faster hopping and normal hopping frequencies. Biomechanically the rhythmic hop produced continuous fluctuations of centre of mass (CM) of a subject, which induced a certain level of mechanical energy (i.e., the sum of kinetic energy and potential energy). The faster hopping frequency

having higher level of mechanical energy would be beneficial to enhance the maximum kicking speed with utilizing a high level of mechanical energy.

The rhythmic hop stimulates the stretch-shortening cycle of elastic component of muscles continuously (Aura & Komi, 1986; Bosco et al., 1981), which utilizes the stored elastic energy of muscles. Farley, Blickhan, Saito and Taylor (1991) investigated the variation of hopping frequency on a treadmill and in place and found different results between the higher frequency and the lower frequency than preferred hopping frequency. In this study, the faster hopping frequency tends to reduce a response time and to induce faster maximum kicking speed such a simple spring-mass system. The slower hopping frequency, however, showed disadvantage in response time. This would be because of the improper utilization of storage and recovery of elastic energy in optimizing the cost of generating muscular force (Blickhan et al., 1991). The optimal hopping frequency for maximizing kicking performance might not be the preferred hopping frequency (normal hopping frequency) but the normal hopping frequency would be the point minimizing the cost of generating muscular force in order to keep longer durations of hopping motions in Taekwondo sparring.

There are a couple of limitations in this study. The number of subject (eleven subjects) would not be sufficient to find strong statistical power so that more subject across diverse levels of skilled athletes are required to induce a general conclusion. In addition, elite adult athletes are required to verify this results in future study.

CONCLUSION: This study identified the effect of hopping frequency on kicking performance in Taekwondo sparring. Results indicated that the 15% faster hopping frequency than normal frequency (i.e., preferred frequency) would be beneficial to maximum kicking speed. The 15% slower hopping frequency would deteriorate the response time in comparison with the faster hopping. Coaches should remember followings in sparring. In order to enhance athlete's kicking speed, an athlete should increase his/her hopping frequency than preferred normal frequency. And coaches carefully watch the rhythm of hopping of an athlete and should not let his/her hopping frequency down below his/her normal hopping frequency because of slower response to an external stimulus.

REFERENCES:

- Aura, O., & Komi, P. V. (1986). Effects of prestretch intensity on mechanical efficiency of positive work and on elastic behavior of skeletal muscle in stretch-shortening cycle. *International Journal of Sport and Medicine*, 7, 137-143.
- Bosco, C., Komi, P. V., & Ito, A. (1981). Prestretch potentiation of human skeletal muscle during ballistic movement. *Acta Physiologica Scandinavia*, 111, 135-140.
- Farley, C. T., Blickhan, R., Saito, J., & Taylor, C. R. (1991). Hopping frequency in humans: a test of how springs set stride frequency in bouncing gaits. *Journal of Applied Physiology*, 71, 2127-2132.
- Kim, Y.-K., & Kim, Y.-H. (2014). Effects of rhythmic hop on response times and kicking velocities. *Korean Journal of Sports Biomechanics*, 24, 367-373.
- Melvill-Jones, G., & Watt, D. G. D. (1971). Observation on the control of stepping and hopping movements in man. *Journal of Physiology*, 219, 709-727.

Acknowledgement

This research project was supported by the Sports Promotion Fund of Seoul Olympic Sports Promotion Foundation from Ministry of Culture, Sports and Tourism.

STUDY ON THE INFLUENCE OF CHANGES OF AIR RESISTANCE ATHLETES' TAKING-OFF SPEED IN FREESTYLE SKIING AERIALS

Zhao Le¹, Ma Yi² and Wang Xin³

Graduate School, Shenyang Sport University, Shenyang, China ¹

Shenyang Sport University, Shenyang, China ²

Sport Science College, Shenyang Sport University, Shenyang, China³

Freestyle skiing is a competitive sport in the open-air environment. The air resistance that athlete meets in the process of slipping, transition and entering stage determines the athletes' taking-off speed, thus affecting the performance in competition. This paper set up a function model of frontal area and time about L, T, F, DF, F and other single action in the process completed, and establishes the function between windward area and time in specific action. It studies and analyses the influence of air resistance on athlete's taking-off speed, combining with the results of the taking-off speed calculation software. The main findings are shown as follows: When the wind speed each increases 0.8 m/s in the leaving platform phase, athlete's taking-off speed will decrease 0.4m/s. When the wind speed is low, the change of wind direction exerts little impact on athletes' taking-off speed.

KEY WORDS: research, reverse modelling, three-dimensional solid model, the finite element method, the flow field model, calculation software

INTRODUCTION: Our country began to carry out the project of Freestyle Skiing Aerials from 80's in 20th Century. Because main outstanding skills, flexibility and agility in the project are in line with its motion characteristics and physical characteristics of Chinese, the Freestyle Skiing Aerials has become an important breakthrough of Chinese players in the Winter Olympics gold medal of the project on the snow. The air resistance is affected by the change of the frontal area, changed with the change of posture when athletes pedal to accelerate in the different positions on slope. So we should consider the changes of players sliding posture and sliding speed when we calculate the air resistance. Finally, we researched and analysed the influence of air resistance on athlete's taking-off speed by simulating the air resistance, established a mathematical equation, and got the function of the change of air resistance in sliding process.

METHODS: In this study, we chose the Freestyle Skiing Aerials athletes of China as the research objects. According to the theory of reverse modeling, we established a three-dimensional solid model player (athletes' surface is divided into 87 seamless patches) by small plane modeling, repaired the arrancar and entity processes^[1-2] in 3D virtual design software. Geomagic Studio with more than 200,000 points cloud data generated by our outstanding freestyle athletes used 3D laser scanner (3D body scanner in Beijing Sport University --Anthroscan 3D VITUS), as shown in figure 2. Adopting the module insert/merge and inherited functions of 3D virtual design in pro/ENGINEER, established the flow field around the space model of athletes, as shown in figure 3. Finally, Import into the Adina software to calculate resistance of air and lift by using the established flow field around the space model of players.

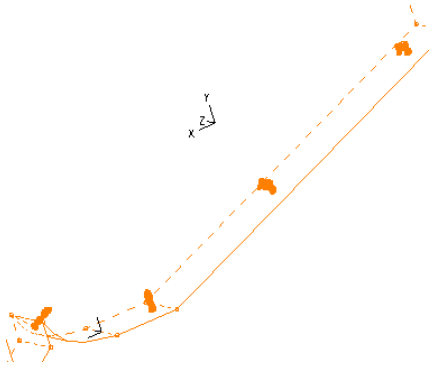


Figure 1: The flow around space model in the sliding process



Figure 2: 3D entity model of in the curve segments

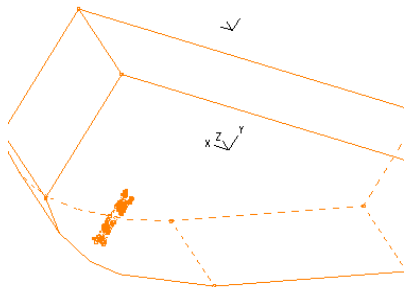


Figure 3: The flow field around the space model curve

RESULTS: Effect of air on freestyle players' action effect is huge. Air resistance of athletes is resultant of forces by force of pressure and friction. It can calculate by solving the flow field of the athletes. The control equation of the flow field around a player is the turbulence model^[3,4]. The finite element method^[5] is used to solve the governing equation. The established flow field space model mesh rezoning (divided into more than 80,000 units), as shown in figure 4. Considering the large velocity gradient in the relatively of boundary layer closed to the surface of the athletes and complex surface of athletes, The grid division of the surface on athletes is specially thickened, as shown in figure 5. The surface of athletes and snow road were defined as the wall in the calculation (athletes surface as the moving wall). And the rest of the surfaces were open surface. In this study, supposed the game environment temperature is -20°C (density and dynamic viscosity of air are 1.395kg/m^3 , $1.62 \times 10^{-5}\text{Pa}\cdot\text{s}$).

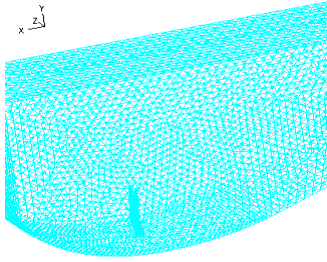


Figure 4: Mesh of the space model in flow field

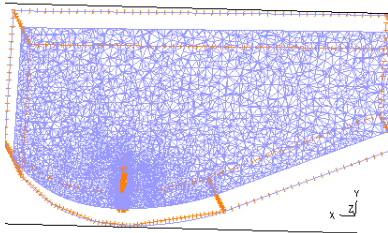


Figure 5: Thicken mesh of athletes' surface

Through the calculation, this paper has obtained the influence of taking-off speed by wind speed and direction against the wind. The results are shown in figure 6 and figure 7.

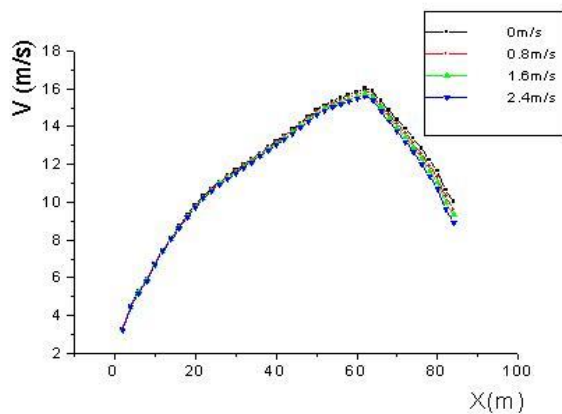


Figure 6: Effect of taking-off speed by different wind speed

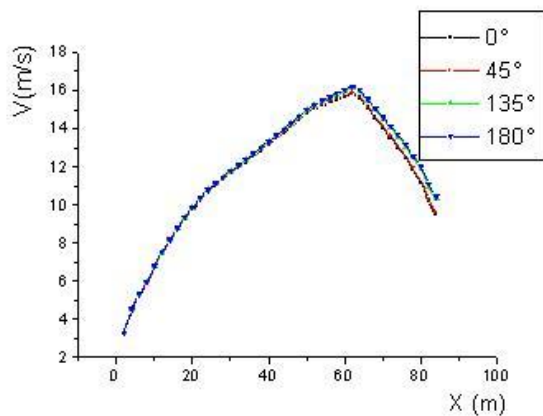


Figure 7: The impact of changes in wind direction on taking-off speed (wind speed is 0.8m/s)

DISCUSSION: Considering the influence of wind on the taking-off speed, the first one is the effect of wind speed. When wind speed is higher, it will exert more influences. The second one is the direction of the wind. The speed increases with the wind, and the speed slows down against the wind. In order to increase the realization of the model, in the study wind direction is set as 0 degree, 180 degree, 45 degree and 135 degree respectively. In accordance with the international customs of the game, when the wind speed is too high, the game will be stopped. In order to ensure the safety of athletes, the wind speed is set as 0--3m/s.

As can be seen from Fig. 6, the taking-off speed will reduce with the each increase of wind speed. When the wind speed each increases 0.8m/s in the leaving platform phase , the taking-off speed will reduce 0.4m/s.

As can be seen from Fig. 7, the influence of changes of wind direction on taking-off speed is small when the wind speed is low. But when the wind speed increases, the influence will increase.

CONCLUSION: The taking-off speed will reduce with the increase of wind speed. When the speed of increases by 0.8m/s, the taking-off speed will reduce 0.4m/s compared with the windless condition. The influence of changes in wind direction on taking-off speed is small when the wind speed is low. But when the wind speed increases, the influence will increase. In the game, we can compensate the influence of wind speed by increasing 10m sliding distance or squat speed.

REFERENCES:

- Dong Xiujun. 3D laser scanning technology and its application in engineering [D]. Chengdu: *Chengdu University of Technology*, 2007.
- J.H.Hart, T.Allen, M.Holroyd. Downhill skateboard aero dynamics[J]. *Procedia Engineering*, 2010, 2 (2): 2523-2528.
- Lei Yansheng, Zhou Zhenggui. Wind turbine oscillating airfoil dynamic stall characteristics of CFD of [J]. *Solar Sinica*, 2010, 31 (3): 367 ~ 372
- Zhang Benzhaoh, Yin Jianan, Zhang Hongji. Numerical method of fluid mechanics [M]. *Machinery Industry Press*, 2003 June: 1 ~ 246.
- Zhou Yu, the money Weiqi, Deng Youqi, Ma Ming. The parameters of SST two equation turbulence model in the preliminary analysis of the aerodynamic effect [J]. *Journal*, 2010, 28 (2): 213 ~ 217.

Acknowledgement

This work was financially supported by the National Natural Science Foundation (11102120) a the Higher School Project supported by Doctoral Research Fund (20090042110003, 20120042120031).

KINEMATICAL ANALYSIS OF FOREHAND STROKE TECHNIQUE OF EXCELLENT WOMEN'S TENNIS PLAYER SHARAPOVA

Zuqing Li, Shuai Wang, Jun Guo, Jihe Zhou

Chengdu Sport University , Chengdu, Sichuan Province, China

Forehand stroke is one of the most important and basic tennis techniques, with the highest rate of utilization. Good forehand stroke technique may serve as a powerful offensive weapon for a player, it can have a profound impact on the tennis game result and lay a solid foundation for learning other tennis techniques. In virtue of three-dimensional photograph analytical method, this research presents a kinematical analysis on key links of forehand stroke technique by Maria Sharapova, the champion of women's singles in 2014 China Open, so as to obtain kinematical parameters of forehand stroke technique by the world excellent women's tennis player, reveal kinematics characteristics of forehand stroke technique and offer theoretical instructions to coaches and athletes for proper understanding and mastery of such a technique during training.

KEY WORDS: Tennis, Forehand stroke, Kinematical analysis.

INTRODUCTION: Tennis is a highly technical sport event. To some extent, forehand stroke technique is one of the most important tennis techniques and can be regarded as the very life of each tennis player. The power of forehand stroke lies in reasonability of technical actions and its outstanding and distinct technique style (Yanming et al., 2014). So it is of great importance for a tennis player to improve his or her technical actions; while reasonable actions must be subject to sports biomechanical principle of a stroke, which is a key factor determining the level of tennis forehand stroke. As a result, it is especially significant to take kinematical analyses on key links in forehand stroke technique of a tennis player (Huifang 2014). Accordingly, three-dimensional photograph analytic method in this paper is adopted to carry out a kinematical analysis of key links in forehand stroke technique of the world excellent women's tennis player Sharapova, in order to understand and master kinematical characteristics and parameters of her forehand stroke technique and provide theoretical bases for tennis players in improving their forehand stroke techniques.

METHODS: three-dimensional photograph analysis. 2014 China Open employed two made-in-Japan JVC9800 cameras (shooting frequency:50fps at a constant speed) in the form of three-dimensional fixed point to shoot the entire forehand stroke of Sharapova from different angles, with No.1 camera right behind the side line of the tennis court, No.2 camera right in front of the base line, showing an included angle of about 95° between main optical axes of the two cameras. Both of the cameras were arranged in the right serve court of the athlete, where 24 control points were placed to demarcate the space in a three-dimension scale so that entire action of the athlete were kept within the frame. To ensure the reliability of analytic data and dotting accuracy of the frame during analysis, staff members moved horizontally or rotated the frame before formal shooting according to the locations of two cameras so as to reduce any unnecessary error due to overlapping of individual poles.

To facilitate the synchronization of camera starting points, the selected videos were cut at first by Boilsoft Video Cutter which was cutting software, and then imported into star high titanium 3-D Signal TEC V3.2HDC analysis system developed by Beijing Senmiaoxing Science and Technological Development Co., Ltd, so as to analyze the shot videos via such steps as spatial model, space demarcation, video analysis, calculation and so forth, with available original data processed smoothly by low-pass digital filtering method and cutting frequency up to 8Hz. When defining the synchronization point, the starting point was pushed 5 frames forward while the end point 5 frames backward in the premise that characteristic pictures had been determined in order to reduce the smooth filtering processing error.

RESULTS AND DISCUSSION: (1) Backswing: at the end of backswing, Sharapova made her left and right hip angles of 158.8° and 142.2° respectively, left and right knee angles of 149.8° and 135.7°, left and right shoulder angels of 43.3° and 106.6°, left and right elbow angles of 158.2° and 127.8°, and the angle between racket and her arm up to 116.9°. During the backswing, the speeds of her right shoulder, right elbow, right wrist joint, racket head and center of gravity were 0.53m/s, 1.65m/s, 2.04m/s, 8.98m/s and 1.12 m/s respectively.

Table 1
Analysis of Joint Angle Parameters of Sharapova at the End of Backswing

Name	Angle
Left hip angle	158.8°
Right hip angle	142.2°
Left knee angle	149.8°
Right knee angle	135.7°
Left shoulder angle	43.3°
Right shoulder angle	106.6°
Left elbow angle	158.2°
Right elbow angle	127.8°
Angle between racket and arm	116.9°
Angle between shoulder and hip	62.5°

analyses on kinematical parameters above show that: Sharapova made a comparatively sufficient body turning during backswing, in which main muscle group participating in the stroke stretched in advance. At the end of the backswing, both her hip joint and knee joint were flexed so that the center of body weight lowered (Jifang et al., 2013). Shoulder joint and elbow joint angles can reflect the extension state of racket and the arm relative to the trunk of an athlete at the end of backswing. Sharapova swung back the racket farther away from her trunk to lengthen the distance of body work and improve the effect of a stroke. Keeping arm joints at a certain speed, and the wrist joint and racket head at a faster speed at the end of backswing will benefit the generation of faster racket head speed at the moment of stroke (Jian 2009).

(2) Racket swinging at the ball: Sharapova made the horizontal shoulder-hip projected angle of 62.5° at the end of backswing and 16.1° at the moment of stroke, with a rotation

of 46.4° at the angle between shoulder and hip. It took 0.18s from the end of the backswing to the moment when the ball touched the racket. At the moment of touch, left and right knee joint angles were 155.4° and 161.5° respectively, left and right hip joint angles of 163.2° and 174.6°, right shoulder joint angle of 38.9°, right elbow joint angle of 142.1° and the angle between racket and the arm up to 132.3°. While, at the moment of stroke, the speeds of Sharapova's right shoulder, right elbow, right wrist, right hand joint and racket hand were 1.84m/s, 3.28m/s, 5.06m/s, 6.02m/s and 17.56 m/s respectively.

Table 2
Analysis of Joint Angle Parameters of Sharapova at the Moment of Touch

Name	Angle
Left hip angle	163.2°
Right hip angle	174.6°
Left knee angle	155.4°
Right knee angle	161.5°
Right shoulder angle	38.9°
Right elbow angle	142.1°
Angle between racket and arm	132.3°
Angle between shoulder and hip	16.1°

During swinging the racket at the tennis ball, a player should employ a full shoulder and hip turning and his or her lower legs should extend towards the ground forcefully, with shoulder joint as axis so that the swinging of the upper arm drives the lower arm which drives the wrist, namely the arm holding the racket delivers force successively (Wenlin et al., 2012). Kinematical parameters obtained from racket swinging at the tennis ball, Sharapova could make a full shoulder and hip turning and keep a certain center of body weight and reasonable shoulder & elbow joint angles, which would play an important role in giving a fast and powerful forehand stroke. Due to shorter time for swinging the racket at the ball, the right elbow joint angle increased gradually and the speed of joints of the arm holding the racket from near side to far side of her body had a gradual progressive increase, with racket head, hand and wrist joint speeds reaching the maximum. During the stroke, thereout, Sharapova moved smoothly at a heat. The inward turning of Sharapova's elbow joint drove the joggling of her wrist so as to generate more spins of the ball and improve the stability of stroke while she swung at the ball forward (Marchar et al., 2013).

(3) Follow-through: at the end of follow-through, Sharapova's speeds for her center of body weight (V_x , V_y and V_z) were 0.04 m/s, 0.36 m/s and 0.56m/s respectively, with her left and right shoulder angles of 43.1° and 112.8° as well as left and right elbow angles of 45.2° and 91.8°. A follow-through action is the continuity of a racket-swinging action and plays an important role in keeping integrity and consistency of a stroke, improving the stroke effect of the stroke and preventing any injury (Rogowski et al., 2011). Sharapova maintained her body balanced throughout the follow-through, with her trunk and all links at a good rotating speed and a satisfactory buffering effect. The change in shoulder and elbow joint angles indicated that Sharapova significantly lifted

her elbow and swung her arm forward during the follow-through to prolong the action time of the racket to the ball, resulting in a fast and powerful stroke with a fast spin .

CONCLUSION: In conclusion, forehand stroke technique of Sharapova in stages ranging from backswing, racket swinging at the racket to follow-through conforms to the theory of sports biomechanical principle. Actions, including shoulder turning and body inclining for preparing a stroke and completing the stroke, are smooth and extended comparatively, with stroke technique being reasonable and normative. Her kinematical technical parameters at each stage are worth of learning by tennis coaches and athletes.

REFERENCES:

Sun Yanming & Chang Chunfang. (2014). Kinematical Analysis of Technical Characteristics of Forehand Topspin in Tennis. *Journal of Capital University of Physical Education and Sports*, 02, 189-192.

Wang Huifang. (2014). Kinematical Analysis of Forehand Topspin Technique of Male Athletes in ATP Chengdu Open, Chengdu Sport University,.

Wang Jifang, Zhou Jihe, Gao Zhanle & Li Yirong. (2013). Kinematical Analysis of Forehand Topspin Action of Thomas Enqvist [A]. Sports Biomechanics Branch of China Sport Science Society. Thesis Collection for the 16th National Academical Communication Conference of Biomechanics in Sports (CABS 2013) [C]. Sports Biomechanics Branch of China Sport Science Society.

Guo Jian. (2009). Biomechanical Analysis and Evaluation of Forehand Stroke Technique. *Bulletin of Sport Science & Technology*, 12, 53-55.

Hu Wenlin, Zhou Jihe & Cheng Liang. (2012). Kinematical Analysis of Forehand Receiving Technique of Moya [A], Sports Biomechanics Branch of China Sport Science Society; Collection of Abstracts of the 15th National Academical Communication Conference of Biomechanics in Sports (CABS2012) [C], Sports Biomechanics Branch of China Sport Science Society.

Reid Machar, Elliott Bruce & Crespo Miguel. (2013). Mechanics and Learning Practices Associated with the Tennis Forehand: A Review. *Journal of sports science & medicine*, 122.

Rogowski Isabelle, Rouffet David, Lambalot Frederic, Brosseau Olivier, & Hautier Christophe. (2011). Trunk and upper limb muscle activation during flat and topspin forehand drives in young tennis players. *Journal of Applied Biomechanics*, 271.